Synthesis, in vitro antibacterial and antiprotozoal evaluation of 2-phenyl-4-amino quinazolines

HJ Neethling

orcid.org/0000-0003-3231-2685

Dissertation accepted in fulfilment of the requirements for the degree Master of Science in Pharmaceutical Chemistry at the North-West University

Supervisor:	Dr R Beteck
Co-Supervisor:	Prof L Legoabe
Assistant-Supervisor:	Mrs KT Angula

Graduation: December 2023

PREFACE

This dissertation is presented in article format in accordance with the academic regulations of North-West University (A.13.7.3). It contains four chapters:

Chapter 1: Introduction and problem statement

Chapter 2: Literature review

Chapter 3: Manuscript to be submitted for publication

Synthesis, *in vitro* antibacterial and antiprotozoal evaluation of 2-phenyl-4-amino quinazolines

The manuscript was prepared following the author guidelines provided by the journal, which are availableon the journal's website.

https://onlinelibrary.wiley.com/page/journal/17470285/homepage/forauthors.html

Chapter 4: Summary and conclusion

ACKNOWLEDGEMENTS

I would like to express my gratitude to my supervisor, **Prof. R.M. Beteck**, for providing me with the opportunity to conduct research in their lab and for their patience and guidance throughout the study. Your commitment is invaluable.

I am also thankful to my co-supervisor, **Prof. L.J. Legoabe**, for their motivation and support.

A special thanks goes to my assistant supervisor, **Dr K.T. Angula**, for their expertise in the laboratory and their constant willingness to assist me in learning the necessary lab skills.

I would like to acknowledge **Drs J. Jordaan** and **D. Otto** for their assistance with HRMS and NMR spectroscopy.

I extend my appreciation to **Audrey Jordaan** and **Prof. D. Warner** for conducting the antitubercular screening at the University of Cape Town in South Africa.

Furthermore, I am grateful to the **South African Research Council** for their additional financial support towards the antitubercular screening.

I would like to express my heartfelt appreciation to my **colleagues** at the Centre of Excellence for Pharmaceutical Sciences (Pharmacen – NWU) for their invaluable assistance and support.

To my **parents**, I am incredibly grateful for this lifetime opportunity and for your unwavering love and unconditional support in all aspects of my life. Your encouragement has been instrumental in my journey, and I am truly blessed to have you by my side.

I want to extend my sincere gratitude to my friend, **Carla Hartman**. Your continuous words of encouragement and unwavering moral support have been invaluable during challenging times. You have played a crucial role in my success, and for that, I will be eternally grateful. Thank you very much!

ABSTRACT

ESKAPE pathogens, including *Enterococcus faecium, Staphylococcus aureus, Klebsiella pneumoniae, Acinetobacter baumannii, Pseudomonas aeruginosa*, and *Enterobacter* species, are prominent contributors to global nosocomial infections. These pathogens possess the ability to evade the biocidal action of antibiotics, representing a paradigm shift in resistance, transmission, and pathogenesis. Multidrug resistance is common, with currently very few to no effective drugs. There is, therefore, an urgent need to identify new compounds active against ESKAPE pathogens.

Human African trypanosomiasis (HAT) is caused by *Trypanosoma brucei (T.b.)* parasites. Greater than 90% of HAT cases are primarily attributed to *T.b. gambiense,* which is prevalent in western and Central Africa, and causes the chronic form of the disease. *T.b. rhodesiense*, primarily infects animals and occasionally humans, causing HAT in southern and eastern Africa. HAT disease progresses through an early stage involving parasites residing in the lymphatic system and bloodstream (haemolymphatic stage), followed by a late stage during which trypanosomes cross the blood-brain barrier into the central nervous system and cause neurological damage (meningoencephalitic stage). *T.b. brucei* causes severe and often fatal disease referred to as nagana in domestic animals. Drugs available for both nagana and HAT are limited in number, efficacy, and spectrum of activity. They have poor drug-like properties such as low oral bioavailability and high toxicities, hence the need to identify new compounds with antitrypanosomal activity.

Leishmaniasis, caused by *Leishmania* parasites and transmitted by infected sandflies, manifests in various clinical forms depending on the infecting *Leishmania* species and the host's immune response. Cutaneous leishmaniasis affects the skin, mucosal leishmaniasis affects the mucous membranes, and visceral leishmaniasis affects internal organs such as the lungs and liver. Visceral leishmaniasis is considered an opportunistic infection in immunocompromised individuals, notably those with the human immunodeficiency virus (HIV) infection. Current leishmanial treatments are not ideal due to intravenous administration, toxicity concerns, and high cost.

Tuberculosis (TB), caused by the bacterium *Mycobacterium tuberculosis* (*M. tuberculosis*), is one of the oldest diseases affecting humans and remains a significant global health threat. TB is classified into pulmonary TB and extrapulmonary TB based on clinical manifestations. Pulmonary TB affects the lungs, while extrapulmonary TB affects other organs. The emergence of drug-resistant *M. tuberculosis* strains

and the co-infection of TB with HIV have exacerbated the management of TB, and TB treatment failure is currently on the rise. This makes it necessary to search for new molecules for treating TB.

Quinazoline is a heterocyclic ring system composed of fused benzene and pyrimidine rings. Its discovery dates back to 1903 when the first quinazoline-based compound, 2-methyl-1,3-aryl-4-quinazoline, was isolated from the Chinese plant *aseru*. This compound possesses sedative and somniferous properties. Subsequent research focused on creating chemical derivatives of quinazoline and exploring their biological activities. By 1980, there were approximately 50 different derivatives, many with various pharmacological effects, including sedative, tranquilising, analgesic, anticonvulsant, antitussive, myorelaxant, antirheumatic, hypotensive, antiallergic, bronchodilating, antidiabetic, cholagogue, diuretic, antimalarial, and spermicidal activities.

Several drug molecules containing the quinazoline ring have been developed for various therapeutic purpose, including bunazosin, trimetrexate, vandetanib, prazosin, alfuzosin, gefitinib, and erlotinib. These compounds are used in cardiovascular medicine, antimicrobial therapy, and cancer treatment. Overall, their diverse pharmacological activities have made this scaffold valuable for drug discovery.

In this project, a series of 2,4-disubstituted quinazolines were synthesised successfully. These compounds were subjected to *in vitro* screening to evaluate their potential as antitubercular, antiprotozoal, antibacterial and antifungal agents, as well as their cytotoxicity.

Among the tested compounds, **3a–3c, 3e, 3f, and 5a–5c** demonstrated promising antitubercular activity, with minimum inhibitory concentration (MIC), which represents the lowest concentration at which a substance inhibits bacterial/fungal growth, values below 9 µM. This indicates they are potent against the TB-causing bacterium. However, none of the compounds showed activity against ESKAPE pathogens. The MIC values against these bacteria were higher than 32 µg/mL and a $D_{max} < 50$. D_{max} (maximum non-inhibitory concentration) values below 50 indicate the concentration at which the compound does not have any inhibitory effect. In terms of antifungal activity, **Compounds 2b**, **3b**, **3d**, and **3f** exhibited activity against *Cryptococcus neoformans var. grubii*, with MIC values equal to or below 32 µg/mL. **Compound 2b** also displayed potent activity against *Candida albicans*, with an MIC value below 32 µg/mL. **Compounds 5a–5c** displayed the best antitrypanosomal activity ($IC_{50} < 7$ µM).

Overall, the synthesised 2,4-disubstituted quinazolines demonstrated promising antitubercular, antifungal, and antiprotozoal activities *in vitro*. The compounds demonstrating promising antitubercular,

antifungal, and antitrypanosomal activities in this study hold significant potential for future drug development. Their effectiveness against Mtb, *Cryptococcus neoformans var. grubii*, and *Candida albicans* suggests they could contribute to the development of novel treatments against these human pathogens. Additionally, the potent antitrypanosomal activity of **Compounds 5a–5c** highlights their potential in addressing trypanosomiasis. These findings pave the way for further research and exploration of these compounds as potential candidates for new drugs or therapeutic interventions against a range of infectious diseases.

In summary the synthesis of the 2,4-disubstituted quinazolines includes the following key steps: As a starting material, 2-aminobenzamide was used to react with different aldehydes in a cyclisation reaction mediated by iodine to form **Compound 1** in 61% yield. **Compound 1** underwent chlorination using thionyl chloride to form **Compound 2** in 55% yield. **Compound 3** underwent nucleophilic substitution reaction (nucleophilic substitution reactions belong to a category of chemical reactions where an electron-rich nucleophile reacts with a positively charged electrophile, leading to the displacement of a leaving group) in the presence of appropriate amines under refluxing conditions to furnish **Compounds 3–5** with yields ranging from 5–54%. Reactions were monitored using thin-layer chromatography (TLC).

Keywords: Quinazolines, ESKAPE pathogens, Trypanosomiasis, Tuberculosis, Leishmaniasis.

TABLE OF CONTENTS

LIST OF FIGURES

LIST OF TABLES

LIST OF SCHEMES

ABBREVIATIONS AND NOMENCLATURE

µg	microgram
µL	microlitre
µM	micromolar
^{13}C NMR	carbon nuclear magnetic resonance
^{1}H NMR	proton nuclear magnetic resonance
A. baumannii	*Acinetobacter baumannii*
AAT	African animal trypanosomiasis
ADC	albumin
AIDS	acquired immunodeficiency syndrome
CAS	casein
CSF	cerebrospinal fluid
d	doublet
Da	Dalton
DMSO-d_6	deuterated dimethyl sulfoxide
DNA	deoxyribonucleic acid
DNDi	Drugs for Neglected Diseases Initiative
dt	doublet of triplets
E. faecium	*Enterococcus faecium*
EPTB	extrapulmonary tuberculosis
eqvi	equivalence
ESKAPE	*Enterococcus faecium*, *Staphylococcus aureus*,*Klebsiella pneumoniae*, *Acinetobacterbaumannii*, *Pseudomonas aeruginosa*, and *Enterobacter* spp.

ESP	enterococcal surface protein
FTIR	Fourier-transform infrared
HAT	human African trypanosomiasis
HIV	human immunodeficiency virus
HPLC	high-performance liquid chromatography
HRMS	high-resolution mass spectrometry
Hz	Hertz
IC_{50}	half-maximal inhibitory concentration
ICU	intensive care unit
INH	isoniazid
J	coupling constant
K. pneumoniae	*Klebsiella pneumoniae*
L. aethiopica	*Leishmania aethiopica*
L. amazonensis	*Leishmania amazonensis*
L. braziliensis	*Leishmania braziliensis*
L. donovani	*Leishmania donovani*
L. infantum	*Leishmania infantum*
L. major	*Leishmania major*
L. mexicana	*Leishmania mexicana*
L. panamensis	*Leishmania panamensis*
L. tropica	*Leishmania tropica*
LCL	localised cutaneous leishmaniasis
m	multiplet

M. tuberculosis	*Mycobacterium tuberculosis*
m.p.	melting point
mcg	microgram
MDR-TB	multidrug-resistant tuberculosis
MHz	megahertz
MIC	minimal inhibitory concentration
MRC-5	lung fibroblast tissues
MRSA	methicillin-resistant *Staphylococcus aureus*
MW	molecular weight
NECT	nifurtimox-eflornithine combination therapy
nm	nanometre
NMR	nuclear magnetic resonance
P. aeruginosa	*Pseudomonas aeruginosa*
PKDL	post kala-azar dermal leishmaniasis
ppm	parts per million
PMM	primary mouse macrophages
PTB	pulmonary tuberculosis
PZA	pyrazinamide
qd	quartet of doublets
qt	quartet of triplets
RIF	rifampicin
RIPE	rifampicin, isoniazid, pyrazinamide, ethambutol
RNA	ribonucleic acid

s	singlet
S. aureus	*Staphylococcus aureus*
Sb(v)	pentavalent antimony
t	triplet
T. b.	*Trypanosoma brucei*
T. congolense	*Trypanosoma congolense*
T. cruzi	*Trypanosoma cruzi*
T. vivax	*Trypanosoma vivax*
T.b. brucei	*Trypanosoma brucei brucei*
T.b. gambiense	*Trypanosoma brucei gambiense*
T.b. rhodesiense	*Trypanosoma brucei rhodesiense*
TB	tuberculosis
td	triplet of doublets
TLC	thin-layer chromatography
UK	United Kingdom
US	United States (of America)
V	volt
Vpp	peak-to-peak voltage
VRE	vancomycin-resistant *Enterococc*i
WHO	World Health Organization

CHAPTER 1 – INTRODUCTION AND PROBLEM STATEMENT

1.1 Introduction

Numerous disease-causing agents, including those mentioned in the subsequent sections, have evolved to withstand the lethal impact of antibiotics. Consequently, it is crucial to investigate the mechanisms through which these organisms acquired resistance and to create innovative antimicrobial solutions for effective treatment.

1.1.1 ESKAPE pathogens

The acronym ESKAPE (*Enterococcus faecium*, *Staphylococcus aureus*, *Klebsiella pneumoniae*, *Acinetobacter baumannii*, *Pseudomonas aeruginosa*, and *Enterobacter* species) includes six pathogenic bacteria (Mulani *et al.*, 2019:1). These bacteria are termed ESKAPE pathogens because of their exceptional capability to 'escape' the biocidal action of antibiotics, which thus represents new paradigms in drug resistance, transmission, and pathogenesis (Pendleton *et al.*, 2013:297). These bacteria exhibit resistance to multiple drugs and possess various virulence traits, contributing to their association with high rates of illness and death (Rice, 2010). Infection with ESKAPE pathogens necessitates longer stays in hospital and the use of expensive antibiotics, which lead to an increased cost in healthcare (Mulani *etal.*, 2019:2).

The United States (US) Centers for Disease Control and Prevention observed that antibiotic-resistant microorganisms cause more than 2 million infections and lead to at least 23 000 deaths in the US each year (Ma *et al.*, 2020:1). The increasing impact of antimicrobial resistance on morbidity, mortality, and healthcare expenditures makes it one of the most alarming public health issues in the world. Antimicrobial resistance is linked to more than 700 000 fatalities each year (Arbune *et al*., 2021:2369). An antibiotic-resistant bacteria is predicted to be responsible for over 33 000 deaths in the European Union in the year 2050 (Ma *et al*., 2020:1). Antimicrobial resistance is a result of natural evolution and bacterial adaptation processes, which are sped up by the selection pressure brought on by insufficient or excessive antibiotic use. It is difficult to treat infections due to the ongoing spread of multidrug resistance, which necessitates the use of reserve medicines that can have greater cost-to-benefit ratios and lower security profiles (Arbune *et al*., 2021: 2370).

The most significant effect of multidrug-resistant pathogens on healthcare-associated illnesses was caused by ESKAPE pathogens (Arbune *et al.*, 2021:2370). Data from the National Healthcare Safety Network revealed that slightly more than 40% of patients in intensive care units (ICUs) are infected with ESKAPE pathogens (Rice, 2010). Infections caused by ESKAPE pathogens may become unmanageable because of insufficient antibacterial therapy (Rice, 2010). Around the world, the deaths per year related to antimicrobial resistance are anticipated to increase ten-fold by 2050 (Ma *et al*.,2020:1). There is, therefore, an urgent need to identify and develop new drugs against ESKAPE pathogens.

Enterococcus faecium (E. faecium), which is resistant to vancomycin and ampicillin, is one example of an organism with a rate of resistance that practically eliminates antibiotics from contemplation in empirical therapy. Other organisms with higher rates of resistance, such as carbapenem-resistant *Pseudomonas aeruginosa (P. aeruginosa)* or *Acinetobacter baumannii (A. baumannii)*, may make definitive therapy useless. *E. faecium's* resistance, as well as the method of resistance in staphylococci, to fluoroquinolones, linezolid, aminoglycosides, clindamycin, and erythromycin has been established. Nevertheless, the exact method of resistance to the lipopeptide antibiotic daptomycin is under continuous study. Aminoglycosides, trimethoprim-sulfamethoxazole, and fluoroquinolones are frequently ineffective against carbapenem-resistant *Klebsiella pneumoniae (K. pneumoniae)*, leaving only colistin and the more recent tigecycline as therapy options. There have been reports of the emergence of colistin and tigecycline resistance, leading to pan-resistant organisms (Rice, 2010).

Until outbreaks of infection with multidrug-resistant strains occurred in various regions of the world, *A. baumannii* was regarded as an insignificant bacterium. Both *A. baumannii* and *P. aeruginosa* are reported to have 'slow' porins, giving them a fundamental dominance against a vast number of antimicrobial medications. Due to degrees of resistance conferred against a variety of antimicrobial drugs brought on by two distinct resistance-nodulation cell division multidrug-resistant efflux pumps, *A. baumannii* is resistant to β-lactam antibiotics. As a result of *P. aeruginosa's* importance in the deaths of patients with febrile neutropenia and its intrinsic resistance to several antimicrobial therapies, there have been major efforts to identify novel antibiotics effective against it (Rice, 2010). *Staphylococcus aureus (S. aureus)* has developed resistance against methicillin because of the widespread usage of penicillin (De Oliveira *et al.*, 2020:3).

The antibiotic resistance mechanisms of ESKAPE pathogens are divided into four main groups, namely: (i) inactivation or alteration of the antimicrobial molecule; (ii) bacterial target site modifications; (iii) reduced antibiotic penetration/accumulation; and (iv) formation of bacterial biofilms (De Oliveira *et al.*, 2020:8).

1.1.2 Human African trypanosomiasis/sleeping sickness

Sleeping sickness, also called human African trypanosomiasis (HAT), is a protozoal disease that shares common endemicity with malaria (another protozoal disease); hence, both diseases present the possibility of co-infection (Nsubuga *et al.*, 2019:2). HAT is spread through the bite of a tsetse fly infested with *Trypanosoma brucei* (*T. b.*) parasites (Brun *et al.*, 2010:148). Activities such as fishing, farming, and hunting expose people to the vector of this disease (Brun *et al.*, 2010:148). The three main subspecies of *T. b.* causing HAT include *T.b. gambiense* (mainly found in Central and West Africa), *T.b. rhodesiense* (commonly found in eastern and southern Africa), and *T.b. brucei* that typically infects wild and domestic animals (Brun *et al.*, 2010:148).

HAT is known as the most neglected tropical disease (Brun *et al.*, 2010:148). It progresses through two stages. The first stage is called the haemolymphatic stage and the second stage the meningoencephalitic stage. In the first stage, the signs and symptoms include headaches, both intermitted and chronic fever, hepatosplenomegaly, pruritis, and lymphadenopathy. The clinical features in the second stage include neuropsychiatric disorders and sleep abruptions (Brun *et al.*, 2010:150).

The trypanosome, the causative agent of HAT, possesses a remarkable capability known as antigenic variation. This mechanism enables the trypanosome to evade the adaptive immune response of the host. As a result, the development of effective vaccines against HAT has been challenging as the parasite constantly changes its surface antigens, making it difficult for the immune system to recognise and mount a specific response. Consequently, chemotherapy remains the primary intervention for HAT as there are no viable vaccine options available to combat the disease in individuals (Brun *et al.*, 2011:678).

Despite the continued endemic nature of the disease, significant efforts to reduce morbidity and mortality associated with HAT have yielded remarkable success. These efforts have led to a notable decline in the number of reported cases in sub-Saharan Africa, with the count dropping to fewer than 3 000 cases in 2015. This achievement signifies the effectiveness of interventions aimed at prevention, early detection,

and treatment of HAT, contributing to improved health outcomes and a reduction in the burden of the disease in the region (Büscher *et al.*, 2017:1).

The medical needs for the treatment of HAT are still unmet as the current available drugs are limited in number and pose challenges in terms of their pharmacokinetic properties and side effects. The existing drugs used for HAT treatment often exhibit poor pharmacokinetics, which can affect their absorption, distribution, metabolism, and excretion in the body. Additionally, these drugs are associated with numerous side effects that affect patient compliance and overall treatment outcomes.

Given these limitations, there is an urgent and critical need for the development of more efficient drugs for HAT. These drugs should possess improved pharmacokinetic profiles, allowing for better drug delivery and efficacy. Furthermore, they should have a reduced risk of side effects to enhance patient safety and tolerability. The development of novel and more effective treatment options for HAT is essential to address the ongoing medical challenges associated with this disease and improve the overall management and outcomes for affected individuals (Welburn *et al.*, 2001). The first drug of choice against first-stage HAT caused by *T.b. gambiense* is pentamidine, while suramin is the first-line drug for *T.b. rhodesien*se disease (Brun *et al.*, 2010:152-153).

Melarsoprol is commonly used for second-stage disease in *T.b. gambiense* and is also the priority choice in second-stage *T.b. rhodesiense.* The frequency of melarsoprol side effects are great and can be fatal and severe (Brun *et al.*, 2010:154). Another molecule registered for the treatment of second-stage HAT is eflornithine, which shows favourable outcomes and fewer fatalities than melarsoprol; therefore, it is recommended as a first-line treatment for second-stage disease caused by *T.b. gambiense*. On the other hand, *T.b. rhodesiense* is not susceptible to eflornithine. The administration of this medication is challenging. After an oral formulation was developed, it was quickly discarded due to unsatisfactory pharmacokinetic results (Brun *et al.*, 2010:154). This was resolved through nifurtimox-eflornithine combination therapy (Büscher *et al.*, 2017:7).

There are currently two new molecules, namely acoziborole and fexinidazole, in clinical development for the treatment of both stage 1 and stage 2 of HAT. These drugs are administered orally, which provides a convenient and accessible route of administration for patients. Continued research and development of these molecules are crucial steps in meeting the medical need and addressing the challenges associated with HAT treatment (Büscher *et al.*, 2017:8).

1.1.3 African animal trypanosomiasis/nagana

African animal trypanosomiasis (AAT) or as it is commonly called, nagana, is a trypanosomal infection mostly found in cattle. In affected animals, nagana may either be acute or chronic. Chronic infection is, however, more prevalent. Clinical symptoms include severe anaemia, weakness, and unproductiveness. This disease has a negative impact as it reduces animal fertility, milk and beef yields, and the increase in animal mortality causes the herd size to decrease. In the human population, these impacts have massive negative economic effects (Connor, 1994:379). The protozoans that cause nagana are *Trypanosoma congolense* (*T. congolense), Trypanosoma vivax (T. vivax)*, and *T.b. brucei.* In animal trypanosomiasis, all drugs have been announced as resistant (Matovu *et al.*, 2001:763).

Chemotherapy remains the sole intervention for this disease due to the inadequate availability of vaccines and drugs. Additionally, there is a noticeable dearth of new drug development, primarily stemming from a lack of research interest. The underlying cause of this lack of interest can be attributed to the prevalence of poverty and the disproportionate impact of the disease on underprivileged communities (Matovu *et al.*, 2001:763).

T.b. brucei is responsible for more severe illness in domestic animals and rather mild disease in wild animals. The animals affected and their severity of the illness are divided into three groups, namely mild: cattle and pigs; moderate: sheep and goats; and severe: donkeys, horses, and dogs. Infected animals continue to grow weaker, and this poor state gave the disease its name. The name *n'gana* is a Zulu word meaning powerless or useless (Steverding, 2017:288).

The detection of nagana in animals primarily relies on the observation of clinical signs and the identification of illness. Prior to initiating any treatment, it is crucial to perform parasitological tests (tests involving the examination of body fluids or tissues for the presence of the causative parasite and consist of blood smear examination, lymph node aspiration and cerebrospinal fluid (CSF) examination) to confirm the presence of trypanosomes in the bloodstream. These tests are essential for diagnosing nagana and determining the appropriate course of treatment (Steverding, 2017:290).

Three drugs, namely quinapyramine, diminazene, and isometamidium are available for treatment and prophylaxis of nagana caused by *T. b.*. The compound quinapyramine can be used prophylactically and therapeutically. Quinapyramine showed efficacy against *T. b.* in cattle, pigs, goats and sheep before it was

eliminated from the market in the most African countries in 1970. Now it is used more often as a prophylactic in pigs. Diminazene is used therapeutically because of its fast eradication. It is non-toxic for cattle and, therefore, is used for the treatment of trypanosomiasis in cattle. Isometamidium is used for infection in equids (Steverding, 2017:293).

1.1.4 Leishmaniasis

Leishmaniasis is a disease caused by the *Leishmania* parasite and transmitted by sandflies, specifically phlebotomine females. Several clinical manifestations of leishmaniasis, including localised infection (ulcerative skin lesions), disseminated infection (cutaneous, mucosal, or visceral), and inapparent infection exist. This disease is caused by nearly 24 different *Leishmania* species in both children and adults (Murray *et al.*, 2005:1561). Leishmaniasis affects almost 12 million people, and about 350 million people in 88 countries are at risk of contracting this disease.

Current treatments use a few different classes of drugs, and some commonly used drugs include penta-valent antimonials [Sb(v)], amphotericin B, paromomycin, miltefosine, and pentamidine (Murray *et al.*, 2005). The drawbacks associated with current drugs include the need for expensive formulation, species selective activity, and unwanted side effects such as nausea, vomiting, diarrhoea, hyperglycaemia, and cardiotoxicity (Murray *et al.*, 2005:1569).

1.1.5 Tuberculosis

Mycobacterium tuberculosis (*M. tuberculosis*) is the bacterium that causes tuberculosis (TB) (Russell, 2001:1). TB affects more than 10 million people with ill health each year. Consequently, it is also one of the major global causes of death in adults (Kiazyk & Ball, 2017). In 2021, it was estimated that approximately 10.6 million people contracted TB. This marked an increase of 4.5% compared to the previous year, when the estimated number of TB cases was 10.1 million in 2020 (Bagcchi, 2023: e20). Around one-third of the world's population is infected with *M. tuberculosis* bacteria, which carries a 10% lifetime risk of getting TB disease. Globally, 10.4 million TB cases were reported in 2017, which equates to 133 cases per 100 000 people. Global TB Control reported that they are set back due to their reliance on 40–60-year old drugs and a 100-year old vaccine (Gagneux, 2018:1).

Deaths caused by TB in 2016 tallied up to 1.7 million, with 22% of these coming about in people co-infected with the human immunodeficiency virus (HIV) (Koch & Mizrahi, 2018). Between 2019 and 2021,

there was a global increase in the estimated number of deaths from TB, reversing a trend of declining TB-related deaths that had been observed from 2005 to 2019. In 2021, the estimated number of TB-related deaths consisted of: approximately 1.4 million deaths among individuals who were HIV-negative and approximately 187,000 deaths among individuals who were HIV-positive. This combined total of TB-related deaths in 2021 was 1.6 million, which represented an increase from the best estimates of 1.5 million in 2020 and 1.4 million in 2019. This elevated number of TB-related deaths brought the statistics back to a level similar to what was observed in 2017 (WHO, 2022:2). Therefore, TB epidemics are increasing due to multidrug resistance and extensive drug resistance, in combination with HIV co-infections. Fuelling this epidemic is the occurrence of the comorbidity, type-2 diabetes (Gagneux, 2018:1).

Although there seems to be progress in the reduction of incidences, these are not enough or as anticipated. It is foreseen that the TB health threat will not be terminated by the year of 2035 as planned by the End TB Strategy (Chakaya *et al.*, 2021:2). For instance, the aim was to reduce TB incidence by 20% between 2015 and 2020. Only 9% of the 20% target was met between 2015 and 2020. Likewise, the death rate reduction aim was set at 35% and only a 14% mortality reduction was reached in this period (Chakaya *et al.*, 2021:2).

The most potent known risk factor for *M. tuberculosis* infection and progression to active disease – which increases the chance of latent TB reactivation by a factor of 20 – is HIV infection (Espert *et al.*, 2015:1). In addition, TB is the main cause of acquired immunodeficiency syndrome (AIDS)-related deaths. Thus, HIV and *M. tuberculosis* infection work synergistically. Around 14 million people worldwide are co-infected with both *M. tuberculosis* and HIV (Espert *et al.*, 2015:1).

Individuals infected with TB are classified into two groups, namely those with a latent TB infection and those with an active TB infection. Latent TB infection refers to a state of infection in which the person does not exhibit any symptoms and the disease is not contagious (Kiazyk & Ball, 2017). In this scenario, the host is asymptomatic and not contagious. The lesions usually heal within 6 to 8 weeks. Reports suggest that approximately one-third of the world's population carries *M. tuberculosis* in this latent form, with the majority (90%) never experiencing active disease symptoms. However, in some cases, granulomas may undergo liquefactive necrosis, releasing contagious bacteria and causing lung damage, leading to the development of symptomatic and highly infectious active TB (Luies & du Preez, 2020:4). On the other hand, individuals with an active TB infection are contagious and experience symptomatic manifestations

of the disease (Kiazyk & Ball, 2017). The clinical manifestations of active TB can vary widely, from mild symptoms like a cough to more severe consequences like permanent lung damage and, in some cases, fatal outcomes, depending on the stage and progression of the disease. Besides its clinical symptoms, TB has also been linked to various systemic complications brought on by the disease, including conditions like low sodium levels (hyponatremia) and impaired glucose metabolism (glucose intolerance) (Luies & du Preez, 2020:1). TB is transmitted through individuals infected with pulmonary or laryngeal tuberculosis. These people bring about a droplet containing *M. tuberculosis* through coughing, sneezing, and shouting. These exhalation actions cause the spread of the respiratory infectious aerosols from the airways (Churchyard *et al.*, 2017:630-631). These droplets survive in the air and are inhaled by other people who may become infected with the disease and then develop latent or active TB (Churchyard *et al.*, 2017:629).

1.1.6 Compounds of interest

Various compounds, such as quinazoline, piperazine, and ethylenediamine-containing compounds, have shown potential as therapeutic agents in the fight against antimicrobial resistance. These compounds are being explored for their ability to combat drug-resistant pathogens.

1.1.6.1 Quinazolines

Quinazolines and quinazolinones **(Figure 1.1)** are two structurally related heterocyclic classes of compounds of great interest. The reason being that their varied and expanded range of biological properties such as anti-HIV, anticancer, antifungal, antibacterial, antimutagenic, anticoccidial, anti-convulsant, anti-inflammatory, antioxidant, antileukemic,antidepressant, antiviral, antiprotozoan, anti-tubercular, and antimalarial activities. These biological activities are often achieved through the inhibition of enzymes involved in deoxyribonucleic acid (DNA) replication (Skyrianou *et al.*, 2009:1617). Moreover, they are chemically tractable, allowing for a wide range of derivatisation at different positions, which have ultimately led to diverse compounds that interact differently with different biological targets (Asif, 2014:1). Due to the antibacterial and antiprotozoan properties associated with quinazolines, novel quinazolines incorporating diamino moiety were synthesised in this project and evaluated for their antibacterial and antiprotozoal potentials.

Thus, quinazolines hold significant relevance in addressing the pressing challenge of drug-resistant pathogens across various medical disciplines. Their diverse range of biological properties, including

antibacterial and antiprotozoal activities, positions quinazolines as promising candidates for combating drug-resistant infections. Their ability to inhibit essential enzymes involved in DNA replication, making them valuable tools in the fight against drug-resistant pathogens. Additionally, the chemical tractability of quinazolines allows for structural modifications, offering the potential to create novel compounds that can effectively target and address the evolving landscape of drug resistance. Therefore, the exploration and synthesis of quinazolines, such as those incorporating a diamino motif, represent a crucial step toward developing innovative solutions to combat drug-resistant infections and enhance global health outcomes.

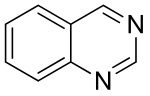

quinazoline

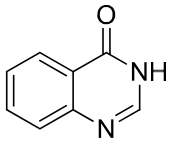

quinazolinone

Figure 1.1: Quinazoline and quinazolinone chemical structures (Source: own)

1.1.6.2 Piperazine

A science known as medicinal chemistry is used to find novel therapeutic compounds to treat a variety of ailments. As a result, intriguing structures have been found. One such structure is the piperazine moiety — an acyclic molecule with four carbon atoms and two nitrogen atoms in positions 1 and 4 (Brito *et al*., 2019:13). Piperazine is a sought-after heterocyclic for the creation of novel medication candidates. Such a ring may be found in a number of well-known, readily available pharmaceuticals. Piperazine compounds have a wide range of pharmacological actions that have made them essential anchoring for the synthesis of innovative therapeutic drugs (Shaquiquzzaman *et al.*, 2015:487). In addition to the antibacterial activity, the central pharmacological activity of many piperazine derivatives is the stimulation of the monoamine pathway. Consequently, research on piperazine compounds has focused on a variety of central therapeutic applications, such as antipsychotic, antidepressant, and anxiolytic uses (Brito *et al.*, 2019:13).

Heterocycles are frequently found in commercially marketed medications as their structural scaffolds. Because of their enormous significance, researchers have focused a significant amount of attention on heterocycles that include nitrogen. The nitrogen-containing, six-membered heterocyclic piperazine **(Figure 1.2)** is noteworthy and significant in medicinal chemistry. According to reports, piperazine derivatives have a wide range of pharmacological effects, including antidepressant, anticancer,

anthelmintic, antibacterial, antifungal, antimycobacterial, antimalarial, and anticonvulsant properties. This heterocyclic is found in a large number of well-known medications from a variety of pharmacological classes (Shaquiquzzaman *et al.*, 2015:487).

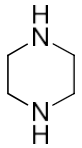

piperazine

Figure 1.2: Structure of piperazine (Source: own)

Several researchers have created a variety of antibacterial compounds with a piperazine moiety, piperazine-based antitubercular drugs, and several piperazine-containing antifungal medicines (Shaquiquzzaman *et al.*, 2015:488-519). Consequently, the exploration of novel compounds like quinazolines incorporating a diamino motif, which builds upon the foundation of piperazine, represents a promising avenue for addressing the challenges of drug resistance and advancing the field of antimicrobial therapeutics.

1.1.6.3 Ethylenediamine-containing compounds

A 1,2-ethylenediamine called SQ109 **(Figure 1.3)** specifically targets MmpL3 in *M. tuberculosis*. The inclusion of mycolic acid in the *M. tuberculosis* cell wall requires the mycolic acid transporter MmpL3. For drug-sensitive TB, SQ109, a novel therapeutic candidate, is undergoing Phase II clinical studies. In order to launch a combinatorial chemistry programme to find a novel TB medicine, Sequella and the Laboratory of Host Defences, National Institute of Allergy and Infectious Diseases, and National Institutes of Health signed a joint research and development agreement in January 1999. During this study, a 63 238-member chemical library was created and screening was performed based on the active 1,2-ethylenediamine pharmacophore present in ethambutol — one of the first-line anti-TB medications (Sacksteder *et al.*, 2012:824-825). Ethylenediamine-containing compounds, offer a promising avenue in addressing the escalating challenges posed by drug-resistant pathogens, especially in the context of TB. Due to the potential antitubercular activity, novel 1,2-ethylenediamine incorporating diamino moiety were synthesised in this project and evaluated for their antitubercular potentials.

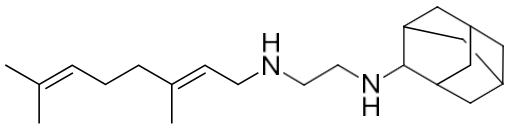

SQ109

Figure 1.3: SQ109 was found using a targeted combinatorial library of small-molecule 1,2-ethylenediamine compounds (Sacksteder *et al.*, 2012:826)

1.2 Problem statement/research problem

Treatment failure due to drug-resistant pathogens has become commonplace in all disciplines of medicines, be it in the treatment of bacterial, viral, fungal, or protozoal infections. It is important to mention that the emergence and spread of drug-resistant pathogens is largely a natural phenomenon; and to keep pace with such a phenomenon, humans have to constantly engage in the identification and development of new drugs. This can easily be achieved through the structural evolution of known drug molecules to target known and/or novel essential metabolic pathways in human pathogens. To this effect, this study aims to synthesise novel quinazolines incorporating diamino motif (see **Figure 1.1**) as potential antibacterial and antiprotozoal agents.

1.3 Aims and objectives

The aim of this project is to synthesise novel quinazolines incorporating piperazine and ethylenediamine and establish their antibacterial and antiprotozoal activities *in vitro*.

The objectives of this study are the following:

- Synthesis and structural elucidation of novel quinazoline-based compounds via nuclear magnetic resonance (NMR) and mass spectrometry.
- *In vitro* antibacterial evaluation of synthesised compounds against ESKAPE pathogens and *M. tuberculosis*.
- *In vitro* antiprotozoal evaluation of synthesised compounds against *T.b. brucei* and *L. donovani*.
- *In vitro* cytotoxicity evaluation of potential hit compounds against HEK293 cells.

*NMR = Nuclear magnetic resonance (NMR) spectroscopy involves the examination of molecules by observing how their nuclei interact with radiofrequency electromagnetic radiation when they are placed within a powerful magnetic field.
*Mass spectrometry = Mass spectrometry is a valuable analytical technique for determining the mass-to-charge

ratio (m/z) of one or more molecules within a sample. These measurements frequently enable the precise determination of the molecular weights of the components in the sample.

REFERENCE LIST – CHAPTER 1

Arbune, M., Gurau, G., Niculet, E., Lancu, A.V., Lupasteanu, G., Fotea, S., … Tatu, A.L. 2021. Prevalence of antibiotic resistance of ESKAPE pathogens over five years in an infectious diseases hospital from South-East of Romania. *Infection and Drug Resistance,* 14(10):2369-2378. doi:10.2147/IDR.S312231

Asif, M. 2014. Chemical characteristics, synthetic methods, and biological potential of quinazoline and quinazolinone derivatives. *International Journal of Medicinal Chemistry*, (2014):1-27, 395637. doi:10.1155/2014/395637

Bagcchi, S. 2023. WHO's global tuberculosis report 2022. *The Lancet Microbe,* 4(1):e20. doi: 10.1016/S266-5247(22)00359-7

Brito, A.F., Moreira, L.K., Menegatti, R. & Costa, E.A. 2019. Piperazine derivatives with central pharmacological activity used as therapeutic tools. *Fundamental & Clinical Pharmacology*, 33(1):13-24. doi:10.1111/fcp.12408

Brun, R., Blum, J., Chappuis, F. & Burri, C. 2010. Human African trypanosomiasis. *The Lancet*, 375(9709): 148-159. doi:10.1016/S0140-6736(09)60829-1

Brun, R., Don, R., Jacobs, R.T., Wang, M.Z. & Barrett, M.P. 2011. Development of novel drugs for human African trypanosomiasis. *Future Microbiology*, 6(6):677-691. doi:10.2217/fmb.11.44

Büscher, P., Cecchi, G., Jamonneau, V. & Priotto, G. 2017. Human African trypanosomiasis. *The Lancet Infectious Diseases*, 390(10110):2397-2409. doi:10.1016/S0140-6736(17)31510-6.

Chakaya, J., Khan, M., Ntoumi, F., Aklillu, E., Fatima, R., Mwaba, P., … Katoto, P.D. 2021. Global tuberculosis report 2020: reflections on the global TB burden, treatment and prevention efforts. *International Journal of Infectious Diseases*, 113(1):S7-S12. doi:10.1016/j.ijid.2021.02.107

Churchyard, G., Kim, P., Shah, N.S., Rustomjee, R., Gandhi, N., Mathema, B., … Cardenas, V. 2017. What we know about tuberculosis transmission: an overview. *The Journal of Infectious Diseases*, 216(6):S629-S635. doi:10.1093/infdis/jix362

Connor, R. 1994. The impact of nagana. *Onderstepoort Journal of Veterinary Research*, 61:379-383 (1994).

De Oliveira, D.M.P., Forde, B.M., Kidd, T.J., Harris, P.N.A., Schembri, M.A., Beatson, S.A., … Walker, M.J. 2020. Antimicrobial resistance in ESKAPE pathogens. *Clinical Microbiology Reviews*, 33(3), e00181-00119. doi:10.1128/CMR.00181-19

Espert, L., Beaumelle, B. & Vergne, I. 2015. Autophagy in *Mycobacterium tuberculosis* and HIV infections. *Frontiers in Cellular and Infection Microbiology*, 5, 49. doi:10.3389/fcimb.2015.00049

Gagneux, S. 2018. Ecology and evolution of *Mycobacterium tuberculosis*. *Nature Reviews Microbiology*, 16(4):202-213.

Kiazyk, S. & Ball, T. 2017. Tuberculosis (TB): latent tuberculosis infection: An overview. *Canada Communicable Disease Report*, 43(3-4):62-66. doi:10.14745/ccdr.v43i34a01

Koch, A. & Mizrahi, V. 2018. *Mycobacterium tuberculosis*. *Trends in Microbiology*, 26(6):555-556. doi:10.1016/j.tim.2018.02.012

Luies, L. & du Preez, I. 2020. The echo of pulmonary tuberculosis: mechanisms of clinical symptoms and other disease-induced systemic complications. *Clinical Microbiological Review,* 33(4):1-19. doi:10.1129/cmr.00036-20

Ma, Y.X., Wang, C.Y., Li, Y.Y., Li, J., Wan, Q.Q., Chen, J.H., … Niu, L.N. 2020. Considerations and caveats in combating ESKAPE pathogens against nosocomial infections. *Advanced Science (Weinh)*, 7(1):(1-43), 1901872. doi:10.1002/advs.201901872

Matovu, E., Seebeck, T., Enyaru, J.C. & Kaminsky, R. 2001. Drug resistance in *Trypanosoma brucei spp*., the causative agents of sleeping sickness in man and nagana in cattle. *Microbes and Infection*, 3(9):763-770. doi:10.1016/S1286-4579(01)01432-0

Mulani, M.S., Kamble, E.E., Kumkar, S.N., Tawre, M.S. & Pardesi, K.R. 2019. Emerging strategies to combat ESKAPE pathogens in the era of antimicrobial resistance: a review. *Frontiers in Microbiology*, 10(539): 1-24. doi:10.3389/fmicb.2019.00539

Murray, H.W., Berman, J.D., Davies, C.R. & Saravia, N.G. 2005. Advances in leishmaniasis. *The Lancet*, 366(9496):1561-1577. doi:10.1016/S0140-6736(05)67629-5

Natarajan, A., Beena, P., Devnikar, A.V. & Mali, S. 2020. A systemic review on tuberculosis. *Indian Journalof Tuberculosis*, 67(3):295-311. doi:10.1016/j.ijtb.2020.02.005

Nsubuga, J., Kato, C.D., Nanteza, A., Matovu, E. & Alibu, V.P. 2019. Plasma cytokine profiles associated with rhodesiense sleeping sickness and falciparum malaria co-infection in north eastern Uganda. *Allergy Asthma Clinical Immunology*, 15(63):1-13. doi:10.1186/s13223-019-0377-7

Pendleton, J.N., Gorman, S.P. & Gilmore, B.F. 2013. Clinical relevance of the ESKAPE pathogens. *Expert Review of Anti-infective Therapy*, 11(3):297-308. doi:10.1586/eri.13.12

Rice, L.B. 2010. Progress and challenges in implementing the research on ESKAPE pathogens. *Infection Control & Hospital Epidemiology*, 31(S1):S7-S10. doi:10.1086/655995

Russell, D.G. 2001. *Mycobacterium tuberculosis*: here today, and here tomorrow. *Nature Reviews Molecular Cell Biology*, 2(8):569-578.

Sacksteder, K.A., Protopopova, M., Barry, C.E., Andries, K. & Nacy, C.A. 2012. Discovery and development of SQ109: a new antitubercular drug with a novel mechanism of action. *Future Microbiology*, 7(7):823-837. doi:10.2217/fmb.12.56

Shaquiquzzaman, M., Verma, G., Marella, A., Akhter, M., Akhtar, W., Khan, M.F., … Alam, M.M. 2015. Piperazine scaffold: a remarkable tool in generation of diverse pharmacological agents. *European Journal of Medicinal Chemistry*, 102:487-529. doi:10.1016/j.ejmech.2015.07.026

Skyrianou, K.C., Efthimiadou, E.K., Psycharis, V., Terzis, A., Kessissoglou, D.P. & Psomas, G. 2009. Nickel-quinolones interaction. Part 1 – Nickel(II) complexes with the antibacterial drug sparfloxacin: structure and biological properties. *Journal of Inorganic Biochemistry*, 103(12):1617-1625. doi:10.1016/j.jinorgbio.2009.08.011

Steverding, D. 2017. Sleeping sickness and nagana disease caused by *Trypanosoma brucei*. In: Marcondes, C.B., ed. *Arthropodborne diseases*. Cham: Springer. pp. 277-297. doi:10.1007/978-3-319-13884-8_18

Welburn, S.C., Fèvre, E.M., Coleman, P.G., Odiit, M. & Maudlin, I. 2001. Sleeping sickness: a tale of two diseases. *Trends in Parasitology*, 17(1):19-24. doi:10.1016/S1471-4922(00)01839-0

WHO (World Health Organization). 2022. *Global tuberculosis report 2022: supplementary material*. Geneva.

CHAPTER 2 – LITERATURE REVIEW

PART 1: ESKAPE PATHOGENS

2.1 Introduction

ESKAPE pathogens are a leading cause of global nosocomial infections. These pathogens exhibit the ability to evade the bactericidal effects of antibiotics, leading to a novel paradigm of resistance, transmission, and pathogenesis (Pendleton *et al.*, 2013:297). Most ESKAPE pathogens are multidrug-resistant due to factors such as extensive drug use, improper antimicrobial use, and inadequate pharmaceuticals. Consequently, a critical demand exist for the development of novel antimicrobials, highlighting the importance of understanding the mechanisms behind bacterial resistance (Santajit & Indrawattana, 2016:1).

2.1.1 *Enterococcus faecium* (E)

E. faecium is an opportunistic, Gram-positive, anaerobic pathogen frequently observed in immunocompromised individuals. *E. faecium* and *E. faecalis* are the two most predominant species identified in nosocomial settings. They are often associated with outbreaks of bacteraemia, urinary tract infections, and endocarditis in hospitals worldwide. These outbreaks pose a consequential risk to vulnerable individuals, leading to potentially life-threatening infections and staggering substantial financial burdens on healthcare systems. The emergence of high-level resistance to multiple antibiotics, either inherent or acquired through the horizontal transfer of plasmids and transposons, further complicates the treatment of these infections. Vancomycin-resistant *E. faecium* has been identified as the most prevalent multidrug-resistant *Enterococcus* species in healthcare facilities (Ayobami *et al.*, 2020:1180).

E. faecium is nearly always resistant to β-lactam antibiotics, with total resistance to imipenem and ampicillin reaching 98.8% in 2006 in the United Kingdom (UK) and Ireland. Vancomycin-resistant *Enterococci* (VRE) first appeared in the late 1980s, and by 2002, 61% of *E. faecium* isolates in North America were resistant to vancomycin. Vancomycin resistance among *E. faecium* isolates has been less common in Europe, but a sentinel British Society for Antimicrobial Chemotherapy study of the UK and Ireland found that non-susceptibility had increased from around 20% in 2001–2002 to > 30% in 2005–

2006. Subsequently, five major forms of resistance, namely VanA–VanE, have been reported. Among these, VanA resistance is the most prevalent and involves alterations in the terminal sequence of cell wall precursors. This type of resistance confers high-level resistance to all glycopeptides, thereby reducing their binding affinity. Despite extensive endeavours to develop novel treatments for VRE bacteraemia, there has been limited progress in improving clinical outcomes. Additionally, challenges have arisen regarding issues of tolerability associated with these treatment options.

VRE isolates exhibit a genetic element known as a pathogenicity island that contains various virulence factors, including a putative enterococcal surface protein (ESP). It is expressed on the bacterial surface, and strains that carry the ESP gene are capable of forming thicker biofilms. The expression of ESP in *E. faecium* is influenced by temperature – a characteristic shared by pathogens that transition between environmental reservoirs and mammalian hosts. This feature promotes initial colonisation and facilitates the formation of biofilms, which can significantly affect the infection of medical devices commonly associated with *enterococci.* Moreover, *enterococci* have the ability to colonise both skin and inanimate surfaces, further enhancing their potential for causing infections (Pendleton *et al.*, 2013:299).

2.1.2 *Staphylococcus aureus* (S)

S. aureus is commonly found in moist areas of the skin such as the underarms and outside areas of the nostrils, and it is a distinguished wound pathogen. Two groups of the human population carry *S. aureus*. One group, named intermittent carriers, represents 60% of the population. This group possesses *S. aureus* sporadically, meaning that the strains fluctuate. The other group, called persistent carriers, comprises approximately 20% of the population. People in this group mostly carry single strains of *S. aureus* (Pendleton *et al*., 2013:299).

S. aureus is a Gram-positive bacterium that primarily grows extracellularly. It is a significant contributor to hospital mortality, causing a wide range of infections. These infections vary from skin infections to more severe conditions such as abscesses in various organs, skin and soft tissue infections, central nervous system infections, pulmonary infections, infections related to medical devices, pneumonia, osteomyelitis, endocarditis, arthritis, sepsis, chronic lung infections associated with cystic fibrosis, as well as syndromes related to exotoxins and enterotoxins, including food poisoning, scalded skin syndrome, and toxic shock syndrome. The bacterium is enveloped by a cell wall consisting of interconnected polypeptides and poly-

saccharides. Surface proteins of *S. aureus* have long been recognised for their ability to adhere to human tissues (Tigabu & Getaneh, 2021:1540).

S. aureus is implicated in both acute and chronic infections and holds the distinction of being the first microorganism observed to develop biofilms. *S. aureus* biofilm formed on the endocardial pacemaker of a 56-year-old man in 1982 and was found to be the cause of persistent bacteraemia despite numerous antibiotic regimens. Since then, it has come to be known that *S. aureus* biofilms are a major contributor to persistent infection after the implantation of medical implants such as arteriovenous shunts, mechanical heart valves, and orthopaedic devices (Pendleton *et al.*, 2013:299).

About 25% of *S. aureus* isolates produce the exotoxin TSST-1, which can cause toxic shock syndrome and gastroenteritis. Fewer than 5% of *S. aureus* strains express Panton–Valentine leukocidin, a pore-forming exotoxin that causes severe necrotic haemorrhagic pneumonia. However, Panton–Valentine leukocidin is involved in the majority of community-acquired methicillin-resistant *S. aureus* (MRSA) infections globally. Furthermore, the carotenoid pigment staphyloxanthin found in *S. aureus* contains an innate immuno-evasive mechanism. Staphyloxanthin is an antioxidant that works as a virulence factor, sequestering the reactive-oxygen species used by neutrophils and promoting cell survival. It also contributes to the distinctive golden yellow hue of *S. aureus* colonies (Pendleton *et al.*, 2013:299).

The first clinical reports of methicillin resistance date back to the 1960s, but extensive media coverage over the past 10 years has increased public awareness of so-called superbugs, of which MRSA is currently the most prominent. Any *S. aureus* strain that has gained resistance to β-lactam antibiotics, which include all penicillins, cephalosporins, and carbapenems, is known as MRSA (Pendleton *et al.*, 2013:299). Furthermore, *S. aureus* exhibits a notable ability to develop resistance to a wide range of antimicrobial drugs, including tetracycline, aminoglycosides, macrolides, penicillins, and methicillin. The emergence of MRSA can be attributed to the extensive use of methicillin and other semisynthetic penicillins in the late 1960s. MRSA continues to be prevalent in both community and healthcare settings to this day (Tigabu & Getaneh, 2021:1540).

MecA expression, which encodes a low-affinity penicillin-binding protein, is the cause of this resistance. Currently, MRSA makes up over 25% of *S. aureus* isolates in more than a third of European Union nations, with certain regions reporting prevalence levels of over 50%. Vancomycin and teicoplanin are frequently used as first-line treatments for MRSA infections around the world; however, this intense selection

pressure has caused the expected appearance of vancomycin-intermediate and vancomycin-resistant *S. aureus* (Pendleton *et al.*, 2013:299).

2.1.3 *Klebsiella pneumoniae* (K)

K. pneumoniae is a Gram-negative bacterium commonly present in the environment, such as water and soil, as well as on the mucous surfaces of animals. In humans, it is primarily found in the gastrointestinal system and to a lesser extent in the nasopharynx. When it enters the bloodstream or other organs, it can cause infections. In the pre-antibiotic era, *K. pneumoniae* was a major cause of community-acquired pneumonia, particularly among individuals with diabetes and alcoholism. With the advent of antibiotics, *K. pneumoniae* has become a significant contributor to healthcare-associated infections in hospitals and a risk factor for severe community-acquired illnesses (Wang *et al.*, 2020:1).

K. pneumoniae is a growing pathogenic danger because of its widespread distribution in hospitals and among the public. *Klebsiella* spp. cause between 4.7% and 6.0% of bacteraemia in the UK (Livermore *et al.*, 2008:ii41),with the most frequent cases observed in the young, elderly, or immunocompromised individuals. *K. pneumoniae* is innately virulent and capable of intrusive infection due to its fimbrial adhesins and thick capsule, which serves as an assumed antiphagocytic factor (Pendleton *et al.*, 2013:300). Additionally, over the past 10 years, *K. pneumoniae* has acquired a wide variety of β-lactamase enzymes that are able to hydrolyse the β-lactam ring common in penicillins, cephalosporins, and even carbapenems (Pendleton *et al.*, 2013:300). *K. pneumoniae* is notorious for the accumulation and quick spread of multidrug-resistant determinants.

Carbapenem-resistant *K. pneumoniae* poses a significant challenge for clinicians, especially in the USA, where *K. pneumoniae* carbapenemase — a broad-spectrum Class A, serine carbapenemase, capable of interspecies dissemination — has been met with limited treatment options, resulting in numerous large-scale epidemics (Pendleton *et al*., 2013:300). Traditionally, carbapenems are reserved for the most difficult Gram-negative infections. The global emergence of the New Delhi metallo-β-lactamase-1 super-enzyme in *K. pneumoniae* has led to an increased prevalence of carbapenem-resistance and could foretell the clinical redundancy of β-lactams (Pendleton *et al.*, 2013:300).

Adopting rigorous infection control methods has been demonstrated to prevent the spread of carbapenem-resistant *K. pneumoniae*, which may help to end these outbreaks. Since the development of

an extended-spectrum β-lactamase alone is regarded as an independent predictor of higher mortality (Schwaber & Carmeli, 2007:913), extended hospital admission, and a delay in the commencement of effective antibiotic therapy, the clinical impact of carbapenemase-mediated multidrug resistance is quite concerning (Pendleton *et al.*, 2013:300).

2.1.4 *Acinetobacter baumannii* (A)

A. baumannii is an opportunistic pathogen mostly found in surgical wards and ICUs, where widespread antibiotic use has allowed for the selection of resistance to every known antibacterialagent (Pendleton *et al.*, 2013:300). This bacterium is recognised for its environmental persistence, living for up to five months on inert surfaces (Kramer *et al.*, 2006:3). Through a widening of the periplasmic gap and subsequent thickening of the cell wall, *Acinetobacter* spp. Exhibit greater resistance to dry circumstances than other Gram-negative bacteria (Pendleton *et al.*, 2013:300). *A. baumannii* is well adapted to surviving in both human and environmental vectors since it can thrive in a variety of temperatures and pH and nutritional levels (Vila *et al.*, 2007:1210). This accounts for its increased nosocomial cross-contamination rates (Pendleton *et al.*, 2013:300). Additionally, *A. baumannii* has a cytotoxin called Omp38, an outer membrane protein, which causes apoptosis in epithelial cells by localising in mitochondria and starting the release of cytochrome C and apoptosis-inducing factor (Choi *et al.*, 2005:1278).

A. baumannii is innately resistant to antibiotics due to the defence provided by a Gram-negative outer membrane, constitutively expressed active efflux pump systems, and the low quantity expression of small-aperture outer membrane porins. The permeability of antimicrobials is drastically decreased by the synergistic interaction of these innate characteristics (Vila *et al.*, 2007:1210). Similar to VRE, multiresistant *A. baumannii* strains have an island of resistance that contains a collection of genes that code for antibiotics resistance and heavy metals, as well as tiny multidrug efflux pumps that confer resistance to ammonium-based disinfectants. Epidemic strains of bacteria have been found to possess open reading frames for all recognised families and superfamilies of efflux pumps acquired from other species. These strains also harbour a resistance island, further contributing to their ability to withstand antimicrobial treatments (Pendleton *et al.*, 2013:300).

Oftentimes, *A. baumannii* is a pioneer in the discovery of new β-lactamases. *A. baumannii* isolates contained the first imipenem metallo-β-lactamase and oxacillinase serine carbapenemases, both of which are carbapenemases. There are 102 known sequences of oxacillinase carbapenemases, the great majority

of which have been isolated from *A. baumannii* to date. Some isolates have acquired universal resistance to all known antimicrobials, including imipenem and colistin, as a result of the widespread acquisition of extended-spectrum β-lactamases (Pendleton *et al.*, 2013:301). *A. baumannii* is a paradigm of pathogenicity due to its intrinsic virulence and multiple resistance factors. The lack of candidate drugs in late-stage development for treating multidrug-resistant *Acinetobacter* infections represents the mismatch between the current clinical demand for novel antimicrobials and the supply of the pharmaceutical industry (Boucher *et al.*, 2009:7).

2.1.5 *Pseudomonas aeruginosa* (P)

P. aeruginosa is a Gram-negative, rod-shaped, facultative anaerobic bacterium that can survive in micro-aerobic environments such as the thick mucus produced by cystic fibrosis lung patients. *P. aeruginosa* is known to break down a variety of chemical compounds for sustenance, including hydrocarbons such as petroleum and jet fuel. This ability to adapt to a variety of nutritional conditions allows it to live in harsh conditions, including benzalkonium chloride solutions (Pendleton *et al.*, 2013:301). Unsurprisingly, the prevalence of *P. aeruginosa* compromises the hospital setting and is a major contributor to nosocomial infections. As an opportunistic pathogen that preferentially colonises immunocompromised individuals, *P. aeruginosa* is frequently linked to cystic fibrosis, cancer patients, and burn victims (Pendleton *et al.*, 2013:301).

Through the OprF outer membrane porin, which is required for the passage of most foreign chemicals, the Gram-negative outer membrane of *P. aeruginosa* enforces an exclusion limit of 500 Da. By losing OprD, another outer membrane porin, permeability is further decreased. *P. aeruginosa* is intrinsically resistant to a variety of antimicrobials because of the decreased permeability of the outer membrane (Pendleton *et al.*, 2013:301). The absence of this transmembrane channel, which carbapenems primarily employ to obtain cytoplasmic access, is linked to imipenem resistance and diminished susceptibility to meropenem (Livermore, 2002:635). OprD and MexEF-OprN, an efflux pump system, are co-regulated, which worsens the situation and leads to highly impermeable mutants with elevated efflux. In addition to sulphonamides, β-lactams, cephalosporins, fluoroquinolones, and macrolides, the upregulation of the single efflux pump system MexAB-OprM also adversely affects meropenem, chloramphenicol, tetracycline, and trimethoprim, as well as a variety of other colours and detergents (Livermore, 2002:634).

2.1.6 Enterobacter species

The genus *Enterobacter*, a member of the *Enterobacteriaceae* family, is primarily associated with healthcare-related infections. *Enterobacter* is a genus of Gram-negative, rod-shaped bacteria that are facultatively anaerobic. *Enterobacter* species are characterised by their ability to ferment lactose, possession of flagella for motility, positive reaction to the urease test, and inability to form spores. Currently, there are 22 different types of *Enterobacter*. However, not all species are known to cause illness in humans. *Enterobacte*r species are responsible for various nosocomial infections and, less frequently, community-acquired diseases, including osteomyelitis, endocarditis, lung infections, soft tissue infections, and urinary tract infections. While some *Enterobacter* species are found on human skin surfaces, water, certain foods, soil, and sewage, other species are part of the natural microbial population in the gastro-intestinal system of mammals.

Enterobacter bacteria have developed resistance to numerous antibiotics, rendering many previously effective drugs ineffective. Carbapenem-resistant *Enterobacteriaceae* is classified as a critical priority in the urgent need for the development of new antibiotics. The World Health Organization (WHO) included carbapenem-resistant *Enterobacteriaceae* in its list of antibiotic-resistant bacteria published in 2017, highlighting the pressing need for effective treatment options against these drug-resistant strains (Ramirez & Giron, 2022). *E. aerogenes, E. cloacae*, and *E. hormaechei* are the most commonly isolated species of *Enterobacter* in clinical infections. These bacteria have shown a remarkable ability to adapt to antimicrobial agents and act as opportunistic pathogens. They are frequently identified in infections among immunocompromised patients and those admitted to ICU (Davin-Regli *et al.*, 2019:2).

With plasmid-encoded extended-spectrum β-lactamases and carbapenemases such as *K. pneumoniae* carbapenemase, Verona integron-encoded metallo-β-lactamase, oxacillinase, and even metallo-β-lactamase-1, *Enterobacter* spp. are known to cause bloodstream infections and are increasingly associated with serious nosocomial infections. These bacteria commonly infect the urinary and respiratory tracts. As with many other ESKAPE pathogens, only a small number of antimicrobials, including colistin and tigecycline, are effective against these resistant organisms, and there are few, if any, drugs in the pipeline capable of effectively addressing this escalating health crisis (Pendleton *et al.*, 2013:301).

2.2 Mechanisms of drug resistance

In response to the detrimental effects of antibiotics, bacteria employ defence mechanisms as a means of survival. Over time, these defence mechanisms can lead to the loss of antibiotic efficacy in inhibiting bacterial growth. In general, there are four kinds of mechanisms that help ESKAPE pathogens become resistant to antibiotics. These are discussed in the subsections that follow.

2.2.1 Inactivation/alteration of antibiotics

The development of enzymes that permanently degrade or neutralise antibiotics is one of the most frequent antimicrobial resistance mechanisms used by ESKAPE bacteria. Such enzymes, which are more common in Gram-negative pathogens, include those that break down the antibiotic (such as when β-lactamases hydrolyse the β-lactam ring) or covalently modify important drug structural components to prevent bacterial target site interaction (such as aminoglycoside-modifying enzymes that catalyse hydroxyl/amino group modifications) (De Oliveira *et al.*, 2020:8).

2.2.2 Modifications to the target site

Modifying the antibiotic target site to lower the affinity or prevent the antibiotic molecule from binding is another frequent antimicrobial resistance tactic used by the ESKAPE bacteria. These processes include modification of the target enzyme, modification of the ribosome target site, and modification of the cell wall precursor (De Oliveira *et al.*, 2020:11).

2.2.3 Decreased antibiotic accumulation and penetration

Outer membrane protein channels and bacterial efflux pumps reduce antibiotic accumulation and penetration, leading to antibiotic resistance.

2.2.3.1 Porins

Additionally, among Gram-negative ESKAPE pathogens, mutations that result in the loss of function, and/ or downregulation of the outer membrane protein channels (porins) play a significant role as antimicrobial resistance mediators. Particularly affected are hydrophilic drugs that depend on porins to permeate the outer membrane barrier, such as β-lactams (including carbapenems) and several fluoroquinolones. These changes can also occur during treatment (De Oliveira *et al*., 2020:14). They are crucial because they

increase the effectiveness of other resistance mechanisms such efflux pumps and drug target modification (Miller *et al.*, 2014:1).

2.2.3.2 Efflux pumps

Antimicrobial resistance is also significantly influenced by the development of bacterial efflux pumps, which actively extrude medicines out of the cell. Efflux pump genes can be found on chromosomes or inside mobile genetic elements. The resistance-nodulation division, major facilitator superfamily, multidrug and toxic compound extrusion, small multidrug resistance, adenosine-triphosphate-binding cassette, and proteobacterial antimicrobial compound efflux families are the six major families of efflux pumps that have been characterised to date (De Oliveira *et al.*, 2020:14).

2.2.4 Additional mechanisms and survival techniques

In addition to the drug resistance mechanisms mentioned above, microbes have also evolved survival strategies, including forming biofilms to hinder antimicrobial action, exhibiting antibiotic tolerance and resistance, and thriving within host cells.

2.2.4.1 Biofilms

It is now understood that development in biofilms can further obstruct antimicrobial activity in addition to the aforementioned classic antimicrobial resistance pathways. The extracellular matrix-encased, surface-attached microbial communities known as biofilms show a considerably better resilience to antimicrobial treatments than non-adherent planktonic cells by providing an additional barrier that drug(s) need to cross before reaching their target (De Oliveira *et al.*, 2020:15).

2.2.4.2 Antibiotic tolerance and persistence

There is growing evidence that some ESKAPE isolates can resist treatment through antibiotic tolerance in addition to antibiotic resistance, which is characterised by the existence of inheritable resistance-encoding genes or mutations that result in a higher minimal inhibitory concentration (MIC). A complete bacterial population may resist brief exposures to large dosages of bactericidal antibiotics (such as β-lactams and fluoroquinolones) due to antibiotic tolerance, which prevents the MIC from changing (Balaban *et al.*, 2019:442). This happens when there are no genetic resistance factors present, and it is

often accompanied by a halted (or dormant) growth condition that is reverted when antibiotic exposure is stopped. Genetically altered organisms may be more tolerant to antibiotics, although adverse environmental circumstances such as nutritional deficiency, host characteristics, temperature, and antibiotic use may also contribute to this trait (De Oliveira *et al.*, 2020:15).

2.2.4.3 Intracellular survival

The finding that some ESKAPE pathogen species can be internalised and then persist for lengthy durations inside host cells suggests another potential cause for antimicrobial resistance among these diseases (De Oliveira *et al.*, 2020:16).

PART 2: HUMAN AFRICAN TRYPANOSOMIASIS/SLEEPING SICKNESS

2.3 Introduction

HAT, also known as sleeping sickness, is a disease caused by *T. b.* parasites (Franco *et al.*, 2014:257), specifically *T.b. gambiense* or *T.b. rhodesiense*. Approximately 95% of HAT cases are attributed to *T.b. gambiense* (Kennedy & Rodgers, 2019:1). The *gambiense* form is a chronic form of this disease that occurs in both western and Central Africa. People are the main reservoir in the transmission of this disease (Franco *et al.*, 2014:257). *T.b. rhodesiense* causes HAT in southern and eastern Africa. It infects mainly animals and in some cases humans (Brun *et al.*, 2010:148).

HAT develops clinically in two stages. During the first stage, often known as the early stage, parasites live in the lymphatic system and bloodstream (haemolymphatic stage). A late or second stage begins when the trypanosomes pass the blood-brain barrier and enter the central nervous system (meningoencephalitic stage), followed by increasing neurological damage. Penetration of the trypanosomes over the blood-brain barrier happens actively (Brun *et al.*, 2010:150). HAT can be fatal if left untreated (Jamonneau *et al.*, 2012:1). Individuals gradually deteriorate into a state of severe organ failure, coma, and eventually pass away (Franco *et al.*, 2014:258).

The two kinds of HAT have different clinical presentations. Both kinds have similar indications and symptoms overall, but they differ in terms of their frequency, seriousness, and kinetic appearance (Franco *et al.*, 2014:258). *T.b. rhodesiense* causes acute HAT disease, which typically results in mortality within six

months (Odiit *et al.*, 1997). The *gambiense* form of HAT is characterised by a more chronic progression and typically lasts for an average duration of approximately three years (Checchi *et al.*, 2008:8). In both forms of the disease, the clinical signs and symptoms are non-specific and can vary among individuals and geographical areas. The primary symptoms of the first stage include intermittent fever, headache, itching, skin problems, swollen lymph nodes, weakness, fatigue, anaemia, heart abnormalities, hormonal disturbances, muscle and joint pain, and enlargement of the liver and spleen. The second stage is characterised by neuropsychiatric symptoms, including sleep disturbances. Differentiating between the stages based on clinical features can be challenging because many symptoms overlap. Neuropsychiatric issues and other fever-related disorders may sometimes be misdiagnosed (WHO, 2013a:103).

2.4 Epidemiology

Trypanosomes are transmitted by the blood-sucking tsetse fly (Diptera, genus *Glossina*). *T.b. gambiense* can potentially be passed from parent to foetus. Other transmission methods, such as sexual contact, lab mishaps, blood transfusions, and organ donation, are theoretically possible but not well understood (Büscher *et al.*, 2017:1).

Devastating epidemics that spread across western African nations in the early twentieth century, including Uganda, the Congo Free State (now the Democratic Republic of the Congo), Cameroon and others, were likely brought on by ecological disruptions and forcible population movements brought on by colonialism (Büscher *et al.*, 2017:1). Since then, there has been a direct correlation between the level of control efforts and the extent of *T. brucei* transmission. Changes in land use, human migration and climate significantly reduced tsetse fly populations and halted *T. brucei* transmission in some endemic regions (Courtin *et al.*, 2008:335). Because of societal or political unrest, HAT will inevitably return if it is neglected constantly (Büscher *et al.*, 2017:1).

In 2015, the WHO received reports of 2 804 cases of HAT. Among these cases, 2 733 (or 90% of cases) were attributed to *T.b. gambiense*, while 71 (10% of cases) were caused by *T.b. rhodesiense* (Büscher *et al.*, 2017:1). It is noteworthy that these cases were identified in both endemic and non-endemic countries, highlighting the widespread nature of the disease. The Democratic Republic of the Congo continues to have the highest case load of *T.b. gambiense* illness (86% of cases), followed by the Central African Republic, and Chad (5% and 2%, respectively). These were the only nations reporting more than 50 cases annually as of 2015. However, while evaluating stated incidence, it is important to consider the likely

underdetection of HAT cases. For instance, the reported and real incidence of disease may differ significantly in South Sudan experiencing civil instability and Guinea experiencing an Ebola virus disease outbreak. These challenges regarding detection and reporting of cases can be due to limited infrastructure, displacement of populations, limited accessibility to remote areas, and disruption of efforts to report incidences during periods of civil unrest. Eighty-two percent of the cases of *T.b. rhodesiense* disease are localised in Malawi and Uganda (Büscher *et al.*, 2017:1).

HAT is distinguished by a markedly focused distribution, whereas AAT, or nagana, is common in all tsetse-infested locations. This uneven distribution is the result of intricate, poorly understood interactions between the parasite, vector, host, and environment. The disease is typically prevalent in rural settings where the tsetse fly vector can thrive and there is a high frequency of human–tsetse contact. Additional affected are peri-urban areas, particularly those where riverine tsetse species have adapted to habitation (Büscher *et al.*, 2017:2). While farming, fishing, hunting, gathering water or wood, or while taking part in any other activity that exposes them to a tsetse fly bite, people can become sick. Both sexes and all age groups are at risk, while the prevalence is higher in adults. The distribution of risky activities differs by gender, such as the predominately male activities of hunting and fishing or the predominately female activities of fetching water and small-crop farming (Büscher *et al.*, 2017:2).

The primary reservoirs of *T.b. rhodesiense* and *T.b. gambiense* are believed to be humans and domestic animals, and wild animals, respectively. Although *T.b. gambiense* can also be found in domestic and wild animals, its epidemiological significance is still unknown (Njiokou *et al.*, 2010:61).

HAT cases have been documented across five continents (Simarro *et al.*, 2012:45), with *T.b. rhodesiense* disease being the most common type in travellers who have visited Tanzania's national parks and game reserves, as well as those in Kenya, Malawi, Uganda, Zambia, and Zimbabwe. Rarer *T.b. gambiense* disease cases include long-term expats, exiles, and migrants (Büscher *et al.*, 2017:2). *T.b. gambiense* disease should be taken into consideration in the differential diagnosis in everyone who has ever resided in an area where the disease is endemic because extremely lengthy intervals (up to 30 years, and potentially more) can exist between infection and diagnosis (Sudarshi *et al.*, 2014:2).

2.5 Transmission of HAT

The transmission of HAT in any given area is determined by three key factors. Firstly, the mammalian reservoirs of parasites, which can include humans or animals, play a crucial role and can also be the hosts that are affected by their interactions with the environment through behaviour. Secondly, Glossina or tsetse flies act as cyclical transmission vectors, relying entirely on environmental conditions. Lastly, the trypanosome itself, the parasite responsible for HAT, is a central component of the transmission process (Franco *et al.*, 2014:258).

2.5.1 The trypanosome (*T. b.*)

Protozoa of the genus *Trypanosoma* hemoflagellates are responsible for HAT (Franco *et al.*, 2014:258). There are other trypanosome species (WHO, 2013a), but only two subspecies of the *T.b.* group, namely *T.b. gambiense* and *T.b. rhodesiense*, cause sleeping sickness (Franco *et al.*, 2014:258). *T.b. brucei*, the third member of the group, is utilised frequently in experimental models of HAT despite not being harmful to humans; however, it parasitises domestic (Bovidae, Suidae, and Canidae) and wild animals (Franco *et al.*,2014:258). Although trypanosomes are extracellular parasites that can be distinguished from one another under the microscope, the two subspecies harmful to humans are morphologically similar. Therefore, other methods of distinguishing might be necessary (WHO, 2013a:42).

The parasites travel to the midgut as bloodstream trypomastigote develops after they enter the Glossina. Even though tsetse flies are vulnerable to infection by trypanosome, the population of parasites in the midgut can be reduced by a factor of 1 000 after three to five days, rendering the infection unsustainable at this stage (Oberle *et al.*, 2010:1). Nevertheless, some trypomastigote forms may arrive in the insect's midgut to differentiate into procyclic forms, which replicate *in situ* and pass the peritrophic membrane to reach the proventriculus, where they become mesocyclic trypomastigotes and eventually epimastigote forms (Rotureau & Van Den Abbeele, 2013:4).

Thereafter, they move to the salivary gland via the oesophagus and hypopharynx, where they can multiply and some of them change into contagious metacyclic forms. This process is called metacyclogenesis (Dyer *et al.*, 2013:193). The parasite population significantly decreases during this transition from the midgut to the salivary glands. The variable surface glycoprotein coat that the parasite needs to survive on the host is present in the metacyclic form, which is the only stage that can infect vertebrates. Once infected, a tsetse

fly is contagious for the remainder of its life. The entire cycle in the vector lasts 18–35 days. However, it has been found in laboratory settings that the majority of trypanosomes ingested by flies do not mature, and about 2–5% of the parasites develop to the metacyclic forms (Franco *et al.*, 2014:259).

During a tsetse fly's blood meal (initial byte), metacyclic forms (parasites) are injected subdermally into the mammalian host. They multiply at the injection site and change into long, thin forms when the draining lymph nodes carry them to the systemic organs, where they reproduce (Kennedy, 2019:2334). The bloodstream of infected individuals can harbour two distinct forms of the parasite *T. brucei*. Firstly, there is the proliferative, long, slender bloodstream trypomastigote form, which is well-suited for survival in the mammalian bloodstream. Secondly, the non-proliferative, short, stumpy bloodstream trypomastigote form is present, which is specialised for differentiating into the replicative procyclic form in the tsetse fly. The coexistence of these two forms in the bloodstream is crucial for the parasite's ability to persist in the mammalian host and ensure transmission through the tsetse fly vector (MacGregor& Matthews, 2010:866). Additionally, there are transitory intermediate forms that fall in between the slender and stumpy forms (MacGregor & Matthews, 2010:866). The bloodstream forms can initially only pass through the blood and lymph systems, whereas it can infiltrate the brain parenchyma and cerebrospinal fluid (CSF) in later stages (Brun *et al.*, 2010:149).

Although trypanosome sexual reproduction is not required, it can happen in salivary glands, opening the possibility of genetic exchange and the quick transmission of vital traits such as virulence and drug resistance (Peacock *et al.*, 2011:3671). Compared with *T.b. gambiense, T.b. rhodesiense* exhibits relatively frequent genetic exchange (Franco *et al.*, 2014:259).

2.5.2 The human/host/reservoir in the transmission cycle

In the two types of HAT, the roles of human and animal reservoirs are different. *Rhodesiense* HAT is a zoonotic illness that mostly affects animals (livestock and game), with people serving as incidental hosts. *Gambiense* HAT is an anthroponotic disease with a minor role for animal reservoirs (Franco *et al.*, 2014: 261). The main epidemiological reservoir of *T.b. gambiense* is commonly thought to be humans (WHO, 1998:39). The protracted duration of human infection with an extended paucisymptomatic interval is thought to be adequate to establish a human-fly-human transmission cycle, despite the tsetse fly's comparatively poor competence as a vector for *T.b. gambiense* and parasitemia in humans being generally low (Franco *et al.*, 2014:261).

Although humans rarely participate in the *T.b. rhodesiense* transmission cycle due to their limited reservoir capacity, non-human reservoirs predominantly facilitate transmission for this pathogen as indicated by WHO (2013a:5-6). The typical cycle involves animal-to-tsetse fly transmission to animals, while occasionally, transmission occurs from animals to human through tsetse flies. Human-to-human transmission via tsetse flies is considered very unlikely.

2.6 Signs and symptoms

The *T. b.i* subspecies, host reaction, and disease stage all affect how HAT presents clinically (Büscher *et al.*, 2017:4). Different parasite strains are said to differ in virulence and pathogenicity (Büscher *et al.*, 2017:4). Both disease types typically result in death if left untreated, yet healthy carriers of *T.b. gambiense* illness and self-cure have been reported (Jamonneau *et al.*, 2012:1). Despite having a significant level of inter-individual variability, the chronic, progressive nature of *T.b. gambiense* disease has a mean estimated duration of three years (Checchi *et al.*, 2008:7-9). Both kinds of the disease have non-specific clinical indications and symptoms that differ between persons and foci. The primary signs and symptoms of the first stage include intermittent fever, headache, pruritus and other dermatologic issues, lympha-denopathies, weakness, asthenia, anaemia, heart abnormalities, endocrine disturbances, musculoskeletal aches, and hepatosplenomegaly. The second stage is characterised by neuropsychiatric signs and symptoms, including sleep problems (WHO, 2013a:103). Daytime somnolence, sudden intense desires to sleep, and nocturnal sleeplessness are the hallmarks of the sleep condition that gives rise to the moniker sleeping sickness (Buguet *et al.*, 2001:147). The frequency and severity of neuropsychiatric symptoms rise as the disease progresses (Blum *et al.*, 2006:62). However, as the majority of the symptoms in both stages overlap, it is difficult to distinguish the stages based solely on clinical criteria but neurological problems, especially sleep disorders, are distinctive of the second stage (Büscher *et al.*, 2017:4). Regular re-evaluation is necessary as new clinical evidence is incorporated (Sahlas *et al.*, 2002:752). Neuropsychiatric issues have been misdiagnosed and *T.b. gambiense* have frequently been misdiagnosed as malaria (Simarro *et al.*, 2012:44).

2.7 Treatment

Unfortunately, since the re-emergence of HAT in the 1980s, there has been little to no new treatment options (Legros *et al.*, 2002:437). Existing drugs for the treatment of the condition are either in limited supply, exhibit significant toxicity, or face challenges due to the emergence of drug-resistant parasites

(Legros *et al.*, 2002:438). The likelihood of a successful treatment and cure for HAT improves with early detection and treatment. The causal agent and disease stage determine the appropriate course of treatment. In most cases, second-stage disease cannot be cured by first-stage medications (pentamidine and suramin). Similarly, using second-stage medications (nifurtimox, eflornithine, and melarsoprol) to treat first-stage disease is not ideal. This is because second-stage treatments must be capable of penetrating the blood-brain barrier and are more difficult to administer compared to first-stage medications (Büscher *et al.*, 2017:6). For example, melarsoprol, an arsenic-based compound must also be delivered intravenously, and regrettably, it has a very narrow therapeutic range. Moreover, its significant toxicity necessitates slow administration over a minimum period of ten days (Álvarez-Rodríguez *et al.*, 2022:09).

See **Figure 2.1** for the structures of the first- and second-stage drugs against HAT.

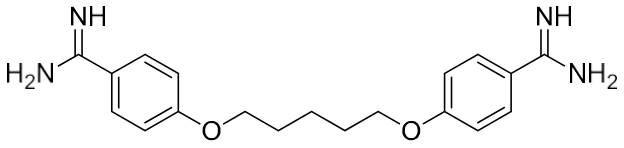

pentamidine

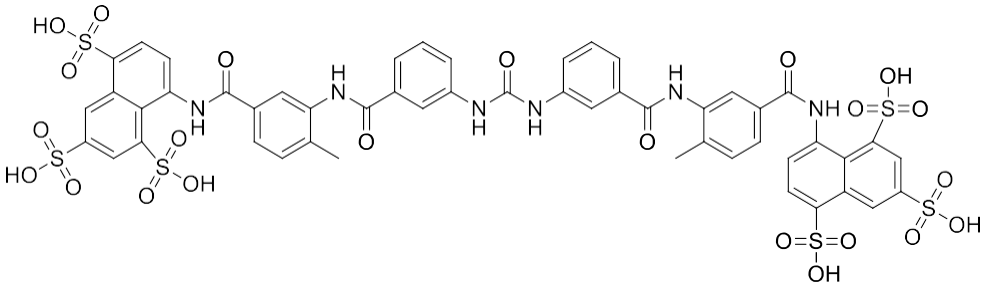

suramin

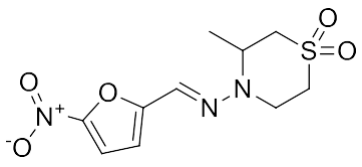

nifurtimox

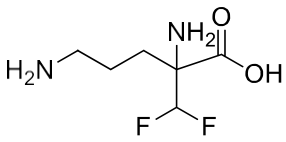

eflornithine

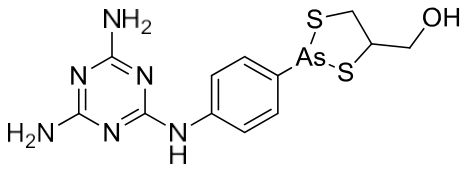

melarsoprol

Figure 2.1: Structures of pentamidine, suramin, nifurtimox, eflornithine, and melarsoprol (Source: own)

2.7.1 First-stage drugs

The first-stage drugs include pentamidine and suramin. Pentamidine is a drug mainly used for *T.b. gambiense* HAT since 1940 **(Figure 2.1)**. The current suggested dosage is 7–10 intramuscular injections of 4 mg/kg administered once daily (Legros *et al.*, 2002:438). Pentamidine isethionate is a first-line treatment for *T.b. gambiense* disease and an alternative for *T.b. rhodesiense* sickness, albeit there is less evidence for its effectiveness in the latter situation (Büscher *et al.*, 2017:6). Pentamidine is typically administered intramuscularly in endemic nations. To avoid the consequences of hypoglycaemia, administration should be preceded by the consumption of sugar (10–20 g), and it should be followed by 1–2 hours of rest in the supine posture. Pain and temporary swelling are side effects of the intramuscular injection (Büscher *et al.*, 2017:6). Hypoglycaemia, hypotension, stomach pain, and digestive issues are some other negative side effects (Pohlig *et al.*, 2016:14).

Suramin has only been used to treat early-stage *T.b. rhodesiense* HAT **(Figure 2.1)** since the early 1920s. The standard regimen is gradual intravenous injections of 5 mg/kg on day 1, 10 mg/kg on day 3, and 20 mg/kg on days 5, 11, and 30. There have been numerous reports of serious adverse effects, including cases of renal failure, severe skin responses, and anaphylactic shock (Legros et al., 2002:438).

2.7.2 Second-stage drugs

The second-stage drugs include nifurtimox, eflornithine, and melarsoprol (Legros *et al.*, 2002:438).

Nifurtimox-eflornithine combination therapy (NECT) is the first-line treatment for second-stage *T.b. gambiense* illness **(Figure 2.1)**. NECT was added to the WHO Essential Medicines List in 2009. NECT has better safety benefits, less severe side effects, has higher cure rates (95-98%), and it is thought to prevent the parasite from developing medication resistance compared with melarsoprol or eflornithine

monotherapy (Priotto *et al.*, 2009:56). NECT consists of the intravenous administration of eflornithine and oral administration of nifurtimox. NECT is simpler to give than eflornithine monotherapy, requiring only 14 infusions as opposed to 56, which lowers expenses and demands fewer hospital resources. Even though eflornithine has a short half-life and theoretically needs four daily infusions to maintain a trypanostatic effect, infusions every 12 hours are quite successful when used in conjunction with oral nifurtimox (Büscher *et al.*, 2017:7).

Melarsoprol is an organo-arsenical substance that has been used for both types of HAT since 1949 **(Figure 2.1)**. The most typical treatment regimen entails three to four series of intravenous injections (one intravenous injection per day), interspersed by resting intervals. Melarsoprol is a medication known to possess significant hazards. One of the most severe adverse reactions linked to this drug is reactive encephalopathic syndrome, which occurs in approximately 5–10% of cases. This syndrome has an average case fatality rate of 50%, indicating its life-threatening nature. Prednisolone and melarsoprol are frequently provided together in order to avoid the development of this condition (Legros *et al.*, 2002:438).

2.7.3 Treatments used in combination

Combination therapies delay resistance development. In addition, these interventions have the potential to enhance the efficacy of HAT treatment and, when used together, may enable a reduction in drug dosage and potentially decrease drug toxicity (Legros *et al.*, 2002:439). However, only a few combinations have been compassionately used in humans, and our understanding of the effectiveness and safety of these regimens is insufficient to suggest their regular usage. Between 1983 and 1992, 616 patients in the former Zaire received treatment for early-stage *T.b. gambiense* with a pentamidine and suramin combination; nonetheless, the cure rate did not improve and 46 patients relapsed eventually (Pepin & Khonde, 1996:183). After numerous unsuccessful treatments with melarsoprol and oral eflornithine for late-stage *T.b. gambiense* infection, one patient reportedly recovered entirely in Equatorial Guinea in 1996 (Simarro & Asumu, 1996:16). Therapeutic combinations of suramin with eflornithine, and suramin with metronidazole have been attempted with some efficacy, albeit in very small case series, for late-stage *T.b. rhodesiense* infection (Legros *et al.*, 2002:439).

2.7.4 Drugs currently in development

Treating HAT is challenging due to the restricted availability of effective trypanocidal drugs, their potential toxicity, complicated administration methods, and the growing occurrence of treatment failures. This predicament underscores the need for intensified research and development efforts aimed at creating new protocols, including combination treatments, in the short term. Additionally, clinical development of promising compounds is essential to ensure the availability of new drugs in the long term (Legros *et al.*, 2002:439). Currently, only two treatment choices exist for *rhodesiense* HAT patients. Suramin is employed for early-stage infections, while the treatment of the meningoencephalitic stage relies on the highly toxic arsenic-based melarsoprol regimen. Consequently, even though *T. b. rhodesiense* is not the primary cause of HAT, further research is essential to enhance treatment options (Álvarez-Rodríguez *et al*., 2022:09).

There are several promising new drugs under development or undergoing testing for the treatment of late-stage HAT. One such drug is fexinidazole (see **Figure 2.2**), a nitroimidazole medication, which has garnered significant attention recently (Kennedy & Rodgers, 2019:8). In a recent phase 2/3 randomised non-inferiority trial, oral fexinidazole demonstrated successful treatment outcomes in 91% of patients with late-stage *T.b. gambiense* HAT in the Democratic Republic of Congo and the Central African Republic at the 18-month assessment. This success rate was comparable to the 98% treatment success rate achieved with standard NECT. Both treatment groups also experienced similar side effects related to the treatment (Mesu *et al.*, 2018:144).

Recognising the need for a simplified treatment approach that eliminates the need for extensive parasitological investigations, the development of a novel oral therapy was pursued. A medication called acoziborole (SCYX-7158) (see **Figure 2.2**), which is a unique boron-containing therapeutic candidate, was included in the Drugs for Neglected Diseases Initiative (DNDi) lead optimisation programme in 2007. Collaboration between DNDi, Anacor, SCYNEXIS, and the Swiss Tropical and Public Health Institute contributed to the development of acoziborole as a potential solution for the treatment of HAT (Tarral *et al.*, 2023:482).

A first-in-human study was conducted in 2012 to evaluate the efficacy and safety of acoziborole. The study was prompted by the excellent *in vitro* activity of acoziborole against *T. brucei* spp., its favourable physico-chemical properties, and promising toxicokinetics, indicating a potential long half-life in humans (Tarral *et al.*, 2023:482). In the trial, healthy male participants of sub-Saharan origin were administered acoziborole

at doses up to 1 200 mg, which demonstrated an outstanding safety profile unrelated to the dosage. Acoziborole exhibited significant and sustained exposure in both plasma and CSF when administered as a single oral dose to fasting patients. The preclinical efficacy studies supported the potential effectiveness of acoziborole in treating HAT patients, and the prolonged exposure observed further supports these findings. Acoziborole represents a promising single-dose oral medication for this potentially life-threatening condition (Tarral *et al.*, 2023:490).

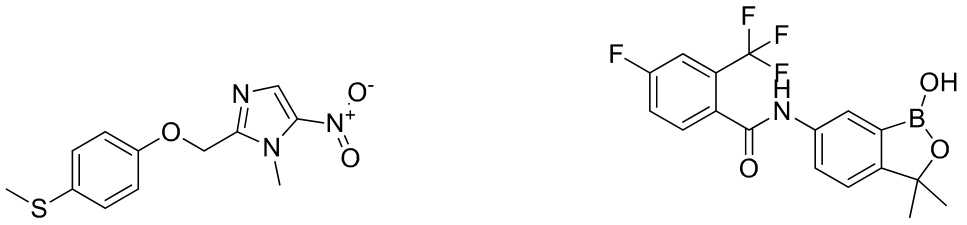

fexinidazole acoziborole

Figure 2.2: Structures of new antitrypanosomal drugs in development (Source: own)

The current treatments for HAT encounter substantial obstacles, encompassing limited drug options, toxicities, intricate administration, and rising instances of treatment failures, with varying effectiveness dependent on HAT type and stage. However, there is optimism in the development of novel medications like fexinidazole and acoziborole, which offer potential advantages such as enhanced treatment success rates and simplified administration procedures. These emerging drugs represent a crucial response to the shortcomings of existing treatments, fostering optimism for more effective and accessible HAT therapy. As research and development endeavours advance, they not only aim to enhance treatment outcomes but also to secure the availability of safer and more efficient drugs in the long run, addressing the disease's challenges and mitigating the limitations of current medications.

HAT, in conclusion, is a deadly disease caused by *T.b.* parasites, primarily *T.b. gambiense* and *T.b. rhodesiense*, with the former being more chronic and widespread. HAT progresses through two stages, with neurological damage in the second stage if left untreated. Diagnosis and differentiation of stages can be challenging due to overlapping symptoms. HAT is transmitted by tsetse flies, and while efforts to control the disease have shown success, it can resurge if neglected. Treatment options have limitations, but promising drugs like fexinidazole and acoziborole offer hope for improved efficacy and accessibility in the battle against this devastating disease.

PART 3: AFRICAN ANIMAL TRYPANOSOMIASIS/NAGANA

2.8 Introduction

T.b. brucei can cause severe and often fatal disease in domestic animals. However, it typically causes only minor infections in wild animals. The progression of the disease varies across different domestic animal species. Cattle and pigs generally exhibit a mild course of the disease. In sheep and goats, the severity is moderate. However, horses, donkeys, and dogs are more susceptible to experiencing severe forms of the disease (Marcondes, 2017:287).

2.9 Symptoms and clinical presentation

Signs and symptoms of the illness in animals affected by *T.b. brucei* include fever, lethargy, weight loss, reduced milk production, hair loss, discharge from the eyes, swelling (oedema), anaemia, and paralysis (Büscher, 2013:192). As the disease advances, affected animals gradually lose their ability to perform labour, becoming increasingly weak. The name of the disease, *n'gana*, originates from the Zulu word meaning helpless or worthless, reflecting the debilitated state of the affected animals (Marcondes, 2017:288).

2.10 Treatment

Only three medications, namely quinapyramine, diminazene, and isometamidium, are available for the treatment and prevention of nagana (see **Figure 2.3**). These medications were created and made available between 1950 and 1961.

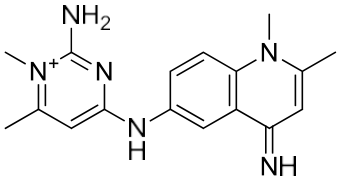

quinapyramine

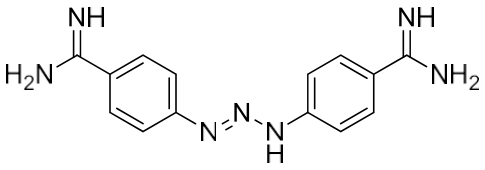

diminazene

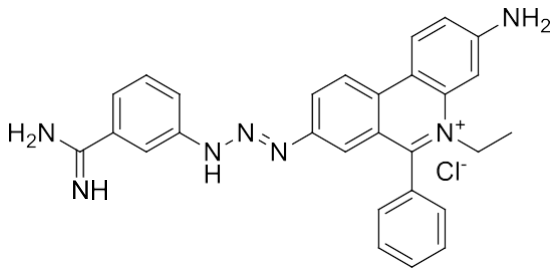

isometamidium

Figure 2.3: Structures of antitrypanosomal drugs used in nagana (Source: own)

Quinapyramine was initially effective in treating nagana in pigs, sheep, goats, and cattle. However, in the 1970s, quinapyramine was taken off the market in several regions of Africa due to the emergence of drug-resistant parasites. Quinapyramine is now mostly used preventively in pigs to avoid *T.b. brucei* infections (Marcondes, 2017:293).

Diminazene, like pentamidine, belongs to the class of aromatic diamidines (Venturelli *et al*., 2022:12). It is primarily utilised in the treatment of bovine trypanosomiasis due to its relatively low toxicity to cattle. In addition to its use in the treatment of bovine trypanosomiasis, diminazene is also employed in the treatment of *T.b. brucei* infection in dogs. A phenanthrinium derivative called isometamidium is effective in treating *T.b. brucei* infections in horses. The medications have both therapeutic and preventative uses (Marcondes, 2017:293).

2.11 Aetiology, transmission, and geographical distribution

More than 80% of AAT affecting domesticated animals (cattle, goats, sheep, horses, pigs, and dogs) in southern, East, and Central Africa is caused by *T. congolense*, which continues to be one of the leading causes of AAT in livestock, even in western Africa (Magez & Radwanska, 2014:243). Intermittent fever, abortion, cachexia, anaemia, lymphadenopathy, lethargy, anorexia, oedema, ocular discharge, and mortality are among the atypical clinical symptoms of *T. congolense* infection in animals (Calvet *et al.*, 2020:2).

Three further varieties of *T. congolense* have been identified, namely *savannah, forest,* and *Kilifi* (Magez & Radwanska, 2014:244). In the sub-Saharan African savannah ecosystem, *T. congolense* strains of the *savannah* type are thought to be the most pathogenic and virulent (Bengaly *et al.*, 2002:1). *T. congolense Kilifi* appears to be more restricted to East Africa and to a lesser extent to southern Africa, whereas

T. congolense forest occurs in humid forest environments of West, Central, and East Africa (Magez & Radwanska, 2014:244). Despite individuals of the *Glossina* species cyclically transmitting *T. congolense,* mechanical transmission by other haematophagous arthropods *(T. evansi)* has also been documented (Desquesnes & Dia, 2004:9). The latter is crucial since *T. congolense* may still cause AAT in areas where tsetse flies are not present but other biting flies are (Magez & Radwanska, 2014:244).

Mild pathogenic *T. congolense* parasites circulate in endemic regions where animals serve as the primary reservoir of infection, leading to more chronic AAT and a typically low impact of the illness. However, *T. congolense* AAT epidemics could have serious effects (higher animal deaths and lower calving rates), particularly in the wake of recent livestock introductions to tsetse-infested areas, which often happen along livestock/wildlife interface zones. Tsetse flies or other haematophagous flies spread highly virulent *T. congolense* strains from wildlife reservoirs to domestic animals in these circumstances (Magez & Radwanska, 2014:244).

In sub-Saharan Africa, *T. vivax* is the second most significant cause of nagana in ruminants, including horses and pigs. AAT caused by *T. vivax* is typically less severe than AAT brought on by *T. congolense*. Most AAT cases in West Africa are caused by *T. vivax*. In Latin America, *T. vivax* is also frequently reported to be the cause of trypanosomiasis, which primarily affects ruminants (Galiza *et al.*, 2011:359-360).

The most widespread trypanosome species in Africa is *T.b. brucei*, which is transmitted cyclically by tsetse flies. This parasite has the ability to affect a wide range of domesticated mammals, including ruminants (such as cattle), horses, and dogs. *T.b. brucei* infection, as well as the human-infective *T.b. rhodesiense*, can cause acute fulminant disease in horses and dogs (Magez & Radwanska, 2014:244). *T.b. brucei* and *T.b. rhodesiense* are generally considered to have a low pathogenicity in ruminants and are not typically associated with severe disease manifestations in these animals. However, it is important to note that while they may exhibit low pathogenicity in ruminants, they can still cause significant health issues in other mammalian species, including humans. Ruminants are thought to be domestic reservoirs for this particular trypanosome subspecies (Fèvre *et al.*, 2001:625). However, pigs, and to a lesser extent sheep and goats, are implicated as domestic animal reservoirs in West and Central Africa (Magez & Radwanska, 2014:244).

In the tsetse-infested sub-Saharan Africa, *T. simiae* (subgenus *Nannomonas*) causes an acute deadly disease that mostly affects pigs and, to a lesser degree, camels, and sheep. Despite the possibility that the

aforementioned trypanosome species and subspecies will result in monolytic infections in particular domestic animals, co-infections with two or more distinct trypanosome species and/or subspecies are regularly documented in the field (Magez & Radwanska, 2014:244).

Understanding AAT is of paramount importance due to its significant impact on livestock, wildlife, and even human populations in sub-Saharan Africa. AAT, caused by various *Trypanosoma* species, can lead to severe economic losses in agriculture, particularly affecting cattle, sheep, goats, horses, and pigs. This disease results in reduced productivity, weight loss, and even death among infected animals, affecting food security and livelihoods. Furthermore, AAT has complex transmission dynamics involving tsetse flies and other vectors, making control efforts challenging. Comprehensive knowledge of AAT, its causative agents, clinical presentations, treatment options, and reservoir hosts is essential for designing effective strategies to combat this devastating disease, safeguarding both livestock and the communities that rely on them for sustenance and income.

PART 4: LEISHMANIASIS

2.12 Introduction

Leishmaniasis is a protozoan disease caused by *Leishmania* parasites and spread by infected sandflies. The many clinical signs of leishmaniasis depend both on the *Leishmania* species infecting the host and the host's immunological response. Depending on the kind of leishmaniasis, the infection may only affect the skin (cutaneous leishmaniasis), the mucous membranes (mucosal leishmaniasis), or internal organs (visceral leishmaniasis). Visceral leishmaniasis is an opportunistic illness in immunocompromised individuals, especially in those with HIV infection (Choi & Lerner, 2001:175).

2.13 Epidemiology and parasite life cycle

Leishmaniasis is a disease that affects people worldwide, but it is more prevalent in the tropics and subtropics of Africa, South and Central America, the Middle East, southern Europe, and Asia. Leishmaniasis affects people in roughly 88 developing and developed nations where 350 million people live (Bessat *et al.*, 2015:1). The current incidence of cutaneous leishmaniasis is estimated to be between 700 000 and 1.2 million cases per year, with the majority (over 95%) of cases occurring in the Americas, the

Mediterranean Basin, the Middle East, and Central Asia. It is important to note that these numbers are likely underreported (Mann *et al.*, 2021:121). Visceral leishmaniasis accounts for more than 95% of the cases reported to WHO each year, and the main countries affected are Brazil, China, Ethiopia, India, Kenya, Nepal, Somalia, and Sudan. The current annual estimates for visceral leishmaniasis are fewer than 100 000, which represents a significant decrease compared with previous estimates of 400 000 cases (Mann *et al.*, 2021:121). **Figure 2.4** illustrates the geographical distribution of *Leishmania*.

Figure 2.4: Geographical distribution of Leishmaniasis (Maia & Depaquit, 2016:5)

Leishmaniasis can be roughly divided into three major clinical forms based on its signs (Murray *etal.*, 2005:1561): visceral leishmaniasis, the most severe; cutaneous leishmaniasis, the most prevalent form, and mucocutaneous leishmaniasis. The cutaneous form of leishmaniasis manifests as a papule at the site of the vector sandfly bite and affects the epidermal layer of the skin (Mann *et al.*, 2021:121-123). The papule enlarges and, after some time, develops into a crust that may ulcerate. The majority of cutaneous cases will eventually heal on their own within 2–10 months, unless they are worsened by secondary infections. The incubation time for the mucocutaneous type of the illness is one to four months. The mucocutaneous type of lesions extends from the skin to the nose, oral cavity, and pharynx and is associated with breathing and eating difficulties as well as significant mortality risks (Bessat *et al.*, 2015:1). Visceral leishmaniasis has an incubation period between three and eight months. Severe symptoms range from fever, weight loss, and skin pigmentation (kala-azar or black disease) to more serious lesions such as hepatosplenomegaly, lymphadenopathy, pancytopenia, and death (Guerin *et al.*, 2002:494).

Leishmania species have intermediate sandfly hosts and a final mammalian host as part of their life cycle. The sandfly vector acquires the *Leishmania* infection from an infected mammal's blood through macrophages carrying amastigotes during feeding. Round non-flagellated amastigotes (2–7 mm) change into elongated flagellated promastigotes (10–20 mm) once inside the midgut of an infected fly. In turn, promastigotes multiply and pass through the midgut on their way to the salivary gland and proboscis, where they change into metacyclic promastigotes. Infective metacyclic promastigotes are injected into the wound of the affected host by the infected sandfly vector when it feeds on a new host. Promastigotes are ingested by macrophages at the bite and wound sites, where they lose their flagella and transform back into amastigotes (Bessat *et al.*, 2015:2). **Figure 2.5** illustrates the life cycle of the *Leishmania* parasite.

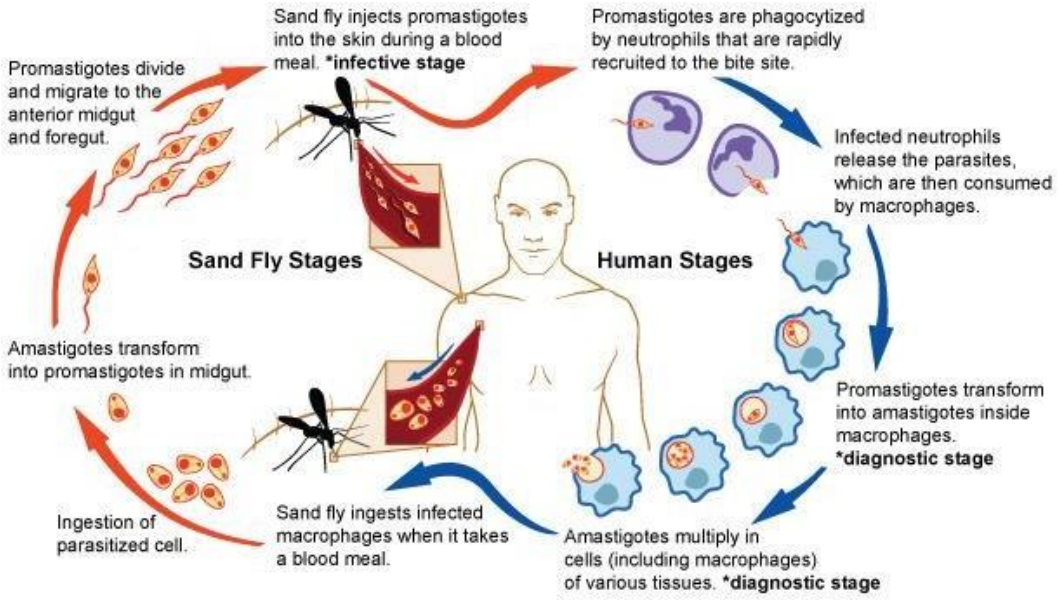

Figure 2.5: Life cycle of the *Leishmania* parasite (Bekele *et al*., 2016:50)

2.14 Diagnosis of leishmaniasis

Accurate and appropriate diagnosis of patients infected with *Leishmania* parasites is of utmost importance as the choice of treatment depends on the specific *Leishmania* species involved. Unfortunately, both cutaneous leishmaniasis and visceral leishmaniasis cases are often underreported, and there is a notable challenge in diagnosing *Leishmania* infections due to a lack of understanding among medical practitioners. Efforts should be made to enhance awareness and knowledge among healthcare professionals regarding the clinical manifestations and diagnostic techniques for different forms of leishmaniasis. Improved diagnostic tools and strategies, including laboratory tests and clinical algorithms,

are crucial for early and accurate detection of *Leishmania* infections. This will facilitate appropriate treatment selection and help mitigate the impact of this neglected tropical disease (Bessat *et al.*, 2015:2).

The majority of time, a diagnosis is made based on the disease's clinical symptoms with direct (parasite) and indirect (immunologic) confirmation, such as nodular and ulcerated skin lesions associated with a history of sandfly bites (Mann *et al.*, 2021:125). However, the diagnosis of current cases is a difficult and problematic process due to the considerable variation in the clinical presentation of leishmaniasis. A differential diagnosis must also be made against other illnesses with strikingly similar clinical spectra in the most severe instances of leishmaniasis, such as leprosy, skin malignancies, and TB for cutaneous leishmaniasis, and malaria and schistosomiasis for visceral leishmaniasis (Reithinger & Dujardin, 2007:21). The most often used approach of diagnosing visceral leishmaniasis relies on the precise detection of diagnostic stages (amastigotes) in tissue aspirate or biopsy samples taken from internal tissues and organs in settings where microscopy and technical expertise are accessible and present (Murray *et al.*, 2005:1570). Contrarily, the majority of cases of cutaneous leishmaniasis are identified through the identification of diagnostic stages in microscopic smears from skin lesions or biopsies, which are typically taken by scarping from the edge of lesions. Although quick and inexpensive in both circumstances, direct microscopic inspection has relatively limited sensitivity, especially when parasites are not plentiful such as in the case of chronic infections (Bessat *et al.*, 2015:2).

2.15 Clinical features

There are several clinical manifestations of leishmaniasis, including localised and diffused cutaneous leishmaniasis, post kala-azar dermal leishmaniasis, mucocutaneous leishmaniasis, and visceral leishmaniasis. These are discussed in detail below.

2.15.1 Localised cutaneous leishmaniasis

All continents, with the exception of Australia and Antarctica, are home to leishmaniasis in one form or another. *L. tropica* and *L. major* are the two organisms that largely cause localised cutaneous leishmaniasis (LCL), which is common across the Old World and endemic in the New World, namely Central and South America. *L. braziliensis* and *L. mexicana*, two separate parasitic species or complexes, are the cause of New World LCL (Choi & Lerner, 2001:175).

LCL typically affects exposed body regions including the face, neck, and arms that are vulnerable to sandfly bites (Mann *et al.*, 2021:123). Old World illness frequently has several primary lesions, but New World leishmaniasis frequently only has one primary lesion, namely a red papule that develops into a plaque or nodule after an average incubation period of one week to three months. The lesion frequently turns into an ulcer with a violaceous border and well-defined margin (Choi & Lerner, 2001:175).

Lymph nodes that are draining may expand and lesion biopsy smears results may show parasites (Bessat *et al.*, 2015:4). Sometimes, inflammatory satellite papules and subcutaneous induration may appear around the original lesion as a consequence to local parasite spread or its antigenic byproducts (Kubba *et al.*, 1987:304). The ulcer spontaneously regresses between one and 36 months, depending on the patient and the infecting organism, leaving a scar with either hypo- or hyperpigmentation. Although research conducted in a Saudi Arabian community indicated reinfection rates of up to 10% among individuals, it is generally believed that immunity to leishmaniasis provides complete protection (Choi & Lerner, 2001:175).

2.15.2 Diffuse cutaneous leishmaniasis

An anergic variation of LCL, namely diffuse cutaneous leishmaniasis, has diffuse lesions that resemble lepromatous leprosy. Either *L. aethiopica* or, in Central and South America, *L. amazonensis* may be the cause of the infection. The disease typically starts with a primary lesion that subsequently spreads to other skin regions. The lesions associated with leishmaniasis often manifest as non-ulcerative nodules filled with parasites, which can spread to various parts of the body such as the limbs, buttocks, and face. In contrast to lepromatous leprosy, no nerves are affected. Diffuse cutaneous leishmaniasis typically does not invade internal organs and primarily affects the skin, but it can become chronic and often exhibits partial response to treatment with a tendency for frequent relapses (Choi & Lerner, 2001:175-176).

2.15.3 Post kala-azar dermal leishmaniasis

L. donovani, which is native to East Africa and India, is the main cause of post kala-azar dermal leishmaniasis (PKDL). Up to 56% of individuals in Africa who are recovering from visceral leishmaniasis have PKDL (Zijlstra *et al.*, 1994:826). The cheekbones, chin, ears, and extensor portions of the forearms are the most common areas where the rash manifests as isolated skin-coloured or hyperpigmented papules (Mann *et al.*, 2021:125). In the majority of cases, lesions associated with PKDL tend to heal

spontaneously over a period of several months. Indian PKDL, in contrast to African PKDL, affects 20% of patients about one to two years after recovery (Choi & Lerner, 2001:176).

PKDL typically begins as little hypopigmented macules, which grow to produce big uneven patches. The majority of lesions are bilateral and symmetrical. Hair colour above the lesions remains unchanged, and although there may be some pigmentary loss, it is typically not completely absent. The next stage of development is erythematous macules, which frequently appear on the face in a malar distribution but can also appear elsewhere. Finally, hypopigmented and erythematous macules are replaced by soft, painless, non-ulcerating, yellowish-pink nodules. The hands and feet get nodules less frequently than the face, earlobes, trunk, and genitalia. PKDL cases are challenging to treat and necessitate longer-term systemic treatment (Choi & Lerner, 2001:176).

2.15.4 Mucocutaneous leishmaniasis

Unlike cutaneous leishmaniasis, mucocutaneous leishmaniasis can be life-threatening and necessitates prompt medical attention. Mucocutaneous leishmaniasis is primarily associated with *Leishmania* species of the *Viannia* subgenus, commonly found in the Americas, such as *L. (V) braziliensis*, *L. (V) amazonensis*, *L. (V) panamensis*, and *L. (V) guyanensis.* The development of mucosal disease depends on the presence of both parasite virulence and host cell-mediated immunity. The infection spreads to the mucosal tissues in approximately 1–10% of individuals in an infected population. The exact host factors that determine which patients will develop mucocutaneous leishmaniasis and which will not remain uncertain. Patients who have had cutaneous leishmaniasis may experience mucosal involvement in the form of primary lesions, typically occurring one to five years after the healing of the initial cutaneous lesion. These primary lesions can manifest as either single or multiple ulcers. It is important to note that the ulcers associated with *Leishmania* species found in the Americas are generally ulcerative, in contrast to the potentially non-ulcerative lesions associated with *Leishmania* species found in other regions (David & Craft, 2009:497).

Hematogenous or lymphatic dissemination, or possibly a direct extension of neighbouring skin lesions, are the most likely causes of mucous membrane involvement. The disease frequently starts in the nasal septum, which gets infected and inflamed before perforating. The two main medical conditions that cause death in mucocutaneous leishmaniasis patients are malnutrition and pneumonia (Choi & Lerner, 2001: 176).

2.15.5 Visceral leishmaniasis

The spread of *L. donovani* or *L. infantum* is the cause of the systemic disease kala-azar, often known as visceral leishmaniasis (Ready, 2014:148). The introduction of HIV has expanded the population of people with visceral leishmaniasis. Fever, splenomegaly, lymphadenopathy, emaciation, pancytopenia, and hyperglobulinemia are typical signs and symptoms of visceral leishmaniasis (Choi & Lerner, 2001:176). The name kala-azar, which means black fever, comes from a generalised blackening of the skin that occurs during the active phase of visceral leishmaniasis. Until addressed, it runs an elusive chronic course after a two- to eight-month incubation period (Ready, 2014:148-149). The patient is more vulnerable to several secondary infections despite the disease's association with an increase in serum immunoglobulin G and immunoglobulin M levels due to a reduction of cell-mediated immunity (Choi & Lerner, 2001:176).

2.16 Treatment

Even though there are almost 25 substances with antileishmanial properties, only a small number are considered human antileishmanial medications, of which the majority must be administered parenterally (Singh & Sivakumar, 2004:307). The sections below discuss some options.

2.16.1 Antimonials [Sb(v)]

Sb(v) continues to be the first choice treatment for all types of leishmaniasis. The most widely utilised organic antimony compounds are meglumine antimoniate and sodium antimonygluconate. Antimonials are known to block glycolytic enzymes and fatty acid oxidation in *Leishmania* amastigotes, and there is a dose-dependent decrease in the net synthesis of adenosine triphosphate and guanosine triphosphate. However, the exact mechanism of action is not entirely understood (Singh & Sivakumar, 2004:309). Pancytopenia and reversible peripheral neuropathy are side effects of antimonial treatment (Brummitt *et al.*, 1996:878). Cardiotoxicity, which can result from Sb(v) therapy and lead to sudden death, has been reported in patients who also received single courses of pentostam (20 mg/kg/day) for up to 28 days (Singh & Sivakumar, 2004:309).

2.16.2 Pentamidine

Pentamidine isethionate was tested in India for the treatment of visceral illness to get around the issue of clinical resistance to Sb(v) (Singh & Sivakumar, 2004:309). *Pneumocystis jirovecii* pneumonia was the main

condition this medication was used to treat. Pentamidine isethionate's specific mode of operation involves targeting kinetoplast DNA and interfering with DNA synthesis (David & Craft, 2009:496). In the late 1970s and early 1980s, Jha (1983:167) employed pentamidine successfully and reported a cure rate of 98.8% without any relapses. The dosage was 4 mg/kg administered three times per week for three to four weeks (10 to 12 injections). However, the success rate began to drop in the 1980s when only 75.2% of patients were healed even after 20 injections (Singh & Sivakumar, 2004:309). Myalgias, discomfort at the injection site, nausea, and headache are common side effects of the low-dose, short-course regimens for cutaneous leishmaniasis. Less often reported side effects include a metallic taste, a burning feeling, numbness, and hypotension. Two per cent of cases of hypoglycaemia were reversible. When visceral illness is treated with high-dose, long-course regimens, the incidence and severity of these adverse effects are increased (Singh & Sivakumar, 2004:309).

2.16.3 Amphotericin B and lipid-associated amphotericin B

A bacterium of the genus *Streptomyces* yielded the polyene antifungal antibiotic drug known as amphotericin B, which was first isolated in 1956 (Singh & Sivakumar, 2004:309). Amphotericin B deoxycholate, a broad-spectrum antifungal, has shown effectiveness against protozoan *Leishmania* species. When antimonial medications lost their efficacy for treating visceral leishmaniasis in India, amphotericin B deoxycholate was selected as the primary treatment option (Roatt *et al.*, 2020:8967). It binds ergosterol, which is a significant cell membrane sterol in fungi and *Leishmania* to produce holes in the parasite's membrane. However, it binds less strongly to cholesterol in human cell walls, which results in its harmful effects. Because of its known infusion-related side effects, such as fever, chills, bone pain, and, occasionally, cardiac arrest, as well as its delayed side effects, such as hypokalaemia and nephrotoxicity, amphotericin B was rarely used before 1990 (Singh & Sivakumar, 2004:310). Compared with the deoxycholate form, liposomal amphotericin B is considered to be less toxic as it primarily targets macrophages (David & Craft, 2009:496). Liposomal amphotericin B is the only drug approved by the US Food and Drug Administration (Roatt *et al.*, 2020:8967).

2.16.4 Paromomycin (aminosidine)

An aminoglycoside called paromomycin is used to treat bacterial illnesses. However, unlike other amino-glycosides, paromomycin has also been discovered to have wide antiparasitic action. Oral paromomycin is advised for the clinical management of intestinal amoebic and tapeworm infections. Paromomycin

injections, administered at doses of 14–16 mg/kg/day for up to three weeks, achieved a cure rate of 79% for visceral leishmaniasis (Chunge *et al.*, 1990:221-222). The aminoglycoside nature of paromomycin makes it potentially hazardous to the eighth cranial nerve and kidneys (Singh & Sivakumar, 2004:310). Paromomycin is available in both topical and parenteral formulations. While the topical form offers a new alternative to parenteral and intralesional treatments, it is not considered sufficient for the treatment of cutaneous leishmaniasis. However, when administered parenterally, paromomycin has been found to be equally effective as antimonials in treating cutaneous leishmaniasis (David & Craft, 2009:496).

2.16.5 Cytokines

Human recombinant interferon-γ was first used as an adjuvant to antimony therapy for visceral leishmaniasis. These researchers discovered that the combination of interferon-γ administered for 28 days might have a cure rate of 80% with Sb(v)-resistant kala-azar. An additional trial revealed that interferon-γ alone was only marginally effective. It was discovered that using interferon-γ together with Sb(v) could hasten the parasite removal process in patients who had not previously received treatment. When given the combination for 28 days instead of antimony alone, both Kenyans and Indians saw a quicker parasite removal. Contrary to initial expectations, the combination of interferon and antimony proved successful in curing nine (69%) out of 13 Indian patients with antimony-resistant visceral illness. However, two patients passed away from medication toxicity, possibly as a result of the interaction between the combination therapy and the cumulative effects of the prior therapy. Additionally, it is outrageously expensive for a poor population (Singh & Sivakumar, 2004:311).

2.16.6 Oral agents

All the aforementioned medications are administered parenterally, which has a number of drawbacks including hospitalisation or frequent hospital visits, injection cost, and the risk of spreading blood-borne illnesses including HIV and hepatitis B and C due to injections. As a result, oral therapy has a clear appeal and benefit, especially for cutaneous leishmaniasis and PKDL, which can be treated as outpatients. Only a few of the more than 20 medications that have been researched or attempted to treat leishmaniasis have been shown to be successful (Singh & Sivakumar, 2004:311), some of which are discussed below.

2.16.6.1 Allopurinol

Allopurinol, an oral medication, was initially used for the treatment of leishmaniasis. It is a hypoxanthine analogue that inhibits the purine anabolism and catabolism in both *Leishmania* parasites and mammalian cells. The underlying principle is based on the inability of *Leishmania* spp. to synthesise purines. Allopurinol is metabolised to allopurinol riboside, which is incorporated into leishmanial ribonucleic acid (RNA) instead of adenosine triphosphate. This integration disrupts the parasite's normal purine salvage pathway, leading to the impairment of protein production (Singh & Sivakumar, 2004:311).

Despite being used to treat leishmaniasis for many years, a recent placebo-controlled double-blinded experiment in Colombian patients with cutaneous leishmaniasis brought on by *L. panamensis* revealed that allopurinol (20 mg/kg/day for 28 days) was no more effective than a placebo. Allopurinol mono-therapy was found to be ineffective in treating Colombian cutaneous illness, and it is thus unlikely to be effective in treating other leishmaniasis types (Berman, 1997:689). Jha, as cited by Singh and Sivakumar (2004:311), reported its effectiveness against Indian kala-azar for the first time in 1983.

2.16.6.2 Imidazole derivatives

Numerous oral medications, including metronidazole, itraconazole, and other imidazole derivatives, have been investigated as potential antileishmanial treatments (Pradhan *et al.*, 2022:516). Even when utilised at its maximal serum levels (30 g/mL) following intravenous administration, metronidazole only completely eradicated 30% of parasites (Singh & Sivakumar, 2004:311). In terms of inhibiting the growth of most *Leishmania* strains, itraconazole has been found to be more effective than fluconazole and ketoconazole (Pradhan *et al.*, 2022:516). The sterol content of *Leishmania* species is comparable to that of yeast and other fungi according to the principle underlying the use of imidazole as an antileishmanial medication. Ketoconazole's significant impact on sterol synthesis was demonstrated even before the *Leishmania* sterol structure was defined, suggesting disruption of ergosterol production (Singh & Sivakumar, 2004:311).

2.16.6.3 Miltefosine

Miltefosine, originally developed as an antineoplastic medication, has been approved for the treatment of leishmaniasis due to its demonstrated antileishmanial properties since the 1980s. This medication exerts its effect by inducing apoptosis, leading to the death of parasites both in laboratory settings (*in*

vitro) and living organisms (*in vivo*). It achieves this by modulating cell membrane production and interfering with signalling pathways within the parasites. Regrettably, after a decade of treatment, there has been an observed increase in resistance and a decline in effectiveness, resulting in a doubling of the relapse rate. According to a clinical trial, miltefosine has shown effectiveness in treating cutaneous leishmaniasis caused by *L. panamensis* in Colombia. However, it has been found to be ineffective against cutaneous leishmaniasis caused by *L. braziliensis* in Guatemala (Roatt *et al.*, 2020:8967).

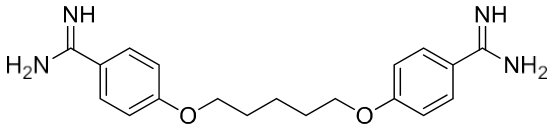

pentamidine

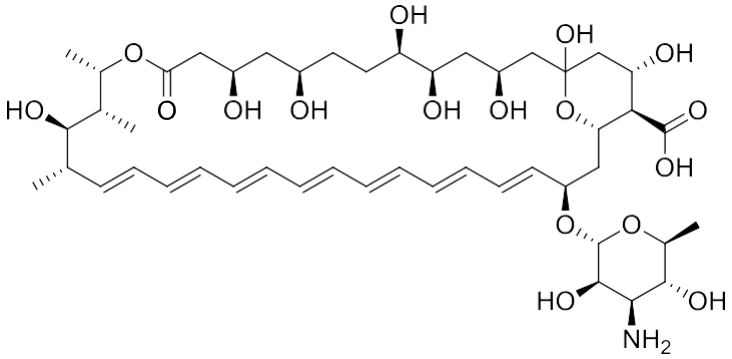

amphotericin B

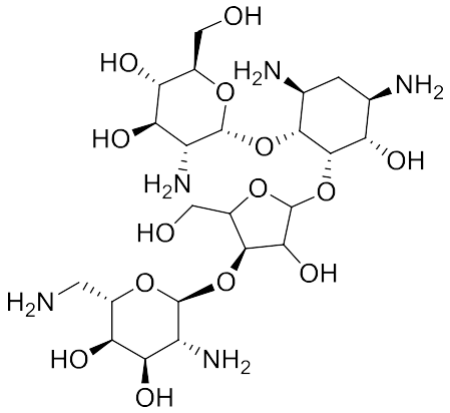

paromomycin

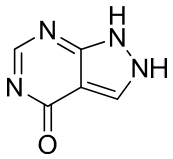

allopurinol

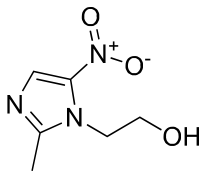

metronidazole

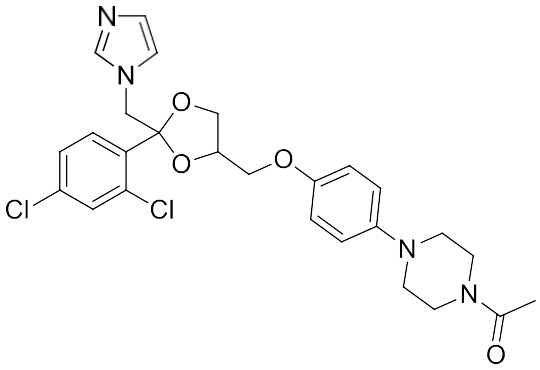

ketoconazole

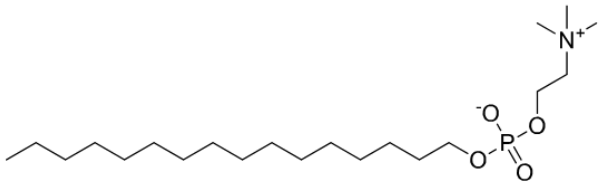

miltefosine

Figure 2.6: Structures of antileishmanial drugs (Source: own)

2.16.7 Combination therapy

With the decreasing effectiveness of most monotherapeutic regimens over time, the use of combination therapy has emerged as a promising approach for treating both cutaneous leishmaniasis and visceral leishmaniasis. This strategy has opened up new possibilities for improving treatment outcomes and combating drug resistance (Singh & Sivakumar, 2004:313). Recently, a combination therapy using sodium antimony gluconate and indolylquinoline derivative A [2-2(2”-dichloroacetamidobenzyle)-3-(39-indolylquinoline)] demonstrated 100% clearance of the parasites from hamsters’ livers and spleens, compared with 93% and 80%, respectively, when indolylquinoline derivative A and sodium antimony gluconate were used separately (Pal *et al.*, 2002:260). Similarly, 91.25% of kala-azar patients who received low-dosage pentamidine and allopurinol as a combination experienced an ultimate cure as opposed to 74.35% of patients who received pentamidine alone. When compared with topical paromomycin plus

methylbenzethonium chloride, which cure 85.7–91.4% of cases, all monotherapies for cutaneous leishmaniasis are less successful. Atovaquone, roxithromycin, and edelfosine were also tested as medications. Medications with a long half-life and low therapeutic ratio, such as miltefosine, may cause drug resistance. As a result, these medications should only be administered in conjunction with medications that have a short half-life and higher therapeutic ratio (Singh & Sivakumar, 2004:313).

Table 2.1 lists the common treatment regimens for leishmaniasis.

Table 2.1: Common treatment regimens of leishmaniasis (Bessat *et al.*, 2015:5)

Disease pattern	**Drug**	**Dose**	**Comments**
Visceral leishmaniasis	Sb(v), sodium stibogluconate or meglumine antimonate	20 mg/kg intramuscular or intravenously for 28 days, depending on species or the clinical syndrome.	Increasing resistance to antimonials is a major problem. Reducing the treatment period for 10 days course may minimise the resistance effect. The cure rate is 90% to 95%.
	Liposomal form of amphotericin B	3 mg/kg per day intravenously for 5 days plus an additional 3 mg/kg dose on the tenth day.	The preferred treatment method in southern Europe. Highly effective, less toxic and tend to be expensive, although shorter course duration may result in improving cost benefits. The cure rate is up to 98%.
	Miltefosine	2.5 mg/kg per day for 28 days.	The first effective orally active drug. It has a very good safety profile. The potential is high for using this drug in poor areas with limited health access. The cure rate ranges from 95% to 100% after 3 or 4 weeks of continuous application. Treatment outcomes vary based on age of patients.
	Pentamidine	300 mg dose as intravenous injection.	The drug use is now very limited due to its substantial toxicity.
	Paromomycin (aminosidine)	16–20 mg/kg per day intramuscularly for 21 days.	Cost saving. High potential developing nephrotoxicity or ototoxicity. Needs further evaluation. The cure rate is 93–97%.
Cutaneous leishmaniasis	Paromomycin	Two ointments per day for 10–30 days.	Mainly for *L. major* while less effective in the case of *L. tropica* lesions. The cure rate varies from 74% to 86%, and it is higher with repeated application.
	Miltefosine	2.5 mg/kg per day orally for 28 days.	In Colombia, it is used for *L. (V) panamensis*. In Guatemala, it is used for *L. (V) braziliensis* and *L. mexicana*. Also, it is a useful oral agent against cutaneous leishmaniasis due to *L. (V) panamensis* in Colombia but not against leishmaniasis due to *L. (V) braziliensis* in Guatemala. The cure rate varies: it is 91% in Colombia and 53% in Guatemala.

Disease pattern	Drug	Dose	Comments
	Pentamidine isethionate	4 mg/kg pentamidine-base.	Used to treat cutaneous leishmaniasis in France. It is highly recommended to use the minimal or lower doses of this medicine.
		Or it can be appliedthrough the intramuscular route on days 1 and 3 as 2 mg/kg every other day for 7 days.	For *L. braziliensis* the cure rate is less than 50%.
	Pentavalent antimony [Sb(v)]	Applied intralesionally as 1 mL per lesion every other day for 8–15 injections.	For *L. major* the cure rate is equal or more than 75%.
		Or used as 1 mL per lesion every other day weekly for 8–11 injections (on average).	For *L. tropica* the cure rate is equal or more than 90%.

PART 5: TUBERCULOSIS

2.17 Background

TB is one of the oldest diseases known to afflict humans and is caused by a bacterium called *M. tuberculosis*. TB continues to be a serious threat to humankind, and the poor socioeconomic segment of the population and marginalised groups in the community are particularly susceptible (Natarajan *et al.*, 2020:1-2). The rise of drug-resistant TB and the co-infection with HIV worsened the situation to the extent that WHO designated TB a worldwide emergency in 1993 (Sharma & Mohan, 2013:456).

Based on clinical manifestation, TB is separated into two types, namely pulmonary TB (PTB) and extrapulmonary TB (EPTB) (Lee, 2015:47). TB that affects organs other than the lungs, such as the pleura, lymph nodes, belly, genitourinary system, skin, joints, and bones, or meninges, is referred to as EPTB. A patient with EPTB is classified as having PTB (such as military TB) if they additionally have a tubercular lesion in their lung parenchyma (Sharma & Mohan, 2013:457). EPTB is defined as the presence of intra-thoracic mediastinal and/or hilar lymph node TB, TB pleural effusion, or both, without radiographic abnormalities in the lung (WHO, 2013b:31).

Pulmonary TB presents with gradual and non-specific symptoms such as a persistent cough with mucus, chest pain exacerbated by deep breathing, coughing up blood, difficulty breathing, weakness, significant weight loss, reduced appetite, chills, fever, night sweats, and malaise. TB is also linked to secondary

systemic complications like increased oxidative stress, low sodium levels, reduced cholesterol, glucose intolerance, blood-related problems, vitamin D deficiency, and alterations in the host's microbiota (Luies & du Preez, 2020:2). EPTB frequently presents a significant challenge for early diagnosis due to its heterogeneity of presentation. Constitutional symptoms including fever, anorexia, weight loss, malaise, and exhaustion may be present (Natarajan *et al.*, 2020:2).

The global TB outbreak in 1993 prompted the WHO to designate TB as a matter of high priority. The emergence of drug-resistant variants of *M. tuberculosis* has made the treatment of TB even more difficult and challenging. The presence of mutations and structural alterations in the genome *M. tuberculosis* can enable these bacteria to resist the drugs typically employed to suppress them. This emergence of drug resistance has added substantial complexity to the efforts to control and treat the disease, particularly in cases where the patient is also infected with the HIV virus (Khawbung *et al*., 2021:1).

2.18 Epidemiology of TB

Nearly one-third of the world's population is infected with *M. tuberculosis*, and about 10% of these cases are likely to develop to TB disease (Bhardwaj *et al.*, 2015). According to WHO estimates, approximately 10.6 million individuals worldwide would be affected by TB (EPTB and ETB) in 2021, a 4.5% increase from 10.1 million in 2020 (WHO, 2022a:2). Geographically, the regions of South-East Asia (43%), Africa (25%), and the Western Pacific (18%) had the highest proportions of TB cases. In contrast, the regions of eastern Mediterranean (8.3%), the Americas (3.0%), and Europe (2.3%) had the lowest proportions. Among the 30 countries with the highest burden of TB, eight countries including India (26%), China (8.5%), Indonesia (8.4%), the Philippines (6.0%), Pakistan (5.8%), Nigeria (4.6%), Bangladesh (3.6%), and South Africa (3.3%) accounted for 86% of all estimated incident cases worldwide (WHO, 2022b:12). Among the reported TB cases, 90% were in adults aged 15 and older. Of these adult cases, 64% were males, and 9% involved individuals who were HIV-positive, with 72% of them residing in Africa. Nearly half of the estimated 558 000 new cases of drug-resistant TB (range: 483 000–639 000) were found in three nations, namely India (24%), China (13%) and the Russian Federation (10%) (Natarajan *et al.*, 2020:3).

According to data from the Revised National Tuberculosis Control Programme, EPTB is present in 50% of HIV-positive individuals and 15–20% of HIV-negative patients in India. The distribution of EPTB could be ranked as pleural nodes (47%); pleural cavity (30%); abdominal nodes (10%); bones and joints (8%); central nervous system (2%); and others (3%) (Natarajan *et al.*, 2020:3).

There has been a 42% decrease in TB mortality between 2000 and 2017. The annual rate of TB incidence has decreased by an average of 2%, and the case fatality rate has decreased from 23% in 2000 to 16% in 2017. The annual decline rates in the incidence of TB cases and the absolute number of cases slowed down in 2020 compared with the previous year. The incidence rate decreased by 1.9% and the absolute number of cases decreased by 0.87% between 2019 and 2020, compared with 2.3% and 1.2%, respectively between 2018 and 2019. However, these rates still followed the downward trends observed since 2000 (Natarajan *et al.*, 2020:3). Between 2020 and 2021, the main drivers of the global increase in TB cases were India, Indonesia, and the Philippines, where TB incidence collectively rose by approximately 0.4 million cases. This aligns with their significant roles in reducing the reported number of newly diagnosed TB cases worldwide in both 2020 and 2021. Globally, it's estimated that the TB incidence rate decreased by 30% from 2000 to 2020.The cumulative decrease in TB incidence per 100 000 people from 2015 to 2021 was 10%, which was only halfway to the first milestone target set by the End TB Strategy (WHO, 2022a:2). Multidrug-resistant tuberculosis (MDR-TB) and, more recently, extensively drug-resistant tuberculosis, pose a danger to the worldwide TB control programme (Natarajan *et al.*, 2020:3).

Drug-resistant TB, encompassing MDR-TB and extensively drug-resistant TB, is recognized as a significant impediment to the global eradication of TB. When combined with HIV infection, drug-resistant TB poses an even more complex challenge and is a potential menace that is difficult to manage. There have been documented cases indicating unfavourable treatment outcomes and alarmingly elevated mortality rates among individuals who are both living with HIV and coinfected drug-resistant TB (Singh *et al*., 2020:9). This underscores the urgent need for innovative approaches and improved strategies to address the growing problem of drug-resistant TB, especially in the context of HIV coinfection.

2.19 Pathogenesis of *M. tuberculosis*

TB is an airborne disease as the infectious bacilli are transmitted through inhalation of droplets in the atmosphere. Alveolar macrophages in the lung phagocytose the bacterium (Jordao & Vieira, 2011:2). The generation of chemokines and cytokines, which act as infection signals, is caused by interactions between *Mycobacterium* components and macrophage receptors such as toll-like receptors (Means *et al.*, 1999: 3920). These signals cause dendritic cells and macrophages produced from monocytes to move from the bloodstream to the site of infection in the lung. Following maturation, dendritic cells, which have taken up pathogens, migrate to the lymph nodes. Thereafter, the CD4 and CD8 T-lymphocytes are prepared to

recognise mycobacterial antigens. In response to mediators released by infected cells, primed T-cells grow and go back to the lung infection site. A granuloma, the TB hallmark, is formed as a result of this characteristic of cell migration toward the infection site. T-cells, macrophages, B-cells, dendritic cells, endothelium and epithelial cells, among others, contribute to the formation of the granuloma in proportions that change with age. This granuloma creates an immunological milieu that makes it easier for macrophages and T-cells to interact as well as preventing the dissemination of bacilli that are resident in macrophages. However, over a lengthy period of time, the granuloma also serves as a home for *M. tuberculosis*. If the cytokine balance is disrupted, the dormant bacilli may later become active, reactivating the disease (Jordao & Vieira, 2011:2).

When a person is exposed to the tubercle bacilli in the air from someone with active PTB, only a small number of the bacilli reach the alveoli of the lungs and cause *M. tuberculosis* infection. Once inside the alveoli, the *M. tuberculosis* bacteria are quickly engulfed by specialised alveolar macrophages, which are highly efficient in phagocytosis. The innate immune response triggered by the macrophages helps in the destruction of the invading bacteria (Urdahl *et al.*, 2011:289-291). If the bacilli manage to get past this first line of defence, they begin multiplying actively in macrophages and spread to neighbouring cells such as epithelial and endothelial cells, building up a significant bacterial burden in a matter of weeks through exponential growth (Natarajan *et al.*, 2020:3).

M. tuberculosis can spread to other organs during these early stages of infection via the lymphatic system and by haematogenous dispersion, where it can infect more cells (Natarajan *et al.*, 2020:3). Neutrophils, lymphocytes, and other immune cells move to the site of the primary infection after the adaptive immune response has begun, forming a cellular infiltration that later takes on the typical structure of a granuloma (Ottenhoff & Kaufmann, 2012:3).

The granuloma is covered in fibrotic components as it hardens and becomes calcified, keeping the bacilli enclosed and safeguarded by the host immune response (Delogu *et al.*, 2013). When a calcified granuloma, also known as Ghon's focus or lesion, coexists with a calcified or infected lymph node, this combination is referred to as a Ghon or Ranke complex. Typically, this complex doesn't exhibit noticeable clinical symptoms and is commonly found in the lower lung lobes, positioned just beneath the pleural surface (Luies & du Preez, 2020:6). The Ghon's complex, was once considered to be the haven of *M. tuberculosis* during latent infection, with bacilli remaining there for years, decades or, most frequently,

patients' whole lives. In this case, active disease would result if, during latent infection, for unknown reasons, bacilli started reproducing inside this initial lesion. That reactivation of TB arose from this same initial site of infection was a significant corollary of this idea with substantial pathophysiology and clinical implications (Delogu *et al.*, 2013).

2.20 Transmission of *M. tuberculosis*

Patients with active PTB are the main source of infection of this contagious disease. When these patients cough, they release small particles called droplet nuclei that contain *M. tuberculosis*. These droplet nuclei have a diameter of 1–5 µM and can remain suspended in the air for a significant period of time (Ahmad, 2011:3). These tiny respiratory droplets containing bacteria travel into the respiratory tract. Here, most of the bacteria are captured by goblet cells that produce mucus, which serves as a protective mechanism to block the entry of foreign substances and remove them. However, in some cases, these droplets can bypass this initial defence system, reaching the upper, well-ventilated regions of the lungs. When this happens, the body's second-line or innate immune defences come into play. Alveolar macrophages are activated and work to engulf the invading bacteria, attempting to destroy them through the use of proteolytic enzymes and cytokines. This response triggers the transfer of T lymphocytes to the infection site, initiating a cell-mediated immune response. This response can lead to either the elimination of the infecting organism or the formation of granulomas. A granuloma is a recognizable pathological feature commonly associated with PTB. It can be described as a disorganized cluster of immune cells, including macrophages, monocytes, neutrophils, natural killer cells, and others, working together to contain the spread of the microbe (Luies & du Preez, 2020:2).

The risk of contracting an infection depends on various factors, including the infectiousness of the source, the proximity of the contact to the infected individual, the number of bacilli inhaled, and the immune system of the potential host (Ahmad, 2011:3).

In summary, the host's immune system is vital in controlling TB infection. A robust and well-coordinated immune response is required to prevent the bacteria from causing active disease. However, in cases where the immune response is compromised, as in immunosuppressed individuals, the risk of TB reactivation or progression to active disease increases significantly. Understanding the immune response to TB is crucial for developing effective vaccines and treatments.

2.21 Clinical manifestations

TB can affect various parts of the body, not just the lungs. The specific location of the TB infection determines the symptoms experienced. In the case of PTB, which primarily affects the lungs, common symptoms include a persistent cough, chest pain, coughing up blood (haemoptysis), weakness or fatigue, weight loss, fever, and night sweats. However, when TB affects other organs such as the brain, intestines, kidneys, or spine, the symptoms may differ based on the specific site of infection (Zaman, 2010:111).

EPTB can affect the larynx, lymph nodes, pleura, gastrointestinal tract, genitourinary tract, central nervous system, or bones and is caused by hematogenous dissemination or direct extension from nearby organs. With the exception of laryngeal TB, the majority of extrapulmonary diseases are not communicable. Chest radiographs may not reveal any indication of TB. Extrapulmonary illness is more likely to affect young children and those with impaired immune systems. Miliary TB is a haematogenously distributed illness that causes a variety of small lesions that range in size from 1 mm to 3 mm and can affect many organs including the lungs, liver, spleen, and central nervous system (Nachiappan *et al.*, 2017:54).

2.22 Treatment of active TB

By the beginning of the 1950s, streptomycin had been combined with para-aminosalicylic acid, and eventually isoniazid (INH) to create the first efficient three-drug regimen. The success was adequate but not tremendous, the length was typically 18 months, and toxicity was frequent. Over the following 10 years, the compounds pyrazinamide (PZA), ethionamide, cycloserine, and ethambutol were identified as TB drugs. However, rifampicin (RIF) was the game-changer (Fox *et al.*, 1999:237-239; Mitchison, 2000: 796-799). When added to INH-containing regimens, RIF halved the time needed to cure TB to nine months. The 'short-course' era began with the addition of PZA to INH and RIF, which allowed for the treatment of drug-sensitive TB in just six months. The current treatment plan, known as RIPE, consists of RIF, INH, PZA, and ethambutol for two months (Peloquin & Davies, 2021).

In the event that the patient responds to treatment and there is no higher risk for treatment failure, RIPE decreases to RI (RIF and INH) for an additional four months - totalling to six months. Patients who are severely underweight, have extensive cavitary lung lesions, and have bone or central nervous system disorders often need treatment exceeding six months. While clinicians await susceptibility data on the slowly expanding *M. tuberculosis*, ethambutol is added to safeguard RIF. Approximately 1 in 10 (10%)

M. tuberculosis isolates in the US are currently INH-resistant, and 9 in 10 (90%) are RIF-resistant, while the prevalence varies by country (Peloquin & Davies, 2021).

When the isolate is resistant to both INH and RIF (so-called MDR-TB), the course of treatment becomes significantly more challenging. Extensive drug-resistant TB is characterised by further resistance to fluoroquinolone and at least one of three second-line drugs (Peloquin & Davies, 2021). Drug-resistant TB poses a significant global health threat, perpetuating the ongoing TB epidemic and raising TB-related illness and death rates worldwide. When TB treatment is not completed or is insufficient, it can result in the development of antimicrobial resistance (Tiberi *et al*., 2022: S20).

The second-line anti-TB medications para-aminosalicylic acid, ethionamide, and cycloserine were used for many years in various combinations with whichever other drugs showed *in vitro* susceptibility and/or had not been used in a particular patient before. This method is known as an individual, or optimised, MDR-TB regimen, and it typically consists of five to seven medications. These regimens typically last 18 to 24 months (Peloquin & Davies, 2021).

2.22.1 First-line TB treatment

Isoniazid (INH)

The mode of action of INH makes it effective against *M. tuberculosis*. Upon passive diffusion of INH into *M. tuberculosis*, a catalase peroxidase enzyme called KatG activates the prodrug by forming an INH-NAD+ adduct. This activated form of INH inhibits essential enzymes involved in mycolic acid synthesis and cell wall formation, leading to the bacterium's demise. Since its identification, INH has continued to be used as a first-line antibiotic in conjunction with RIF, ethionamide, and PZA for treating TB (Erwin *et al.*, 2019:4).

Rifampicin (RIF)

RIF inhibits transcription by attaching to the beta subunit of the mycobacterial DNA-dependent RNA polymerase enzyme (Friedman *et al.*, 2020). RIF is approximately 70% bioavailable. The hepatic organic anion transporter, SLCO1B1, is involved in the complicated absorption of RIF (Peloquin & Davies, 2021). As the most significant TB-sterilising medication, RIF has a modest early bacterial activity but significantly lowers the bacillary population to avoid relapse. RIF-free regimens generally have lower cure rates and have to be used for a longer time (typically 12 to 18 months). The main characteristic of RIF is its capacity to operate against what are known as non-replicating persisters (Friedman *et al.*, 2020).

Pyrazinamide (PZA)

PZA is a prodrug that is converted to pyrazinoic acid by human and mycobacterial amidases. Protonated pyrazinoic acid builds up in *M. tuberculosis* and disrupts a number of critical cellular functions. The *pncA* gene mutation is mostly linked to resistance. Testing for PZA phenotypic and genotypic resistance can be difficult. PZA is typically used at a dose of 25 mg/kg once day, which is less than the 35 mg/kg amount examined by the British Medical Research Council. When intermittent therapy is required, a dose of 50–70 mg/kg three times a week may be administered (Peloquin & Davies, 2021). Plasma-like concentrations can be found in the CSF (Peloquin & Davies, 2021). PZA does not accumulate in alveolar macrophages but does so significantly in epithelial lining fluid (Friedman *et al.*, 2020). PZA does reasonably penetrate pulmonary lesions (Peloquin & Davies, 2021).

Ethambutol

Ethambutol's D-isomer inhibits mycobacterial arabinosyltransferases, which results in the depletion of arabinogalactan and lipoarabinomannan, and consequently inhibition of cell wall formation. The oral bioavailability of ethambutol is about 80%. Roughly 70% of the substance is eliminated unchanged in the urine, and renal function affects this process. The concentrations in CSF are typically less than 1 mcg/mL, or 50%, of the concentrations in plasma. Ethambutol does not build up in the fluid of the epithelial lining but rather concentrates heavily in pulmonary lesions and alveolar macrophages. The early bacterial activity of ethambutol is moderate (Peloquin & Davies, 2021). The present first-line usage of ethambutol aims to stop the establishment of RIF resistance. Ethambutol is dosed at 15–25 mg/kg each day or 50 mg/kg three times per week. Both C_{max}/MIC and area under the curve (AUC)/MIC are used to predict the effectiveness of ethambutol (Märtson *et al.*, 2021:26).

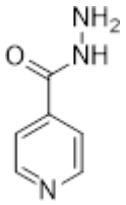

isoniazid

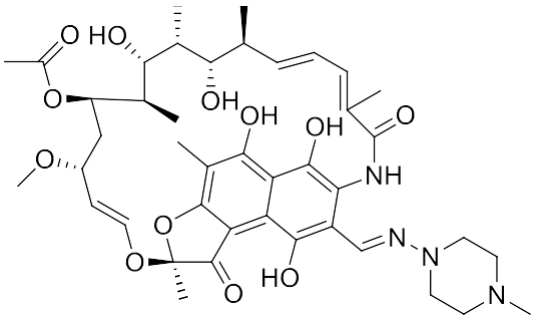

rifampicin

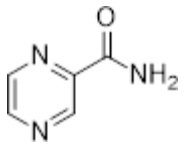

pyrazinamide

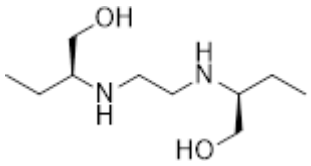

ethambutol

Figure 2.7: Structures of first-line TB drugs (Source: own)

2.22.2 Second-line TB treatment

As shown in **Table 2.2**, Falzon *et al*. (2017:6) divided these drugs in four groups for the treatment of RIF-resistant TB and MDR-TB. The classification of medications used in the treatment of MDR-TB and XDR-TB has been updated based on discussions by the Guideline Development Group and the latest evidence reviews regarding their effectiveness and safety. These medications, which constitute the essential second-line components of extended MDR-TB regimens, are now categorized into four groups: A, B, C, and D. Group D is further divided into three subgroups: first-line anti-TB medicines (D1), bedaquiline and delamanid (D2), and other agents with uncertain roles in MDR-TB treatment (D3) (Falzon *et al*., 2017:5).

Table 2.2: Second-line treatment of MDR-TB and RIF-resistant TB (Falzon *et al.*, 2017:6)

Step	Medicine	
	Group	**Options**
Fluoroquinolones	A	Levofloxacin Moxifloxacin Gatifloxacin
Second-line injectables	B	Amikacin Capreomycin Kanamycin (Streptomycin)
Second-line agents	C	Ethionamide/prothionamide Cycloserine/terizidone Linezolid Clofazimine
Pyrazinamide + first-line agent	D1	Pyrazinamide Ethambutol High-dose isoniazid
+ Bedaquiline or Delamanid	D2	Bedaquiline Delamanid

Step	Medicine	
	Group	Options
Add if regimen cannot be composed	D3	p-aminosalicylic acid Imipenem-cilastatin Meropenem Amoxicillin-clavulanate (Thioacetazone)

2.22.3 Treatment of latent TB infection

Latent TB refers to a state in which the immune system shows recognition of *M. tuberculosis* through skin or blood tests, but no symptoms or signs of active disease are present. In this situation, it is believed that the host's immune system has confined or controlled the bacteria, and there are likely fewer than 1000 live bacilli remaining in the body. Importantly, individuals with latent TB infection do not pose an infection risk to others since they lack active pulmonary lesions (Peloquin & Davies, 2021).

After using 300 mg INH per day for six months, the benefits were noticeable, increased after nine months, and nearly reached their peak after 12 months (Comstock, 1999:847). The recommended length of time for INH use is nine months. The challenges arise from the fact that INH is not the most effective medication for the task — it is not regarded as a powerful 'sterilising' medicine, and it bears a risk of drug-induced liver impairment. As a result, better and more efficient alternatives to INH are being investigated. The most effective sterilising medication is RIF, which works by getting rid of persisters and preventing post-treatment recurrence in individuals with active TB disease. RIF should be the treatment of choice for latent TB infection to the extent that the physiological state of a latent TB bacillus mimics the physiological condition of a persister TB bacillus (Peloquin & Davies, 2021). RIF given at a dose of 600 mg daily for four months is quite successful (Sterling *et al.*, 2020:1202).

Combination therapy has also proven successful in latent TB infection treatment. Some nations employ three months of daily INH combined with RIF, which is now recommended in the US. An alternative is INH combined with rifapentine, which is also known as cyclopentyl-rifampin. In people with HIV, a more recent variation that involves daily INH and rifapentine for one month has been researched. Undoubtedly, a one-month course of treatment is shorter in duration (from nine months to four, to three down to one month). Other treatments, such as fluoroquinolones or the brand-new medication bedaquiline, are being considered for latent TB infection. More research is being done on long-acting injectable dosage

formulations that would allow as little as one injection to stop TB transmission in the future (Peloquin & Davies, 2021).

Thus, ongoing research in the field of TB is needed to focus on various aspects to improve TB prevention, diagnosis, and treatment. Some of the key areas of ongoing research and prospects for TB include, drug development, treatment shortening, and health systems strengthening. These research efforts aim to advance our understanding of TB and ultimately reduce its global burden. Collaboration between scientists, healthcare professionals, policymakers, and affected communities is essential to drive progress in TB research and control.

PART 6: COMPOUND CLASSES OF INTEREST

2.23 Quinazolines

Quinazoline is a heterocyclic ring system that contains benzene and pyrimidine rings fused together (**Figure 2.8**). The first quinazoline-based compound, 2-methyl-1,3-aryl-4-quinazoline, was initially isolated from the Chinese plant *aseru* in 1903. This substance has sedative and somniferous properties. When chemical derivatives were created, research on the biological activity of quinazoline compounds began to emerge. Around 50 different derivatives of this class were known by the year 1980, including medications with a variety of biological effects such as soporific, sedative, tranquilising, analgesic, anticonvulsant, antitussive, myorelaxant, antirheumatic, hypotensive, antiallergic, bronchodilating, antidiabetic, cholagogue, diuretic, antimalarial, and spermicidal effects. Following pharmacological testing of quinazoline derivatives with a third-position glycine amide or alanine amide residue that exhibits hypotensive activity, the hunt for compounds of cardiovascular agents began. Unfortunately, more specific problems with the investigation of cardiovascular agents have not been reflected successfully in some evaluations due to the amount and depth of generic information on quinazoline derivatives (Selvam & Kumar, 2015). Some drug molecules containing the quinazoline ring include bunazosin, trimetrexate, vandetanib, prazosin, alfuzosin, gefitinib, and erlotinib (Auti *et al.*, 2020:41354).

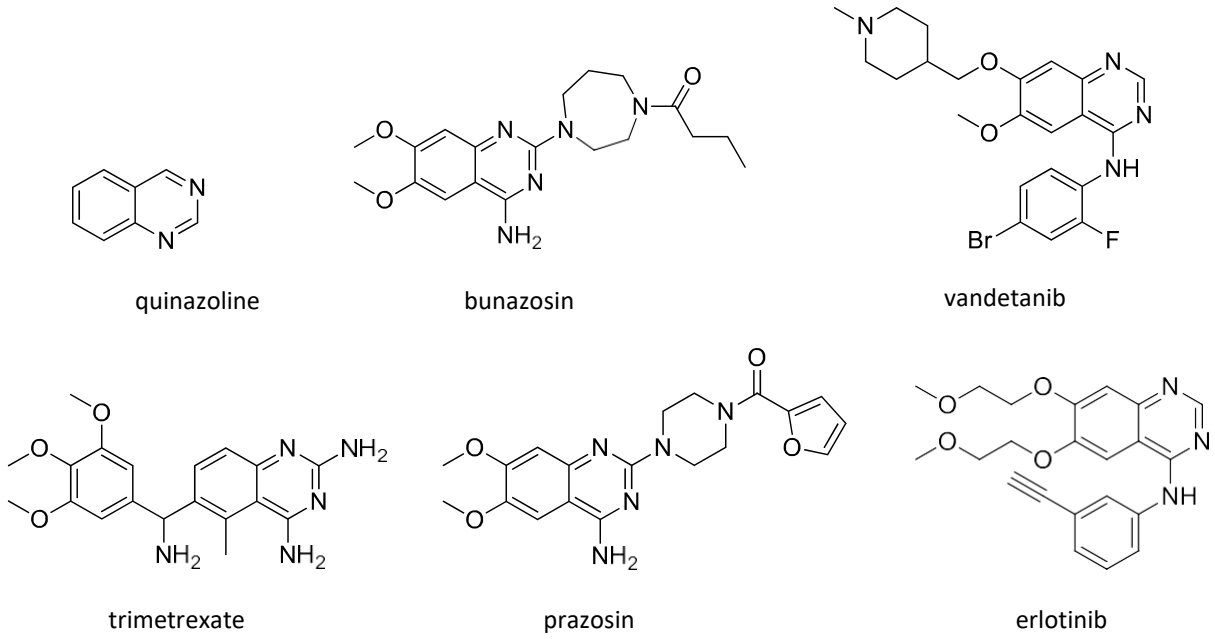

Figure 2.8: Structure of the quinazoline molecule and drugs containing a quinazoline ring (Auti *et al.*, 2020:41354)

2.24 Piperazine/ethyldiamine derivatives

Heterocycles, which include at least one ring with an element other than carbon, are a significant class with biological and pharmacological relevance. These are essential for accomplishing several physiological tasks in both plants and animals. Heterocycles serve as the structural framework for many medications readily available on the market. Because of their enormous significance, researchers have focused significant attention on heterocycles that include nitrogen. The nitrogen-containing, six-membered heterocyclic piperazine is interesting and crucial in medicinal chemistry. Piperazine derivatives have a wide range of pharmacological effects, including depressive, anticancer, anthelmintic, antibacterial, antifungal, antimycobacterial, antimalarial, and anticonvulsant properties. This heterocyclic is found in a large number of well-known medications from a variety of pharmacological classifications. Piperazine is the subject of numerous patent applications (Shaquiquzzaman *et al.*, 2015:4). Numerous derivatives with sundry pharmacological properties have been created based on the different activities of piperazine. Examples of piperazine/ethyldiamine derivatives that are lead/drug molecules include ciprofloxacin, SQ109, RIF, and PBTZ169.

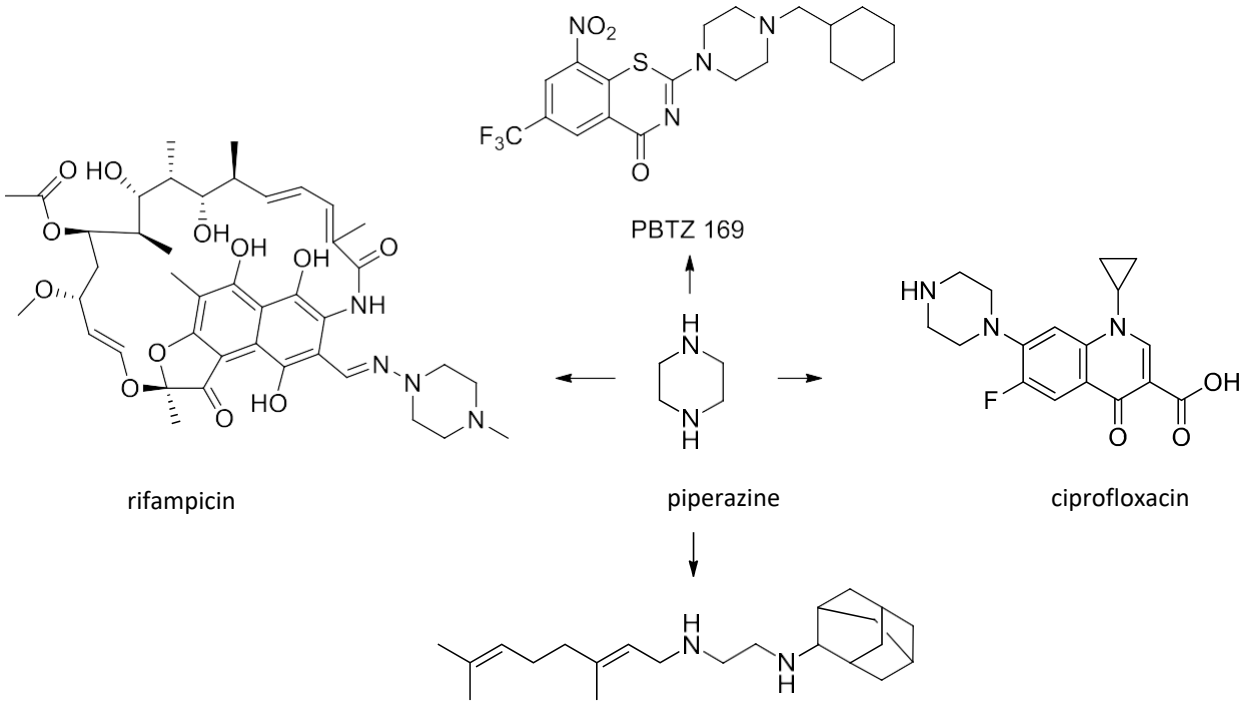

Figure 2.9: Structure of piperazine and piperazine-containing leads/drugs

REFERENCE LIST – CHAPTER 2

Ahmad, S. 2011. Pathogenesis, immunology, and diagnosis of latent *Mycobacterium tuberculosis* infection. *Clinical and Developmental Immunology*, 2011:1-17. doi:10.1155/2011/814943

Álvarez-Rodríguez, A., Jin, B-K., Radwanska, M. & Magez, S. 2022. Recent progress in diagnosis and treatment of Human African trypanosomiasis has made the elimination of this disease a realistic target by 2030. *Frontiers in Medicine*, 9:1037094. doi:10.3389/fmed.2022.1037094

Auti, P.S., George, G. & Paul, A.T. 2020. Recent advances in the pharmacological diversification of quinazoline/quinazolinone hybrids. *Royal Society of Chemistry*, 10(68):41353-41392. doi:10.1039/D0RA06642G

Ayobami, O., Willrich, N., Reuss, A., Eckmanns, T. & Markwart, R. 2020. The ongoing challenge of vancomycin-resistant *Enterococcus faecium* and *Enterococcus faecalis* in Europe: an epidemiological analysis of bloodstream infections. *Emerging Microbes & Infections*, 9(1):1180-1193. doi:10.1080/22221751.2020.1769500

Balaban, N.Q., Helaine, S., Lewis, K., Ackermann, M., Aldridge, B., Andersson, D.I., … Collins, J.J. 2019. Definitions and guidelines for research on antibiotic persistence. *Nature Reviews Microbiology*, 17(7):441-448. doi:10.1038/s41579-019-0196-3

Bekele, E., Awekew, A. & Bassa, T. 2016. The public health significance of leishmaniasis: an overview. *Journal of Natural Sciences Research*, 6(5):2224-3186, ISSN 2225-0921.

Bengaly, Z., Sidibé, I., Ganaba, R., Desquesnes, M., Boly, H. & Sawadogo, L. 2002. Comparative pathogenicity of three genetically distinct types of *Trypanosoma congolense* in cattle: clinical observations and haematological changes. *Veterinary Parasitology*, 108(1):1-19. doi:10.1016/S0304-4017(02)00164-4

Berman, J. 1997. Human leishmaniasis: clinical, diagnostic, and chemotherapeutic developments in the last 10 years. *Clinical infectious diseases*, 24(4):684-703. doi:10.1093/clind/24.4.684

Bessat, M., Okpanma, A. & Shanat, E. 2015. Leishmaniasis: epidemiology, control and future perspectives with special emphasis on Egypt. *Journal of Tropical Diseases*, 2(153):1-10. doi:10.4172/2329-891X.1000153

Bhardwaj, A.K., Kumar, D., Raina, S.K., Sharma, S. & Chander, V. 2015. Assessment of extra pulmonary tuberculosis (EPTB) cases from selected tuberculosis units (TUs) of Himachal Pradesh, India. *International Journal of Health*, 3(2):29-33. doi:10.14419/ijh.v3i2.4567

Blum, J., Schmid, C. & Burri, C. 2006. Clinical aspects of 2541 patients with second stage human African trypanosomiasis. *Acta tropica*, 97(1):55-64. doi:10.1016/j.actatropica.2005.08.001

Boucher, H.W., Talbot, G.H., Bradley, J.S., Edwards, J.E., Gilbert, D., Rice, L.B., … Bartlett, J. 2009. Bad bugs, no drugs: no ESKAPE! An update from the Infectious Diseases Society of America. *Clinical Infectious Diseases*, 48(1):1-12, doi.org/10.1086/595011

Brummitt, C.F., Porter, J.A. & Herwaldt, B.L. 1996. Reversible peripheral neuropathy associated with sodium stibogluconate therapy for American cutaneous leishmaniasis. *Clinical infectious diseases*, 22(5):878-879. doi:10.1093/clinids/22.5.878

Brun, R., Blum, J., Chappuis, F. & Burri, C. 2010. Human African trypanosomiasis. *The Lancet*, 375(9709): 148-159. doi:10.1016/S0140-6736(09)60829-1

Buguet, A., Bourdon, L., Bouteille, B., Cespuglio, R., Vincendeau, P., Radomski, M. & Dumas, M. 2001. The duality of sleeping sickness: focusing on sleep. *Sleep Medicine Reviews*, 5(2):139-153. doi:10.1053/smrv.2000.0130

Büscher, P. 2013. Diagnosis of African trypanosomiasis. In. *Trypanosomes and Trypanosomiasis*: Springer. pp. 189-216. doi: 10.1007/978-3-7091-1556-5_8

Büscher, P., Cecchi, G., Jamonneau, V. & Priotto, G. 2017. Human African trypanosomiasis. *The Lancet*, 390(10110):2397-2409. doi:10.1016/S0140-6736(17)31510-6

Calvet, F., Medkour, H., Mediannikov, O., Girardet, C., Jacob, A., Boni, M. & Davoust, B. 2020. An African canine trypanosomosis case import: is there a possibility of creating a secondary focus of *Trypanosoma congolense* infection in France? *Pathogens*, 9(9), 709. doi:10.3390/pathogens9090709

Checchi, F., Filipe, J.A., Haydon, D.T., Chandramohan, D. & Chappuis, F. 2008. Estimates of the duration of the early and late stage of gambiense sleeping sickness. *BMC Infectious Diseases*, 8(1):1-10. doi:10.1186/1471-2334-8-16

Choi, C.H., Lee, E.Y., Lee, Y.C., Park, T.I., Kim, H.J., Hyun, S.H., … Lee, J.C. 2005. Outer membrane protein 38 of *Acinetobacter baumannii* localizes to the mitochondria and induces apoptosis of epithelial cells. *Cellular Microbiology*, 7(8):1127-1138. doi:10.1111/j.1462-5822.2005.00538.x

Choi, C.M. & Lerner, E.A. 2001. Leishmaniasis as an emerging infection*. International Journal of Investigative Dermatology Symposium Proceedings*. Elsevier, 6(3):175-182. doi:10.1046/j.0022-202x.2001.00038.x

Chunge, C., Owate, J., Pamba, H. & Donno, L. 1990. Treatment of visceral leishmaniasis in Kenya by aminosidine alone or combined with sodium stibogluconate. *Transactions of the Royal Society of Tropical Medicine and Hygiene*, 84(2):221-225. doi:10.1016/0035-9203(90)90263-E

Comstock, G. 1999. How much isoniazid is needed for prevention of tuberculosis among immunocompetent adults? [Counterpoint]. *The International Journal of Tuberculosis and Lung Disease*, 3(10):847-850.

Courtin, F., Jamonneau, V., Duvallet, G., Garcia, A., Coulibaly, B., Doumenge, J., … Solano, P. 2008. Sleeping sickness in West Africa (1906–2006): changes in spatial repartition and lessons from the past. *Tropical Medicine & International Health*, 13(3):334-344. doi:10.1111/j.1365-3156.2008.02007.x

David, C.V. & Craft, N. 2009. Cutaneous and mucocutaneous leishmaniasis. *Dermatologic Therapy*, 22(6):491-502. doi:10.1111/j.1529-8019.2009.01272.x

Davin-Regli, A., Lavigne, J.-P. & Pagès, J.-M. 2019. *Enterobacter* spp.: update on taxonomy, clinical aspects, and emerging antimicrobial resistance. *Clinical Microbiology Reviews*, 32(4), e00002-00019. doi:10.1128/cmr.00002-19

De Oliveira, D.M.P., Forde, B.M., Kidd, T.J., Harris, P.N.A., Schembri, M.A., Beatson, S.A., … Walker, M.J. 2020. Antimicrobial resistance in ESKAPE pathogens. *Clinical Microbiology Reviews*, 33(3), e00181-00119. doi:10.1128/CMR.00181-19

Delogu, G., Sali, M. & Fadda, G. 2013. The biology of *Mycobacterium tuberculosis* infection. *Mediterranean Journal of Hematology and Infectious Diseases*, 5(1), e2013070. doi:10.4084/MJHID.2013.070

Desquesnes, M. & Dia, M.L. 2004. Mechanical transmission of *Trypanosoma vivax* in cattle by the African tabanid Atylotus fuscipes. *Veterinary Parasitology*, 119(1):9-19. doi:10.1016/j.vetpar.2003.10.015

Dyer, N.A., Rose, C., Ejeh, N.O. & Acosta-Serrano, A. 2013. Flying tryps: survival and maturation of trypanosomes in tsetse flies. *Trends in Parasitology*, 29(4):188-196. doi:10.1016/j.pt.2013.02.003

Erwin, E.R., Addison, A.P., John, S.F., Olaleye, O.A. & Rosell, R.C. 2019. Pharmacokinetics of isoniazid: the good, the bad, and the alternatives. *Tuberculosis*, 116:S66-S70. doi:10.1016/j.tube.2019.04.012

Falzon, D., Schünemann, H.J., Harausz, E., González-Angulo, L., Lienhardt, C., Jaramillo, E. & Weyer, K. 2017. World Health Organization treatment guidelines for drug-resistant tuberculosis, 2016 update. *European Respiratory Journal*, 49(3):1-12. doi:10.1183/13993003.02308-2016

Fèvre, E.M., Coleman, P., Odiit, M., Magona, J., Welburn, S. & Woolhouse, M.E. 2001. The origins of a new *Trypanosoma brucei rhodesiense* sleeping sickness outbreak in eastern Uganda. *The Lancet*, 358(9282): 625-628. doi:10.1016/S0140-6736(01)05778-6

Fox, W., Ellard, G.A. & Mitchison, D.A. 1999. Studies on the treatment of tuberculosis undertaken by the British Medical Research Council tuberculosis units, 1946–1986, with relevant subsequent publications. *The International Journal of Tuberculosis and Lung Disease*, 3(10):S231-S279.

Franco, J.R., Simarro, P.P., Diarra, A. & Jannin, J.G. 2014. Epidemiology of human African trypanosomiasis. *Clinical Epidemiology*, 6:257. doi:10.2147/CLEP.S39728

Friedman, L.N., Dedicoat, M. & Davies, P.D., eds. 2020. *Clinical tuberculosis*. 6th ed. Boca Raton, FL: CRC Press.

Galiza, G., Garcia, H., Assis, A., Oliveira, D., Pimentel, L., Dantas, A., … Riet-Correa, F. 2011. High mortality and lesions of the central nervous system in trypanosomosis by *Trypanosoma vivax* in Brazilian hair sheep. *Veterinary Parasitology*, 182(2-4):359-363. doi:10.1016/j.vetpar.2011.05.016

Guerin, P.J., Olliaro, P., Sundar, S., Boelaert, M., Croft, S.L., Desjeux, P., … Bryceson, A.D. 2002. Visceral leishmaniasis: current status of control, diagnosis, and treatment, and a proposed research and development agenda. *The Lancet Infectious Diseases*, 2(8):494-501. doi:10.1016/S1473-3099(02)00347-X

Jamonneau, V., Ilboudo, H., Kaboré, J., Kaba, D., Koffi, M., Solano, P., … Lingue, K. 2012. Untreated human infections by *Trypanosoma brucei gambiense* are not 100% fatal. *PLoS Neglected Tropical Diseases*, 6(6), e1691. doi:10.1371/journal.pntd.0001691

Jha, T. 1983. Evaluation of diamidine compound (pentamidine isethionate) in the treatment of resistant cases of kala-azar occurring in North Bihar, India. *Transactions of the Royal Society of Tropical Medicine and Hygiene*, 77(2):167-170. doi:10.1016/0035-9203(83)90058-5

Jordao, L. & Vieira, O.V. 2011. Tuberculosis: new aspects of an old disease. *International Journal of Cell Biology*, (2011):1-13. doi:10.1155/2011/403623

Kennedy, P.G. 2019. Update on human African trypanosomiasis (sleeping sickness). *Journal of Neurology*, 266:2334-2337. doi:10.1007/s00415-019-09425-7

Kennedy, P.G. & Rodgers, J. 2019. Clinical and neuropathogenetic aspects of human African trypanosomiasis. *Frontiers in Immunology*, 10:39. doi:10.3389/fimmu.2019.00039

Khawbung, J.L., Nath, D. & Chakraborty, S. 2021. Drug resistant tuberculosis: a review. *Comparative Immunology, Microbiology and Infectious Diseases,* 74:101574. doi:10.1016/j.cimid.2020.101574

Kramer, A., Schwebke, I. & Kampf, G. 2006. How long do nosocomial pathogens persist on inanimate surfaces? A systematic review. *BMC infectious diseases*, 6(1):1-8. doi:10.1186/1471-2334-6-130

Kubba, R., El-Hassan, A., Path, F., Al-Gindan, Y., Omer, A., Kutty, M., … Saeed, M.B. 1987. Dissemination in cutaneous leishmaniasis I. Subcutaneous nodules. *International Journal of Dermatology*, 26(5):300-304. doi:10.1111/j.1365-4362.1987.tb00193.x

Lee, J.Y. 2015. Diagnosis and treatment of extrapulmonary tuberculosis. *Tuberculosis and Respiratory Diseases*, 78(2):47-55. doi:10.4046/trd.2015.78.2.47

Legros, D., Ollivier, G., Gastellu-Etchegorry, M., Paquet, C., Burri, C., Jannin, J. & Büscher, P. 2002. Treatment of human African trypanosomiasis: present situation and needs for research and development. *The Lancet Infectious Diseases*, 2(7):437-440. doi:10.1016/S1473-3099(02)00321-3

Livermore, D.M. 2002. Multiple mechanisms of antimicrobial resistance in *Pseudomonas aeruginosa*: our worst nightmare? *Clinical Infectious Diseases*, 34(5):634-640. doi:10.1086/338782

Livermore, D.M., Hope, R., Brick, G., Lillie, M. & Reynolds, R. 2008. Non-susceptibility trends among *Enterobacteriaceae* from bacteraemias in the UK and Ireland, 2001–06. *Journal of Antimicrobial Chemotherapy*, 62(suppl_2):ii41-ii54. doi:10.1093/jac/dkn351

Luies, L. & du Preez, I. 2020. The echo of pulmonary tuberculosis: mechanisms of clinical symptoms and other disease-induced systemic complications. *Clinical Microbiological Review,* 33(4):1-19. doi:10.1129/cmr.00036-20

MacGregor, P. & Matthews, K.R. 2010. New discoveries in the transmission biology of sleeping sickness parasites: applying the basics. *Journal of Molecular Medicine*, 88(9):865-871. doi:10.1007/s00109-010-0637-y

Maia, C. & Depaquit, J. 2016. Can Sergentomyia (*Diptera, Psychodidae*) play a role in the transmission of mammal-infecting Leishmania? *Parasite*, 23:55. doi:10.1051/parasite/2016062

Magez, S. & Radwanska, M. 2014. *Trypanosomes and Trypanosomiasis*. Springer. 2014:1-300. doi:10.1007/978-3-7091-1556-5

Mann, S., Frasca, K., Scherrer, S., Henao-Martínez, A.F., Newman, S., Ramanan, P. & Suarez, J.A. 2021. A review of leishmaniasis: current knowledge and future directions. *Current Tropical Medicine Reports*, 8:121-132. doi:10.1007/s40475-021-00232-7

Marcondes, C.B., ed. 2017. *Arthropod borne diseases*. Cham: Springer. pp. 1-642. doi:10.1007/978-3-319-13884-8

Märtson, A.-G., Burch, G., Ghimire, S., Alffenaar, J.-W.C. & Peloquin, C.A. 2021. Therapeutic drug monitoring in patients with tuberculosis and concurrent medical problems. *Expert Opinion on Drug Metabolism & Toxicology*, 17(1):23-39. doi:10.1080/17425255.2021.1836158

Means, T.K., Wang, S., Lien, E., Yoshimura, A., Golenbock, D.T. & Fenton, M.J. 1999. Human toll-like receptors mediate cellular activation by *Mycobacterium tuberculosis*. *The Journal of Immunology*, 163(7):3920-3927. doi:10.4049/jimmunol.163.7.3920

Mesu, V.K.B.K., Kalonji, W.M., Bardonneau, C., Mordt, O.V., Blesson, S., Simon, F., … Lubaki, J.-P.F. 2018. Oral fexinidazole for late-stage African *Trypanosoma brucei gambiense* trypanosomiasis: a pivotal multicentre, randomised, non-inferiority trial. *The Lancet*, 391(10116):144-154. doi:10.1016/S0140-6736(17)32758-7

Miller, W.R., Munita, J.M. & Arias, C.A. 2014. Mechanisms of antibiotic resistance in *enterococci*. *Expert Review of Anti-infective Therapy*, 12(10):1221-1236. doi:10.1586/14787210.2014.956092

Mitchison, D.A. 2000. Role of individual drugs in the chemotherapy of tuberculosis. *The International Journal of Tuberculosis and Lung Disease*, 4(9):796-806.

Murray, H.W., Berman, J.D., Davies, C.R. & Saravia, N.G. 2005. Advances in leishmaniasis. *The Lancet*, 366(9496):1561-1577. doi:10.1016/S0140-6736(05)67629-5

Nachiappan, A.C., Rahbar, K., Shi, X., Guy, E.S., Mortani Barbosa Jr, E.J., Shroff, G.S., … Hammer, M.M. 2017. Pulmonary tuberculosis: role of radiology in diagnosis and management. *Radiographics*, 37(1):52-72. doi:10.1148/rg.2017160032

Natarajan, A., Beena, P., Devnikar, A.V. & Mali, S. 2020. A systemic review on tuberculosis. *Indian Journalof Tuberculosis*, 67(3):295-311. doi:10.1016/j.ijtb.2020.02.005

Njiokou, F., Nimpaye, H., Simo, G., Njitchouang, G., Asonganyi, T., Cuny, G. & Herder, S. 2010. Domestic animals as potential reservoir hosts of *Trypanosoma brucei gambiense* in sleeping sickness foci in Cameroon. *Parasite*, 17(1):61-66. doi:10.1051/parasite/2010171061

Oberle, M., Balmer, O., Brun, R. & Roditi, I. 2010. Bottlenecks and the maintenance of minor genotypes during the life cycle of *Trypanosoma brucei*. *PLoS Pathogens*, 6(7):e1001023. doi:10.1371/journal.ppat.1001023

Odiit, M., Kansiime, F. & Enyaru, J. 1997. Duration of symptoms and case fatality of sleeping sickness caused by *Trypanosoma brucei rhodesiense* in Tororo, Uganda. *East African Medical Journal*, 74(12): 792-795.

Ottenhoff, T.H. & Kaufmann, S.H. 2012. Vaccines against tuberculosis: where are we and where do we need to go? *PLoS Pathogens*, 8(5), e1002607. doi:10.1371/journal.ppat.1002607

Pal, C., Raha, M., Basu, A., Roy, K.C., Gupta, A., Ghosh, M., … Bandyopadhyay, S. 2002. Combination therapy with indolylquinoline derivative and sodium antimony gluconate cures established visceral leishmaniasis in hamsters. *Antimicrobial Agents and Chemotherapy*, 46(1):259-261. doi:10.1128/aac.46.1.259-261.2002

Peacock, L., Ferris, V., Sharma, R., Sunter, J., Bailey, M., Carrington, M. & Gibson, W. 2011. Identification of the meiotic life cycle stage of *Trypanosoma brucei* in the tsetse fly. *Proceedings of the National Academy of Sciences*, 108(9):3671-3676. doi:10.1073/pnas.1019423108

Peloquin, C.A. & Davies, G.R. 2021. The treatment of tuberculosis. *Clinical Pharmacology & Therapeutics*, 110(6):1455-1466. doi:10.1002/cpt.2261

Pendleton, J.N., Gorman, S.P. & Gilmore, B.F. 2013. Clinical relevance of the ESKAPE pathogens. *Expert Review of Anti-infective Therapy*, 11(3):297-308. doi:10.1586/eri.13.12

Pepin, J. & Khonde, N. 1996. Relapses following treatment of early-stage *Trypanosoma brucei gambiense* sleeping sickness with a combination of pentamidine and suramin. *Transactions of the Royal Society of Tropical Medicine and Hygiene*, 90(2):183-186. doi:10.1016/S0035-9203(96)90132-7

Pohlig, G., Bernhard, S.C., Blum, J., Burri, C., Mpanya, A., Lubaki, J.-P.F., … Deo, G.K.M. 2016. Efficacy and safety of pafuramidine versus pentamidine maleate for treatment of first stage sleeping sickness in a randomized, comparator-controlled, international phase 3 clinical trial. *PLoS Neglected Tropical Diseases*, 10(2), e0004363. doi:10.1371/journal.pntd.0004363

Pradhan, S., Schwartz, R., Patil, A., Grabbe, S. & Goldust, M. 2022. Treatment options for leishmaniasis. *Clinical and Experimental Dermatology*, 47(3):516-521. doi:10.1111/ced.14919

Priotto, G., Kasparian, S., Mutombo, W., Ngouama, D., Ghorashian, S., Arnold, U., … Kazadi-Kyanza, S. 2009. Nifurtimox-eflornithine combination therapy for second-stage African *Trypanosoma brucei gambiense* trypanosomiasis: a multicentre, randomised, phase III, non-inferiority trial. *The Lancet*, 374(9683):56-64. doi:10.1016/S0140-6736(09)61117-X

Ramirez, D. & Giron, M. 2022. Enterobacter infections. In: *StatPearls [Internet]*. Treasure Island, FL: StatPearls Publishing.

Ready, P.D. 2014. Epidemiology of visceral leishmaniasis. *Clinical Epidemiology*:147-154. doi:10.2147/CLEP.S44267

Reithinger, R. & Dujardin, J.-C. 2007. Molecular diagnosis of leishmaniasis: current status and future applications. *Journal of Clinical Microbiology*, 45(1):21-25. doi:10.1128/jcm.02029-06

Roatt, B.M., De Oliveira Cardoso, J.M., De Brito, R.C.F., Coura-Vital, W., De Oliveira Aguiar-Soares, R.D. & Reis, A.B. 2020. Recent advances and new strategies on leishmaniasis treatment. *Applied Microbiology and Biotechnology*, 104:8965-8977. doi:10.1007/s00253-020-10856-w

Rotureau, B. & Van Den Abbeele, J. 2013. Through the dark continent: African trypanosome development in the tsetse fly. *Frontiers in Cellular and Infection Microbiology*, 3, 53. doi:10.3389/fcimb.2013.00053

Sahlas, D.J., MacLean, J.D., Janevski, J. & Detsky, A.S. 2002. Out of Africa. *New England Journal of Medicine*, 347(10):749-753. doi:10.1056/NEJMcps021049

Santajit, S. & Indrawattana, N. 2016. Mechanisms of antimicrobial resistance in ESKAPE pathogens. *BioMed Research International*, 2016, 2475067. doi:10.1155/2016/2475067

Schwaber, M.J. & Carmeli, Y. 2007. Mortality and delay in effective therapy associated with extended-spectrum β-lactamase production in *Enterobacteriaceae* bacteraemia: a systematic review and meta-analysis. *Journal of Antimicrobial Chemotherapy*, 60(5):913-920. doi:10.1093/jac/dkm318

Selvam, T.P. & Kumar, P.V. 2015. Quinazoline marketed drugs. *Research in Pharmacy*, 1(1):1-21.

Sharma, S.K. & Mohan, A. 2013. Tuberculosis: from an incurable scourge to a curable disease-journey over a millennium. *The Indian Journal of Medical Research*, 137(3):455.

Shaquiquzzaman, M., Verma, G., Marella, A., Akhter, W., Khan, M.F., … Alam, M.M. 2015. Piperazine scaffold: a remarkable tool in generation of diverse pharmacological agents. *Europian Journal of Medicinal Chemistry,* 102:487-529. doi:10.1016/j.ejmech.2015.07.026

Simarro, P.P. & Asumu, P.N. 1996. Gambian trypanosomiasis and synergism between melarsoprol and eflornithine: first case report. *Transactions of the Royal Society of Tropical Medicine and Hygiene*, 90(3): 315-315. doi:10.1016/S0035-9203(96)90268-0

Simarro, P.P., Franco, J.R., Cecchi, G., Paone, M., Diarra, A., Ruiz Postigo, J.A. & Jannin, J.G. 2012. Human African trypanosomiasis in non-endemic countries (2000–2010). *Journal of Travel Medicine*, 19(1):44-53. doi:10.1111/j.1708-8305.2011.00576.x

Singh, A., Prasad, R., Balasubramanian, V. & Gupta, N. 2020. Drug-resistant tuberculosis and HIV infection: current perspectives. *HIV/AIDS-Research and Palliative Care*:9-31. doi: 10.2147/hiv.s193059

Singh, S. & Sivakumar, R. 2004. Challenges and new discoveries in the treatment of leishmaniasis. *Journal of Infection and Chemotherapy*, 10(6):307-315. doi:10.1007/s10156-004-0348-9

Singh, S., Kumar, J., Singh, R. & Dwivedi, S.N. 2000. Hepatitis B and C viral infections in Indian kala-azar patients receiving injectable anti-leishmanial drugs: A community-based study. *International Journal of Infectious Diseases*, 4(4):203. doi:10.1016/S1201-9712(00)90110-3

Sterling, T.R., Njie, G., Zenner, D., Cohn, D.L., Reves, R., Ahmed, A., … Burgos, M. 2020. Guidelines for the treatment of latent tuberculosis infection: recommendations from the National Tuberculosis Controllers Association and CDC, 2020. *American Journal of Transplantation*, 20(4):1196-1206. doi.10.1111/ ajt.15841

Sudarshi, D., Lawrence, S., Pickrell, W.O., Eligar, V., Walters, R., Quaderi, S., … Vincent, A. 2014. Human African trypanosomiasis presenting at least 29 years after infection: what can this teach us about the pathogenesis and control of this neglected tropical disease? *PLoS Neglected Tropical Diseases*, 8(12), e3349. doi:10.1371/journal.pntd.0003349

Sundar, S. & Murray, H.W. 1995. Effect of treatment with interferon-γ alone in visceral leishmaniasis. *Journal of Infectious Diseases*, 172(6):1627-1629. doi:10.1093/infdis/172.6.1627

Tarral, A., Hovsepian, L., Duvauchelle, T., Donazzolo, Y., Latreille, M., Felices, M., … Blesson, S. 2023. Determination of the optimal single dose treatment for acoziborole, a novel drug for the treatment of human African trypanosomiasis: first-in-human study. *Clinical Pharmacokinetics*, 62(3):481-491. doi:10.1007/s40262-023-01216-8

Tiberi, S., Utjesanovic, N., Galvin, J.,Centis, R., D'Ambrosio, L., van den Bloom, M., …Migliori, G.B. 2022. Drug resistant TB-latest developments in epidemiology, diagnostics and management. *International Journal of Infectious Diseases,* 124:S20-S25. doi:10.1016/j.ijid.2022.03.026

Tigabu, A. & Getaneh, A. 2021. *Staphylococcus aureus*, ESKAPE bacteria challenging current health care and community settings: a literature review. *Clinical Laboratory*, 67(7):10.7754. doi:10.7754/Clin.Lab. 2020.200930)

Urdahl, K., Shafiani, S. & Ernst, J. 2011. Initiation and regulation of T-cell responses in tuberculosis. *Mucosal Immunology*, 4(3):288-293. doi:10.1038/mi.2011.10

Venturelli, A., Tagliazucchi, L., Lima, C., Venuti, F., Malpezzi, G., Magoulas, G.E., … Costi, M.P. 2022. Current tretments to control african trypanosomiasis and the health perspective. *Microorganisms,* 10(7):1298. doi:10.3390/microorganisms10071298

Vila, J., Martí, S. & Sanchez-Céspedes, J. 2007. Porins, efflux pumps and multidrug resistance in *Acinetobacter baumannii*. *Journal of Antimicrobial Chemotherapy*, 59(6):1210-1215. doi:10.1093/jac/dkl509

Wang, G., Zhao, G., Chao, X., Xie, L. & Wang, H. 2020. The characteristic of virulence, biofilm and antibiotic resistance of *Klebsiella pneumoniae*. *International Journal of Environmental Research and Public Health*, 17(17), 6278. doi:10.3390/ijerph17176278

WHO (World Health Organization). 1998. *Control and surveillance of African Trypanosomiasis: report of a WHO Expert Committee*. Geneva.

WHO (World Health Organization). 2013a. C*ontrol and surveillance of human African Trypanosomiasis: report of a WHO Expert Committee*. Geneva.

WHO (World Health Organization). 2013b. *Global tuberculosis report 2013*. Geneva.

WHO (World Health Organization). 2022a. *Global tuberculosis report 2022.* Geneva: World Health Organization; 2022. License: CC BY-NC-SA 3.0 IGO

WHO (World Health Organization). 2022b. *Global tuberculosis report 2021: supplementary material*. Geneva.

Zaman, K. 2010. Tuberculosis: a global health problem. *Journal of Health, Population, and Nutrition*, 28(2):111. doi:10.3329/jhpn.v28i2.4879

Zijlstra, E., El-Hassan, A., Ismael, A. & Ghalib, H. 1994. Endemic kala-azar in eastern Sudan: a longitudinal study on the incidence of clinical and subclinical infection and post-kala-azar dermal leishmaniasis. *The American Journal of Tropical Medicine and Hygiene*, 51(6):826-836. doi:10.4269/ajtmh.1994.51.826

CHAPTER 3 – ARTICLE FOR SUBMISSION

Chapter 3 comprises a manuscript intended for submission to the journal *Chemical Biology & Drug Design*. The manuscript contains an introduction, materials and methods, results and discussion, and conclusion. Additionally, an abstract and graphical abstract have been added to the manuscript. Supporting data for Chapter 3 are found in Appendix A.

The manuscript was written following the journal's instructions to authors, which are available on the journal's website: https://onlinelibrary.wiley.com/page/journal/17470285/homepage/forauthors.html

SYNTHESIS, *IN VITRO* ANTIBACTERIAL AND ANTIPROTOZOALEVALUATION OF 2-PHENYL-4-AMINO QUINAZOLINES

Hendrika Jacoba Neethling,[a] Lesetja J. Legoabe,[a] Klaudia T. Angula,[a] and Richard M. Beteck[a]*

[a]*Centre of Excellence for Pharmaceutical Sciences, North-West University, Private Bag X6001, Potchefstroom 2520, South Africa.*

Correspondence:

* Corresponding author: e-mail: 25159194@nwu.ac.za OR richmbi1@yahoo.com; Tel.: +2718 299 2249

GRAPHICAL ABSTRACT

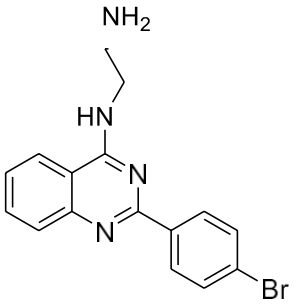

5a

MW: 342.34 g/mol^{-1}

T.b. cruzi: MIC_{50} 0.55 µM

L. infantum: MIC_{50} 1.26 µM

T.b. brucei: MIC_{50} 0.22 µM

T.b. rhodesiense: MIC_{50} 0.13 µM

M. tb: MIC_{50} 0.868 µM

ABSTRACT

Herein we report the synthesis of 2,4-disubstituted quinazoline derivatives. The synthesised compounds underwent *in vitro* testing to assess their antitubercular, antibacterial, antiprotozoal, and cytotoxic properties. Among the tested compounds, **3a–3c, 3e–3f**, and **5a–5c** exhibited antitubercular activity in the casein medium, with activity ranging from 0.488 μM to 8.481 μM, with **Compound 5a** showing the highest antitubercular activity in the series (0.488–0.868 μM). However, none of the compounds showed any activity in the albumin medium. Except for **Compounds 2b, 3b, 3d, and 3f** which exhibited activity against *Cryptococcus neoformansi*, none of the compounds demonstrated antibacterial or antifungal activity. Most of the tested compounds were inactive or showed low specificity against the protozoal parasites.

Keywords: Quinazoline, Ethylenediamine, Protozoans, Bacteria, Fungi

3.1 Introduction

ESKAPE pathogens, which include *Enterococcus faecium*, *Staphylococcus aureus*, *Klebsiella pneumoniae*, *Acinetobacter baumannii*, *Pseudomonas aeruginosa*, and *Enterobacter* species, are multidrug-resistant bacteria, which are resistant to three or more classes of antibiotics (Magiorakos *et al.*, 2012:268). The prevalence of these bacteria is on the rise, while the number of effective antibiotics is declining; as such, ESKAPE pathogens pose a global threat to human health (Sommer *et al.*, 2017:1). The acquisition of antimicrobial resistance genes by these pathogens has limited the treatment options for the diseases they cause, leading to increased disease burden and mortality rates. The United States records over 2 million cases of antimicrobial resistance infections annually, resulting in 29 000 deaths and a healthcare cost exceeding $4.7 billion each year. In Europe, antimicrobial resistance infections are annually responsible for approximately 33 000 deaths and 874 000 disability-adjusted life years, resulting in direct and indirect healthcare costs of $1.5 billion (De Oliveira *et al.*, 2020:1). In February 2017, the World Health Organization (WHO) issued a list to direct and prioritise research and development efforts towards new antibiotics. The list highlighted pathogenic bacteria for which there is an urgent need for the development of new antimicrobial agents. Among the numerous pathogens on this list, most ESKAPE pathogens are listed as priority pathogens (De Oliveira *et al.*, 2020; Rice, 2008:1080).

Sleeping sickness, also known as human African trypanosomiasis (HAT), is a life-threatening parasitic disease that can be fatal if left untreated. The disease is caused by *Trypanosoma brucei*, a protozoan parasite transmitted by tsetse flies. Almost 93% of HAT cases are caused by *T.b. gambiense* subspecies, a parasite that is endemic to West and Central Africa (Brun *et al.*, 2010:148). In 2015, fewer than 3 000 cases were documented, and WHO set a goal to eradicate the disease. Despite reduced cases, HAT remains prevalent in some sub-Saharan African regions, particularly in Central Africa, and is a significant burden on rural communities (Büscher *et al.*, 2017:1). While intravenous suramin has demonstrated efficacy and relatively mild adverse effects in treating early-stage HAT caused by *T.b. rhodesiense*, and intramuscular or intravenous pentamidine has shown effectiveness in treating early-stage HAT caused by *T.b. gambiense*, the therapeutic options available for late-stage disease are highly toxic. Melarsoprol, the primary treatment for central nervous system *T.b. rhodesiense*, is associated with significant discomfort during administration and carries a risk of post-treatment reactive encephalopathy in approximately 10% of cases, with nearly half of cases resulting in death. A recent study revealed a mortality rate of approximately 5% for melarsoprol-treated patients (Kennedy, 2013:192). Nifurtimox-eflornithine

combination therapy (NECT), which has replaced melarsoprol as the first-line treatment for this form of HAT, is ineffective against central nervous system *T.b. rhodesiense* but has shown success in treating central nervous system *T.b. gambiense*. Fexinidazole has emerged as an effective oral monotherapy for the treatment of *T.b. gambiense* (Kennedy, 2019:2335). The recommended regimen involves oral administration of fexinidazole once a day for a total of 10 days, comprising four loading days followed by six maintenance days. Extensive evidence supports its efficacy in addressing both early and advanced stages of the disease. However, it is important to note some limitations associated with this novel medication. Firstly, individuals with pronounced central nervous system involvement may exhibit a reduced response to treatment. Secondly, it is crucial to take the tablets with a meal since their bioavailability diminishes significantly in a fasting state (Lindner *et al.*, 2020:3). Currently, there are only two treatment choices accessible for patients with *T.b. rhodesiense*. These options include suramin for early-stage infections and the highly toxic arsenic-based melarsoprol regimen for the meningoencephalitic stage of the disease. Although *T.b. rhodesiense* is not the primary cause of HAT, further research is imperative to enhance treatment options for this condition. Given that current HAT treatments necessitate a 10-day course, future research should prioritize the development of therapies that can achieve a successful cure in a shorter duration. This pursuit may eventually lead to the discovery of a one-day, one-pill solution for both forms of HAT (Álvarez-Rodríguez *et al*., 2022:09). As such, there still exist a need to identify and develop new agents for treating HAT.

Leishmaniasis is a neglected disease caused by the protozoan parasite *Leishmania* (family *Trypanosomatidae*). It is transmitted by vectors and requires intracellular infection (Mann *et al.*, 2021: 121). Leishmaniasis exhibits diverse clinical presentations, but it can be broadly categorised into three primary phenotypic types, namely cutaneous leishmaniasis, mucocutaneous leishmaniasis, and visceral leishmaniasis (Mann *et al.*, 2021:122). Despite efforts to reduce the disease burden, leishmaniasis remains a significant public health problem affecting 88 countries and presents a health threat to approximately 350 million people. Each year, there are 500 000 new cases of visceral leishmaniasis, 1–1.5 million cases of cutaneous leishmaniasis, and 2.4 million disability-adjusted life years. The disease is influenced by a range of environmental and personal risk factors, including human immunodeficiency virus (HIV), malnutrition, genetics, and urbanisation, deforestation, and new irrigation systems (Desjeux, 2004:305). The treatment of leishmaniasis can be challenging. In general, the approach to leishmaniasis treatment should be tailored to the individual patient, taking their specific requirements, type of leishmaniasis, and

the subspecies of the parasite involved into consideration. There are several systemic treatment options available for leishmaniasis, including pentavalent antimonials such as meglumine antimoniate and sodium stibogluconate, different formulations of amphotericin (deoxycholate and liposomal), pentamidine, and oral therapies such as fluconazole and miltefosine. These treatments suffer from poor pharmacokinetic properties, poor efficacy due to resistance, and some exhibit severe side effects (Mann *et al.*, 2021:128). All these necessitate the search for new treatment for leishmaniasis. On the therapeutic front, issues such as drug toxicity, cost, and emerging drug resistance constrain the available antiparasitic treatment options. Given these limitations, vaccination emerges as the most promising approach to controlling leishmaniasis. The ideal objective is to develop a vaccine that is safe, effective, affordable, and widely accessible. Regrettably, despite years of research and clinical trials, there is currently no approved human vaccine available for this disease (Mann *et al.*, 2021:130).

Tuberculosis (TB) is an infectious disease characterised by progressive granulomas in the lung tissues and is caused by acid-fast bacteria belonging to the *Mycobacterium* genus. *M. tuberculosis* is the major causative agent of TB in humans, predominantly affecting the lungs and causing pulmonary TB (Natarajan *et al.*, 2020:1-2). It can further cause extrapulmonary TB by affecting other body tissues, such as the colon, meninges, bones, joints, lymph nodes, and skin (Natarajan *et al.*, 2020:2). The transmission of TB mainly occurs through droplet nuclei (Jain *et al.*, 2020:1439). The death rate due to TB is alarmingly high, with over 1 million people succumbing to the disease each year, and drug-resistant strains of *M. tuberculosis* are exacerbating the situation (Khan *et al.*, 2019). The primary drugs for TB treatment are rifampicin, isoniazid, ethambutol, and pyrazinamide, which are first-line drugs for the disease (Yew *et al.*, 2011:447). These drugs are associated with severe side effects, poor efficacy due to resistance, and they require a long treatment period to achieve an effective cure, hence there is a need to continuously search for new compounds to curb TB (Peloquin & Davies, 2021).

Quinazolinone, chemically known as quinazolin-4(3H)-one, is a heterocyclic compound that contains two fused aromatic rings, one carbon atom oxidised with a keto oxygen, and two nitrogen atoms. Quinazolinone has two structural isomers, 2 and 4, with the latter being more common. Quinazolinones are used as sedative drugs (such as afloqualone, cloroqualone, and diproqualone) and antiprotozoal agents (such as halofuginone and febrifugine) (Selvam & Kumar, 2015:13). Quinazoline, a derivative of quinazolinone, has also been reported to exhibit various biological activities, including antibacterial and anticancer properties (Hameed *et al.*, 2018:281).

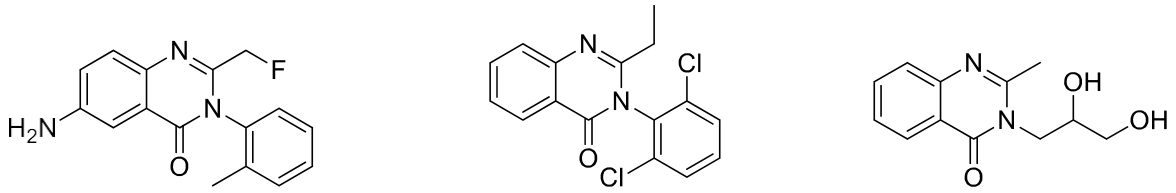

afloqualone cloroqualone diproqualone

Figure 3.1: Structures of quinazolinone-containing drugs (Source: own)

A scientific publication examined the structure-activity relationship of quinazolinone derivatives and suggest that substitution at positions 2 and 3, the presence of halogen atoms at position 6 and 8, and the introduction of amine or substituted amine groups at position 4 can increase antimicrobial effectiveness (as illustrated in **Figure 3.2**) (Jafari *et al.*, 2016:1-2). Based on this, 2,4-substituted quinazolinone derivatives were generated in this study and investigated as potential anti-infective agents. The interest was to generate new derivatives incorporating piperazine or related moiety at position 4. According to a recent statistical analysis of substructures, piperazine (a diamine molecule) is the third most commonly used small molecule in pharmaceuticals (Jalageri *et al.*, 2021:15213).

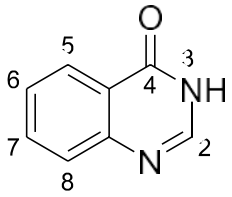

Figure 3.2: Basic structure of quinazolinone

3.2 Results and discussion

This section describes how target compounds were synthesised and evaluated for antiprotozoal, antitubercular, antibacterial and antifungal activities. The toxicity of target compounds were also established.

3.2.1 Chemistry

Target compounds were formed following the synthetic route in Scheme 1. As a starting material, 2-aminobenzamide was used to react with different aldehydes in a cyclisation reaction mediated by iodine to form **Compound 1** with a 61–149% yield. **Compound 1** underwent chlorination using thionyl chloride to form **Compound 2** with a 55–92% yield. **Compound 3** underwent nucleophilic substitution reaction (nucleophilic substitution reactions belong to a category of chemical reactions where an electron-rich

nucleophile reacts with a positively charged electrophile, leading to the displacement of a leaving group) in the presence of appropriate amines under refluxing conditions to furnish **Compounds 3–5** with yields ranging from 5–54%. Reactions were monitored using thin-layer chromatography (TLC) and the results are presented in **Scheme 1**.

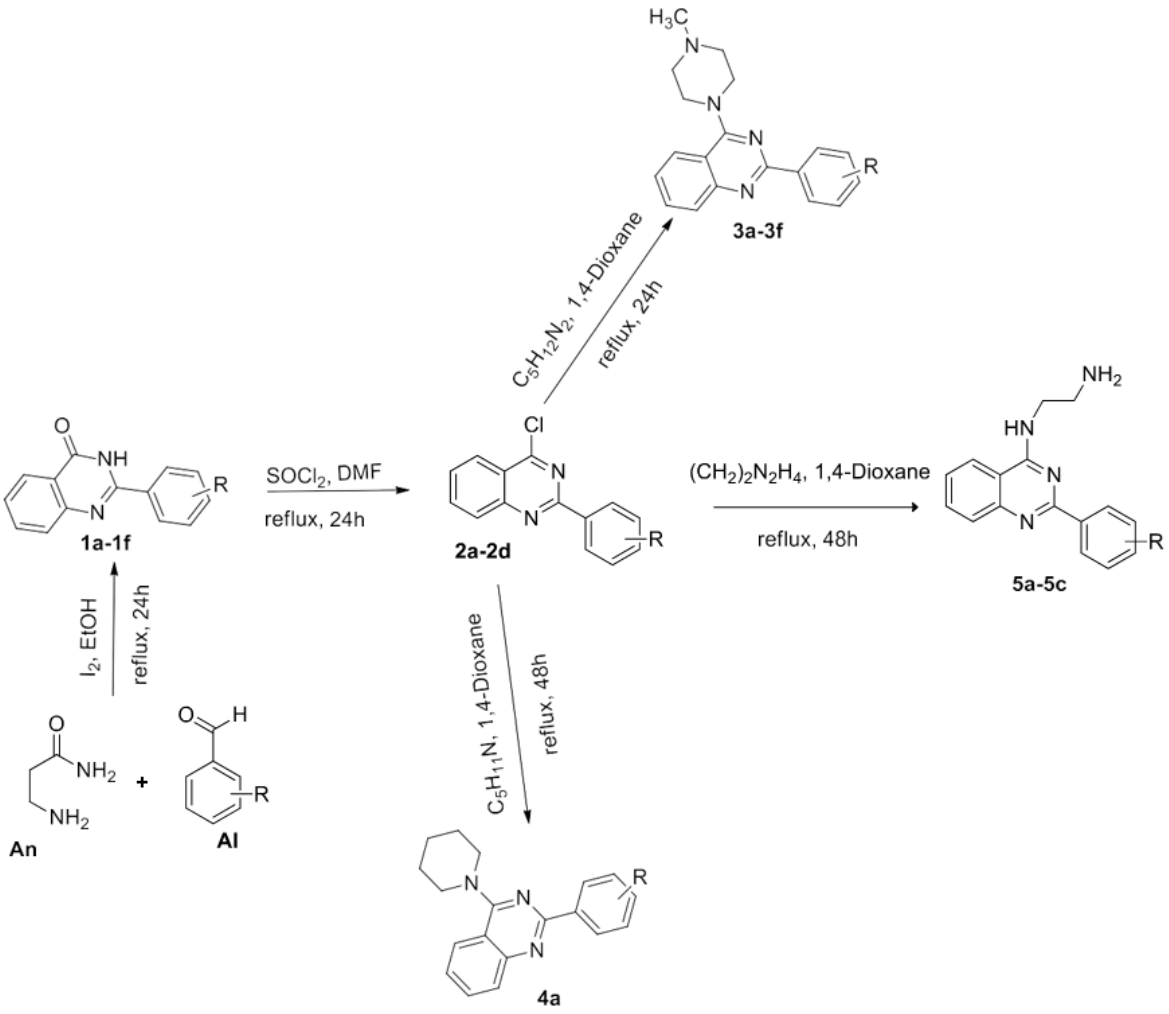

Scheme 1: Synthesis of target compounds (Source: own)

*Percentage yield		R		
1a: 2,4-OCH_3, 100%*	2a: 3-F, 55%	3a: 3-F, 5%	4a: 4-Br, 20%	5a: 4-Br, 32%
1b: 2-CH_3, 83%	2b: 4-F, 78%	3b: 2,4-OCH_3, 41%		5b: 4-F, 7%
1c: 3-Cl, 66%	2c: 3-Cl, 91	3c: 4-F, 18%		5c: 3-Cl, 34%
1d: 3-F, 74%	2d: 4-Br, 92%	3d: 2-CH_3, 25%		
1e: 4-OH, 61%		3e: 4-NO_2, 43%		

1f: 4-Br, 84% 3f: 4-Br, 54%

Using Fourier-transform infrared (FTIR), proton (^{1}H) and carbon-13 (^{13}C) nuclear magnetic resonance (NMR), and high-resolution mass spectrometry (HRMS), the structures of the target **Compounds 1a–1f, 2a–2f, 3a–3f, 4a**,and **5a–5d** were established. The diagnostic visible peaks are listed below:

- The FTIR spectra of **Compounds 1a–1f** showed absorbance at wavelengths indicative of their functional groups. The C=0 group of the quinazolinone is visible as a strong intense peak between 1 650 cm^{-1} and 1 800 cm^{-1}. The N-H group is visible as a broad medium-intensity peak between 3 100 cm^{-1} and 3 500 cm^{-1}.
- The FTIR spectra for **Compounds 2a–2d** showed the C-Cl stretch between 500 cm^{-1} and 730 cm^{-1} as a strong intense peak. The N-H functional group peak of **Compounds 1a–1f** disappears in these spectra.
- For **Compounds 3a–3f**, the -CH_3 group of the piperazine ring stretch is visible between 2 110 cm^{-1} and 3 175 cm^{-1} as a broad weaker peak. The FTIR spectra for **Compounds 5a–5c** showed the N-H peaks between 2 851 cm^{-1} and 3 950 cm^{-1} as broad medium-intensity peaks.
- All target compounds were confirmed using ^{1}H and ^{13}C NMR. In ^{1}H NMR spectra of **Compounds 1a–1f** and **2a–2d**, the quinazolinone and quinazoline rings are represented by doublet and triplet peaks in the 7–8.5 ppm range. This confirms that the cyclisation reaction was successful. The ^{13}C NMR spectra of **Compounds 1a–1f** and **2a–2d** shows all the carbon peaks in the 115–165 ppm range. This is indicative of all the carbons in the compounds and suggests that cyclisation occurred fully and chlorination took place.
- The ^{1}H NMR of **Compounds 3a–3f** contains two triplet peaks occurring at 2.25 ppm and 3.84 ppm. These peaks are representative of the piperazine ring, and the occurrence of a singlet peak at 2.28 ppm is representative of the -CH_3 moiety. The doublets and triplets in the range 7–8.5 ppm are the quinazoline moiety.
- In the ^{13}C NMR spectra of these compounds, the peaks at 49.5 and 54.9 ppm indicate the piperazinyl ring. The peak at 46 ppm is the -CH_3 unit. The peaks in the up-field region are representative of the quinazoline moiety.

HRMS was performed for all compounds (**1–5**) and the results confirmed the masses of the compounds. Trace solvent impurities of ethanol were present in some of the NMR spectra. Prior to biological evaluations, a desiccator was used to dry these compounds for three days.

3.2.2 Antiprotozoal activity

In **Table 3.1** it is evident that **Compound 1e** has low antiprotozoal activity and low toxicity with values of > 64.00 µM, 57.75 µM, 36.76 µM, > 64.00 µM, and > 64.00 µM against MRC-5, *T. cruzi*, *L. infantum*, *T.b. brucei*, and *T.b. rhodesiense*, respectively. **Compounds 2a** and **2c** were generally inactive, with only moderate activity against *T. cruzi* and *L. infantum*. **Compounds 3a–3f** generally exhibited non-intrinsic antitrypanosomal activity. **Compound 3a** exhibited moderate and equipotent activity of 8 µM against *L. infantum* and *T.b. rhodesiense*, and showed low cytotoxicity against MRC-5 cells. **Compound 3c** also demonstrated low micromolar (< 10 µM) activities against *T. cruzi*, *T.b. brucei*, and *T.b. rhodesiense* and moderate cytotoxicity of 18 µM against MRC-5 cells. **Compound 3f** showed the best activity (4.80 µM, 2.52 µM, 2.42 µM, and 1.82 µM against *T. cruzi*, *L. infantum*, *T.b. brucei*, and *T.b. rhodesiense*, respectively) followed by **Compound 3e** (7.04 µM, 2.30 µM, 3.81 µM, 2.05 µM, and 8.00 µM against *T. cruzi*, *L. infantum*, *T.b. brucei*, and *T.b. rhodesiense*, respectively). These compounds, however, exhibited toxicity in MRC-5 and primary mouse macrophages (PMMs). **Compound 4a** exhibited poor to no antitrypanosomal activity with IC_{50} values > 46.48 µM. **Compound 5a** presented the best activity of 0.55 µM, 1.26 µM, 0.22 µM, and 0.13 µM against, *T. cruzi*, *L. infantum*, *T.b. brucei*, and *T.b. rhodesiense*, respectively, but also showed strong cytotoxicity (4.43 µM) against the MRC-5 cell line. Although most of the **Compounds 5a–5d** had good activity compared with the reference drugs, they exhibited high toxicity levels.

Table 3.1: Chemical structures and antitrypanosomal activity of target compounds

		IC-50 (µM)					
ID	**R**	**MRC-5**	***T. cruz***	***L. inf***	***T. bruc***	***T. rhod***	**PMM**
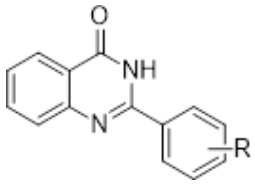							
1d	**3-F**	> 64.00	57.75	36.76	> 64.00	> 64.00	**> 64.00**
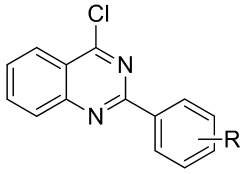							
2a	**3-F**	> 64.00	24.25	29.63	> 64.00	> 64.00	**> 64.00**
2c	**3-Cl**	> 64.00	10.77	28.98	> 64.00	> 64.00	**> 64.00**
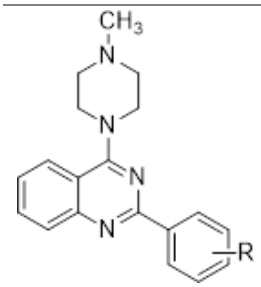							
3a	**3-F**	23.09	24.55	8.00	12.44	8.00	**> 64.00**
3b	**2,4-OCH_3**	4.54	5.43	5.15	5.04	6.73	**32.00**
3c	**4-F**	18.15	8.12	10.08	4.17	4.84	**32.00**
3d	**2-CH_3**	8.44	8.72	27.09	22.03	22.74	**> 64.00**
3e	**4-NO_2**	7.50	7.04	2.30	3.81	2.05	**8.00**
3f	**4-Br**	6.06	4.80	2.52	2.42	1.82	**32.00**
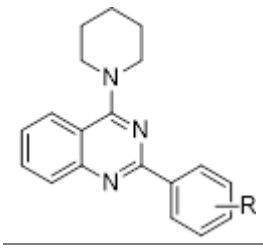							

		IC-50 (µM)					
ID	**R**	**MRC-5**	***T. cruz***	***L. inf***	***T. bruc***	***T. rhod***	**PMM**
4a	**-Br**	> 64.00	> 64.00	46.48	> 64.00	> 64.00	**> 64.00**
	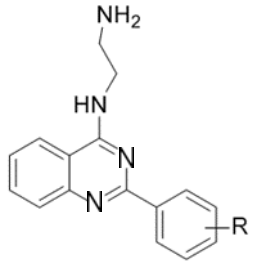						
5a	**4-Br**	4.43	0.55	1.26	0.22	0.13	**8.00**
5b	**4-F**	5.72	6.94	5.54	2.09	0.50	**32.00**
5c	**3-Cl**	5.04	1.99	2.03	0.40	0.50	**2.00**
***Tamoxifen**		17.05	–	–	–	–	**–**
***Benznidazol**		–	1.47	–	–	–	**–**
***Miltefosine**		–	–	6.35	–	–	–
***Suramin**		–	–	–	0.05	0.04	–

*= Reference drugs; MRC-5 = Lung fibroblast tissues; *T. cruz* = *Trypanosoma cruzi*; *L. inf* = *Leishmania infantum*; *T. bruc* = *Trypanosoma brucei brucei; T. rhod* = *Trypanosoma brucei rhodesiense*; PMM = Primary mouse macrophage cytotoxicity.

3.2.3 Antitubercular activity

The antitubercular activity of all compounds was tested *in vitro* against the gfp strain of *M. tuberculosis* in casein (CAS) and albumin (ADC) medium. Rifampicin, the standard antitubercular medication, served as a reference. During day 7 and day 14 of the incubation period, the minimal inhibitory concentration required to inhibit 90% of the growth (MIC_{90}) of mycobacteria was determined. The gfp reporter strain of *M. tuberculosis* was grown in two different media supplements, namely ADC medium supplemented with Tween 80 and CAS medium supplemented with tyloxapol. To determine the MIC, 10 serial dilutions per sample were prepared and their bacterial growth inhibitory effect were evaluated, which allowed for the construction of a dose-response curve. The MIC_{90} value was determined as the sample concentration required to inhibit 90% of bacterial growth. MIC_{90} values were collected from both ADC and CAS media on days 7 and 14. **Table 3.2** summarises the antitubercular activity results of the investigated compounds.

Table 3.2: Antimicrobial and cytotoxic activities of **Compounds 4a**, **3a-3f** and **5a-5c** in CAS and ADC medium

ID	R	MIC_{90} (µM) [Media: 7H9 CAS GLU Tx, Day: 7]	MIC_{90} (µM) [Media: 7H9 CASGLU Tx, Day: 14]	MIC_{90} (µM) [Media: 7H9 ADC GLU Tw, Day: 7]	MIC_{90} (µM) [Media: 7H9 ADC GLU Tw, Day: 14]
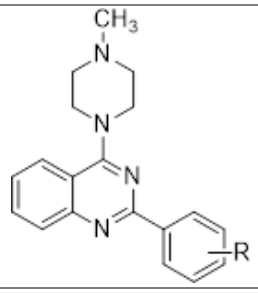					
3a	**3-F**	3.330	8.481	62.5	125
3b	**2,4-OCH_3**	0.488	2.114	38.730	62.500
3c	**4-F**	2.201	7.134	32.468	62.500
3d	**2-CH_3**	9.220	22.413	> 125	> 125
3e	**4-NO_2**	1.546	4.339	32.735	62.500
3f	**4-Br**	0.488	0.873	15.625	31.250
4a	**-Br**	> 125	> 125	> 125	> 125
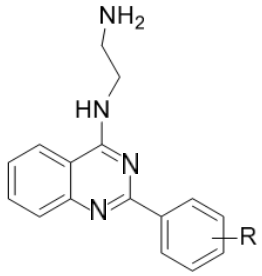					
5a	**4-Br**	0.488	0.868	16.623	31.288
5b	**4-F**	0.488	2.169	62.500	125.000
5c	**3-Cl**	0.488	0.925	31.250	30.069
	RIF	0.011	0.017	0.001	0.002

*RIF (Rifampicin) = Reference drug

*Media: 7H9 CAS GLU Tx = mycobacterial broth base, Middlebrook (7H9) and glucose (GLU) supplement, casitone (CAS) and tyloxapol (Tx)

*Media: 7H9 ADC GLU Tw = mycobacterial broth base, Middlebrook (7H9) and glucose (GLU) supplement, albumin–dextrose–catalase (ADC) and Tween-80 (Tw)

Compounds 3a–3c, **3e**, **3f**, and **5a–5c** presented good antitubercular activity ranging from 0.488–3.330 µM on day 7 and 0.868–8.481 µM on day 14 in the CAS medium. **Compounds 3f** and **5a** exhibited the best activity in the ADC medium out of all the compounds with MIC_{90} values ranging from 15.625–31.25 µM from day 7–14 for **Compound 3f** and 16.623–31.288 µM from day 7–14 for **Compound 5a**. This can be due to the bromine (-Br) group being an electron withdrawing group as both these compounds consist of a bromine attached to the phenyl ring in the para-position. **Compound 3d** presented moderate antitubercular activity in the CAS medium ranging from 9.220–22.413 µM from day 7–14 for **Compound 3d**. **Compound 5a**, having a bromine (-Br) group in the position 2 of the phenyl ring of the quinazoline moiety, presented the best antitubercular activity of 0.488–0.868 µM in the CAS medium. **Compound 3b**, which has a disubstitution of OCH_3, exhibited good antitubercular activity, implying that increasing the number of substitutions can enhance activity. **Compound 4a** showed no antitubercular activity irrespective of the culture media. **Compound 3d**, having a methyl ($-CH_3$) group at the para-position of the phenyl ring attached at position 2 of the quinazoline nucleus showed the least antitubercular activity in the ADC medium.

3.2.4 Antibacterial and antifungal activities

The antibacterial activity of **Compounds 2a–2c, 3a–3f, 4a**, and **5a–5c** were assessed against *E. coli* (ATCC 25922), *K. pneumoniae* (ATCC 700603), *A. baumannii* (ATCC 19606), *P. aeruginosa* (ATCC 27853), *S. aureus*, and methicillin-resistant *S. aureus* (ATCC 43300). Approved antibacterial drugs, namely colistin and vancomycin, were used as reference drugs. Every compound demonstrating an MIC value of equal or less than 16 µg/mL was categorised as a hit. Compounds were generally inactive (MIC: > 32 µg/mL and D_{max} of < 50) against all bacteria deployed.

The antifungal effectiveness of these compounds against *Candida albicans* (ATCC 90028*)* was also examined. Just one substance, namely **Compound 2b** (< 32 µg/mL), showed potent activity against *C. albicans*. The rest of the series was generally inactive, showing MIC: > 32 µg/mL.

3.3 Materials and methods

The section that follows describe the method that was used to synthesise a series of 2,4-disubstituted quinazolines.

3.3.1 General methods

Reagents and solvents were bought from several chemical vendors, such as Ambeed, Labchem, Merck, Rochelle, and AK Scientific. Merck 60F_{254} silica gel sheet supported on aluminium was used to perform TLC to monitor reaction progress. The developed sheets were examined using ultraviolet light (254 nm and 366 nm) or iodine vapour staining. Using a Buchi B-545 device, melting points (m.p.) were calculated. A Bruker ALPHA FTIR Routine spectrometer was used to perform FTIR. Using a Bruker Avance III 600 spectrophotometer, ^{1}H and ^{13}C NMR spectra were recorded at 600 MHz and 151 MHz, respectively, in deuterated dimethyl sulfoxide (DMSO)-d_6. Chemical shifts are given in parts per million (ppm) and were compared with the solvent peaks (DMSO-d_6: 2.50 ppm and 39.52 ppm for ^{1}H and ^{13}C NMR, respectively). Spin multiplicities are denoted as follows: s for singlet, d for doublet, t for triplet, m for multiplet, dt for doublet of triplets, td for triplet of doublets, dd for doublet of doublets, qd for quartet of doublets, and qt for quartet of triplets. Coupling constants (*J*) included are measured in Hz.

HRMS were recorded using a Bruker micrOTOF-Q II mass spectrometer set in positive ion mode. At a capillary voltage of 4 500 V, an end plate offset of −500 V, 1.8 bar nebulisers, and a collision cell radio frequency voltage of 150 Vpp, a complete scan from 50 m/z to 1 600 m/z was performed. High-performance liquid chromatography (HPLC) analysis using an Agilent 1200 series HPLC system outfitted with a quaternary pump and an Agilent 1200 series diode array detector was used to ascertain the purity of the compound. The mobile phase was initially composed of 10% methanol and 90% Milli-Q water at a flow rate of 1 mL/min, and the separation was performed using a Venusil XBP C18 column (4.60 150 mm, 5 m). The substances were dissolved in acetonitrile of HPLC grade, and 10 µl of the mixture was injected. The samples were examined at 280 nm and 400 nm wavelengths with a flow rate of 1 mL/min. Each HPLC run lasted 13 minutes, with an equilibration time of five minutes in between.

3.3.2 Synthesis of target compounds

A series of 2,4-disubstituted quinazolines were synthesised. Some compounds were used as intermediates to form additional target compounds.

3.3.2.1 Synthesis of target Compounds 1a–1f (cyclisation)

A 100 mL round bottom flask was charged with 1 g (1 mole) of anthranilamide, 1.2 equivalence (eqvi) of various aldehydes, 1 eqvi of I_2 and 20 mL of ethanol as solvent. The mixture was heated under reflux for 24 hours and monitored via TLC. After the anthranilamide was consumed completely, the reaction mixture was let to cool to room temperature. Sodium thiosulphate solution (5 g sodium thiosulphate in 50 mL water) was added to the reaction mixture and stirred for five minutes. The formed precipitant was filtered and dried in a fume hood. Some of these compounds were used as intermediates to form target **Compounds 2a–2f**.

3.3.2.2 Synthesis of target Compounds 2a–2d (chlorination)

Into a 100 mL round bottom flask, 0.7–1 g of **Compounds 1a–1f**, 10 mL of thionyl chloride, and 1 mL of dimethylformamide were added. The reaction mixture was refluxed for 24 hours or until it reached completion as indicated by TLC analysis. After reaction completion, the mixture was cooled to room temperature, ice added and the stirred until a precipitation was formed. The resultant precipitate was then filtered, and dried to form **Compound 2a–2d** with a 55–92% yield.

3.3.2.3 Synthesis of target Compounds 3a–3f, 4a, 5a–c (nucleophilic substitution reaction)

A mixture of 0.4–1 g of **Compounds 2a–2d**, 10 eqvi of the appropriate amine, 10 mL of 1,4-dioxane in a round bottom flask was refluxed for 24 hours. After reaction completion, the reaction mixture was cooled to room temperature. H_2O was added to the mixture and the formed precipitation was filtered and dried.

In some cases where a precipitation did not occur after adding water to the reaction mixture, liquid-liquid extraction with ethyl acetate (15 ml) and water (15 ml) was used. With **Compounds 3b** and **3c**, the final solid powders were washed with warm water and filtered to get rid of impurities. All compounds were recrystallised from ethanol.

3.3.2.4 Synthesised target compounds

The following target compounds were synthesised:

2-(2,4-dimethoxyphenyl)quinazolin-4(3H)-one **(1a)**

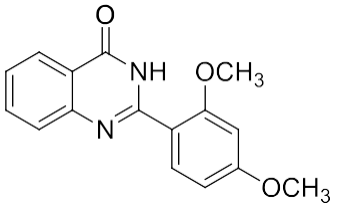

Purple powder; 100% yield; m.p.: 144–148˚C; ^{1}H NMR (600 MHz, Ace-d6) δ 12.62 (s, 1H), 8.17–8.10 (m, 3H), 7.85 (ddd, J = 8.5, 7.0, 1.6 Hz, 1H), 7.78 – 7.73 (m, 2H), 7.56 – 7.52 (m, 1H), 4.35 (s, 3H), 3.85 (s, 3H). ^{1}3C NMR (151 MHz, Ace-d_6) δ 164.23, 160.79, 159.72, 149.64, 149.33, 134.15, 132.55, 127.23, 126.29, 125.76, 121.10, 106.85, 101.97, 98.67, 55.96, 55.20.; IR V_{max} cm^{-1}: 3 319.52 (N-H stretch), 1 678.94 (C=O stretch), 1 612.61 (C=N stretch), 1 250.94 (C-N stretch), 1 593.05 (C-O stretch), 1 210.14 (O-CH_3 stretch). m/z HRMS (APCI) found 238.1082 calcd for $C_{16}H_{15}N_2O_3$ 283.1077 $[M + H]^+$; Purity (HPLC): 86%.

2-(o-tolyl)quinazolin-4(3H)-one **(1b)**

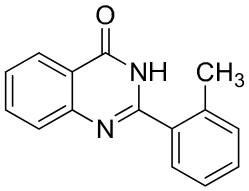

White powder; 83% yield; m.p.: 195–197˚C; ^{1}H NMR (600 MHz, Ace-d_6) δ 8.26 (d, J = 8.0 Hz, 1H), 7.82 (t, J = 7.8 Hz, 1H), 7.73 (d, J = 8.2 Hz, 1H), 7.62 (d, J = 7.8 Hz, 1H), 7.53 (t, J = 7.6 Hz, 1H), 7.43 (d, J = 7.6 Hz, 1H), 7.40–7.28 (m, 2H), 2.52 (s, 3H). ^{13}C NMR (151 MHz, Ace-d_6) δ 161.58, 154.17, 149.23, 136.69, 134.24, 130.78, 129.96, 128.96, 127.64, 126.48, 125.94, 125.75, 125.23, 121.47, 19.19; IR V_{max} cm^{-1}: 3 125.64 (N-H stretch), 1 675.96 (C=O stretch), 1 609.20 (C=N stretch), 1 255.62 (C-N stretch), 2 905.31 (C-CH_3 stretch). m/z HRMS (APCI) found 237.1020 calcd for $C_{15}H_{13}N_2O$ 237.1022 $[M + H]^+$; Purity (HPLC): 87.3%.

2-(3-chlorophenyl)quinazolin-4(3H)-one **(1c)**

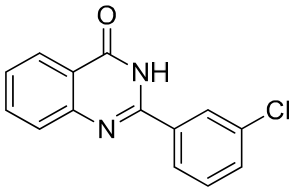

White powder; 66% yield; m.p.: 289–293˚C; ^{1}H NMR (600 MHz, DMSO-d6) δ 12.62 (s, 1H), 8.24 (t, *J* = 2.0 Hz, 1H), 8.16 (td, J = 7.5, 1.5 Hz, 2H), 7.86 (ddd, J = 8.4, 7.1, 1.6 Hz, 1H), 7.77 (dd, J = 8.2, 1.1 Hz, 1H), 7.67 (ddd, J = 8.1, 2.2, 1.1 Hz, 1H), 7.57 (dt, J = 22.9, 7.5 Hz, 2H), ^{13}C NMR (151 MHz, DMSO-*d*$_6$) δ 162.58, 151.29, 148.94, 135.17, 133.93, 131.63, 131.00, 128.09, 128.01, 127.41, 126.90, 126.35, 121.58; IR V_{max} cm^{-1}: 3 381.44 (N-H stretch), 1 672.50 (C=O stretch), 1 564.95 (C=N stretch), 1 270.57 (C-N stretch), 793.13 (C-Cl stretch). m/z HRMS (APCI) found 257.0468 calcd for $C_{14}H_{10}ClN_2O$ 257.0476 $[M + H]^+$; Purity (HPLC): 85.4%.

2-(3-fluorophenyl)quinazolin-4(3H)-one **(1 d)**

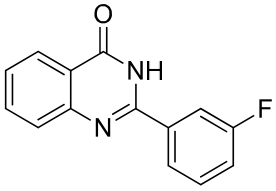

White powder; 74% yield; m.p.: 210°C; ^{1}H NMR (600 MHz, DMSO-*d*$_6$) δ 8.16 (dd, *J* = 7.9, 1.6 Hz, 1H), 8.06 (dd, *J* = 7.6, 1.7 Hz, 1H), 8.01 (dt, *J* = 10.4, 2.3 Hz, 1H), 7.87 – 7.81 (m, 2H), 7.75 (d, *J* = 8.1 Hz, 1H), 7.60 (td, *J* = 8.1, 6.0 Hz, 1H), 7.53 (t, *J* = 7.5 Hz, 1H), 7.44 (td, *J* = 8.5, 2.7 Hz, 1H). ^{13}C NMR (151 MHz, DMSO-*d*$_6$) δ 162.89, 161.28, 148.51, 134.57, 130.74, 130.69, 127.49, 126.78, 125.88, 123.93, 121.13, 118.10, 114.55, 114.45; IR V_{max} cm^{-1}: 3 365.49 (N-H stretch), 1 674. 57 (C=O stretch), 1 580.82 (C=N stretch), 1 278.01 (C-N stretch), 1 199.42 (C-F stretch). m/z HRMS (APCI) found 241.0765 calcd for $C_{14}H_{10}FN_2O$ 241.0772 $[M + H]^+$; Purity (HPLC): 96.5%.

2-(4-hydroxyphenyl)quinazolin-4(3H)-one **(1e)**

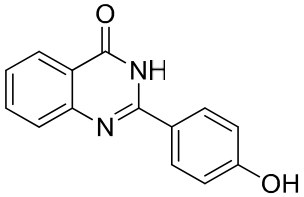

White powder; 61% yield; m.p.: 210°C; ^{1}H NMR (600 MHz, Ace-*d*$_6$) δ 11.20 (s, 1H), 8.83 (s, 1H), 8.23 (dd, J = 7.9, 1.5 Hz, 1H), 7.88–7.81 (m, 1H), 7.79–7.73 (m, 3H), 7.52 (t, J = 7.5 Hz, 1H), 7.41 (t, J = 7.9 Hz, 1H), 7.09 (dd, J = 8.1, 2.5 Hz, 1H). ^{13}C NMR (151 MHz, Ace-*d*$_6$) δ 162.00, 157.84, 152.13, 149.34, 134.59, 134.36, 129.78, 127.77, 126.38, 126.01, 121.51, 118.51, 118.43, 114.44. IR V_{max} cm^{-1}: 3 191.95 (N-H stretch),

1 657.43 (C=O stretch), 1 604.43 (C=N stretch), 1 102.22 (C-N stretch) 3130.36 (C-OH stretch). m/z HRMS (APCI) found 239.0827 calcd for $C_{14}H_{11}N_2O_2$ 239.0815 $[M + H]^+$; Purity (HPLC): 91.5%.

2-(4-bromophenyl)quinazolin-4(3H)-one **(1f)**

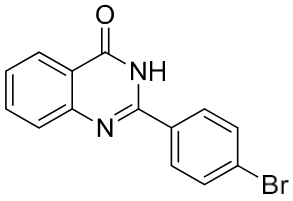

Cream powder; 84% yield; m.p.: 308–309°C; ^{1}H NMR (600 MHz, DMSO-d_6) δ 12.61 (s, 1H), 8.30–7.97 (m, 3H), 7.88–7.82 (m, 1H), 7.76 (dd, J = 11.7, 8.1 Hz, 3H), 7.54 (t, J = 7.5 Hz, 1H). ^{13}C NMR (151 MHz, DMSO-d_6) δ 169.71, 162.63, 151.97, 149.03, 135.15, 132.40, 132.09, 130.28, 127.97, 127.26, 126.35, 125.70, 121.48, 117.12; IR V_{max} cm^{-1}: 3 026.66 (N-H stretch), 1 667.85 (C=O stretch), 1 556.32 (C=N stretch), 1 182.52 (C-N stretch), 547.65 (C-Br stretch). m/z HRMS (APCI) found 300.9967 calcd for $C_{14}H_{10}BrN_2O$ 300.9971 $[M + H]^+$; Purity (HPLC): 98.1%.

4-chloro-2-(3-fluorophenyl)quinazoline **(2a)**

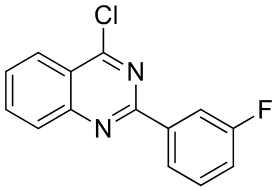

Light green powder; 55% yield; 116°C; ^{1}H NMR (600 MHz, DMSO-d_6) δ 8.17 (dd, J = 7.9, 1.5 Hz, 1H), 8.06 (dt, J = 7.9, 1.2 Hz, 1H), 8.01 (ddd, J = 10.4, 2.6, 1.7 Hz, 1H), 7.87 (ddd, J = 8.5, 7.1, 1.6 Hz, 1H), 7.79 (d, J = 8.1 Hz, 1H), 7.62 (td, J = 8.1, 5.9 Hz, 1H), 7.56 (ddd, J = 8.1, 7.0, 1.2 Hz, 1H), 7.47 (td, J = 8.5, 2.6 Hz, 1H). ^{13}C NMR (151 MHz, DMSO-d_6) δ 163.33, 162.52, 161.71, 151.82, 148.36, 135.25, 131.27, 127.63, 127.50, 126.40, 124.53, 121.51, 118.82, 115.07; IR V_{max} cm^{-1}: 1 564.11 (C=N stretch), 727.07 (C-Cl stretch), 1 548.04 (C=N stretch), 1 262.81 (C-N stretch), 1 188.57 (C-F stretch). m/z HRMS (APCI) found 259.0444 calcd for $C_{14}H_9ClFN_2$ 259.0433 $[M + H]^+$; Purity (HPLC): 86.2%.

4-chloro-2-(4-fluorophenyl)quinazoline **(2b)**

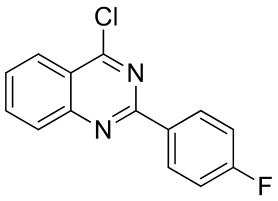

Brown powder; 78% yield; m.p.: 199°C; ^{1}H NMR (600 MHz, DMSO-d_6) δ 8.26–8.23 (m, 1H), 8.17 (dd, *J* = 7.9, 1.5 Hz, 1H), 8.09 (d, *J* = 2.5 Hz, 1H), 7.90–7.85 (m, 1H), 7.80 (d, *J* = 8.1 Hz, 1H), 7.74 (s, 1H), 7.56 (t, *J* = 7.5 Hz, 1H), 7.43 (t, *J* = 8.8 Hz, 1H), 7.32 (s, 1H). ^{13}C NMR (151 MHz, DMSO-d_6) δ 165.55, 163.89, 162.41, 152.66, 147.71, 135.34, 131.25, 128.80, 127.40, 126.88, 126.45, 121.15, 116.24, 116.10; IR V_{max} cm^{-1}: 1 600.05 (C=N stretch), 510 (C-Cl stretch), 1 637.45 (C=N stretch), 1 292.42 (C-N stretch), 1 165.65 (C-F stretch). m/z HRMS (APCI) found 259.0421 calcd for $C_{14}H_9ClFN_2$ 259.0433 $[M + H]^+$; Purity (HPLC): 86%.

4-chloro-2-(3-chlorophenyl)quinazoline **(2c)**

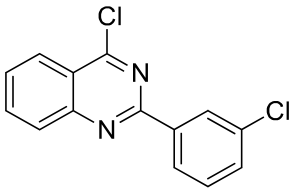

Light pink powder; 91% yield; 207-210°C; ^{1}H NMR (600 MHz, DMSO-d_6) δ 8.23 (t, *J* = 2.0 Hz, 1H), 8.16 (ddd, *J* = 19.9, 8.0, 1.6 Hz, 2H), 7.90–7.86 (m, 1H), 7.81 (d, *J* = 8.1 Hz, 1H), 7.68 (td, *J* = 8.9, 8.5, 1.9 Hz, 1H), 7.63–7.49 (m, 2H). ^{13}C NMR (151 MHz, DMSO-d_6) δ 162.40, 152.03, 147.95, 135.32, 134.57, 133.92, 131.88, 131.02, 128.21, 127.62, 127.33, 127.12, 126.43, 121.44; IR V_{max} cm^{-1}: 1 565.69 (C=N stretch), 725.21 (C-Cl stretch), 1 609.73 (C=N stretch), 1 331.00 (C-N stretch), 714.64 (C-Cl stretch). m/z HRMS (APCI) found 275.0143 calcd for $C_{14}H_9Cl_2N_2$ 275.0137 $[M +H]^+$; Purity (HPLC): 47.3%.

2-(4-bromophenyl)-4-chloroquinazoline **(2d)**

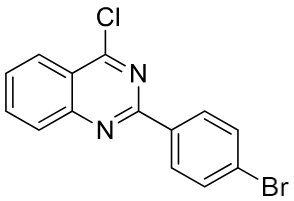

Pink powder; 92% yield; m.p.: 211–214°C; ^{1}H NMR (600 MHz, DMSO-d_6) δ 8.17 (dd, J = 7.9, 1.5 Hz, 1H), 8.14–8.09 (m, 2H), 7.87 (ddd, J = 8.5, 7.0, 1.6 Hz, 1H), 7.80 (td, J = 7.2, 1.6 Hz, 4H), 7.57 (ddd, J = 8.1, 7.0, 1.2 Hz, 1H). ^{13}C NMR (151 MHz, DMSO-d_6) δ 162.43, 152.59, 147.92, 135.32, 133.97, 132.12, 131.68, 130.51, 127.50, 127.16, 126.45, 126.05, 122.12, 121.33.; IR V_{max} cm^{-1}: 1636.69 (C=N stretch), 756.06 (C-Cl stretch), 1 590.33 (C=N stretch), 1 120.57 (C-N stretch), 531.28 (C-Br stretch). m/z HRMS (APCI) found 318.9769 calcd for $C_{15}H_{11}BrClN$ 318.9758 $[M + H]^+$; Purity (HPLC): 96%.

2-(3-fluorophenyl)-4-(4-methylpiperazin-1-yl)quinazoline **(3a)**

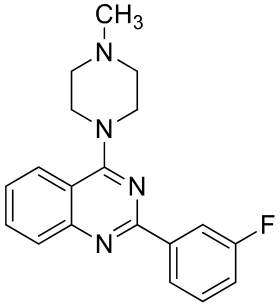

Light brown powder; 5% yield; m.p.: 76–78°C; ^{1}H NMR (600 MHz, Ace-d_6) δ 8.44 (dt, J = 7.8, 1.3 Hz, 1H), 8.30 (ddd, J = 10.8, 2.8, 1.5 Hz, 1H), 8.08 (dd, J = 8.3, 1.5 Hz, 1H), 7.93 (dd, J = 8.5, 1.5 Hz, 1H), 7.82 (ddd, J = 8.4, 6.9, 1.5 Hz, 1H), 7.56–7.51 (m, 2H), 7.25 (td, J = 8.4, 2.6 Hz, 1H), 3.93 (t, J = 4.9 Hz, 4H), 2.68–2.61 (m, 4H), 2.34 (d, J = 2.1 Hz, 3H). ^{13}C NMR (151 MHz, Ace-d_6) δ 164.84, 163.88, 162.27, 157.56, 152.73, 141.60, 141.58, 132.56, 129.93, 128.80, 125.18, 124.04, 116.63, 116.49, 115.49, 114.45, 54.79, 49.61, 45.38; IR V_{max} cm^{-1}: 1 591.08 (C=N stretch), 1 561.69 (C=N stretch), 1 166.38 (C-F stretch), 1 246.64 (C-N stretch), 1 166.38 (C-N stretch), 3 074.24 (C-H stretch), 1 257.11 (C-N stretch), 2843.10 (C-H stretch). m/z HRMS (APCI) found 323.1662 calcd for $C_{19}H_{20}FN_4$ 323.1667 $[M + H]^+$; Purity (HPLC): 98.5%.

2-(2,4-dimethoxyphenyl)-4-(4-methylpiperazin-1-yl)quinazoline **(3b)**

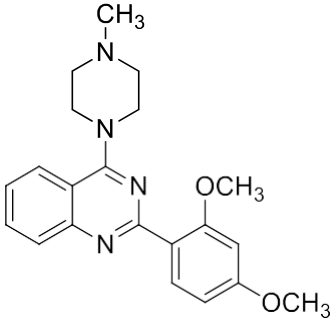

Yellow-brown powder; 41% yield; 90°C; ^{1}H NMR (600 MHz, DMSO-*d*$_6$) *δ* 8.05–8.02 (m, 1H), 7.88 (ddd, *J* = 8.3, 6.5, 1.7 Hz, 1H), 7.56 (ddd, *J* = 8.3, 6.4, 1.9 Hz, 1H), 7.50 (s, 1H), 6.90 (s, 1H), 33.91 (s, 3H), 3.89 (s, 3H), 3.87–3.85 (m, 4H), 3.04 (t, *J* = 5.1 Hz, 4H), 2.41–2.38 (m, 4H). ^{13}C NMR (151 MHz, DMSO-*d*$_6$) *δ* 174.44, 157.83, 155.08, 150.31, 148.67, 142.38, 134.42, 127.37, 126.50, 116.96, 99.35, 97.63, 73.34, 61.06, 57.07, 54.87, 49.47, 46.04, 43.60; IR V_{max} cm^{-1}: 1 599.24 (C=N stretch), 1 562.40 (C=N stretch), 1 206.33 (C-O stretch), 1 284.23 (C-O stretch), 2 935.73 (C-H stretch), 2 793.02 (C-H stretch), 1 141.29 (C-N stretch), 1 284.23 (C-N stretch), 2 840.09 (C-H stretch).

2-(4-fluorophenyl)-4-(4-methylpiperazin-1-yl)quinazoline **(3c)**

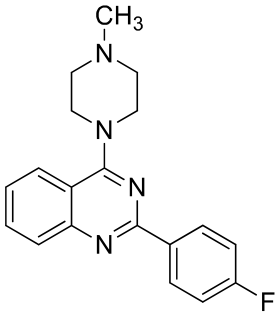

Brown powder; 18% yield; m.p.: 164–166°C; ^{1}H NMR (600 MHz, DMSO-*d*$_6$) *δ* 8.56–8.50 (m, 1H), 8.27–8.22 (m, 1H), 8.16 (dd, *J* = 7.9, 1.6 Hz, 1H), 8.00 (dd, *J* = 8.4, 1.3 Hz, 1H), 7.90–7.79 (m, 1H), 7.74 (dd, *J* = 8.2, 1.2 Hz, 1H), 7.56–7.49 (m, 1H), 7.43–7.37 (m, 1H), 7.36–7.27 (m, 1H), 7.23–7.11 (m, 1H), 3.94–3.67 (m, 2H), 3.39 (d, *J* = 44.7 Hz, 4H), 2.58 (t, *J* = 4.9 Hz, 2H), 2.28–2.12 (m, 1H). ^{13}C NMR (151 MHz, DMSO-*d*$_6$) *δ* 165.34, 164.99, 163.35, 157.65, 152.56, 139.59, 135.10, 133.40, 130.87, 130.71, 129.72, 128.77, 127.07, 125.80, 116.17, 115.03, 54.88, 49.53, 46.11; IR V_{max} cm^{-1}: 1 599.27 (C=N stretch), 1 580.31 (C=N stretch), 1 145.41 (C-F stretch), 1 268.13 (C-N stretch), 1 216.94 (C-N stretch), 2 843.69 (C-H stretch). m/z HRMS (APCI) found 323.1678 calcd for $C_{19}H_{20}FN_4$ 323.1667 $[M + H]^+$; Purity (HPLC): 74%.

4-(4-methylpiperazin-1-yl)-2-(o-tolyl)quinazoline **(3d)**

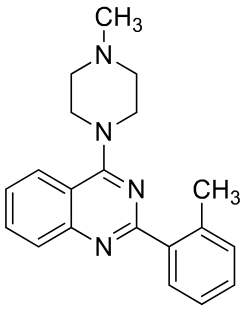

Dark brown powder; 25% yield; m.p.: 124°C; ^{1}H NMR (600 MHz, DMSO-d_6) δ 8.18 (d, J = 7.9 Hz, 1H), 8.02 (d, J = 8.3 Hz, 1H), 7.89 (d, J = 7.5 Hz, 1H), 7.83 (d, J = 7.5 Hz, 1H), 7.69 (d, J = 8.1 Hz, 1H), 7.66–7.60 (m, 1H), 7.57–7.49 (m, 3H), 7.44 (t, J = 7.6 Hz, 1H), 7.33 (dt, J = 23.1, 7.9 Hz, 5H), 7.21–7.17 (m, 1H), 4.13 (s, 1H), 3.76–2.22 (m, 5H). ^{13}C NMR (151 MHz, DMSO-d_6) δ 164.18, 161.82, 137.23, 136.57, 134.92, 133.24, 131.46, 130.99, 130.29, 129.58, 128.75, 127.09, 126.25, 114.51, 66.82, 55.00, 49.67, 46.19, 21.83, 20.01; IR V_{max} cm^{-1}: 1 608.44 (C=N stretch), 1 593.04 (C=N stretch), 3 058.55 (C-H stretch), 1 269.10 (C-N stretch), 1 139.95 (C-N stretch), 2 846.17 (C-H stretch). m/z HRMS (APCI) found 319.1930 calcd for $C_{20}H_{23}N_4$ 319.1917 $[M + H]^+$; Purity (HPLC): 51%.

4-(4-methylpiperazin-1-yl)-2-(4-nitrophenyl)quinazoline **(3e)**

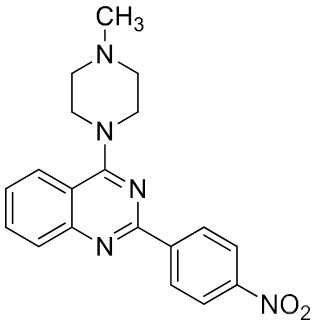

Brown powder; 43% yield; m.p.: 133°C; ^{1}H NMR (600 MHz, DMSO-d_6) δ 8.68 (d, J = 8.4 Hz, 1H), 8.35 (d, J = 8.4 Hz, 1H), 8.20 (d, J = 8.3 Hz, 1H), 8.03 (d, J = 8.3 Hz, 1H), 7.93 (d, J = 8.4 Hz, 1H), 7.86 (t, J = 7.6 Hz, 1H), 7.77–7.71 (m, 1H), 7.57 (t, J = 7.6 Hz, 1H), 3.87 (t, J = 4.9 Hz, 2H), 3.74 (t, J = 5.0 Hz, 1H), 3.34–2.27 (m, 8H). ^{13}C NMR (151 MHz, DMSO-d_6) δ 164.41, 156.63, 152.39, 148.97, 144.57, 133.64, 133.05, 129.94, 129.42, 129.01, 126.57, 125.93, 124.10, 115.21, 113.62, 54.93, 49.54, 46.16, 39.59; IR V_{max} cm^{-1}: 1 561.40 (C=N stretch), 1 533.54 (C=N stretch), 1 338.64 (N-O stretch), 1 508. 66 (N-O stretch), 1 266.39 (C-N stretch), 1 177.75 (C-N stretch), 3 066.69.08 (C-H stretch), 2 842.59 (C-H stretch). m/z HRMS (APCI) found 350.1630 calcd for $C_{19}H_{20}N_5O_2$ 350.1612 $[M + H]^+$; Purity (HPLC): 91.2%.

2-(4-bromophenyl)-4-(4-methylpiperazin-1-yl)quinazoline **(3f)**

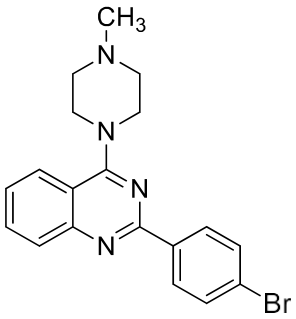

Brown powder; 54% yield; m.p.: 133.8–140.1°C; ^{1}H NMR (600 MHz, DMSO-d_6) δ 8.45–8.37 (m, 1H), 8.14 (d, J = 8.6 Hz, 1H), 8.06–7.97 (m, 1H), 7.88 (dd, J = 8.4, 1.3 Hz, 1H), 7.83 (dd, J = 6.9, 1.4 Hz, 1H), 7.73–7.67 (m, 1H), 7.56–7.42 (m, 1H), 3.85 (t, J = 4.9 Hz, 2H), 3.24 (s, 4H), 2.66–2.42 (m, 6H).^{13}C NMR (151 MHz, DMSO-d_6) δ 164.52, 157.74, 152.58, 137.90, 133.37, 132.06, 131.85, 130.39, 130.27, 128.82, 125.91, 124.49, 117.78, 115.19, 54.95, 49.59, 46.14; IR V_{max} cm^{-1}: 1 671.40 (C=N stretch), 1 605.13 (C=N stretch), 541.31 (C-Br stretch), 1 218.17 (C-N stretch), 1 142.59 (C-N stretch), 3 068.08 (C-H stretch), 1 265.20 (C-N stretch), 2 844.03 (C-H stretch). m/z HRMS (APCI) found 383.0842 calcd for $C_{19}H_{20}BrN_4$ 383.0866 $[M + H]^+$; Purity (HPLC): 94.9%.

2-(4-bromophenyl)-4-(piperidin-1-yl)quinazoline **(4a)**

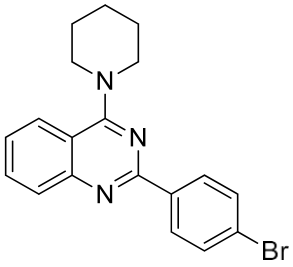

Grey spheres; 20% yield; m.p.: 155.1–157.3°C; ^{1}H NMR (600 MHz, DMSO-d_6) δ 8.44–8.39 (m, 1H), 7.99–7.96 (m, 1H), 7.87 (dd, J = 8.3, 1.3 Hz, 1H), 7.81 (ddd, J = 8.3, 6.8, 1.3 Hz, 1H), 7.75–7.70 (m, 1H), 7.53 (ddd, J = 8.3, 6.8, 1.4 Hz, 1H), 4.35 (t, J = 5.1 Hz, 1H), 3.80 (t, J = 4.9 Hz, 2H), 3.45 (qd, J = 7.0, 4.9 Hz, 2H), 1.76 (tq, J = 11.8, 6.7, 5.6 Hz, 4H), 1.06 (t, J = 7.0 Hz, 3H). ^{13}C NMR (151 MHz, DMSO-d_6) δ 164.66, 157.69, 152.53, 140.94, 137.92, 133.32, 131.87, 130.35, 129.93, 128.73, 125.87, 124.47, 122.06, 115.21, 56.49, 50.77, 25.99, 24.68, 19.02; IR V_{max} cm^{-1}: 1 532.56 (C=N stretch), 1 496.81 (C=N stretch), 544.18 (C-Br

stretch), 1 211.83 (C-N stretch), 1 157.44 (C-N stretch), 3 046.97 (C-H stretch). m/z HRMS (APCI) found 368.0764 calcd for $C_{19}H_{19}BrN_3$ 368.0757 $[M + H]^+$; Purity (HPLC): 98.6%.

N^1,N^2-bis(2-(4-bromophenyl)quinazolin-4-yl)ethane-1,2-diamine **(5a)**

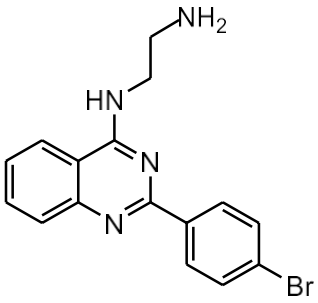

Yellow-brown powder; 32% yield; m.p.: 99-103°C; ^{1}H NMR (600 MHz, DMSO-d_6) δ 8.49–8.38 (m, 1H), 8.34 (s, 1H), 8.29 (d, J = 8.2 Hz, 1H), 8.19 (dd, J = 16.4, 8.2 Hz, 1H), 7.77 (dd, J = 5.4, 1.5 Hz, 1H), 7.72–7.67 (m, 1H), 7.56 (d, J = 8.6 Hz, 1H), 7.50 (ddd, J = 8.3, 5.9, 2.3 Hz, 1H), 3.73–3.67 (m, 1H), 3.57 (s, 3H), 2.93 (t, J = 6.5 Hz, 1H), 2.51 (p, J = 1.8 Hz, 2H). ^{13}C NMR (151 MHz, DMSO-d6) δ 160.40, 158.79, 150.21, 141.17, 138.41, 133.22, 131.70, 130.36, 128.25, 125.88, 124.25, 123.32, 114.41, 66.82, 44.41, 41.02; IR V_{max} cm^{-1}: 1 527.51 (C=N stretch), 1 568.31 (C=N stretch), 540.77 (C-Br stretch), 1 191.91 (C-N stretch), 3 344.78 (N-H stretch), 1 167.73 (N-C stretch). m/z HRMS (APCI) found 343.0519 calcd for $C_{16}H_{16}BrN_4$ 343.0554 $[M + H]^+$;Purity (HPLC): 83.6%.

N^1,N^2-bis(2-(4-fluorophenyl)quinazolin-4-yl)ethane-1,2-diamine **(5b)**

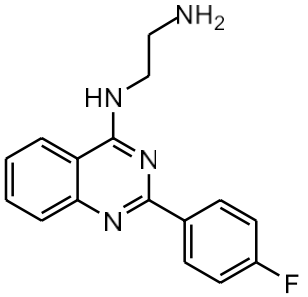

Light brown powder; 7% yield; m.p.: 93–95°C; ^{1}H NMR (600 MHz, DMSO-d_6) δ 8.54 (ddd, J = 12.9, 8.8, 5.9 Hz, 1H), 8.27 (d, J = 8.4 Hz, 1H), 7.92–7.59 (m, 1H), 7.56–7.09 (m, 2H), 4.23–3.70 (m, 6H), 3.22–2.90 (m, 1H), 2.51 (p, J = 1.9 Hz, 3H). ^{13}C NMR (151 MHz, DMSO-d_6) δ 164.89, 160.64, 150.28, 135.57, 133.24, 132.91, 130.58, 128.19, 126.58, 125.73, 124.86, 123.26, 115.46, 114.65, 66.82, 31.15. IR V_{max} cm^{-1}: 1 571.42 (C=N stretch), 1 529.35 (C=N stretch), 1 147.76 (C-F stretch), 1 218.82 (C-N stretch), 3 305.56

(N-H stretch). m/z HRMS (APCI) found 284.1339 calcd for $C_{16}H_{16}FN_4$ 2 484.1306 $[M + H]^+$; Purity (HPLC): 42%.

N^1,N^2-bis(2-(3-chlorophenyl)quinazolin-4-yl)ethane-1,2-diamine **(5c)**

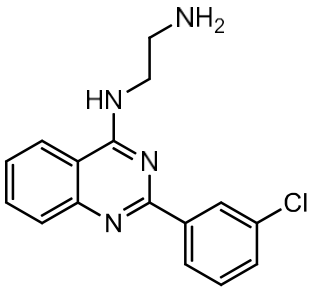

Light brown powder; 34% yield; m.p.: 93°C; ^{1}H NMR (600 MHz, Ace-d_6) δ 8.69–8.45 (m, 1H), 8.16 (s, 1H), 7.82 (ddd, J = 29.5, 7.7, 1.4 Hz, 1H), 7.51 (s, 1H), 7.38–7.17 (m, 1H), 4.32 (s, 1H), 4.18–3.73 (m, 1H), 3.80–3.71 (m, 1H), 3.60 (s, 2H), 3.50–2.10 (m, 6H). ^{13}C NMR (151 MHz, Ace-d_6) δ 160.11, 158.58, 150.41, 141.55, 133.72, 132.53, 132.51, 129.73, 127.90, 126.54, 125.62, 121.91, 114.26, 66.71, 49.93, 41.87; IR V_{max} cm^{-1}: 1 568.40 (C=N stretch), 1 527.77 (C=N stretch), 768.13 (C-Cl stretch), 1 241.43 (C-N stretch), 3 337.91 (N-H stretch). m/z HMRS (APCI) found 299.1058 calcd for $C_{16}H_{16}ClN_4$ 299.1058 $[M + H]^+$; Purity (HPLC): 81.8%.

3.3.3 *In vitro* antiprotozoal evaluation

L. infantum [MHOM/MA (BE)/67] was employed with primary peritoneal mouse macrophages as the host cell to assess anti-*Leishmania* activity. Per well, 4.5×10^5 parasites infected 3×10^4 macrophages. Serial dilutions of compounds were added to the parasite infected cells. After incubation for five days, parasite loads (measured as the average number of amastigotes per macrophage) were examined under a microscope following staining with a 10% Giemsa solution.

The Tulahuen CL2 β-galactosidase strain of *T. cruzi*, which is nifurtimox-sensitive, was utilised and maintained on MRC-5 SV2 (human lung fibroblast). Per well, 4×10^3 cells were infected with 4×10^4 parasites. Serial dilutions of compounds were added to the parasite infected cells and incubated for five days. Substrate CPRG (chlorophenolred ß-d-galactopyranoside) was added and incubated for four hours at 37°C. Parasite burdens were determined spectrophotometrically at 540 nm.

Using a resazurin assay, drug susceptibility testing for *T. brucei* were carried out using *T. brucei Squib 42749* and *T.b. rhodesiense STIB-90050*. Resazurin was added after 24 hours for *T. brucei Squib 427* and after six hours for *T.b. rhodesiense*, respectively. *T. brucei Squib 427* was seeded at 1.5×10^4 parasites per well and *T.b. rhodesiense* at 4×10^3 parasites per well. Plates were incubated for a further 24 hours after the addition of resazurin before fluorescence detection.

The growth of the parasite was compared in all assays to untreated-infected controls (which had 100% growth) and non-infected controls (which had 0% growth). In order to determine the IC_{50} values from the dose-response curves, results were represented as percentages of parasite reduction at various sample concentrations.

3.3.4 *In vitro* antitubercular evaluation

The antitubercular activity, provided as the MIC, was determined by the standard broth microdilution method. This assay was performed according to the protocol provided by Dube *et al*. (2021). In a nutshell, a 10 mL culture of *M. tuberculosis* pMSp12::GFP was grown to an optical density (OD_{600}) of 0.6–0.7 in a Middlebrook 7H9 medium with the addition of either 0.03% casitone, 0.4% glucose, and 0.05% tyloxapol or 0.03% albumin, 0.4% glucose, and 0.05% Tween 80. In a 96-well micro titre plate, test compounds were prepared in two-fold serial dilutions before 50 µL of the diluted *M. tuberculosis* cultures were added to each compound-containing well. The plates were carefully sealed and incubated at 37°C under 5% CO_2 while being humidified. At days 7 and 14, relative fluorescence (excitation 485 nm emission 520 nm) was measured and analysed to get MIC_{90} values. The assay minimum and maximum growth controls, respectively, were rifampicin at 2 × MIC and 5% DMSO (Dube *et al*., 2021:11).

3.3.5 *In vitro* antibacterial and antifungal evaluation

In 384-well, non-binding surface plates, eight-fold serial dilutions of each sample were made starting at 32 µg/mL, while DMSO concentrations below 0.5% were maintained throughout. Bacteria were grown using Cation-Adjusted Mueller Hinton Broth at 37°C overnight, followed by a 40-fold dilution and 1.5–3 hours of incubation at 37°C.

To achieve a volume of 50 µL and a cell density of 5×10^5 CFU/mL, mid-log phase cultures were diluted (CFU/mL determined by OD_{600}) and plated to each compound-containing well plate. Without shaking, plates were incubated at 37°C for 18 hours. Each well's absorbance at 600 nm (OD_{600}) was recorded using

a Tecan M1000 Pro monochromator plate reader, and this information was used to calculate the degree of bacterial growth inhibition.

According to the Clinical and Laboratory Standards Institute's standards and guidelines, the MIC, which is referred as the lowest concentration at which > 80% of bacterial growth is inhibited, was calculated. Hits were defined as compounds with MIC ≤ 16 µg/mL in any replicate (n = 2).

Yeast extract-peptone dextrose agar was used to cultivate *C. albicans* for three days at 30°C. To achieve a final cell density of 2.5×10^3 CFU/mL and a volume of 50 µL, a culture suspension was prepared, diluted, and then applied to each well of the compound-containing plates. The plates were sealed and incubated for a period of 36 hours at 35°C. Thereafter, a final concentration of 0.001% resazurin was added to each plate and incubated for an additional two hours at 35°C. A Biotek Multiflo Synergy HTX plate reader was used to evaluate the amount of growth inhibition by measuring the absorbance at 630 nm (OD_{630}) for each well.

3.3.6 *In vitro* cytotoxicity evaluation

In a nutshell, cells at a concentration of 1.5×10^5 cells/mL were grown with chemical dilutions at 37°C and with 5% CO_2. A comparison of cell growth was made with medium-control wells (0% cell growth) and untreated-control wells (100% cell growth). After three days of incubation and the addition of 50 µL of resazurin per well, cell viability was evaluated fluorometrically. Fluorescence was detected (λ ex 550 nm, λ em 590 nm) after four hours at 37°C. An IC_{50} value was established, and the results were presented as a percentage reduction in cell growth/viability in comparison to control wells.

3.4 Conclusion

In this project, 2,4-disubstituted quinazolines were synthesised successfully. The compounds were screened *in vitro* for antitubercular, antiprotozoal, antibacterial, antifungal, and overt cell toxicity. **Compounds 3a–3c**, **3e**, **3f**, and **5a–5c** exhibited antitubercular activity at less than 9 µM. These compounds were generally inactive against Gram-positive and Gram-negative bacteria with MIC values of > 32 µg/mL and a D_{max} <50. Regarding antifungal activity, **Compounds 2b**, **3b**, **3d**, and **3f** indicated activity against *Cryptococcus neoformans var. grubii* (MIC: ≤ 32 µg/mL). One compound (**2b**) exhibited potent activity against *Candida albicans* (< 32 µg/mL). The results obtained for the antiprotozoal activity suggest

that **Compounds 5a–5c** can be potential antitrypanosomal agents, presenting with the best anti-trypanosomal activity (< 7 µM).

3.5 Acknowledgements

This project was funded by the NWU, Faculty of Health Science. The grant was awarded to RMB. The NMR spectra were recorded by Dr Daniel Otto and Dr Johan Jordaan of the SASOL Centre of Chemistry, North-West University. Antitubercular activity was carried out by Audrey Jordaan, under supervision of Prof. Digby Warner. The authors commend North-West University, Potchefstroom campus, for its financial and infrastructural support. The Welcome Trust (UK) and The University of Queensland (Australia) are acknowledged for providing funding toward antimicrobial testing performed by COADD (The Community for Antimicrobial Drug Discovery). Antiprotozoal activities were conducted by Kayhan Ilbeigi under the supervision of Prof. Guy Caljon.

3.6 Conflict of interest

There are no known conflicts of interest between the authors.

3.7 Data availability statements

The supplemental material contains proton, carbon NMR, FTIR, and HRMS spectra of target compounds.

REFERENCE LIST – CHAPTER 3

Álvarez-Rodríguez, A., Jin, B-K., Radwanska, M. & Magez, S. 2022. Recent progress in diagnosis and treatment of Human African trypanosomiasis has made the elimination of this disease a realistic target by 2030. *Frontiers in Medicine*, 9:1037094. doi:10.3389/fmed.2022.1037094

Brun, R., Blum, J., Chappuis, F. & Burri, C. 2010. Human African trypanosomiasis. *The Lancet*, 375(9709): 148-159. doi:10.1016/S0140-6736(09)60829-1

Büscher, P., Cecchi, G., Jamonneau, V. & Priotto, G. 2017. Human African trypanosomiasis. *The Lancet*, 390(10110):2397-2409. doi:10.1016/S0140-6736(17)31510-6

De Oliveira, D.M.P., Forde, B.M., Kidd, T.J., Harris, P.N., Schembri, M.A., Beatson, S.A., … Walker, M.J. 2020. Antimicrobial resistance in ESKAPE pathogens. *Clinical Microbiology Reviews*, 33(3):e00181-00119. doi:10.1128/cmr.00181-19

Desjeux, P. 2004. Leishmaniasis: current situation and new perspectives. *Comparative Immunology, Microbiology and Infectious Diseases*, 27(5):305-318. doi:10.1016/j.cimid.2004.03.004

Dube, P.S., Legoabe, L.J., Jordaan, A., Jesumoroti, O.J., Tshiwawa, T., Warner, D.F. & Beteck, R.M. 2021. Easily accessed nitroquinolones exhibiting potent and selective anti-tubercular activity. *European Journal of Medicinal Chemistry*, 213, 113207. doi:10.1016/j.ejmech.2021.113207

Hameed, A., Al-Rashida, M., Uroos, M., Ali, S.A., Arshia, Ishtiaq, M. & Khan, K.M. 2018. Quinazoline and quinazolinone as important medicinal scaffolds: a comparative patent review (2011–2016). *Expert Opinion on Therapeutic Patents*, 28(4):281-297. doi:10.1080/13543776.2018.1432596

Jafari, E., Khajouei, M.R., Hassanzadeh, F., Hakimelahi, G.H. & Khodarahmi, G.A. 2016. Quinazolinone and quinazoline derivatives: recent structures with potent antimicrobial and cytotoxic activities. *Research in Pharmaceutical Sciences*, 11(1):1.

Jain, V.K., Iyengar, K.P., Samy, D.A. & Vaishya, R. 2020. Tuberculosis in the era of COVID-19 in India. *Diabetes & Metabolic Syndrome: Clinical Research & Reviews*, 14(5):1439-1443. doi:10.1016/j.dsx. 2020.07.034

Jalageri, M.D., Nagaraja, A. & Puttaiahgowda, Y.M. 2021. Piperazine based antimicrobial polymers: a review. *RSC Advances*, 11(25):15213-15230. doi:10.1039/D1RA00341K

Kennedy, P.G. 2019. Update on human African trypanosomiasis (sleeping sickness). *Journal of Neurology*, 266:2334-2337. doi:10.1007/s00415-019-09425-7

Kennedy, P.G.E. 2013. Clinical features, diagnosis, and treatment of human African trypanosomiasis (sleeping sickness). *The Lancet Neurology,* 12(2):186-194. doi:10.1016/s1474-4422(12)70296-x

Khan, M., Islam, M., Ferdous, J. & Alam, M. 2019. An overview on epidemiology of tuberculosis. *Mymensingh Medical Journal: MMJ*, 28(1):259-266.

Lindner, A.K., Lejon, V., Chappuis, F., Seixas, J., Kazumba, L., Barrett, M.P., … Villanueva, G. 2020. New WHO guidelines for treatment of gambiense human African trypanosomiasis including fexinidazole: substantial changes for clinical practice. *The Lancet Infectious Diseases*, 20(2):e38-e46. doi:10.1016/ S1473-3099(19)30612-7

Magiorakos, A.-P., Srinivasan, A., Carey, R.B., Carmeli, Y., Falagas, M., Giske, C., … Olsson-Liljequist, B. 2012. Multidrug-resistant, extensively drug-resistant and pandrug-resistant bacteria: an international expert proposal for interim standard definitions for acquired resistance. *Clinical Microbiology and Infection*, 18(3):268-281. doi:10.1111/j.1469-0691.2011.03570.x

Mann, S., Frasca, K., Scherrer, S., Henao-Martínez, A.F., Newman, S., Ramanan, P. & Suarez, J.A. 2021. A review of leishmaniasis: current knowledge and future directions. *Current Tropical Medicine Reports*, 8:121-132. doi:10.1007/s40475-021-00232-7

Natarajan, A., Beena, P., Devnikar, A.V. & Mali, S. 2020. A systemic review on tuberculosis. *Indian Journalof Tuberculosis*, 67(3):295-311. doi:10.1016/j.ijtb.2020.02.005

Peloquin, C.A. & Davies, G.R. 2021. The treatment of tuberculosis. *Clinical Pharmacology & Therapeutics*, 110(6):1455-1466. doi:10.1002/cpt.2261

Rice, L.B. 2008. Federal funding for the study of antimicrobial resistance in nosocomial pathogens: no ESKAPE. *The Journal of Infectious Diseases*, 197(8):1079-1081. doi:10.1086/533452

Selvam, T.P. & Kumar, P.V. 2015. Quinazoline marketed drugs. *Research in Pharmacy*, 1(1):1-21.

Sommer, M.O., Munck, C., Toft-Kehler, R.V. & Andersson, D.I. 2017. Prediction of antibiotic resistance: time for a new preclinical paradigm? *Nature Reviews Microbiology*, 15(11):689-696. doi:10.1038/nrmicro.2017.75

Yew, W.W., Lange, C. & Leung, C.C. 2011. Treatment of tuberculosis: update 2010. *European Respiratory Society*: (37):441-462. doi:10.1183/09031936.00033010

CHAPTER 4 – SUMMARY AND CONCLUSION

4.1 ESKAPE pathogens

E. faecium, *S. aureus*, *K. pneumoniae*, *A. baumannii*, *P. aeruginosa*, and *Enterobacter* species comprise a group of six bacteria collectively referred to as ESKAPE pathogens. They have high virulence and are resistant to multiple antibiotics (De Oliveira *et al.*,2020:2). Collectively, these bacteria exemplify novel patterns in transmission and resistance as they possess the ability to evade or 'escape' the biocidal actions of antibiotics (Pendleton *et al.*, 2013:297).

ESKAPE pathogens were granted priority status on WHO's list of pathogenic bacteria requiring urgent development of new antibiotics (Orosz *et al.*, 2022:27). ESKAPE pathogens cause high morbidity, mortality, and associated healthcare cost (Zhen *et al.*, 2019:1) as they annually account for more than 33 000 fatalities and 874 000 disability-adjusted life years each year in Europe (Cassini *et al.*, 2019:56).

E. coli, the primary culprit behind urinary tract infections, *S. aureus*, responsible for surgical site and respiratory tract infections, *P. aeruginosa*, which commonly leads to respiratory tract infections, along with Gram-positive bacteria, collectively represent the most prevalent causative agents of nosocomial infections. The urinary tract system (31%) is the third most common site for nosocomial infections, followed by the respiratory system (24%), and the bloodstream (16%). The skin and other organs may also experience nosocomial infections (Nouri *et al.*, 2020:2366).

The antibacterial activity of **Compounds 2a–2c, 3a–3f, 4a**, and **5a–5c** was evaluated against various bacterial strains, including *E. coli* (ATCC 25922), *K. pneumoniae* (ATCC 700603), *A. baumannii* (ATCC 19606), *P. aeruginosa* (ATCC 27853), *S. aureus* (ATCC 43300), and MRSA (ATCC 43300). Established antibacterial drugs such as colistin and vancomycin were used as reference standards. The findings indicate that the tested compounds demonstrated limited activity (MIC: > 32 μg/mL and D_{max} of < 50) against the bacteria deployed. **Compounds 2a–2c** exhibited low micromolar activity against the above-mentioned pathogens: *E. coli* (> 32 μg/mL), *K. pneumoniae* (> 32 μg/mL), *A. baumannii* (> 32 μg/mL), *P. aeruginosa* (> 32 μg/mL), *S. aureus* (> 32 μg/mL), and MRSA (> 32 μg/mL). **Compounds 4a** and **5a–5c** exhibited low micromolar activity against the above-mentioned pathogens: *E. coli* (> 32 μg/mL), *K. pneumoniae* (> 32 μg/mL), *A. baumannii* (> 32 μg/mL), *P. aeruginosa* (> 32 μg/mL), *S. aureus* (> 32 μg/mL), and MRSA (> 32 μg/mL).

4.2 Protozoan diseases: Human African trypanosomiasis, leishmaniasis and nagana

Sub-Saharan Africa harbours HAT, commonly known as sleeping sickness. This disease is caused by the protozoan parasite *T. brucei*, which is transmitted by tsetse flies. The majority of HAT cases are attributed to *T.b. gambiense*, predominantly found in West and Central Africa. Trypanosomiasis is an under-estimated tropical ailment, with fewer than 12 000 reported cases of this life-threatening and debilitating condition each year. The complex clinical presentation poses challenges for accurate diagnosis and effective treatment. Medications currently available are outdated, cumbersome to administer, and associated with severe and potentially dangerous side effects. Therefore, there is an urgent demand for innovative diagnostic tools and safe, effective drugs to combat this disease (Brun *et al*., 2010:148).

Leishmaniasis is a tropical and subtropical disease that affects people in Europe, Northern Africa, the Middle East, Asia, and parts of South America. It is brought on by an intracellular parasite transmitted to people by the bite of a sandfly, primarily *Phlebotomus* and *Lutzomyia* (Vera-Izaguirre *et al*., 2006:252). Leishmaniasis is one of the seven most significant tropical diseases. It is a critical global health issue that has a wide range of clinical symptoms and a potentially deadly consequence. Except for Oceania, it can be found on every continent. It is native to northeastern Africa, southern Europe, the Middle East, southeastern Mexico, and Central and South America (Torres-Guerrero *et al*., 2017:3).

AAT, also known as nagana, affects 37 sub-Saharan countries, totalling more than 9 million km^2, or roughly one-third of Africa's land mass. The main obstacle to the production of cattle in sub-Saharan Africa, particularly Ethiopia, continues to be AAT. It is brought on by parasitic protozoans of the genus *Trypanosoma*, of which *T. vivax, T. congolense*, and members of the *T. brucei* group are the principal trypanosome species affecting animals. Tsetse flies, among other species, are important in the transmission of these trypanosomes. If the disease is not treated, it results in decreased animal productivity and, in severely affected animals, death. When one or more of the three African animal trypanosomes infect cattle, it can cause subacute, acute, or chronic disease that is frequently fatal and is characterised by intermittent fever, anaemia, sporadic diarrhoea, and rapid loss of condition (Eshetu & Begejo, 2015:117).

The evaluation of various compounds against different protozoan parasites revealed diverse levels of antiprotozoal activity. **Compound 1d** exhibited low antiprotozoal activity with values above 64.00 µM against multiple parasites, coupled with low toxicity. **Compounds 2a** and **2c** demonstrated moderate

activity against *T. cruzi* (24.25 µM and 10.77 µM, respectively) and *L. infantum* (36.76 µM and 28.98 µM, respectively). **Compounds 3a–3f** displayed limited intrinsic antitrypanosomal activity. Among them, **Compound 3a** showed moderate activity against *L. infantum* (8 µM) and *T. rhodesiense* (8 µM). **Compound 3c** exhibited low micromolar activities against *T. cruzi* (8.12 µM), *T. brucei* (4.17 µM), and *T. rhodesiense* (4.84 µM). **Compound 3f** demonstrated the highest activity against *T. cruzi* (4.8 µM), *L. infantum* (2.52 µM), *T. brucei* (2.42 µM), and *T. rhodesiense (*1.82 µM), while **Compound 3e** exhibited significant activity against these parasites as well: *T. cruzi* (7.04 µM), *L. infantum* (2.3 µM), *T. brucei* (3.81 µM), and *T. rhodesiense* (2.04 µM). However, both compounds exhibited toxicity towards MRC-5 and PMM cells. **Compound 4a** showed poor to no antitrypanosomal activity with *T. cruzi* (> 64 µM), *L. infantum* (46.48 µM), *T. brucei* (> 64 µM), and *T. rhodesiense* (> 64 µM). **Compound 5a** demonstrated potent activity against *T. cruzi* (0.55 µM), *L. infantum* (1.26 µM), *T. brucei* (0.22 µM), and *T. rhodesiense* (0.13 µM). Although several compounds displayed good antiprotozoal activities compared with reference drugs, they also showed elevated toxicity levels against MRC-5 and PMM cells.

4.3 Tuberculosis

TB, caused by bacteria belonging to the *M. tuberculosis* complex, is one of the oldest diseases known to humanity and remains a significant global cause of mortality. The disease continues to pose a substantial threat to human health. Vulnerable populations, including socioeconomically disadvantaged individuals and marginalised communities, are particularly susceptible to TB (Natarajan *et al.*, 2020:15).

Conceptualised compounds were evaluated *in vitro* for antitubercular efficacy against the gfp strain of *M. tuberculosis* grown in both CAS and ADC media. In the CAS medium, **Compound 3a** (3.33–8.481 µM), **Compound 3b** (0.488–2.114 µM), **Compound 3c** (2.201–7.134 µM), **Compound 3e** (1.546–4.339 µM), **Compound 3f** (0.488–0.873 µM), **Compound 5a** (0.488–0.868 µM), **Compound 5b** (0.488–2.169 µM), and **Compound 5c** (0.488-0.925 µM) were generally active against *M. tuberculosis* exhibiting activity in the range of 0.488–8.481 µM (day 7–14). The best compound was **Compound 5a** with an activity range of 0.488–0.868 µM.

In the ADC medium, **Compound 3a** (62.5–125 µM), **Compound 3b** (38.73–62.5 µM), **Compound 3c** (32.468–62.5 µM), **Compound 3e** (32.735–62.5 µM), **Compound 3f** (15.625–31.25 µM), **Compound 5a** (16.623–31.288 µM), **Compound 5b** (62.5–125 µM), and **Compound 5c** (31.25–30.069 µM) were

generally active against *M. tuberculosis* exhibiting activity in the range 15.625–125 µM, with **Compound 3f** being the best compound with an activity range of 15.625–31.25 µM (day 7–14).

In summary, **Compounds 3a–3c**, **3e**, **3f**, and **5a–5c** displayed significant antitubercular activity, exhibiting MIC_{90} values ranging from 0.488 µM to 8.481 µM in the CAS culture medium. **Compound 5a** also demonstrated low micromolar activity against protozoal parasites and exhibited a selectivity index of > 10 against the MRC-5 cell line.

REFERENCE LIST – CHAPTER 4

Brun, R., Blum, J., Chappuis, F. & Burri, C. 2010. Human African trypanosomiasis. *The Lancet*, 375(9709): 148-159. doi:10.1016/S0140-6736(09)60829-1

Cassini, A., Högberg, L.D., Plachouras, D., Quattrocchi, A., Hoxha, A., Simonsen, G.S., … Cecchini, M. 2019. Attributable deaths and disability-adjusted life-years caused by infections with antibiotic-resistant bacteria in the EU and the European Economic Area in 2015: a population-level modelling analysis. *The Lancet Infectious Diseases*, 19(1):56-66. doi:10.1016/S1473-3099(18)30605-4

De Oliveira, D.M.P, Forde, B.M., Kidd, T.J., Harris, P.N.A., Schembri, M.A., Beatson, S.A., … Walker, M.J. 2020. Antimicrobial resistance in ESKAPE pathogens. *Clinical Microbiology Reviews*, 33(3):e00181-00119. doi:10.1128/CMR.00181-19

Eshetu, E. & Begejo, B. 2015. The current situation and diagnostic approach of nagana in Africa: a review. *Journal of Natural Sciences Research*, 5(17):117-125.

Natarajan, A., Beena, P., Devnikar, A.V. & Mali, S. 2020. A systemic review on tuberculosis. *Indian Journalof Tuberculosis*, 67(3):295-311. doi:10.1016/j.ijtb.2020.02.005

Nouri, F., Karami, P., Zarei, O., Kosari, F., Alikhani, M.Y., Zandkarimi, E., … Taheri, M. 2020. Prevalence of common nosocomial infections and evaluation of antibiotic resistance patterns in patients with secondary infections in Hamadan, Iran. *Infection and Drug Resistance*, 13:2365-2374. doi:10.2147/IDR.S259252

Orosz, L., Lengyel, G., Ánosi, N., Lakatos, L. & Burián, K. 2022. Changes in resistance pattern of ESKAPE pathogens between 2010 and 2020 in the clinical center of University of Szeged, Hungary. *Acta Microbiologica et Immunologica Hungarica*, 69(1):27-34. doi:10.1556/030.2022.01640

Pendleton, J.N., Gorman, S.P. & Gilmore, B.F. 2013. Clinical relevance of the ESKAPE pathogens. *Expert Review of Anti-infective Therapy*, 11(3):297-308. doi:10.1586/eri.13.12

Torres-Guerrero, E., Quintanilla-Cedillo, M.R., Ruiz-Esmenjaud, J. & Arenas, R. 2017. Leishmaniasis: a review. *F1000Research*, 6, 2017; 6: 750. doi:10.12688/f1000research.11120.1

Vera-Izaguirre, D.S., Vega-Memije, E., Quintanilla-Cedillo, M.R. & Arenas, R. 2006. Leishmaniasis: a review. *Dermatología Cosmética, Médica Y Quirúrgica*, 4(4):252-260.

Zhen, X., Lundborg, C.S., Sun, X., Hu, X. & Dong, H. 2019. Economic burden of antibiotic resistance in ESKAPE organisms: a systematic review. *Antimicrobial Resistance & Infection Control*, 8:1-23. doi:10.1186/s13756-019-0590-7

ANNEXURE A – SUPPLEMENTARY MATERIAL FOR CHAPTER 3

SYNTHESIS, *IN VITRO* ANTIBACTERIAL AND ANTIPROTOZOALEVALUATION OF 2-PHENYL-4-AMINO QUINAZOLINES

Supporting data for chemistry, characterisation and synthesis

Blank HPLC test

To rule out any clearly undesired peaks that might be present in the HPLC data of the test chemicals due to solvent or column contaminants, a blank experimental HPLC control analysis using just acetonitrile as the solvent was carried out. The HPLC data of the target **Compounds 1–5** with identical peaks to the blank were disregarded when calculating the purity for each compound using the area under the curve.

2-(2,4-dimethoxyphenyl)quinazolin-4(3H)-one **(1a)**

^{1}H NMR

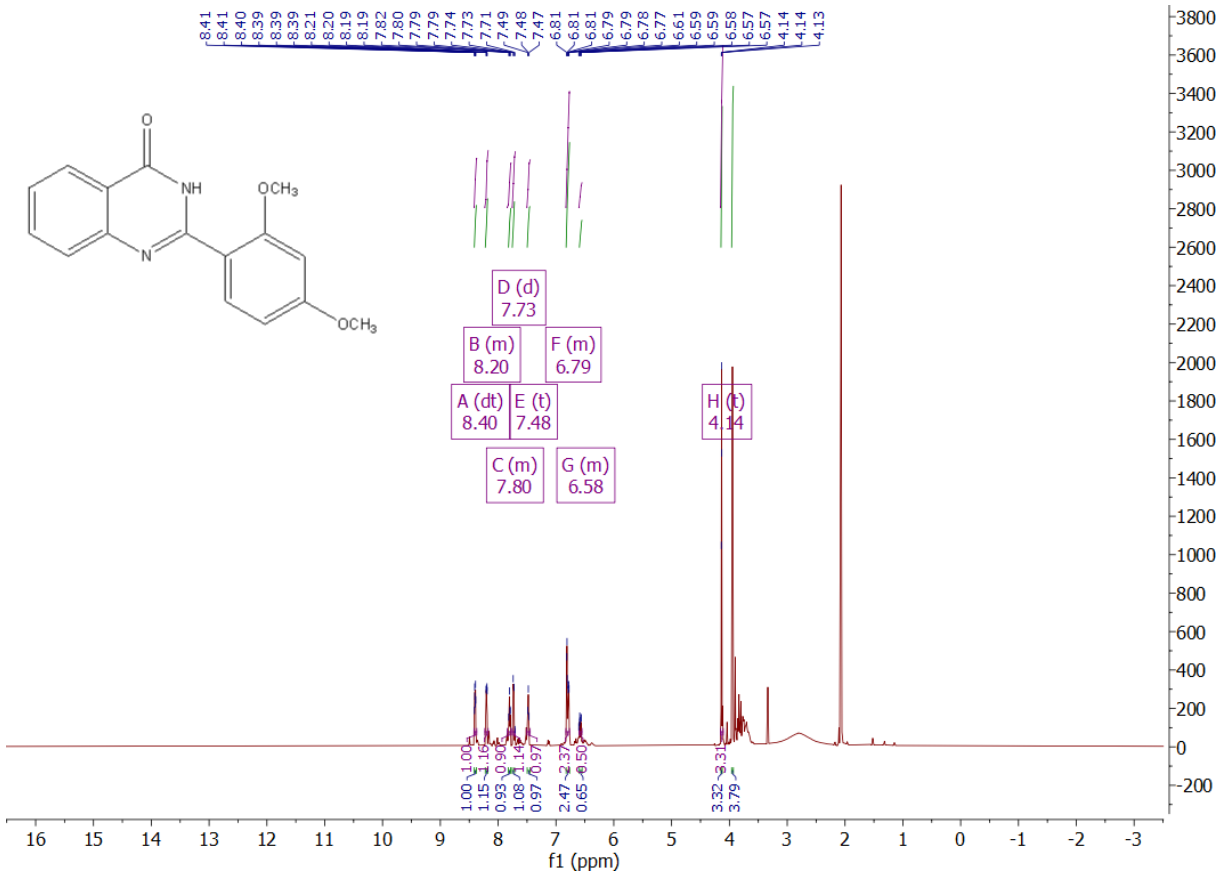

^{13}C NMR

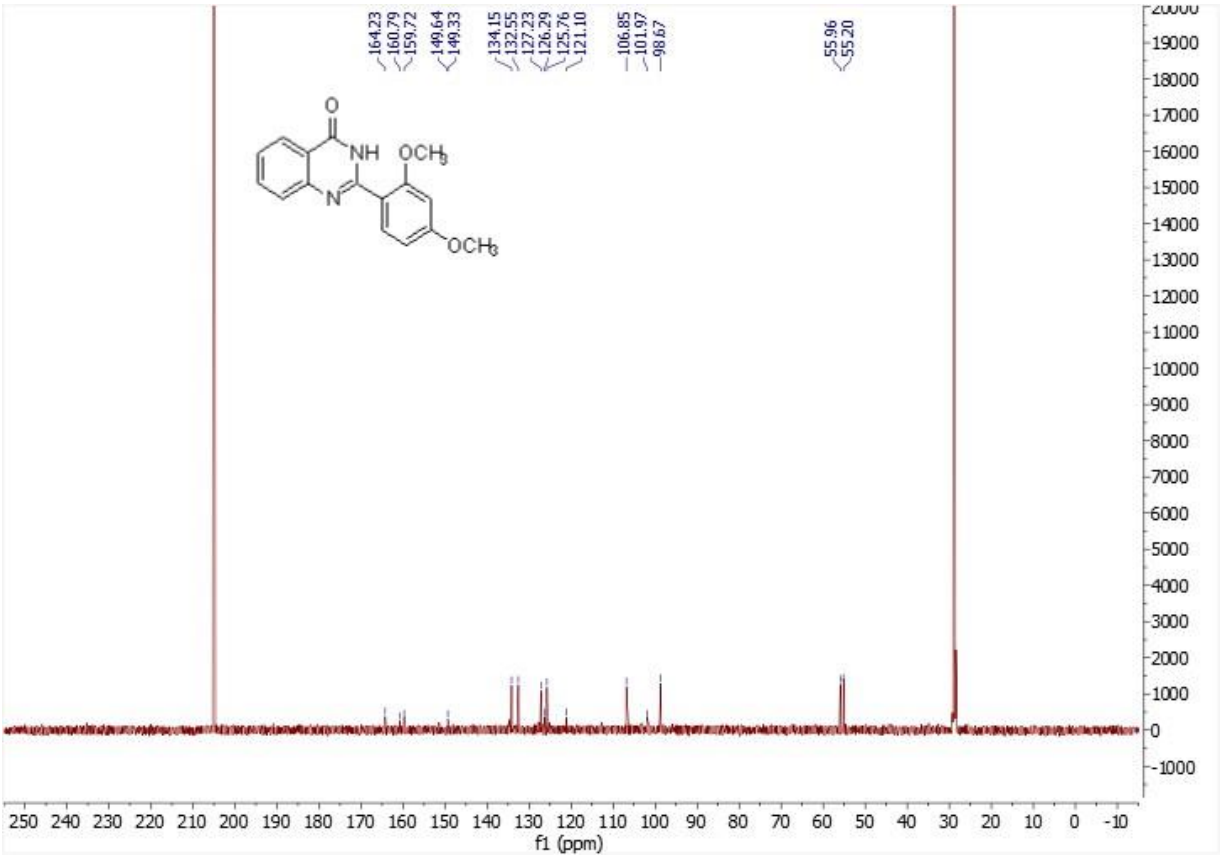
164.23
160.79
159.72
149.64
149.33
134.15
132.55
127.23
126.29
125.76
121.10
106.85
101.97
98.67
55.96
55.20
O
NH
OCH3
N
OCH3
f1 (ppm)

FTIR

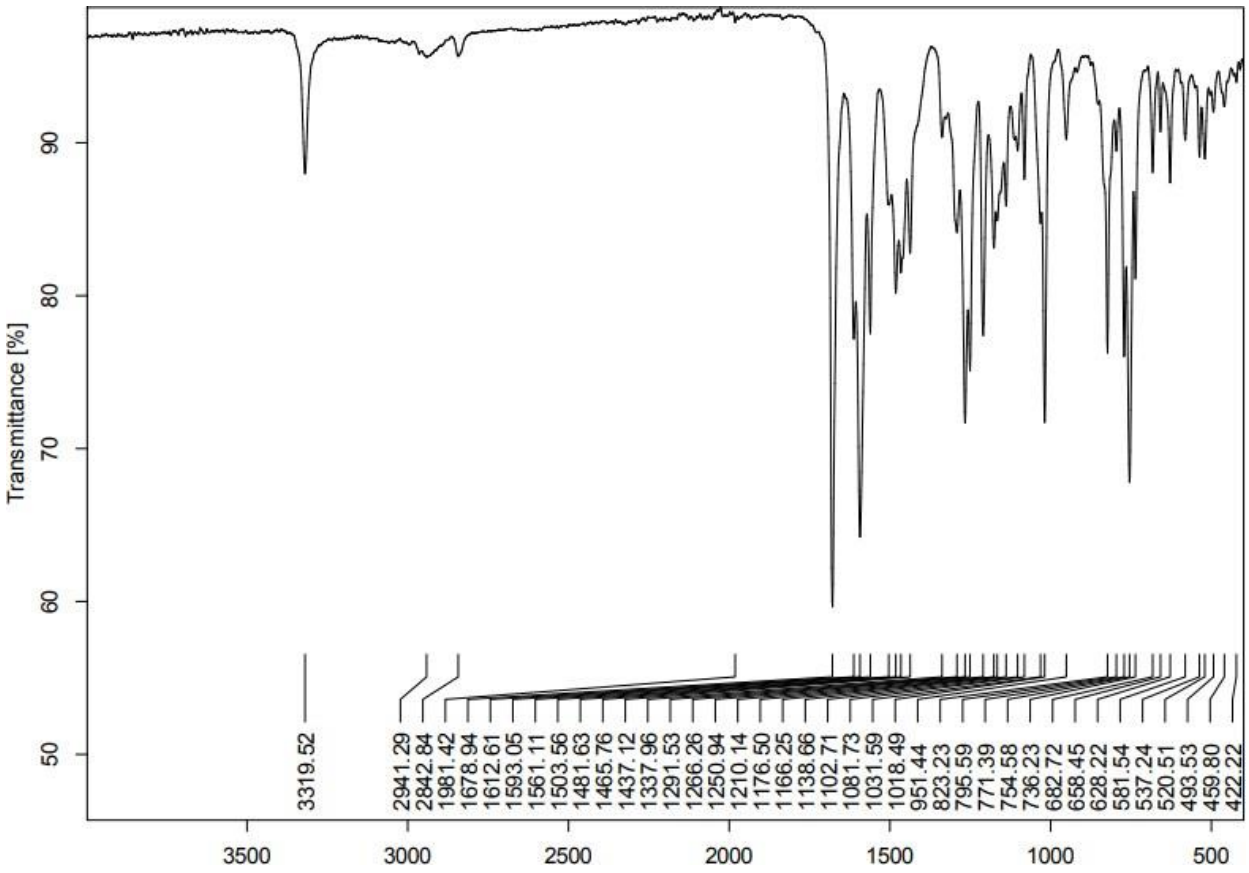

HRMS

Acquisition Parameter

Source Type	APCI	Ion Polarity	Positive	Set Nebulizer	0.8 Bar
Focus	Not active	Set Capillary	4500 V	Set Dry Heater	180 °C
Scan Begin	50 m/z	Set End Plate Offset	-500 V	Set Dry Gas	4.0 l/min
Scan End	2000 m/z	Set Collision Cell RF	100.0 Vpp	Set Divert Valve	Waste

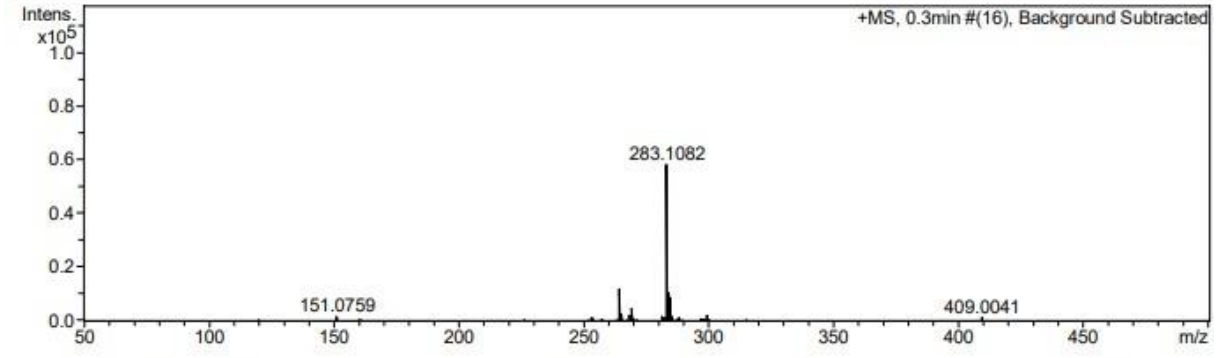

Meas. m/z	#	Formula	Score	m/z	err [mDa]	err [ppm]	mSigma	rdb	e⁻ Conf	N-Rule
283.1082	1	C 16 H 15 N 2 O 3	100.00	283.1077	-0.5	-1.7	5.0	10.5	even	ok

HPLC

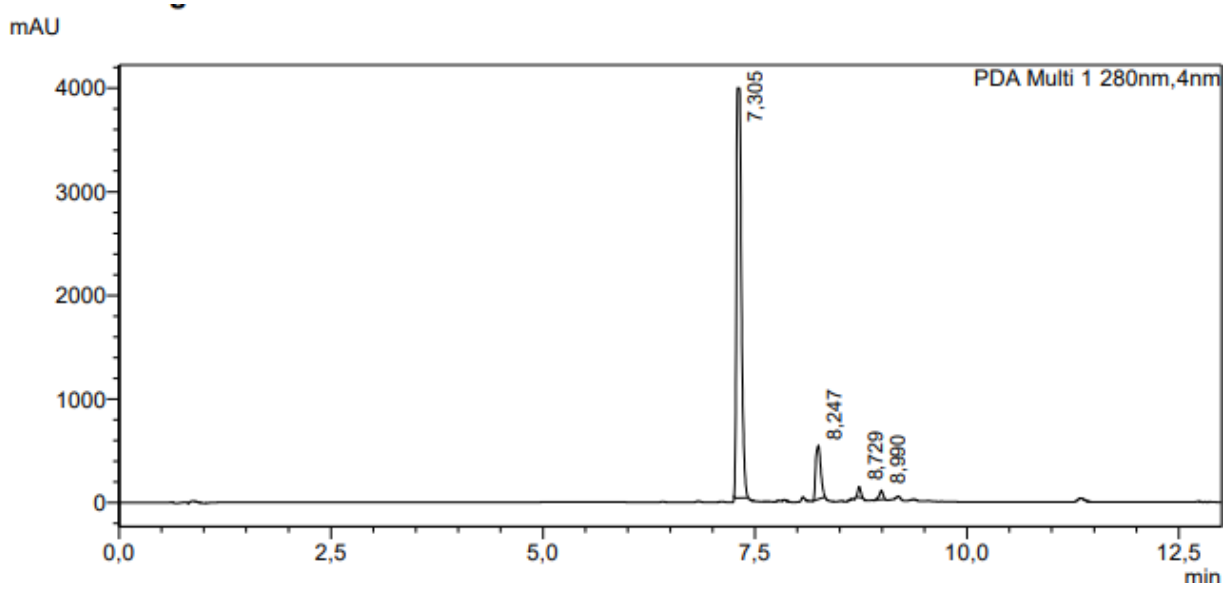

2-(o-tolyl)quinazolin-4(3H)-one (**1b)**

^{1}H NMR

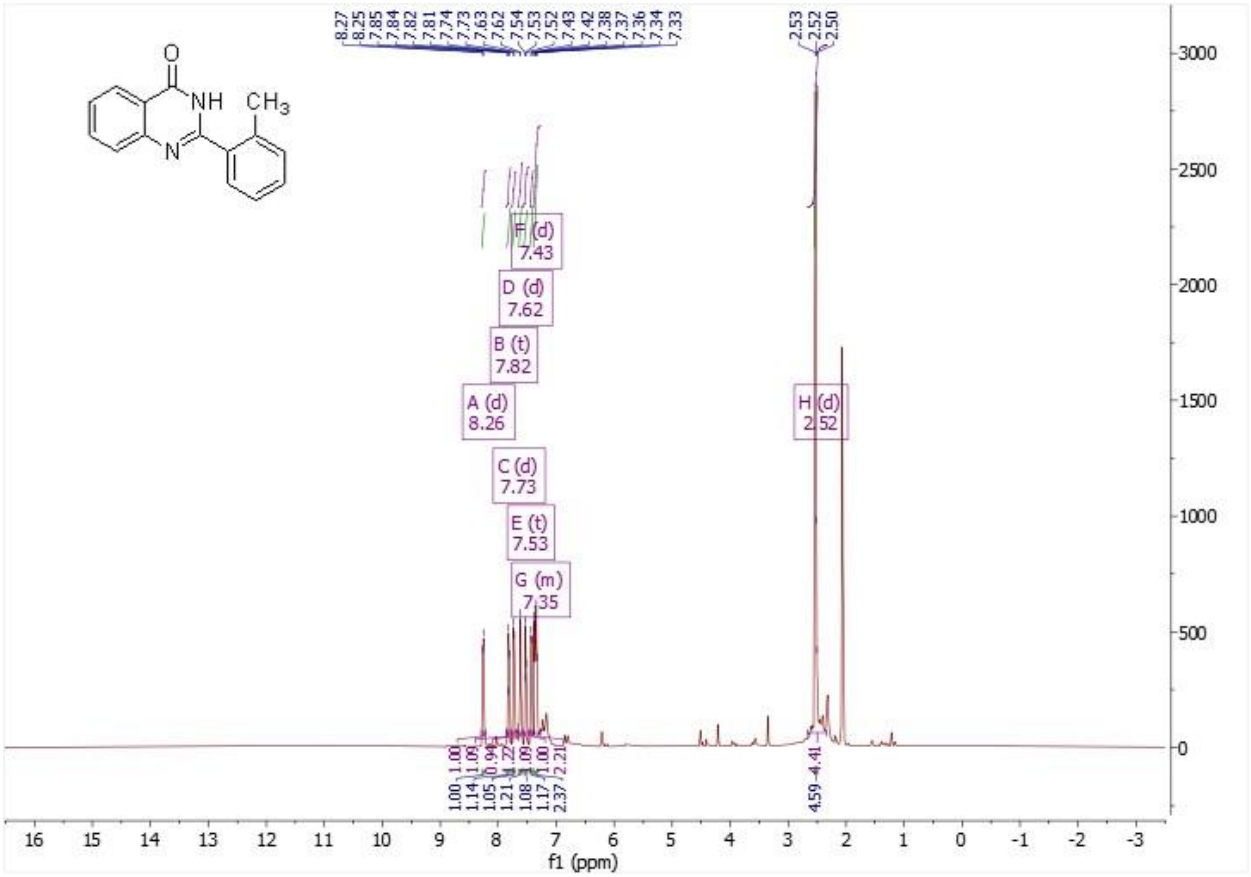

^{13}C NMR

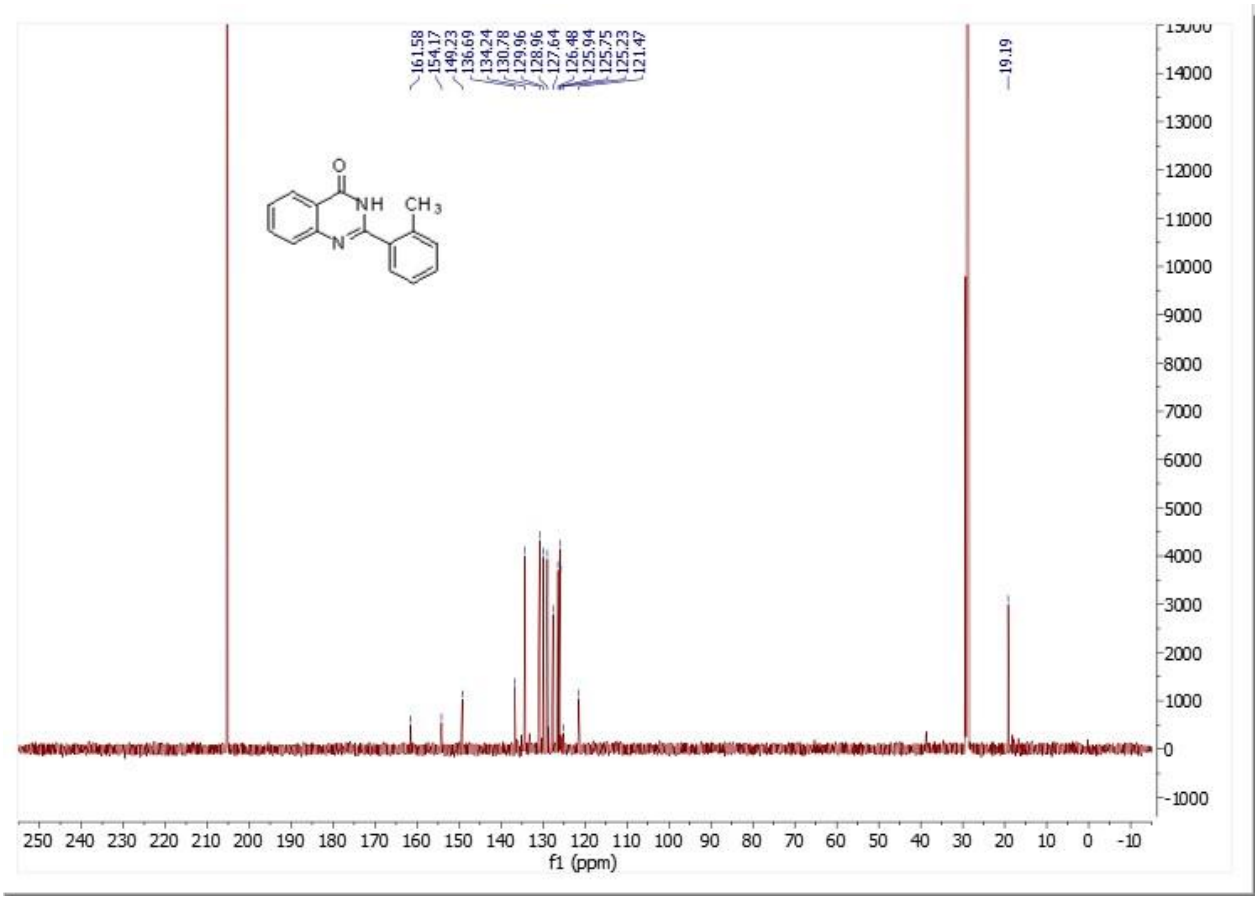
161.58
154.17
149.23
136.69
134.24
130.78
129.96
128.96
127.64
126.48
125.94
125.75
125.23
121.47
19.19
O
NH
CH3
N
f1 (ppm)

FTIR

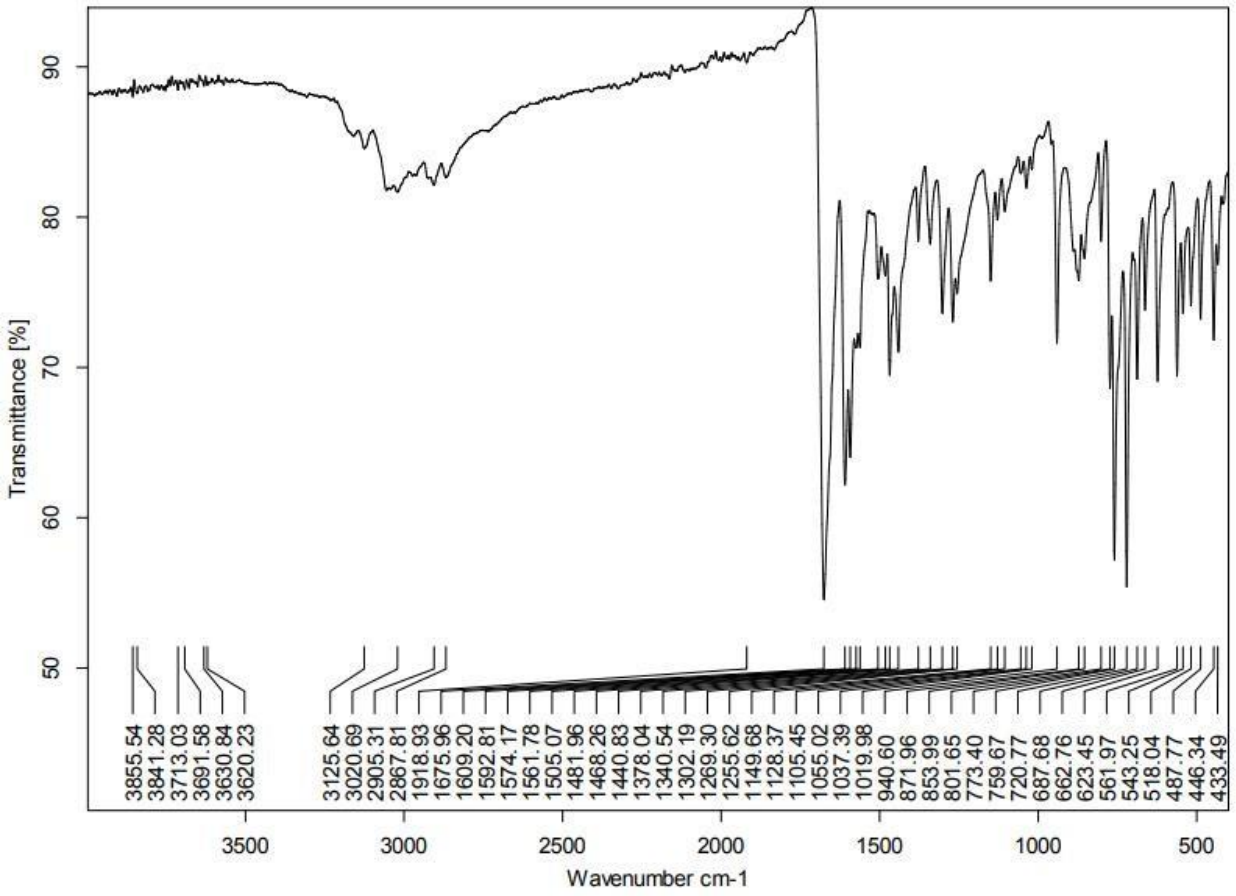

HRMS

Acquisition Parameter

Source Type	APCI	Ion Polarity	Positive	Set Nebulizer	0.8 Bar
Focus	Not active	Set Capillary	4500 V	Set Dry Heater	180 °C
Scan Begin	50 m/z	Set End Plate Offset	-500 V	Set Dry Gas	4.0 l/min
Scan End	2000 m/z	Set Collision Cell RF	100.0 Vpp	Set Divert Valve	Waste

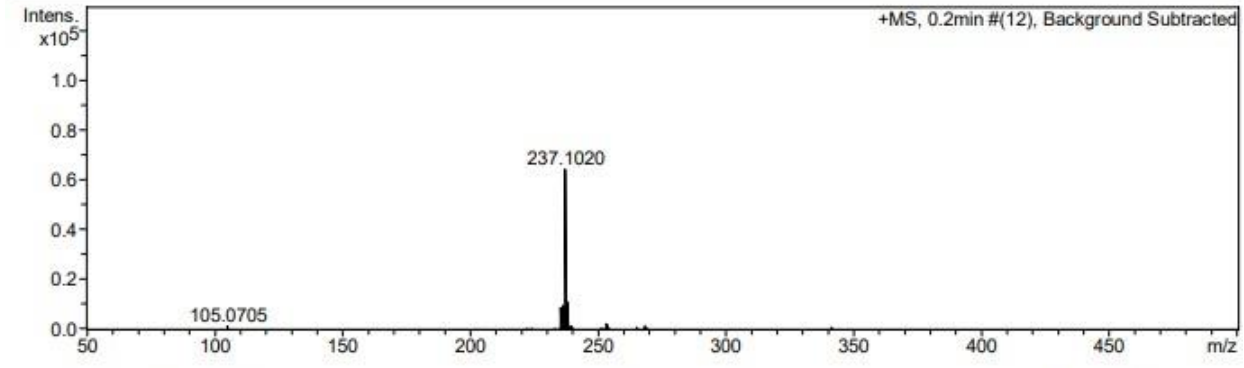

Meas. m/z	#	Formula	Score	m/z	err [mDa]	err [ppm]	mSigma	rdb	e⁻ Conf	N-Rule
237.1020	1	C 15 H 13 N 2 O	100.00	237.1022	0.2	0.9	8.4	10.5	even	ok

HPLC

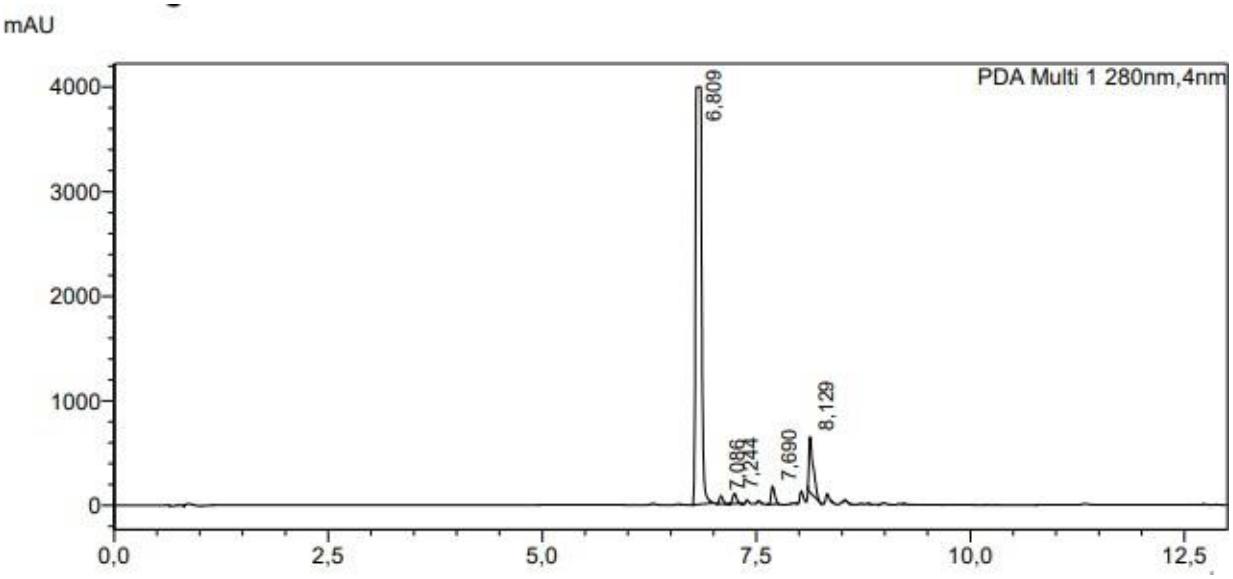

2-(3-chlorophenyl)quinazolin-4(3H)-one **(1c)**

^{1}H NMR

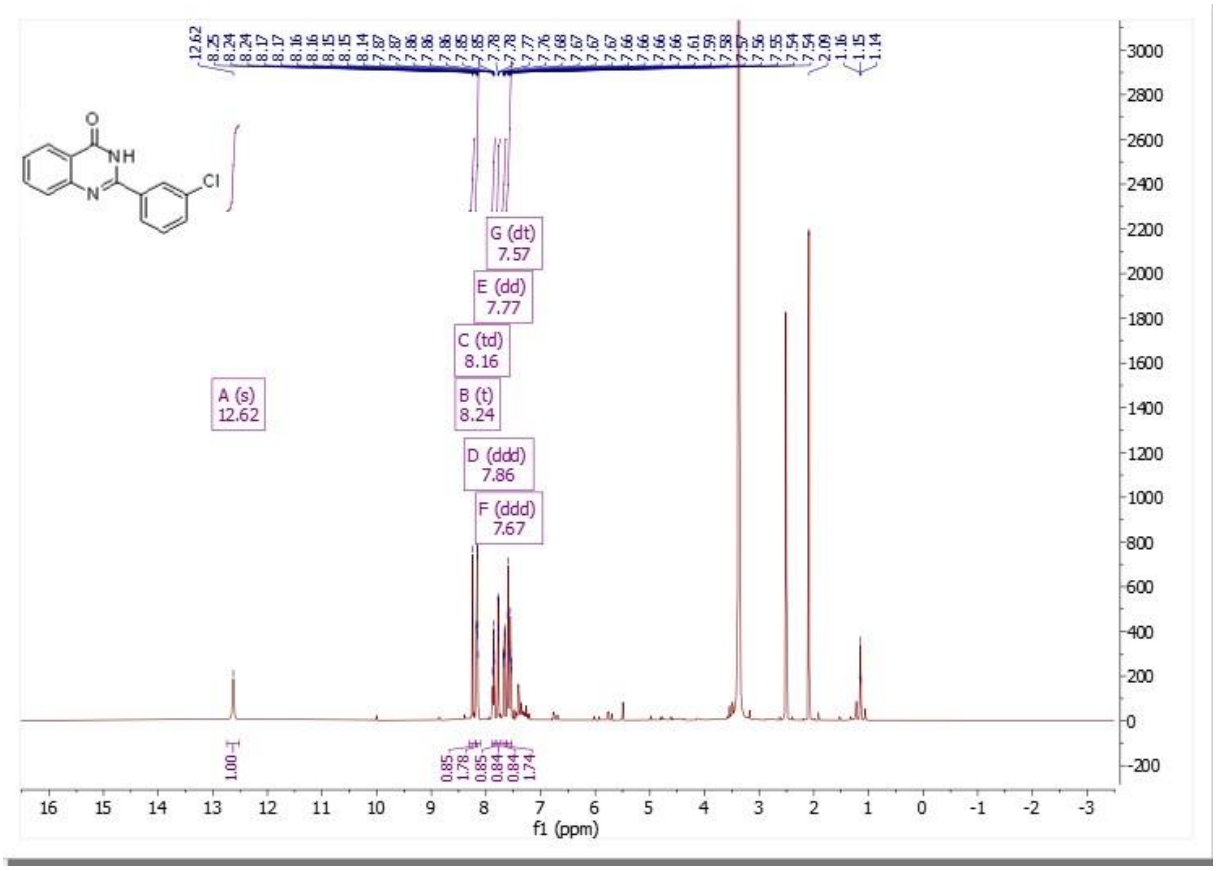

^{13}C NMR

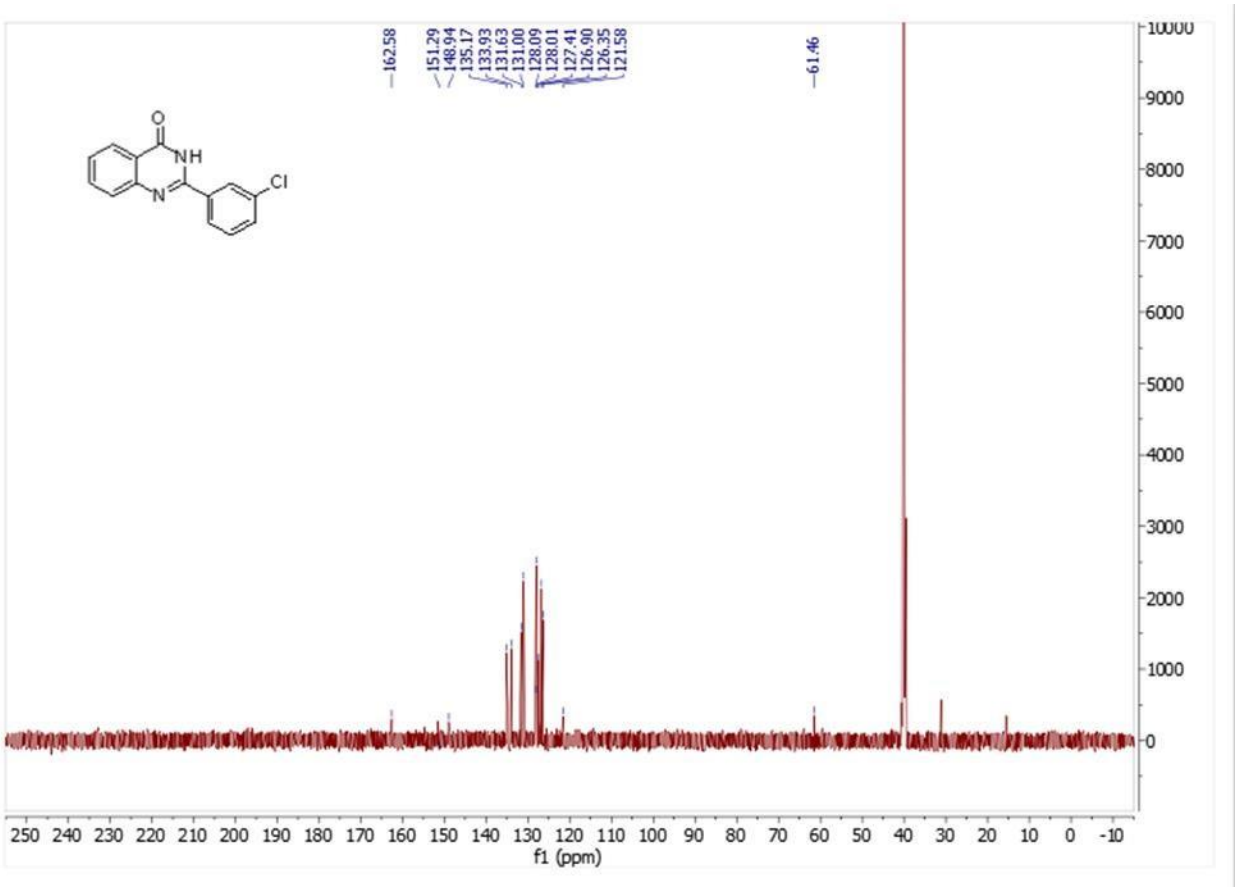
162.58
151.29
148.94
135.17
133.93
131.63
131.00
128.09
128.01
127.41
126.90
126.35
121.58
61.46
O
NH
N
Cl
10000
9000
8000
7000
6000
5000
4000
3000
2000
1000
0
250 240 230 220 210 200 190 180 170 160 150 140 130 120 110 100 90 80 70 60 50 40 30 20 10 0 -10
f1 (ppm)

FTIR

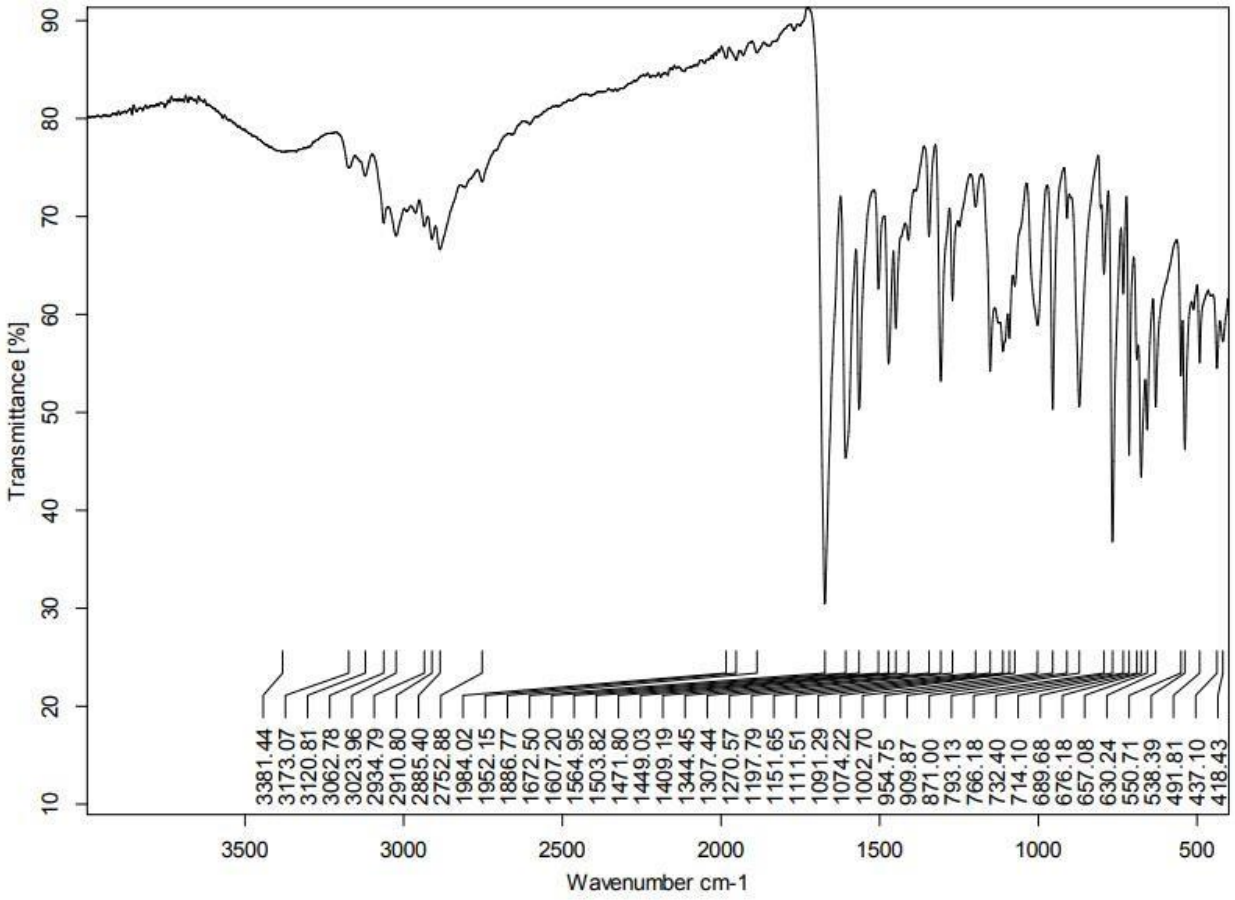

HRMS

Acquisition Parameter

Source Type	APCI	Ion Polarity	Positive	Set Nebulizer	0.8 Bar
Focus	Not active	Set Capillary	4500 V	Set Dry Heater	180 °C
Scan Begin	50 m/z	Set End Plate Offset	-500 V	Set Dry Gas	4.0 l/min
Scan End	2000 m/z	Set Collision Cell RF	100.0 Vpp	Set Divert Valve	Waste

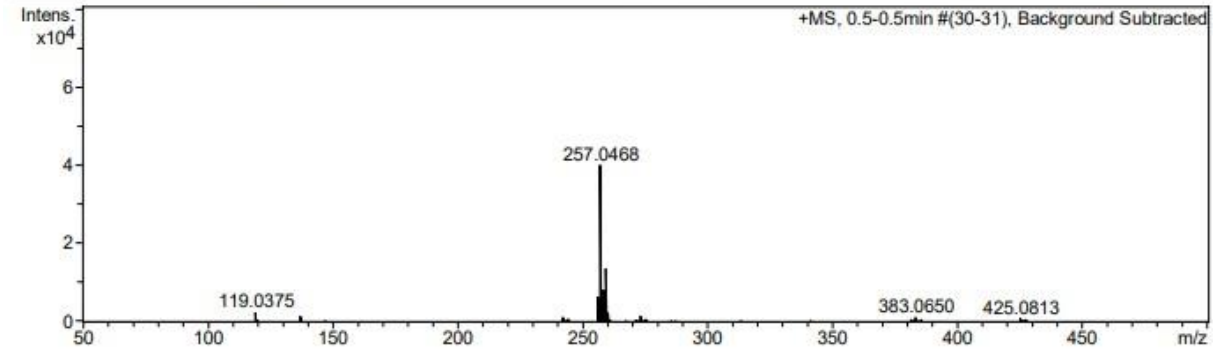

Meas. m/z	#	Formula	Score	m/z	err [mDa]	err [ppm]	mSigma	rdb	e⁻ Conf	N-Rule
257.0468	1	C 14 H 10 Cl N 2 O	100.00	257.0476	0.8	3.2	23.5	10.5	even	ok

HPLC

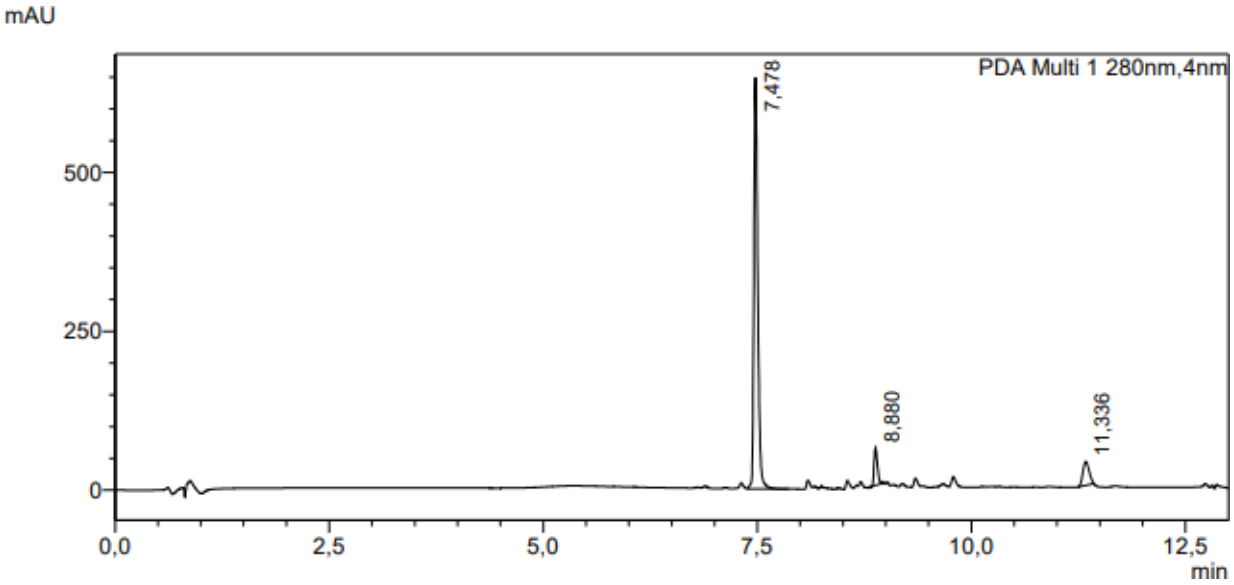

2-(3-fluorophenyl)quinazolin-4(3H)-one **(1d)**

^{1}H NMR

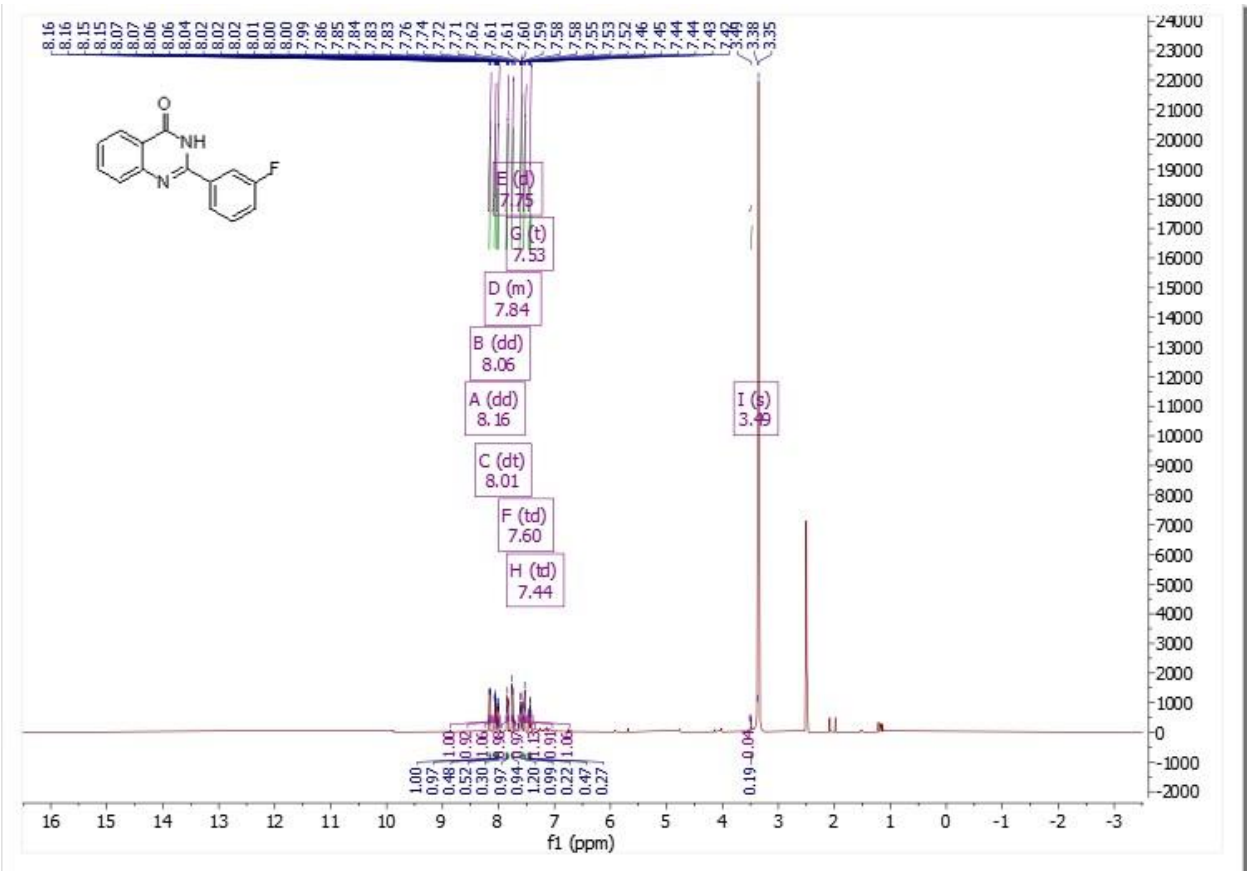

^{13}C NMR

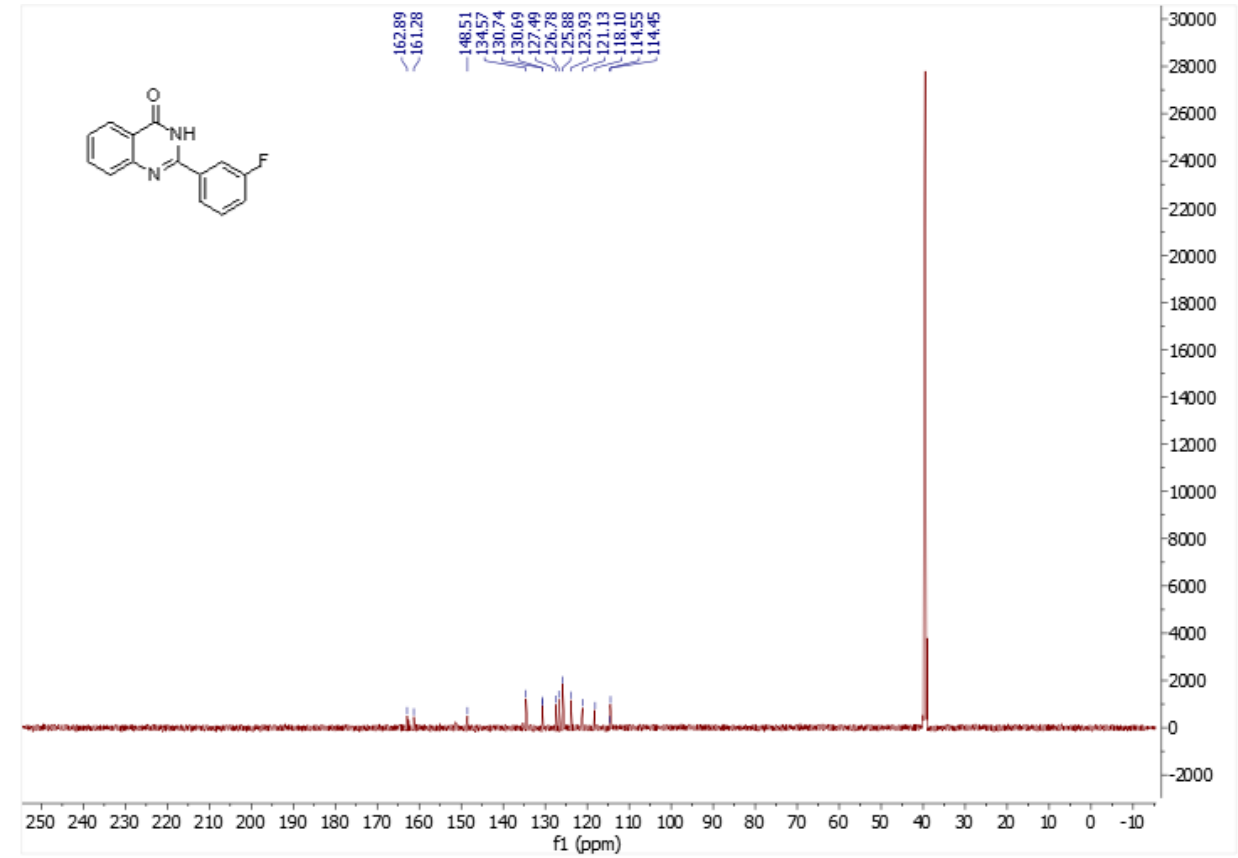
162.89
161.28
148.51
134.57
130.74
130.69
127.49
126.78
125.88
123.93
121.13
118.10
114.55
114.45
O
NH
N
F
30000
28000
26000
24000
22000
20000
18000
16000
14000
12000
10000
8000
6000
4000
2000
0
-2000
250 240 230 220 210 200 190 180 170 160 150 140 130 120 110 100 90 80 70 60 50 40 30 20 10 0 -10
f1 (ppm)

FTIR

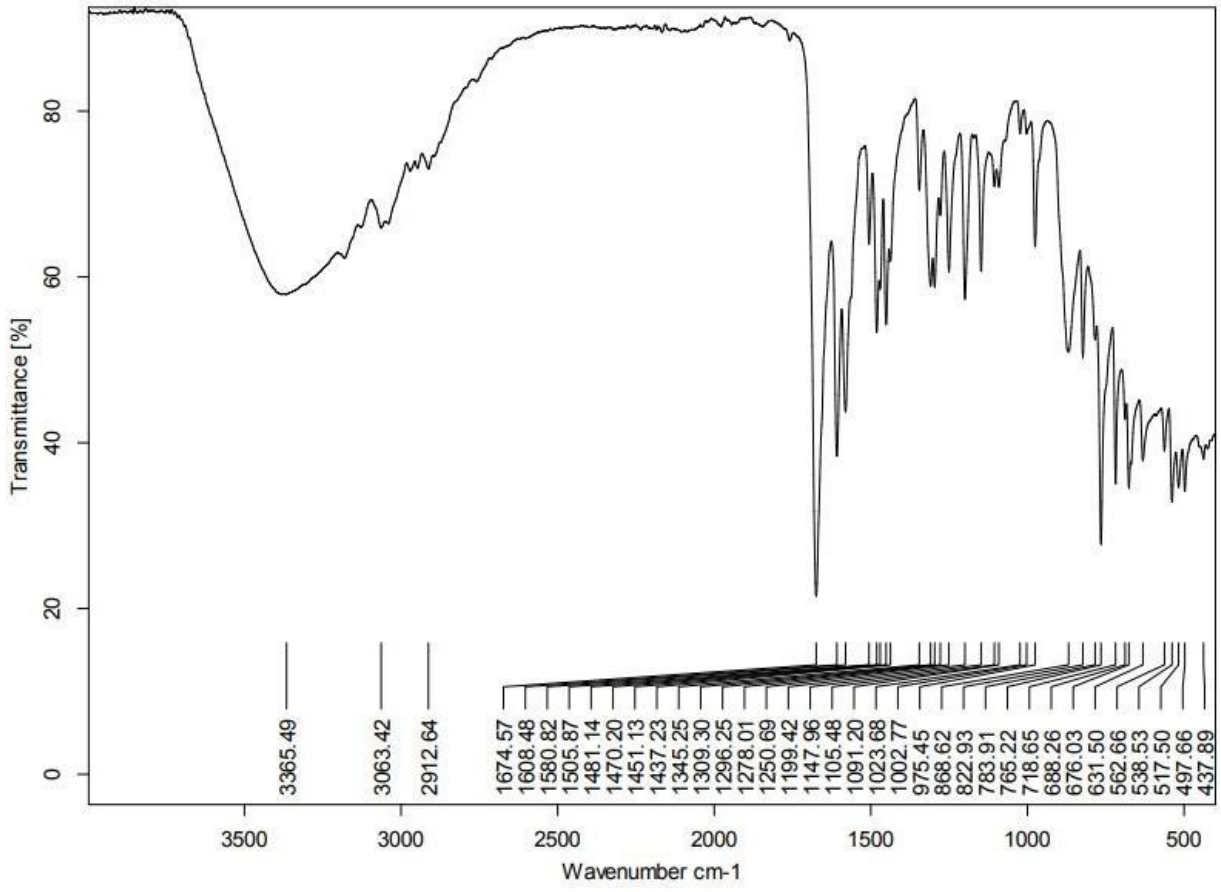

HRMS

Acquisition Parameter

Source Type	APCI	Ion Polarity	Positive	Set Nebulizer	0.8 Bar
Focus	Not active	Set Capillary	4500 V	Set Dry Heater	180 °C
Scan Begin	50 m/z	Set End Plate Offset	-500 V	Set Dry Gas	4.0 l/min
Scan End	2000 m/z	Set Collision Cell RF	100.0 Vpp	Set Divert Valve	Waste

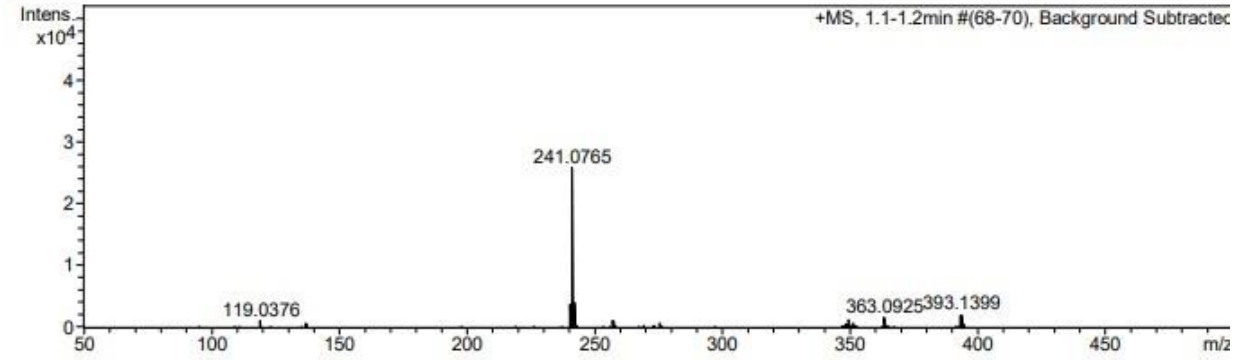

Meas. m/z	#	Formula	Score	m/z	err [mDa]	err [ppm]	mSigma	rdb	e⁻ Conf	N-Rule
241.0765	1	C 14 H 10 F N 2 O	100.00	241.0772	0.7	2.8	7.2	10.5	even	ok

HPLC

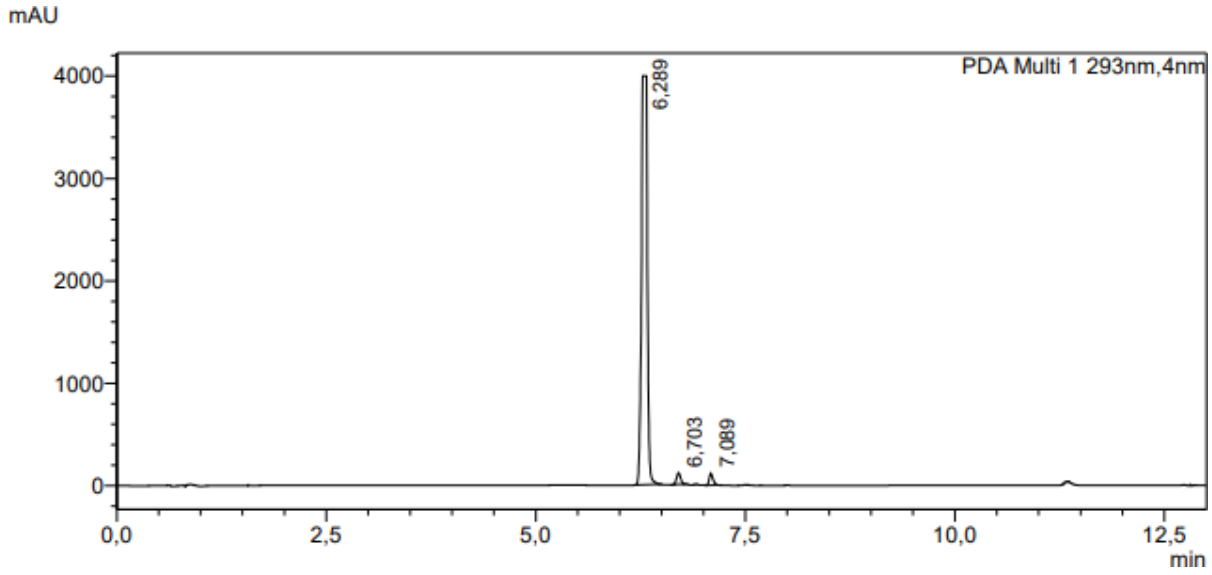

2-(4-hydroxyphenyl)quinazolin-4(3H)-one **(1e)**

^{1}H NMR

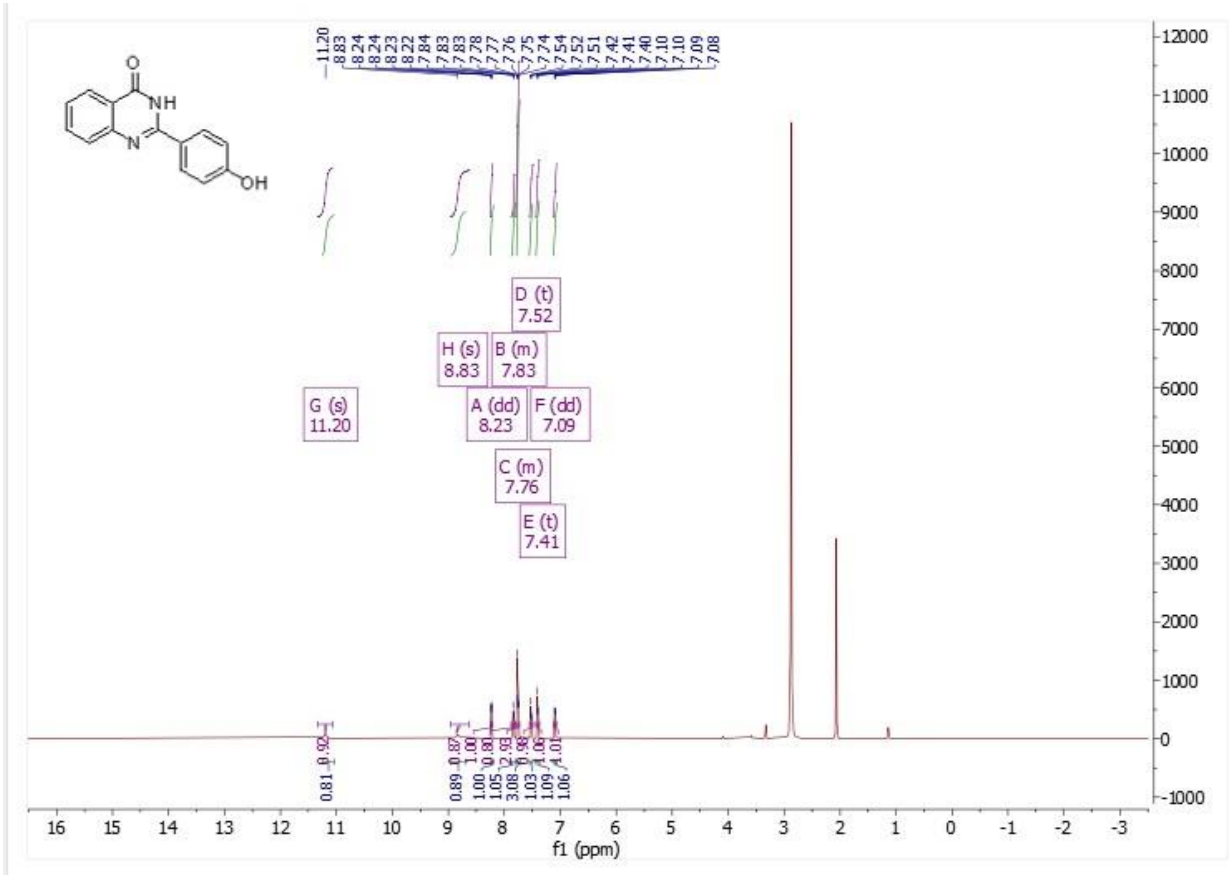

^{13}C NMR

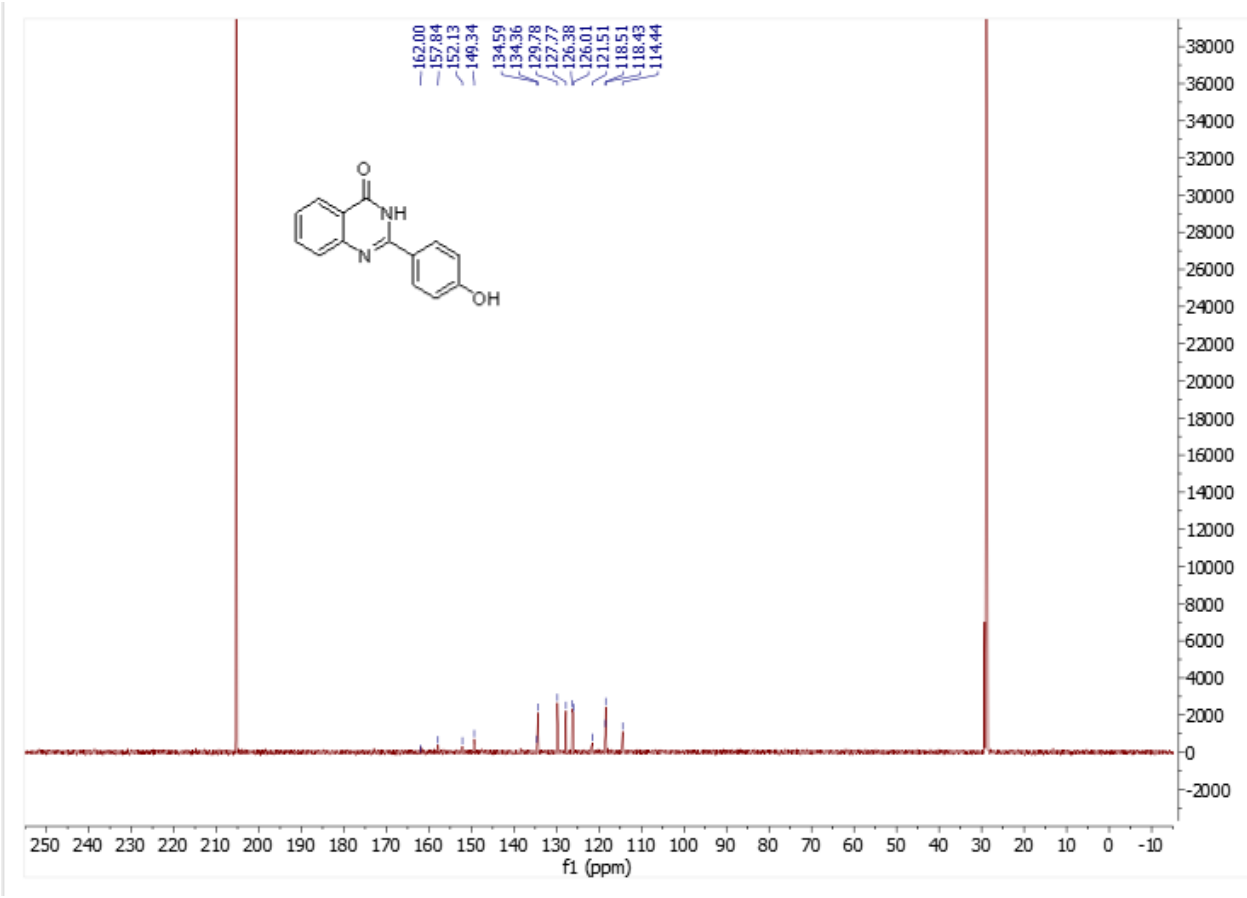
162.00
157.84
152.13
149.34
134.59
134.36
129.78
127.77
126.38
126.01
121.51
118.51
118.43
114.44
O
NH
N
OH
38000
36000
34000
32000
30000
28000
26000
24000
22000
20000
18000
16000
14000
12000
10000
8000
6000
4000
2000
0
-2000
250 240 230 220 210 200 190 180 170 160 150 140 130 120 110 100 90 80 70 60 50 40 30 20 10 0 -10
f1 (ppm)

FTIR

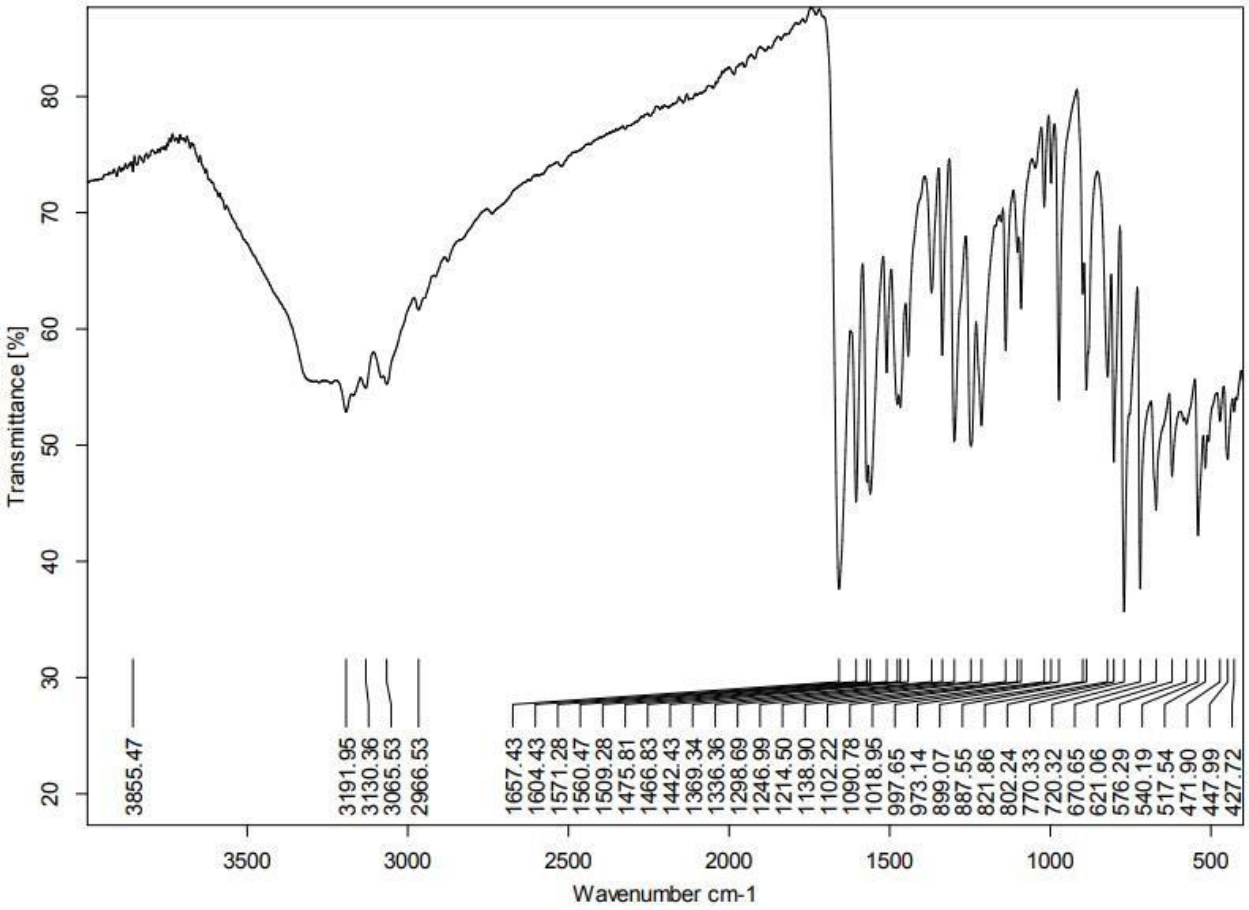

HRMS

Acquisition Parameter

Source Type	APCI	Ion Polarity	Positive	Set Nebulizer	0.8 Bar
Focus	Not active	Set Capillary	4500 V	Set Dry Heater	180 °C
Scan Begin	50 m/z	Set End Plate Offset	-500 V	Set Dry Gas	4.0 l/min
Scan End	2000 m/z	Set Collision Cell RF	100.0 Vpp	Set Divert Valve	Waste

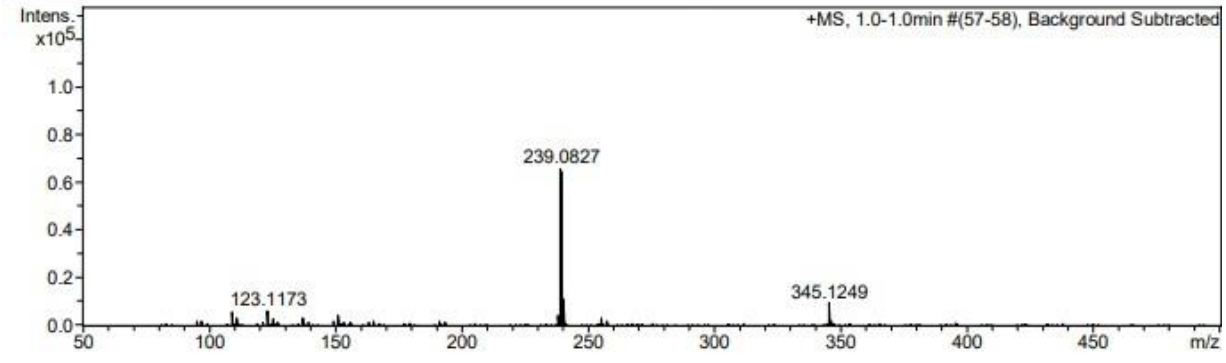

Meas. m/z	#	Formula	Score	m/z	err [mDa]	err [ppm]	mSigma	rdb	e⁻ Conf	N-Rule
239.0827	1	C 14 H 11 N 2 O 2	100.00	239.0815	-1.2	-5.1	5.0	10.5	even	ok

HPLC

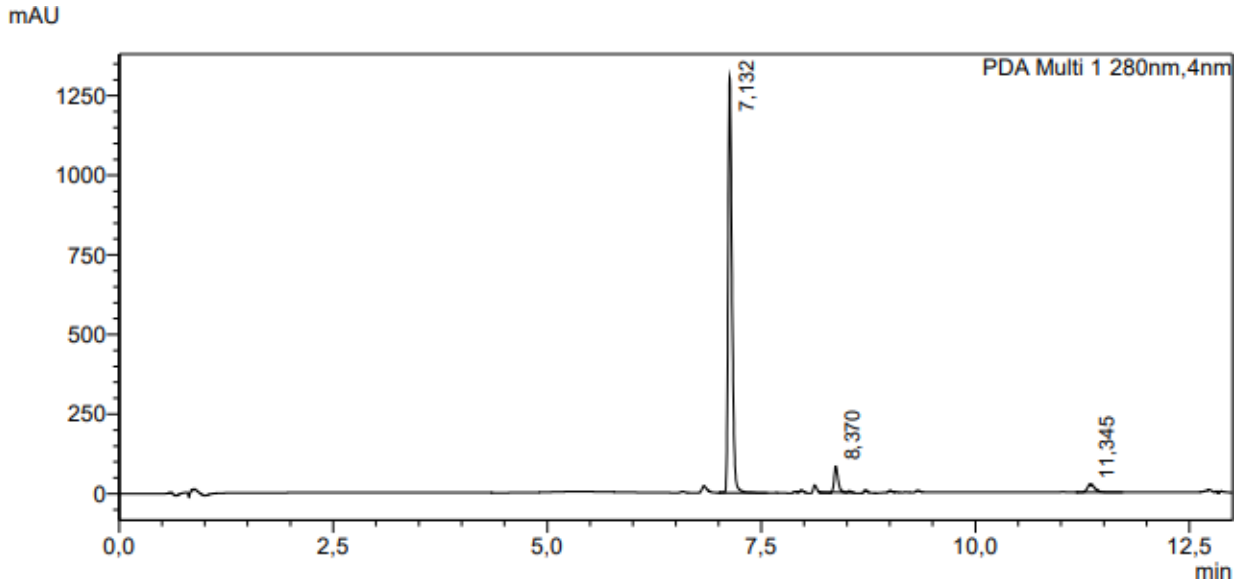

2-(4-bromophenyl)quinazolin-4(3H)-one **(1f)**

^{1}H NMR

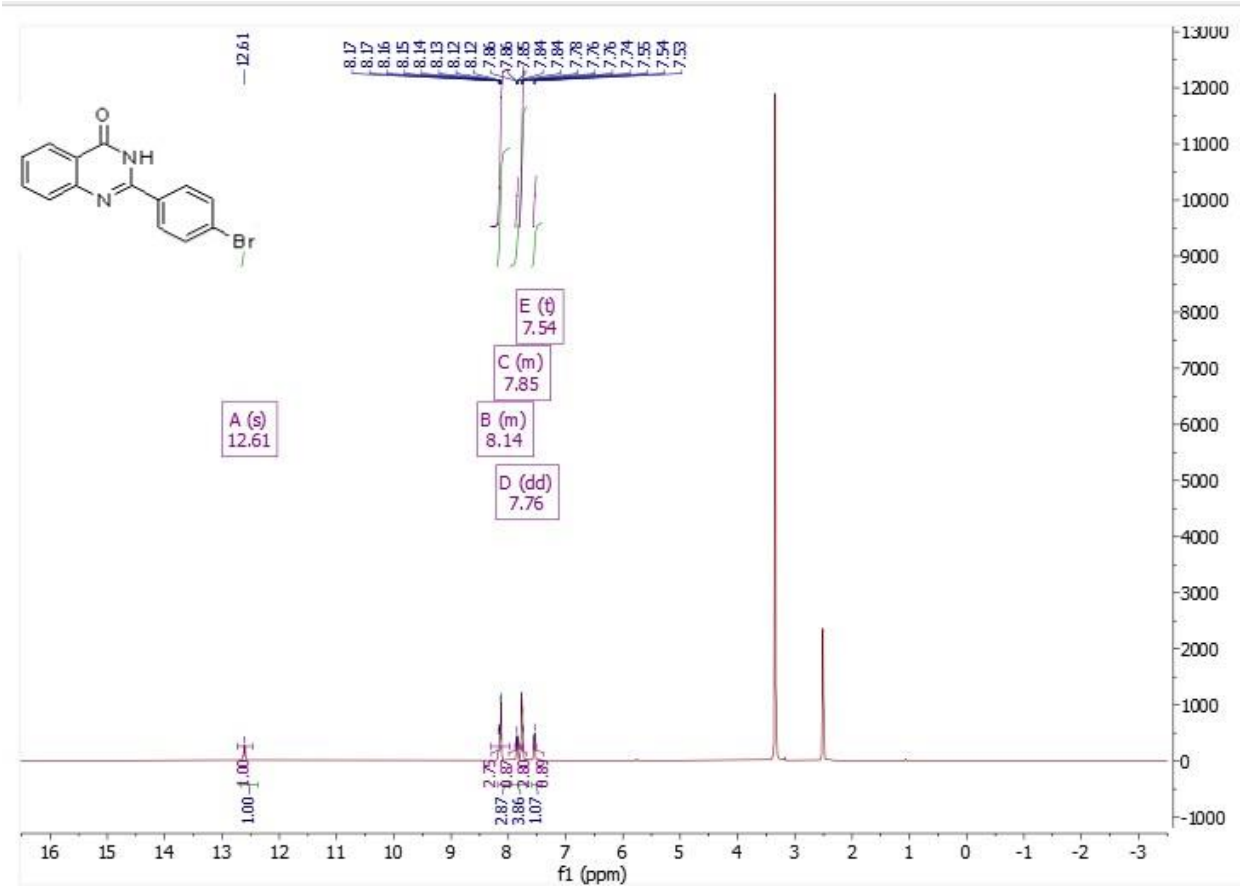

^{13}C NMR

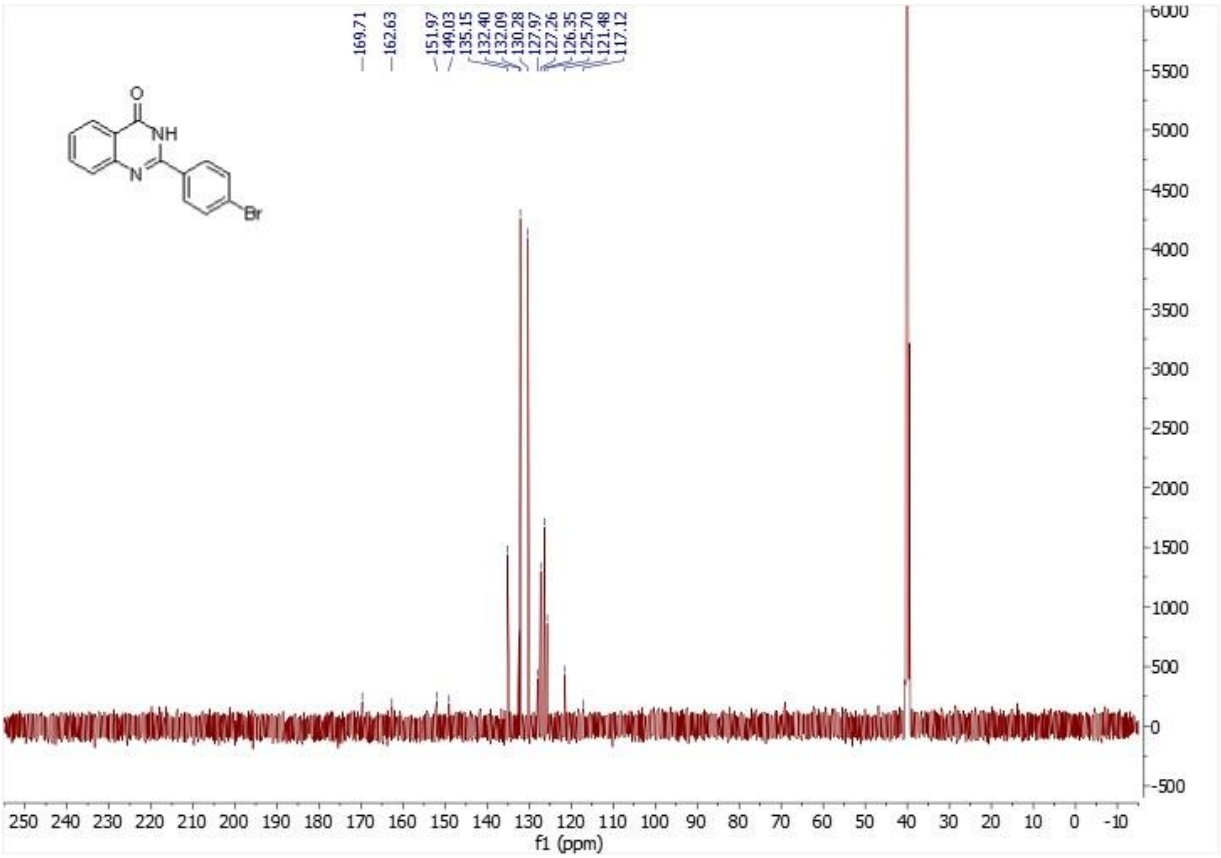
169.71
162.63
151.97
149.03
135.15
132.40
132.09
130.28
127.97
127.26
126.35
125.70
121.48
117.12
O
NH
N
Br
f1 (ppm)

FTIR

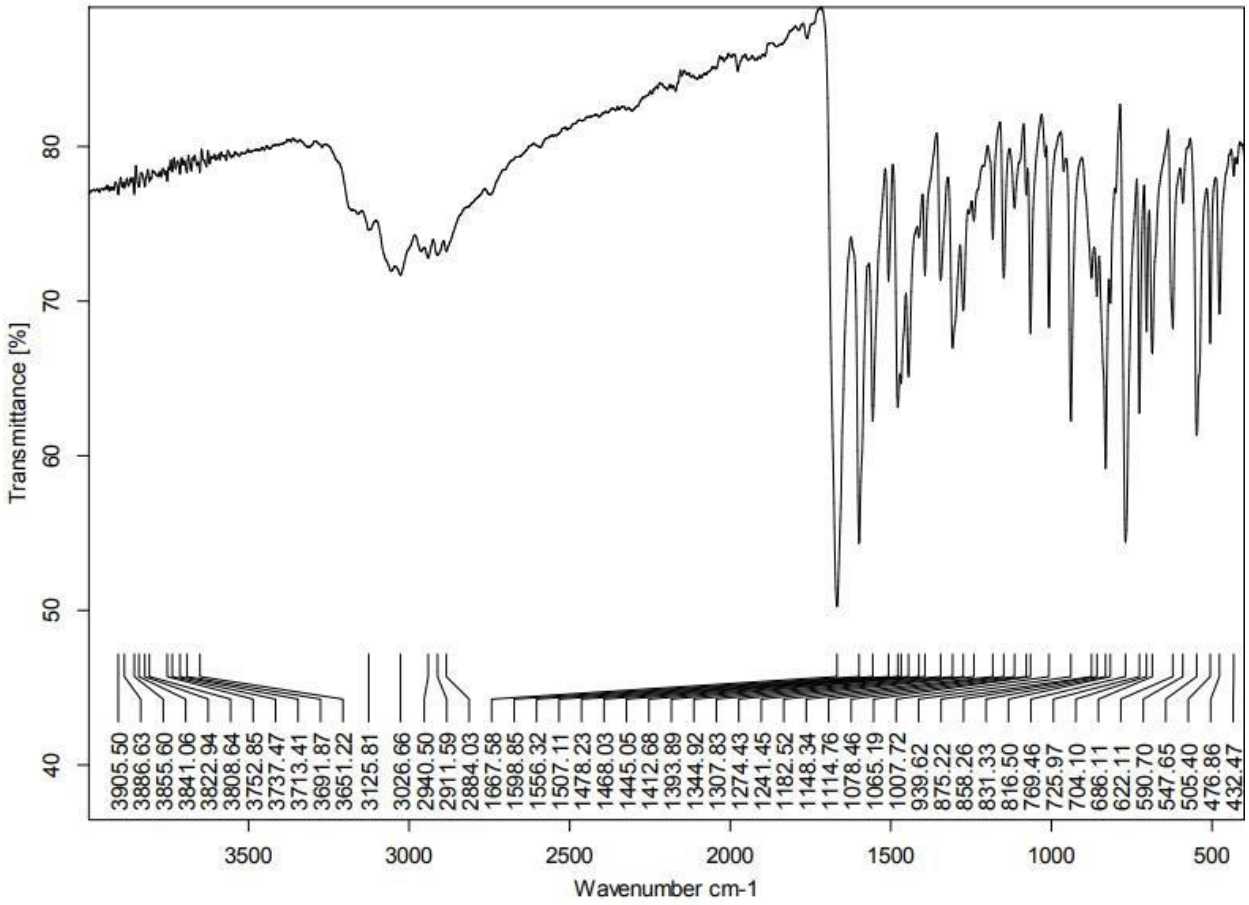

HRMS

Acquisition Parameter

Source Type	APCI	Ion Polarity	Positive	Set Nebulizer	0.8 Bar
Focus	Not active	Set Capillary	4500 V	Set Dry Heater	180 °C
Scan Begin	50 m/z	Set End Plate Offset	-500 V	Set Dry Gas	4.0 l/min
Scan End	2000 m/z	Set Collision Cell RF	100.0 Vpp	Set Divert Valve	Waste

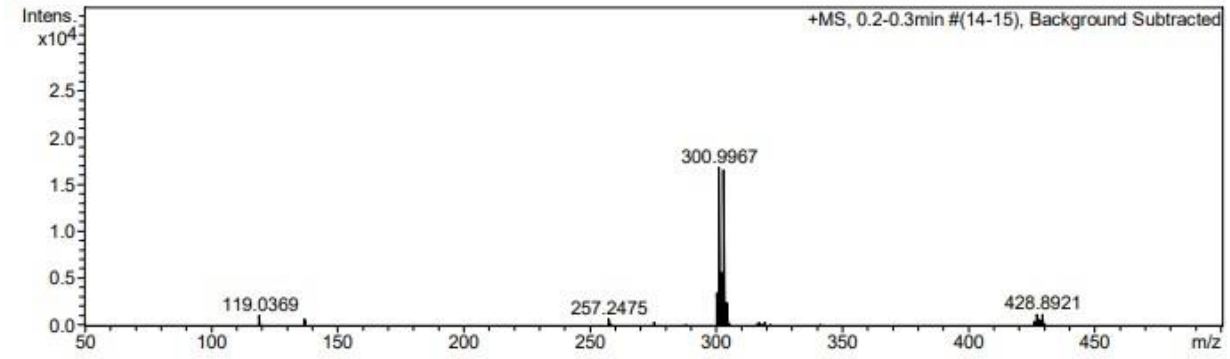

Meas. m/z	#	Formula	Score	m/z	err [mDa]	err [ppm]	mSigma	rdb	e⁻ Conf	N-Rule
300.9967	1	C 14 H 10 Br N 2 O	100.00	300.9971	0.4	1.2	81.8	10.5	even	ok

HPLC

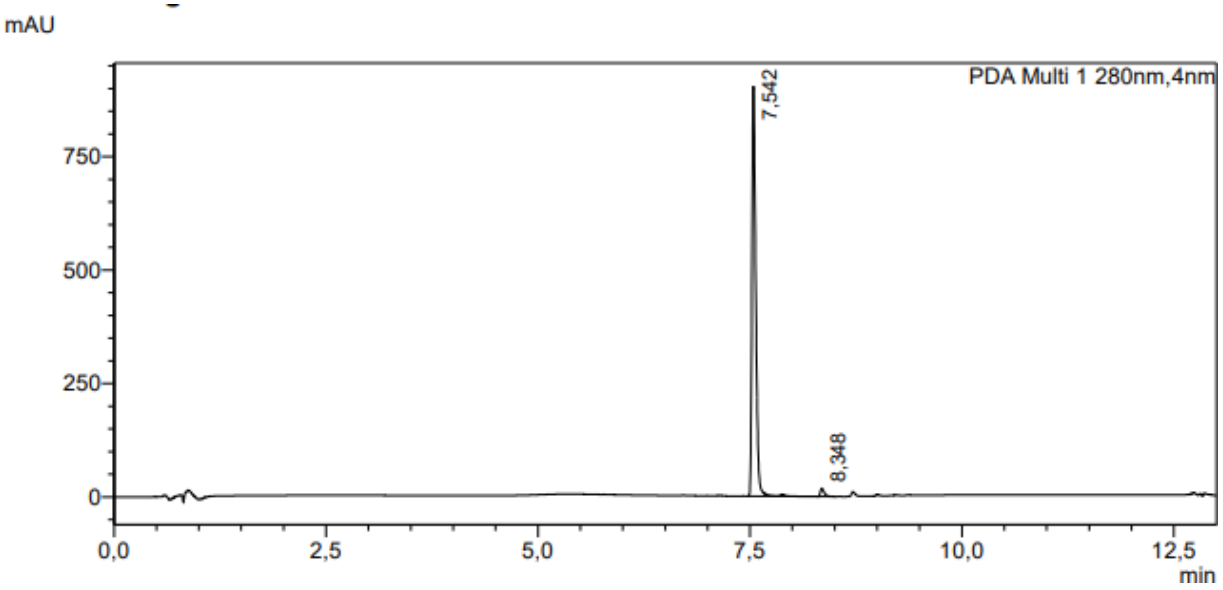

4-chloro-2-(3-fluorophenyl)quinazoline **(2a)**

^{1}H NMR

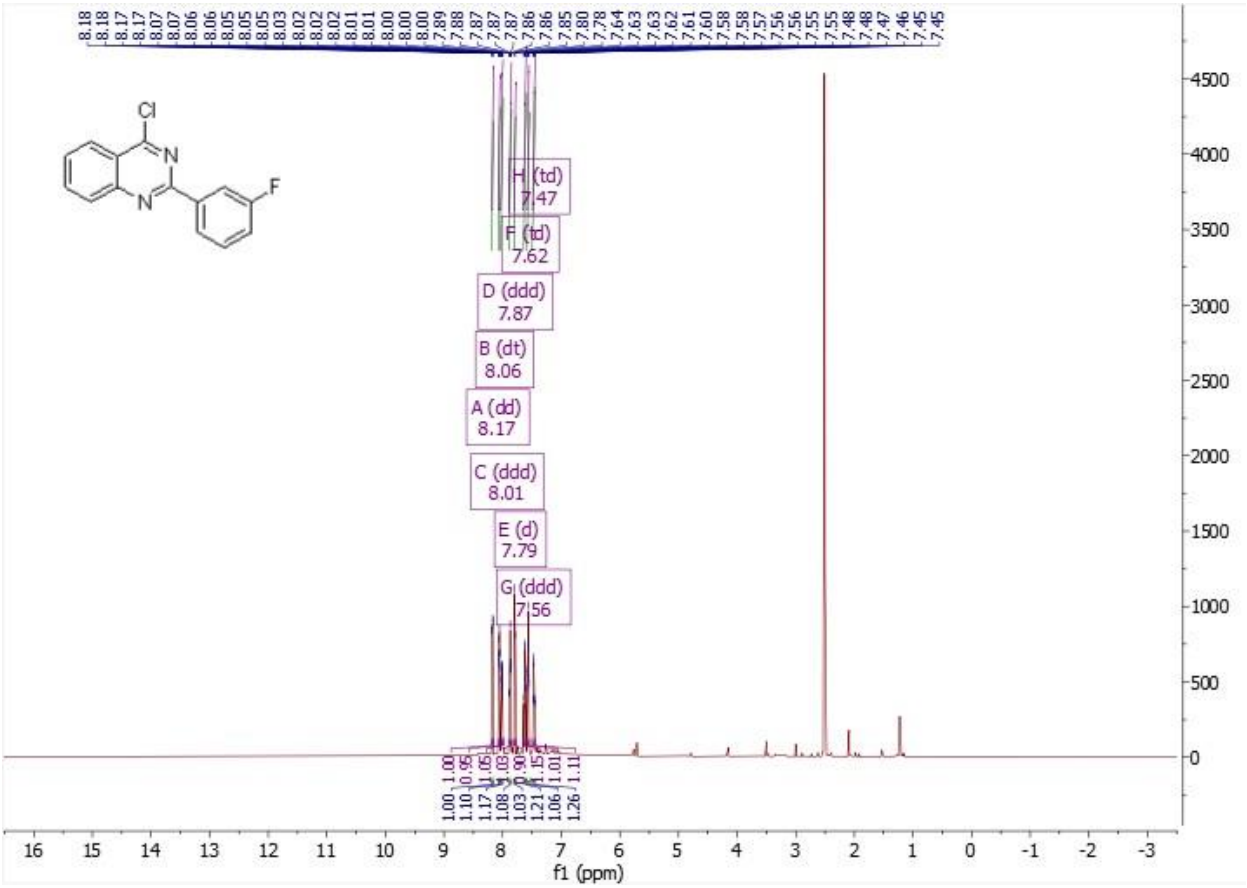

^{13}C NMR

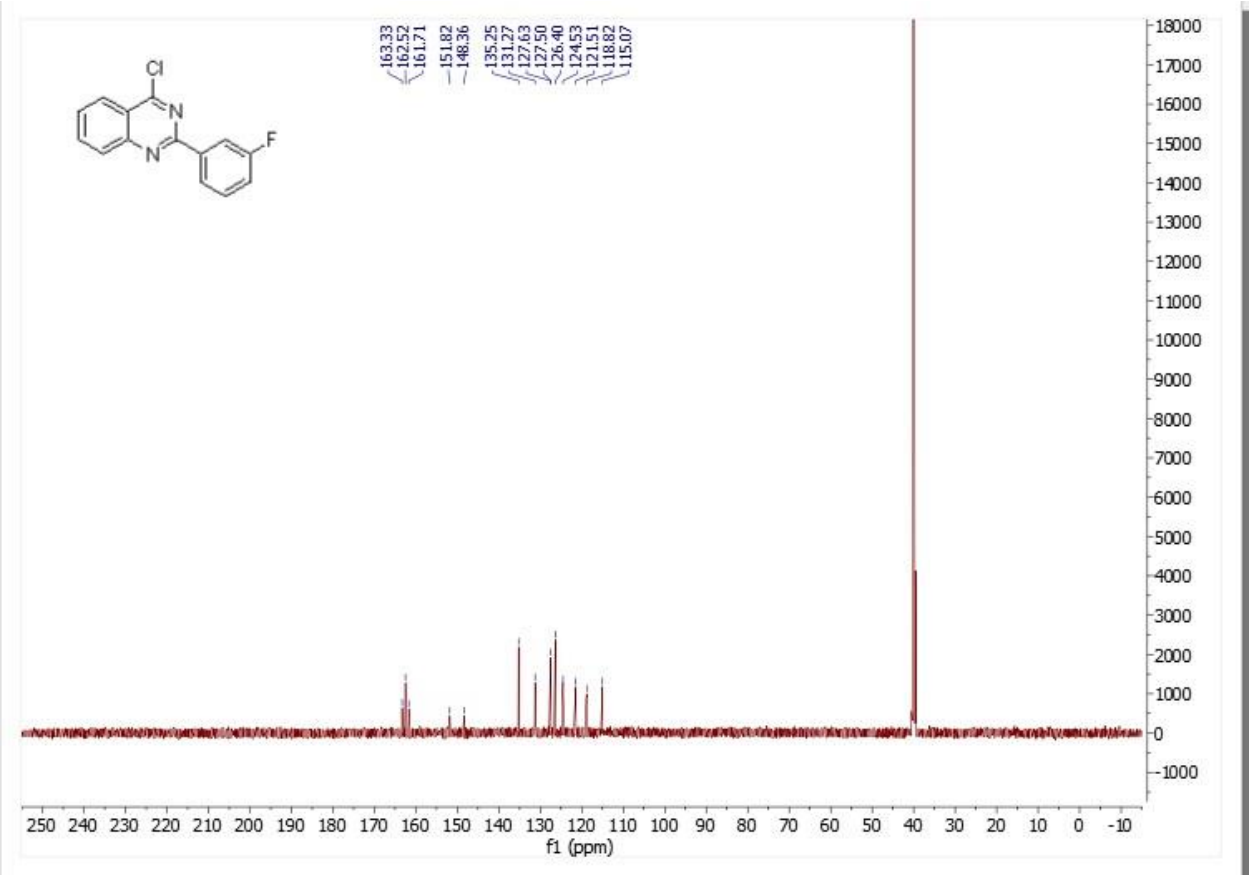
163.33
162.52
161.71
151.82
148.36
135.25
131.27
127.63
127.50
126.40
124.53
121.51
118.82
115.07
Cl
N
N
F
18000
17000
16000
15000
14000
13000
12000
11000
10000
9000
8000
7000
6000
5000
4000
3000
2000
1000
0
-1000
250 240 230 220 210 200 190 180 170 160 150 140 130 120 110 100 90 80 70 60 50 40 30 20 10 0 -10
f1 (ppm)

FTIR

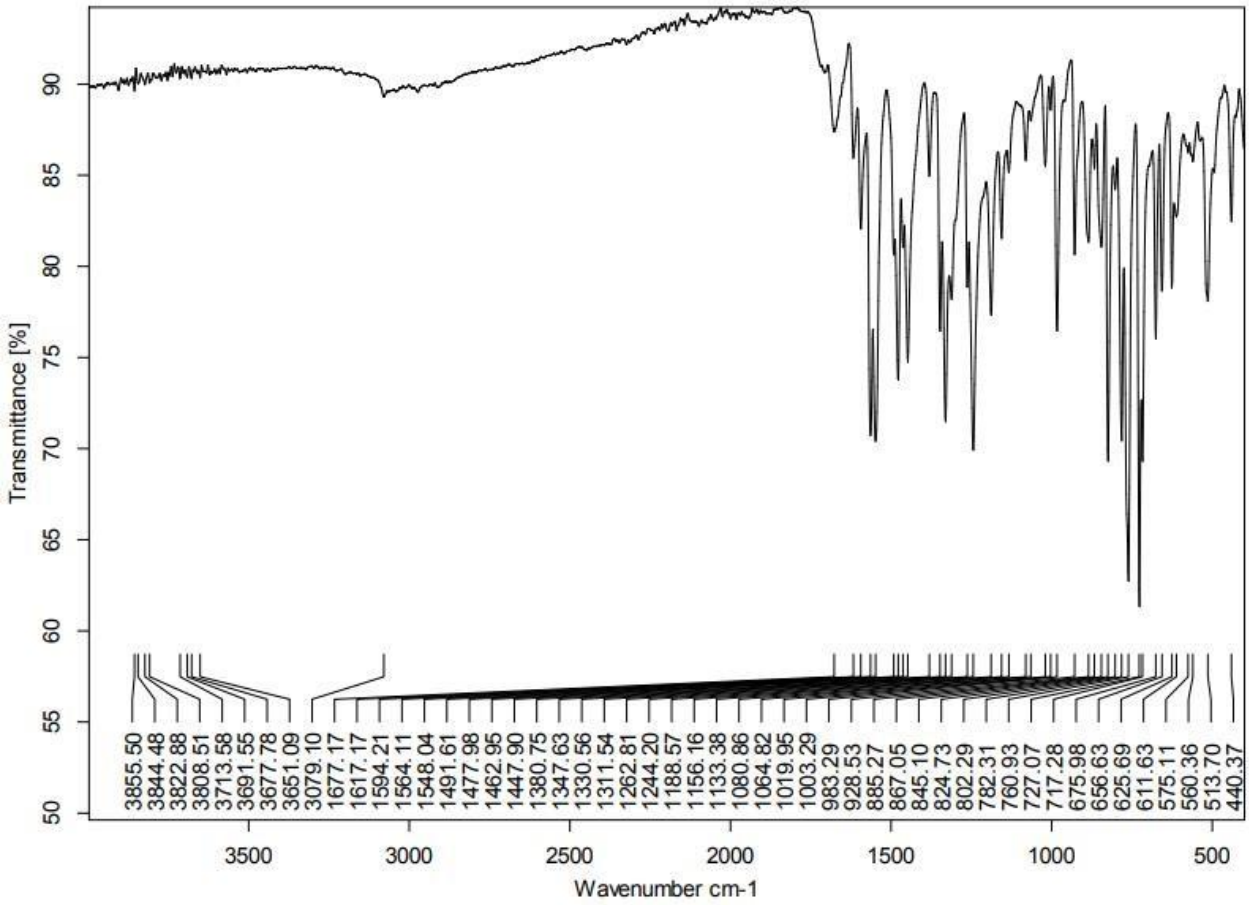

HRMS

Acquisition Parameter

Source Type	APCI	Ion Polarity	Positive	Set Nebulizer	0.6 Bar
Focus	Not active	Set Capillary	4500 V	Set Dry Heater	180 °C
Scan Begin	50 m/z	Set End Plate Offset	-500 V	Set Dry Gas	4.0 l/min
Scan End	2000 m/z	Set Collision Cell RF	100.0 Vpp	Set Divert Valve	Waste

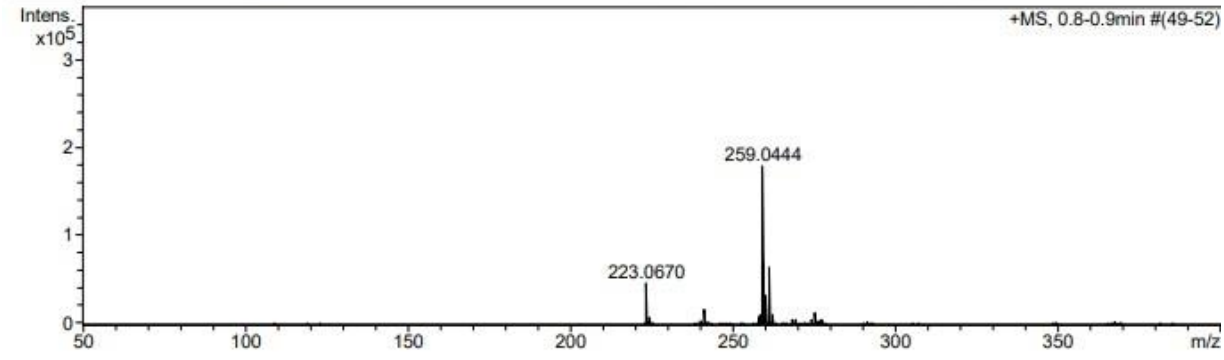

Meas. m/z	#	Formula	Score	m/z	err [mDa]	err [ppm]	mSigma	rdb	e⁻ Conf	N-Rule
223.0670	1	C 14 H 8 F N 2	100.00	223.0666	-0.4	-1.8	3.6	11.5	even	ok
	2	C 13 H 13 Cl F	0.09	223.0684	1.4	6.4	158.0	6.5	even	ok
259.0444	1	C 14 H 9 Cl F N 2	100.00	259.0433	-1.1	-4.3	15.8	10.5	even	ok

HPLC

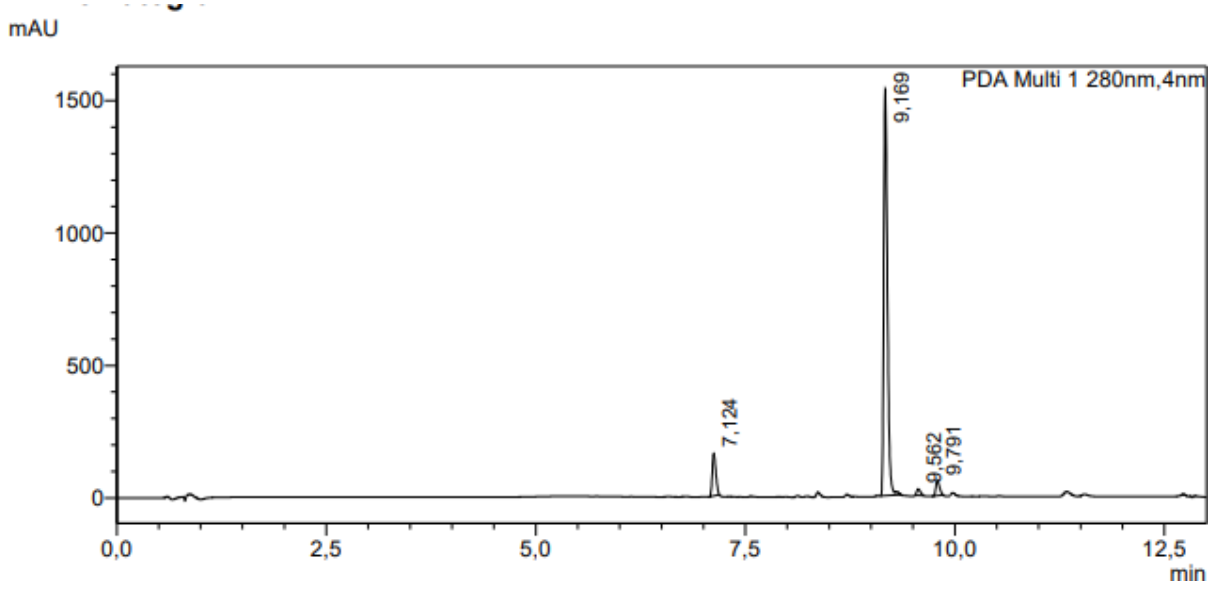

4-chloro-2-(4-fluorophenyl)quinazoline **(2b)**

^{1}H NMR

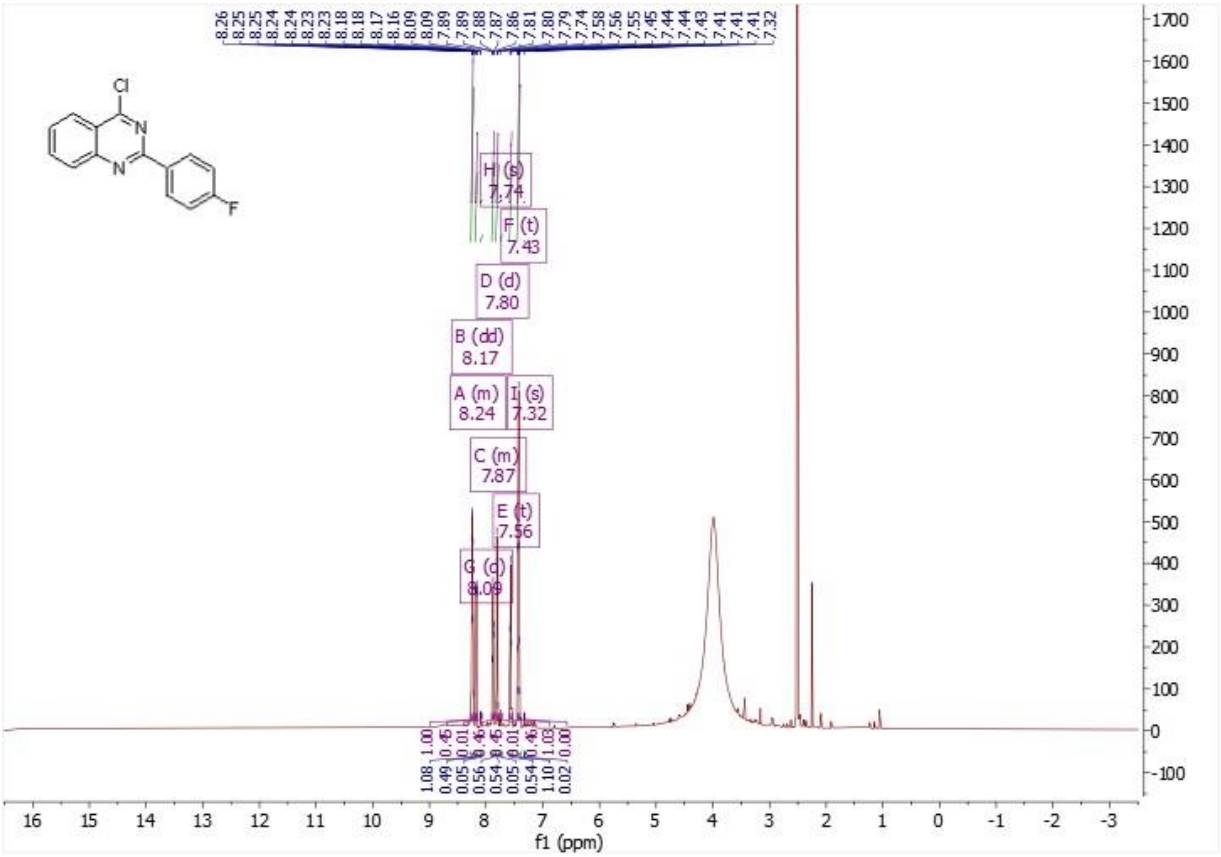

^{13}C NMR

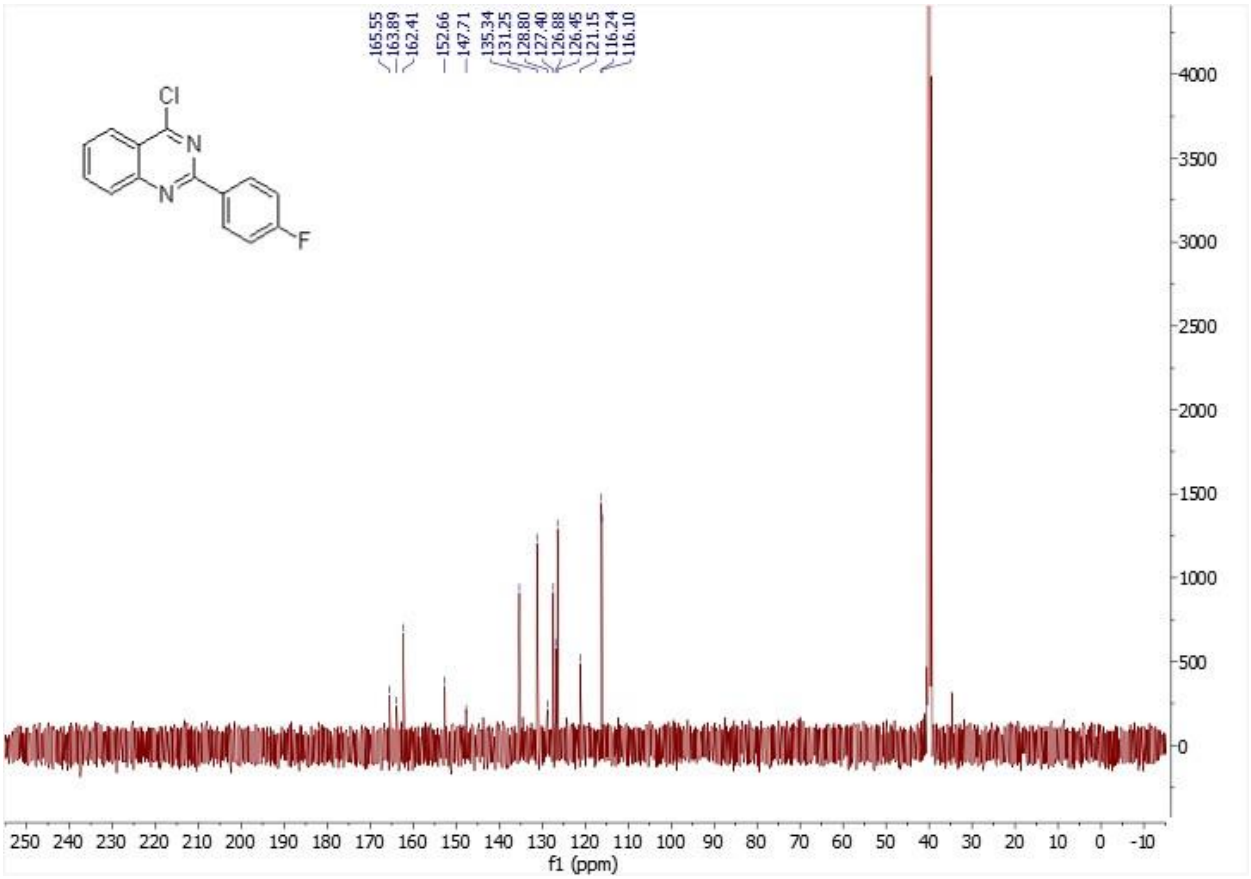
165.55
163.89
162.41
152.66
147.71
135.34
131.25
128.80
127.40
126.88
126.45
121.15
116.24
116.10
Cl
N
N
F
4000
3500
3000
2500
2000
1500
1000
500
0
250 240 230 220 210 200 190 180 170 160 150 140 130 120 110 100 90 80 70 60 50 40 30 20 10 0 -10
f1 (ppm)

FTIR

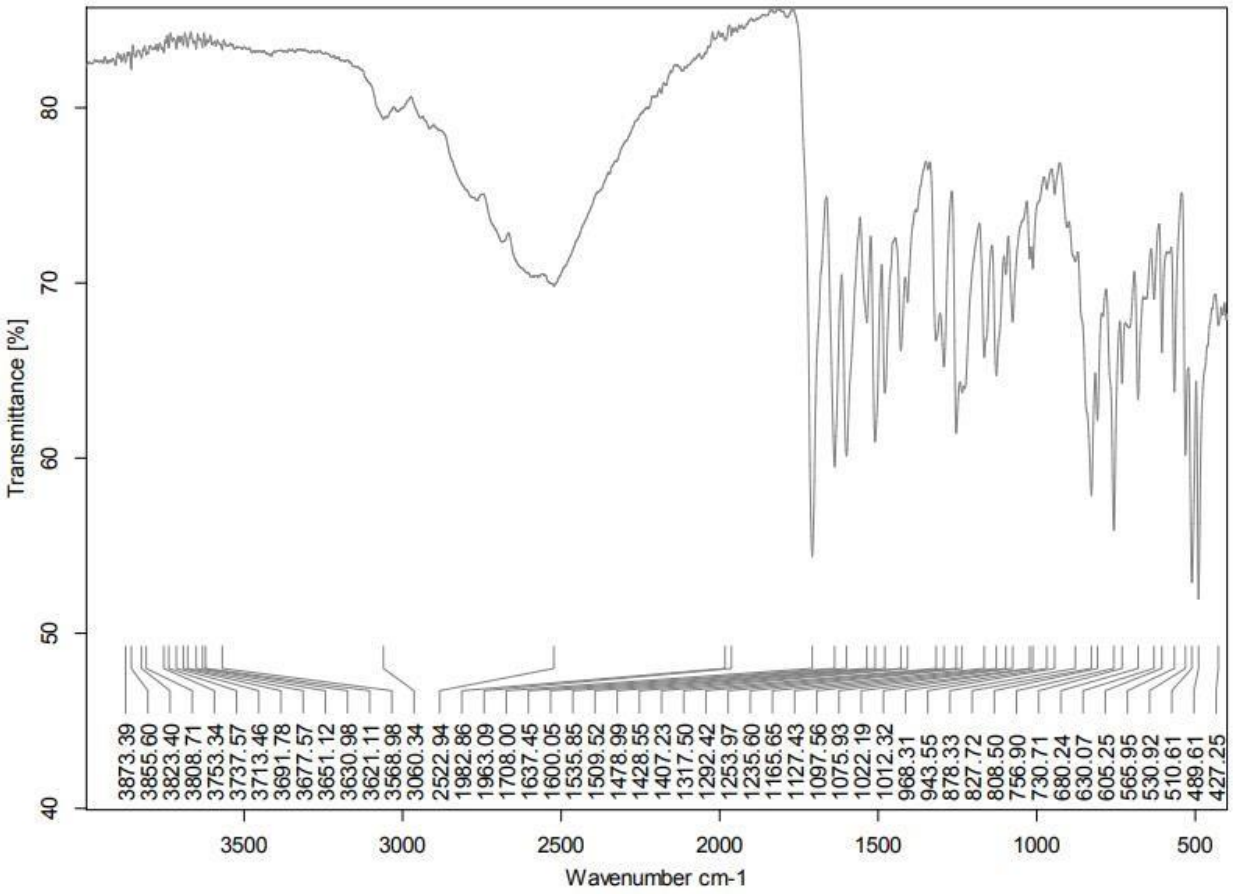

HRMS

Acquisition Parameter

Source Type	APCI	Ion Polarity	Positive	Set Nebulizer	0.6 Bar
Focus	Not active	Set Capillary	4500 V	Set Dry Heater	180 °C
Scan Begin	50 m/z	Set End Plate Offset	-500 V	Set Dry Gas	4.0 l/min
Scan End	2000 m/z	Set Collision Cell RF	100.0 Vpp	Set Divert Valve	Waste

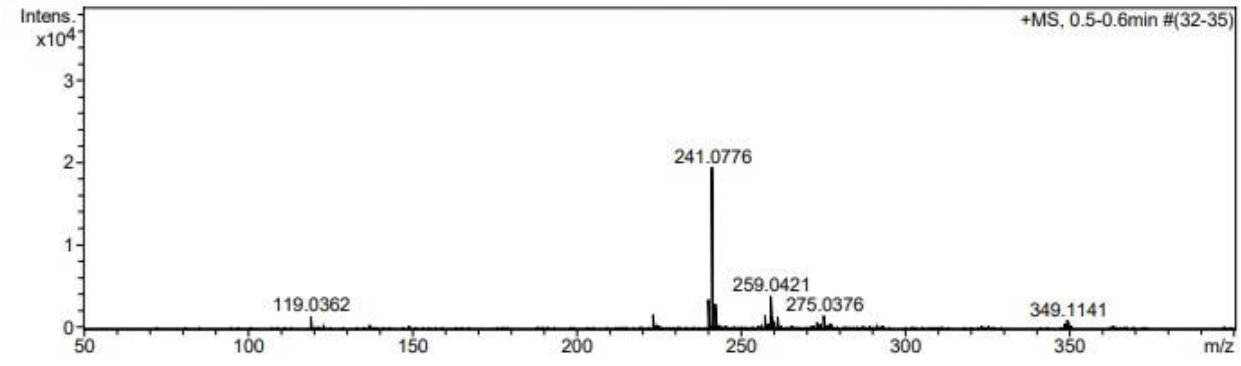

Meas. m/z	#	Formula	Score	m/z	err [mDa]	err [ppm]	mSigma	rdb	e⁻ Conf	N-Rule
259.0421	1	C 14 H 9 Cl F N 2	100.00	259.0433	1.2	4.7	24.7	10.5	even	ok

HPLC

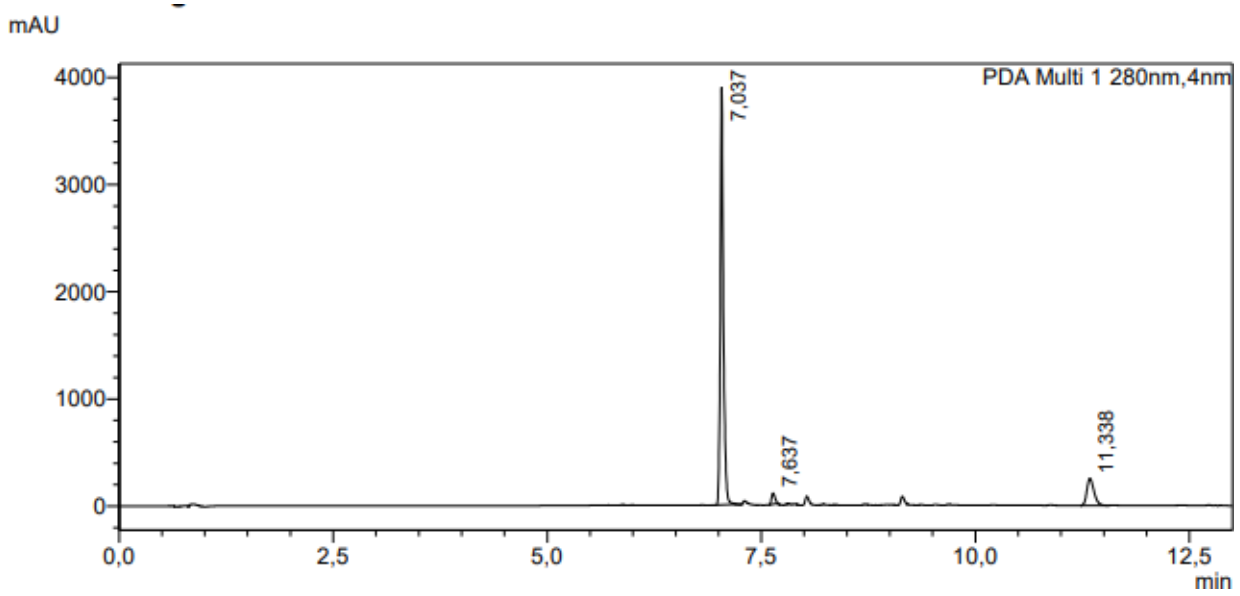
mAU
4000
3000
2000
1000
0
PDA Multi 1 280nm,4nm
7,037
7,637
11,338
0,0
2,5
5,0
7,5
10,0
12,5
min

4-chloro-2-(3-chlorophenyl)quinazoline **(2c)**

^{1}H NMR

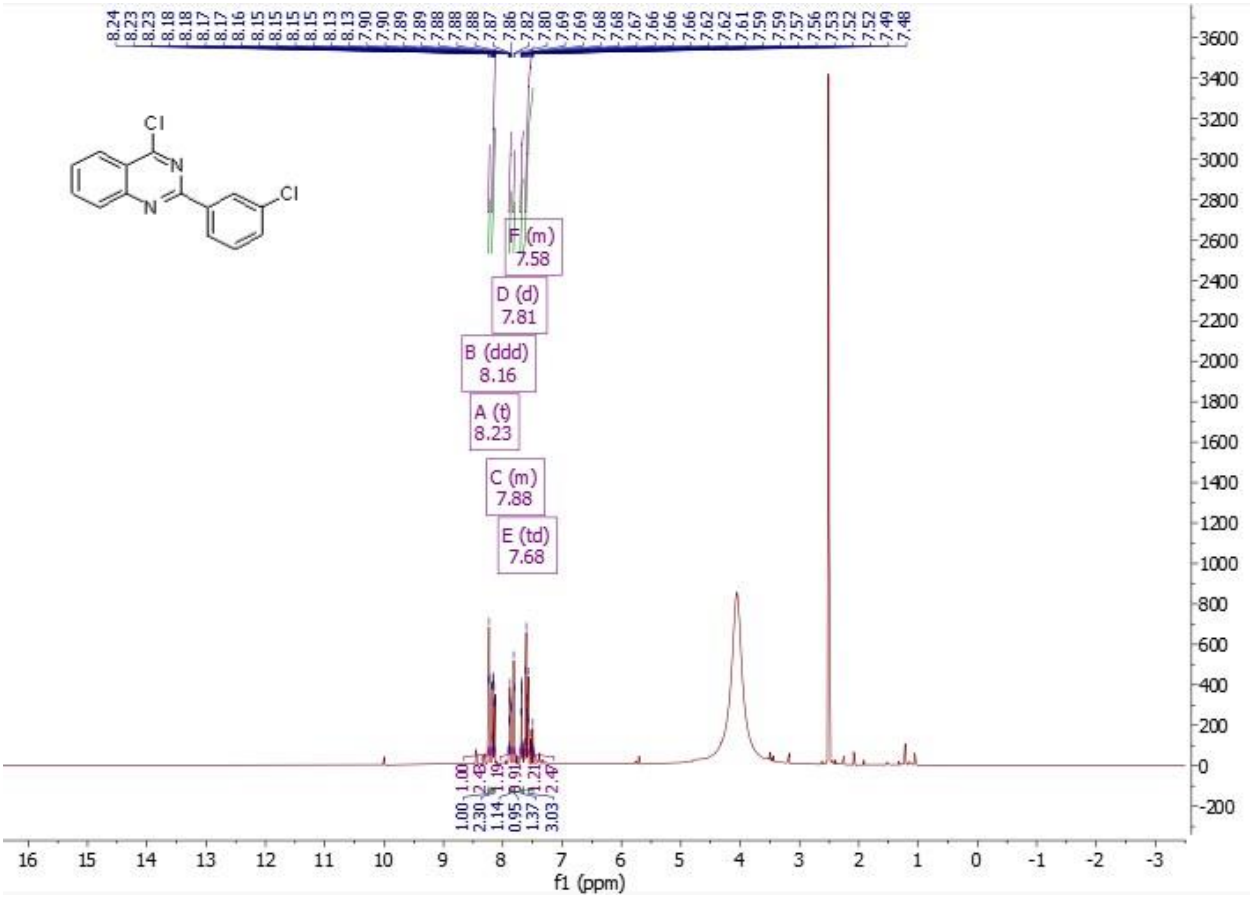

^{13}C NMR

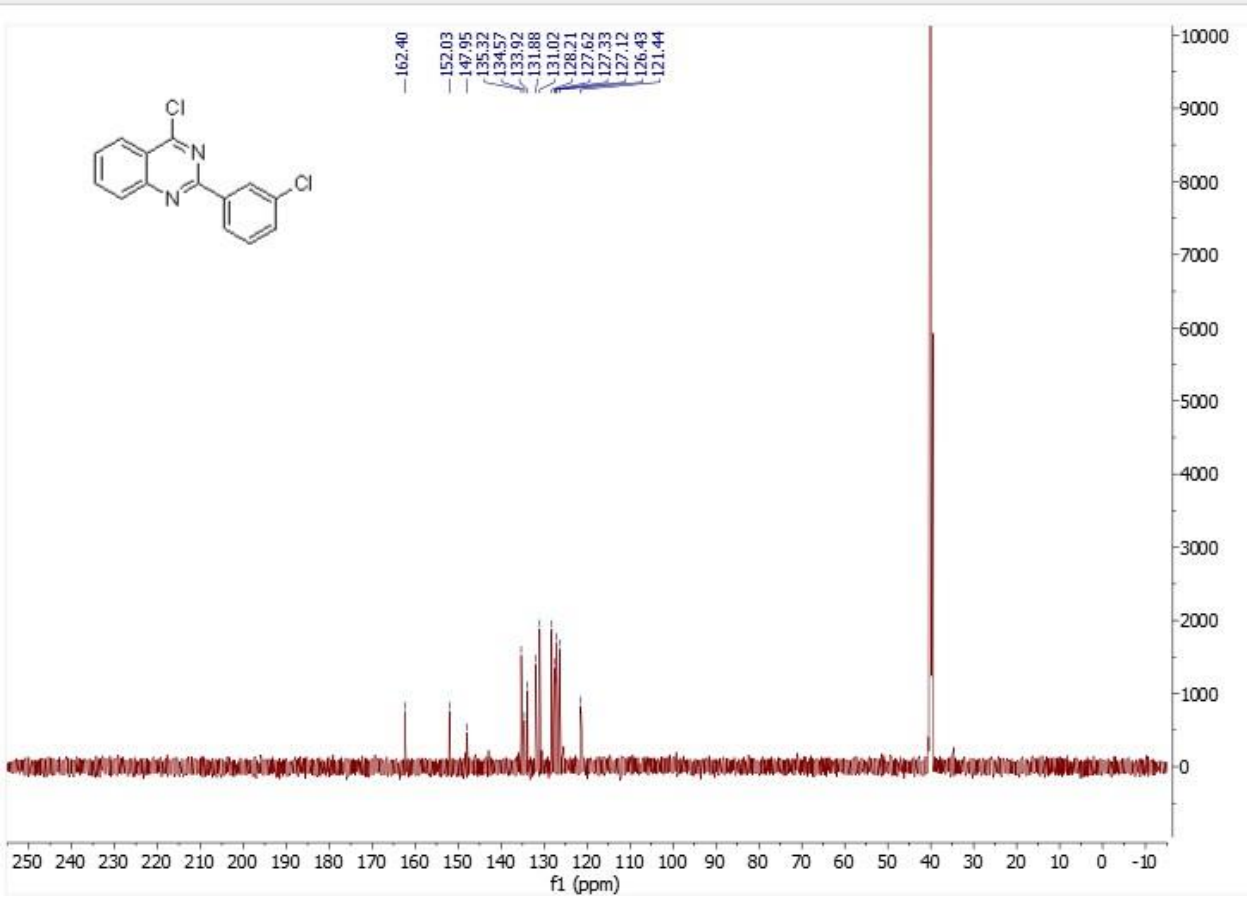
162.40
152.03
147.95
135.32
134.57
133.92
131.88
131.02
128.21
127.62
127.33
127.12
126.43
121.44
Cl
N
N
Cl
10000
9000
8000
7000
6000
5000
4000
3000
2000
1000
0
250 240 230 220 210 200 190 180 170 160 150 140 130 120 110 100 90 80 70 60 50 40 30 20 10 0 -10
f1 (ppm)

FTIR

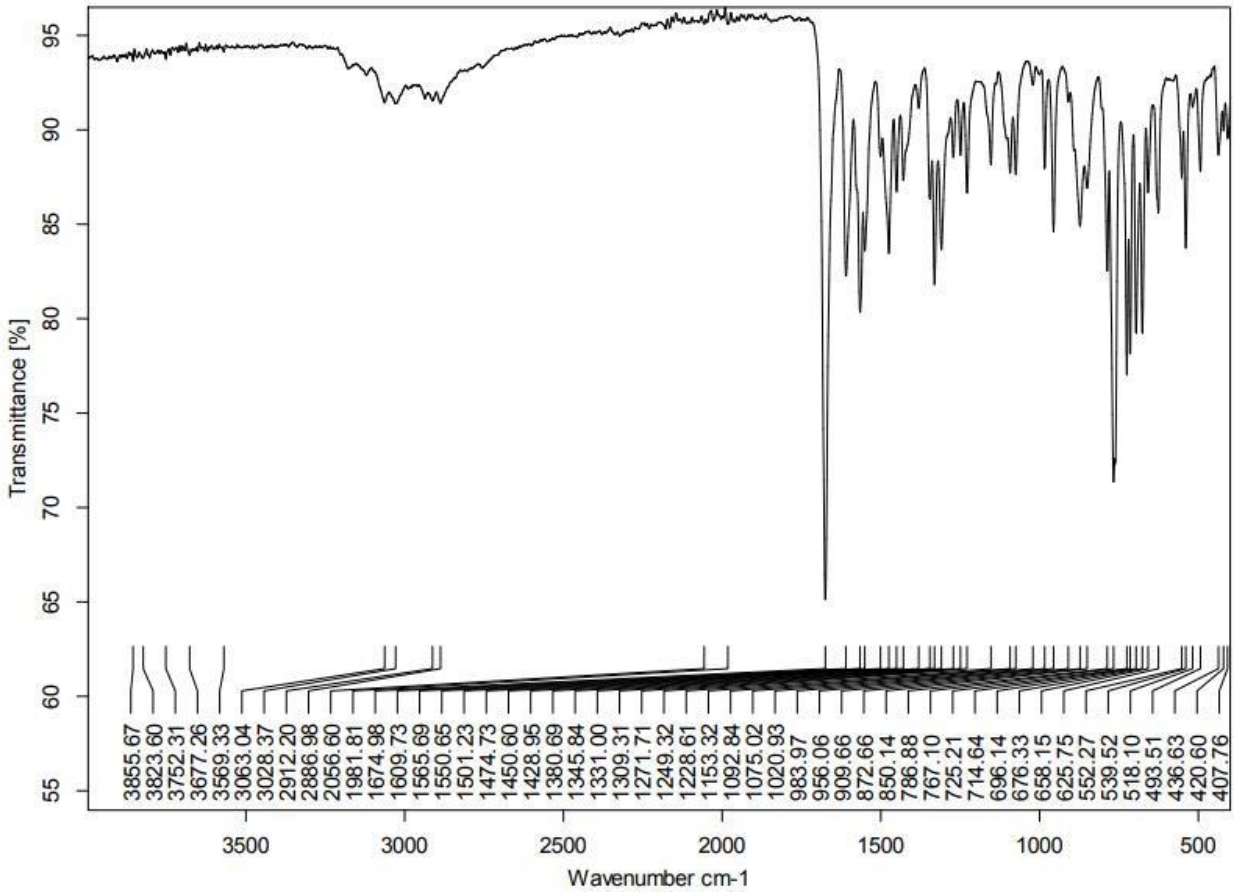

HRMS

Acquisition Parameter

Source Type	APCI	Ion Polarity	Positive	Set Nebulizer	0.8 Bar
Focus	Not active	Set Capillary	4500 V	Set Dry Heater	180 °C
Scan Begin	50 m/z	Set End Plate Offset	-500 V	Set Dry Gas	4.0 l/min
Scan End	2000 m/z	Set Collision Cell RF	100.0 Vpp	Set Divert Valve	Waste

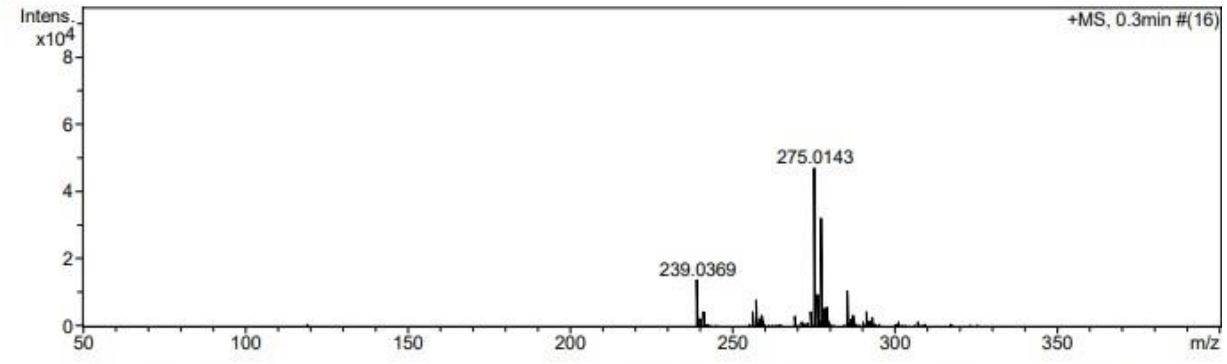

Meas. m/z	#	Formula	Score	m/z	err [mDa]	err [ppm]	mSigma	rdb	e⁻ Conf	N-Rule
275.0143	1	C 14 H 9 Cl 2 N 2	100.00	275.0137	-0.6	-2.2	24.9	10.5	even	ok

HPLC

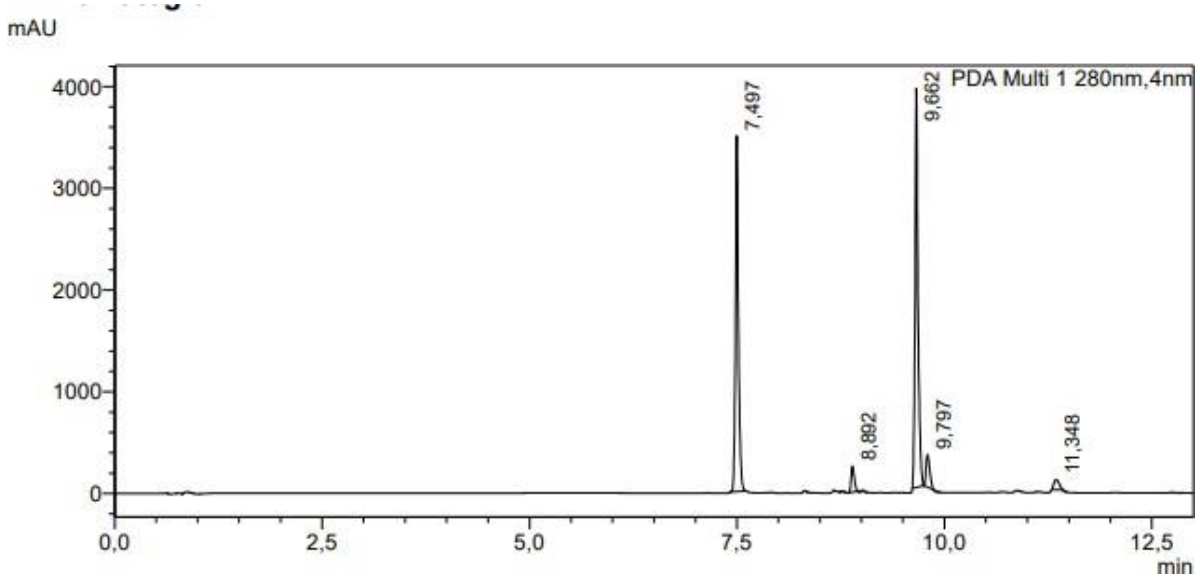

2-(4-bromophenyl)-4-chloroquinazoline **(2d)**

^{1}H NMR

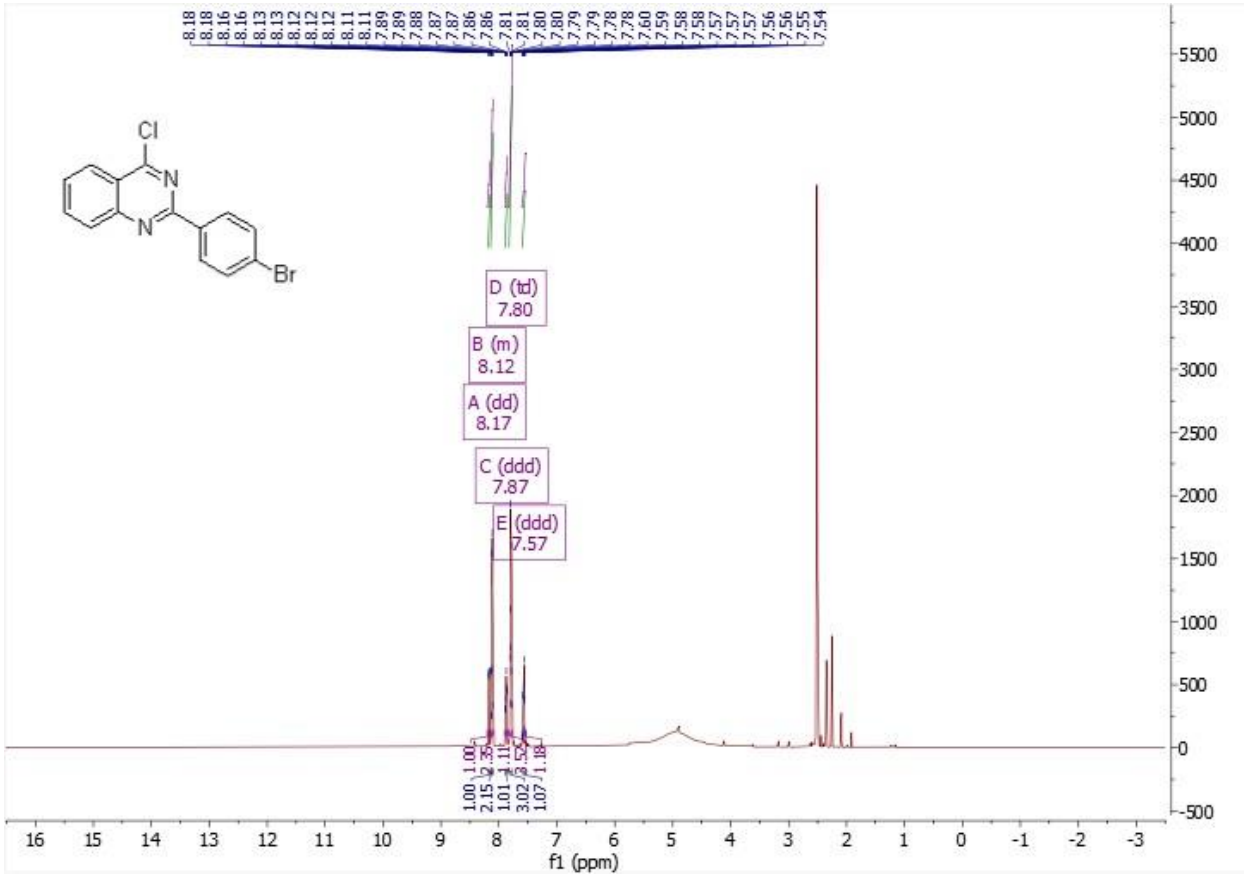

^{13}C NMR

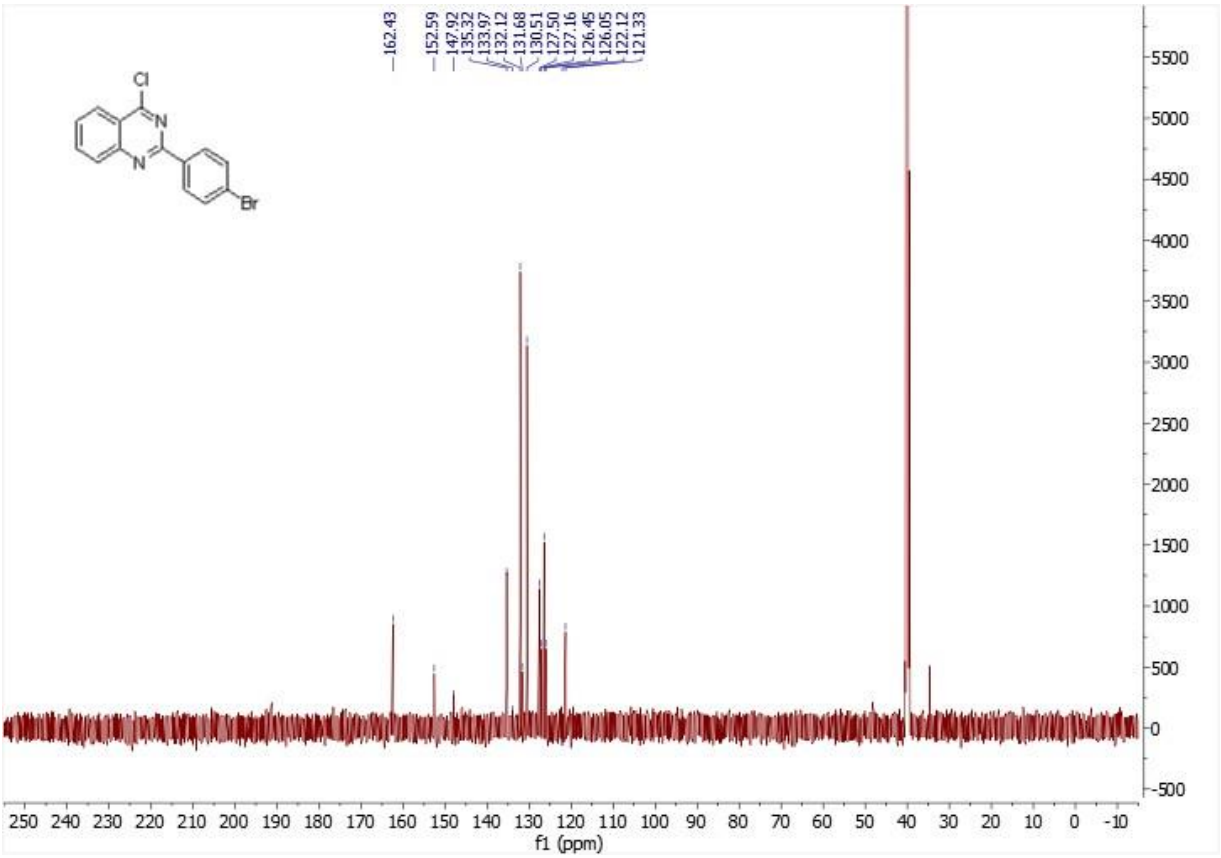
162.43
152.59
147.92
135.32
133.97
132.12
131.68
130.51
127.50
127.16
126.45
126.05
122.12
121.33
Cl
N
N
Br
5500
5000
4500
4000
3500
3000
2500
2000
1500
1000
500
0
-500
250 240 230 220 210 200 190 180 170 160 150 140 130 120 110 100 90 80 70 60 50 40 30 20 10 0 -10
f1 (ppm)

FTIR

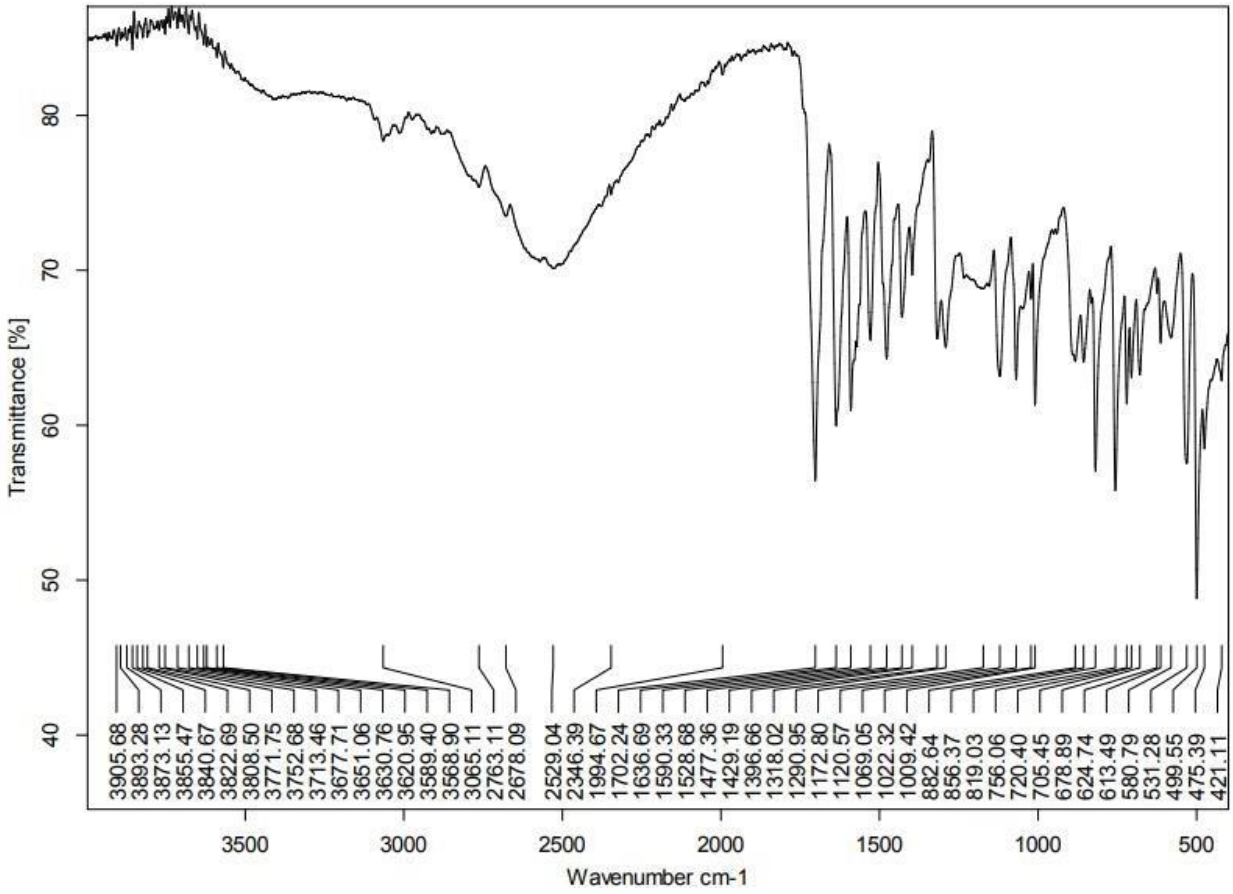

HRMS

Acquisition Parameter

Source Type	APCI	Ion Polarity	Positive	Set Nebulizer	0.8 Bar
Focus	Not active	Set Capillary	4500 V	Set Dry Heater	180 °C
Scan Begin	50 m/z	Set End Plate Offset	-500 V	Set Dry Gas	4.0 l/min
Scan End	2000 m/z	Set Collision Cell RF	100.0 Vpp	Set Divert Valve	Waste

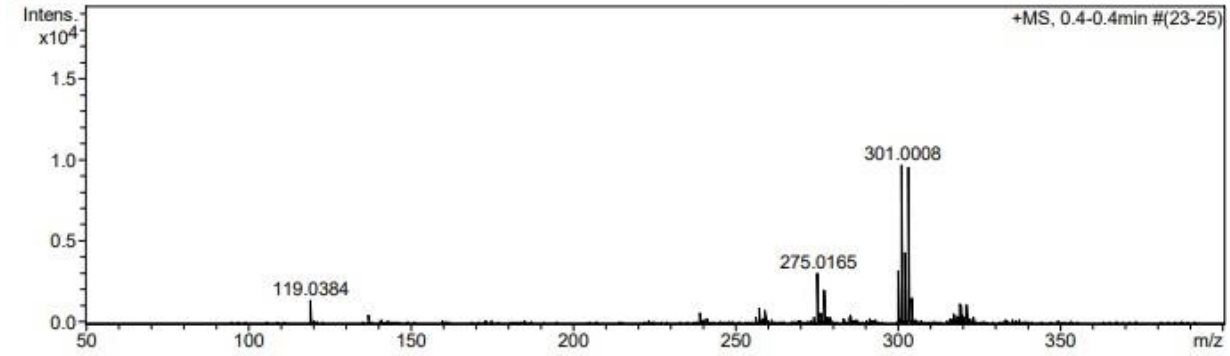

Meas. m/z	#	Formula	Score	m/z	err [mDa]	err [ppm]	mSigma	rdb	e⁻ Conf	N-Rule
299.9930	1	C 12 H 14 Br Cl N 2	100.00	300.0023	9.4	31.2	580.8	6.0	odd	ok
301.0008	1	C 12 H 15 Br Cl N 2	100.00	301.0102	9.4	31.1	191.9	5.5	even	ok
318.9769	1	C 15 H 11 Br Cl N	100.00	318.9758	-1.1	-3.3	130.5	10.0	odd	ok

HPLC

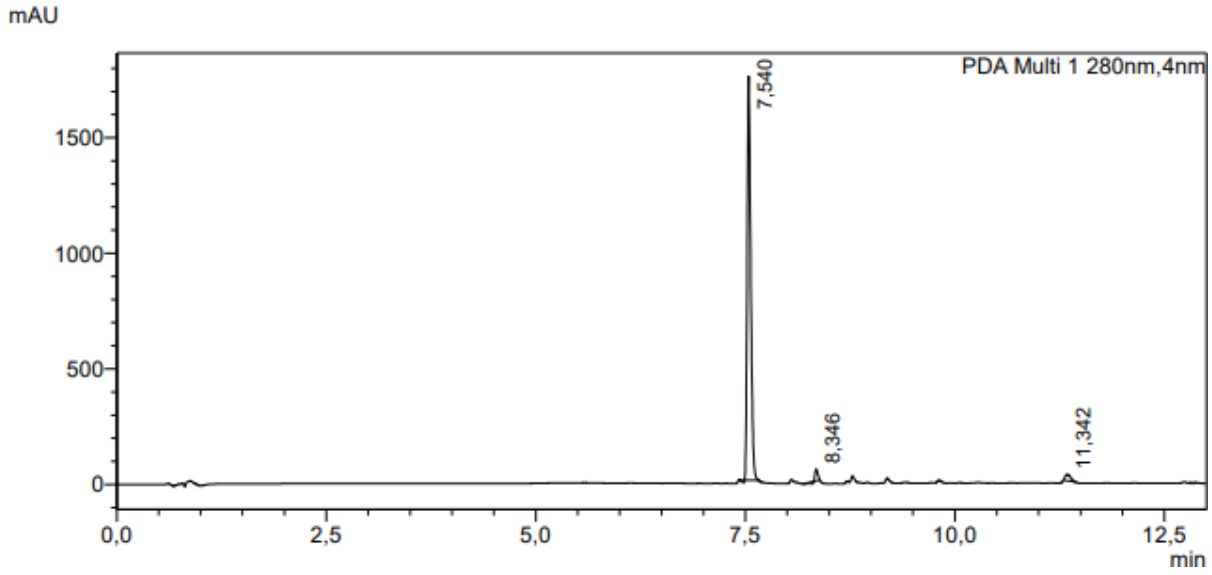

2-(3-fluorophenyl)-4-(4-methylpiperazin-1-yl)quinazoline **(3a)**

^{1}H NMR

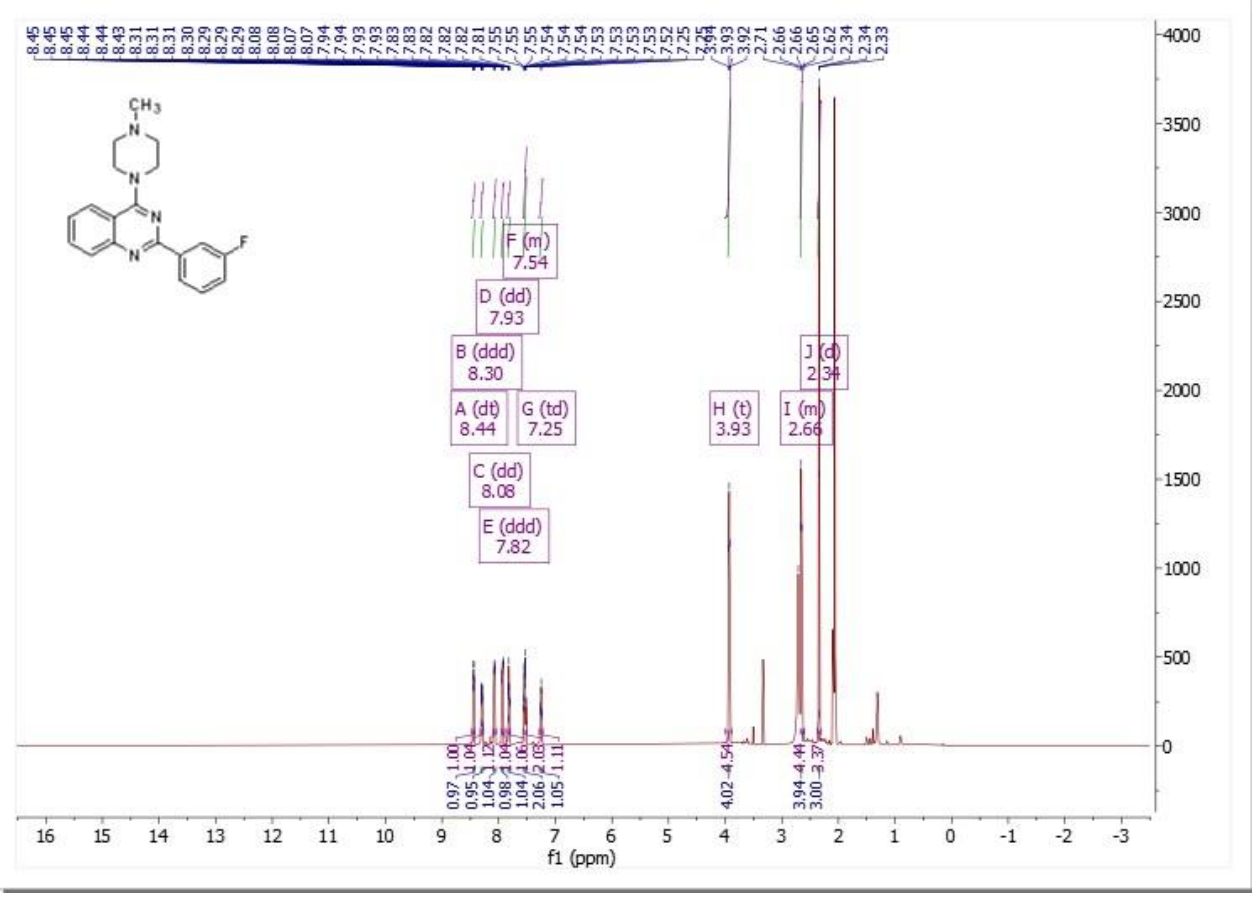

^{13}C NMR

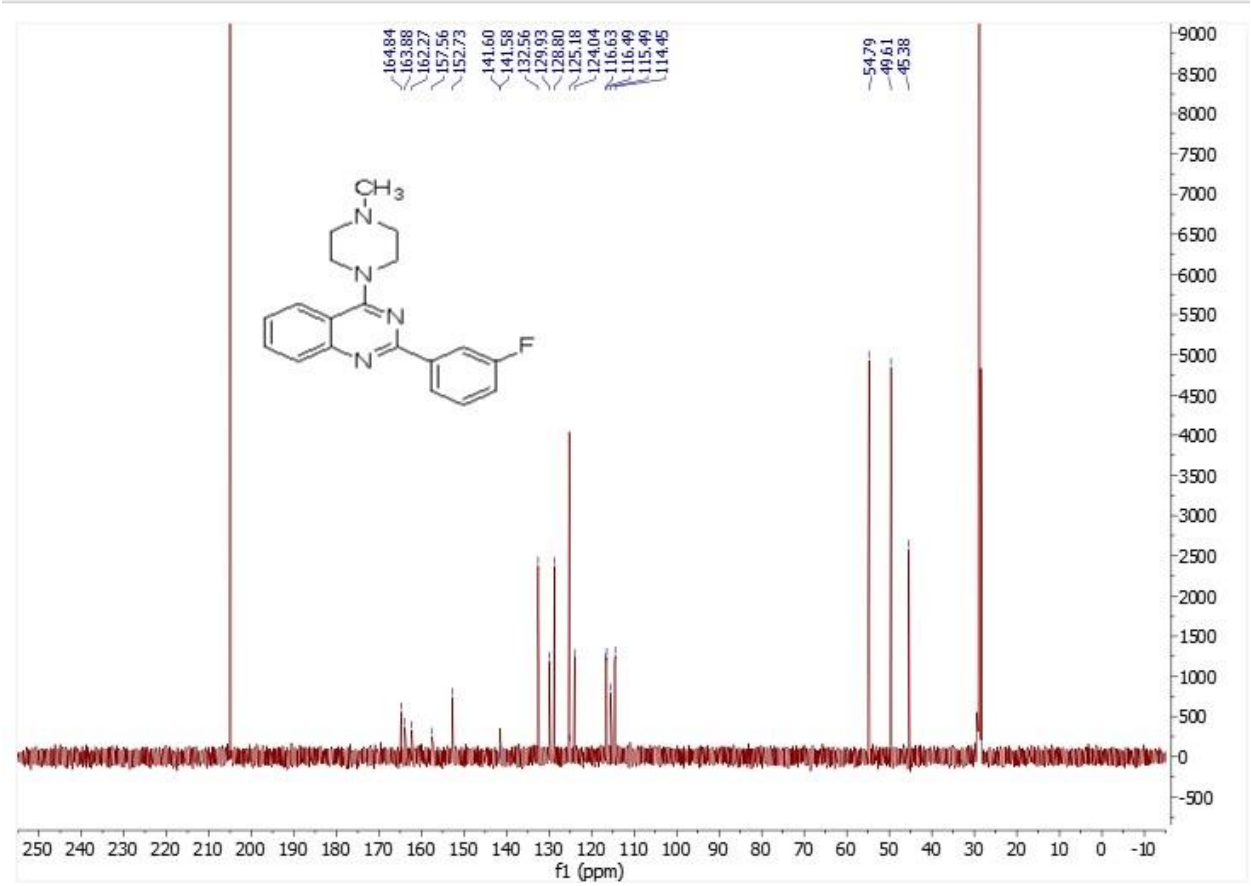
164.84
163.88
162.27
157.56
152.73
141.60
141.58
132.56
129.93
128.80
125.18
124.04
116.63
116.49
115.49
114.45
54.79
49.61
45.38
CH3
N
N
N
N
F
9000
8500
8000
7500
7000
6500
6000
5500
5000
4500
4000
3500
3000
2500
2000
1500
1000
500
0
-500
250 240 230 220 210 200 190 180 170 160 150 140 130 120 110 100 90 80 70 60 50 40 30 20 10 0 -10
f1 (ppm)

FTIR

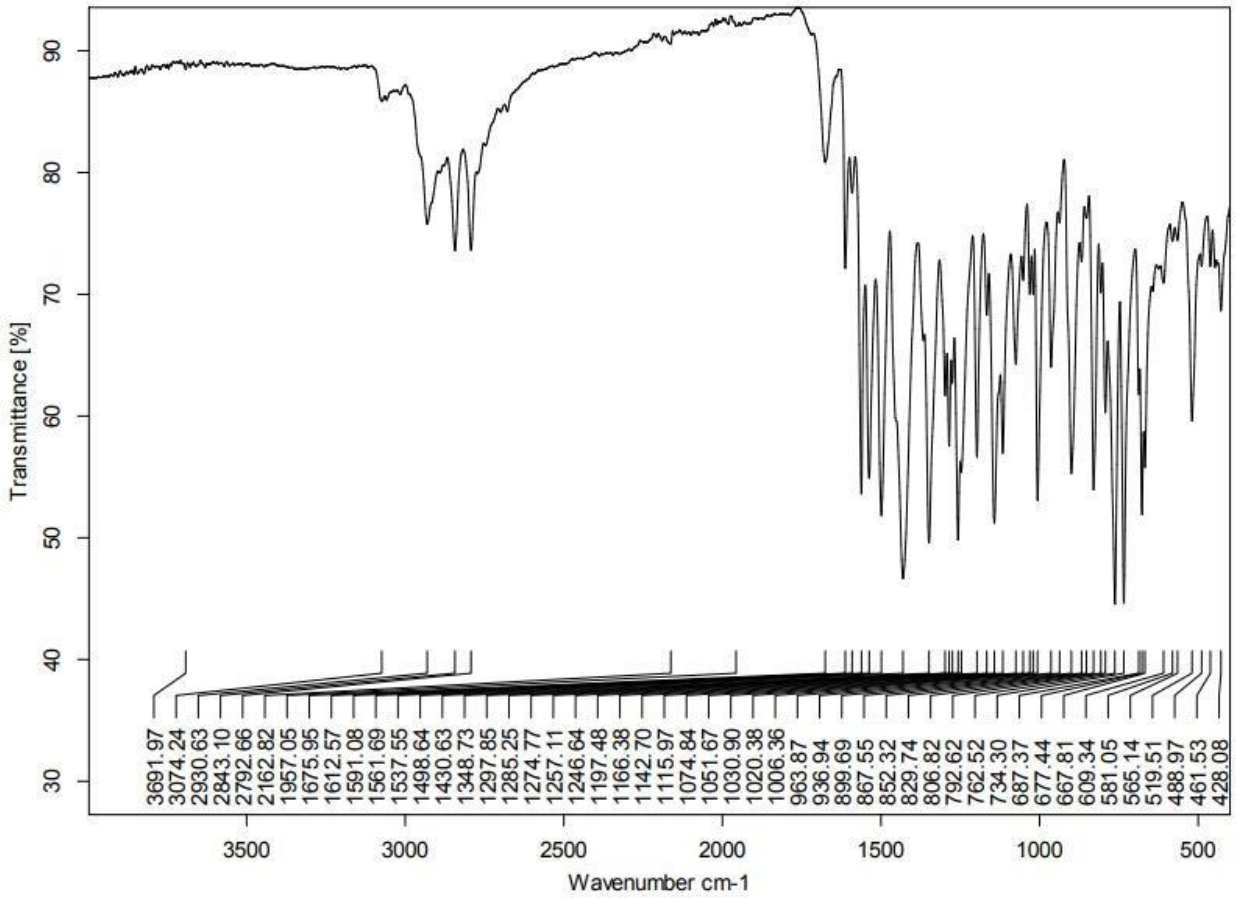

HRMS

Acquisition Parameter

Source Type	APCI	Ion Polarity	Positive	Set Nebulizer	0.8 Bar
Focus	Not active	Set Capillary	4500 V	Set Dry Heater	180 °C
Scan Begin	50 m/z	Set End Plate Offset	-500 V	Set Dry Gas	4.0 l/min
Scan End	2000 m/z	Set Collision Cell RF	100.0 Vpp	Set Divert Valve	Waste

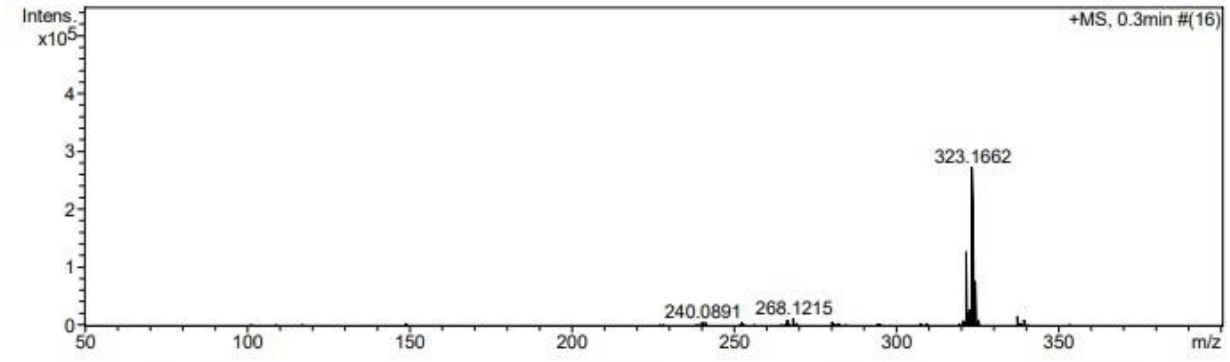

Meas. m/z	#	Formula	Score	m/z	err [mDa]	err [ppm]	mSigma	rdb	e⁻ Conf	N-Rule
323.1662	1	C 19 H 20 F N 4	100.00	323.1667	0.5	1.5	37.4	11.5	even	ok

HPLC

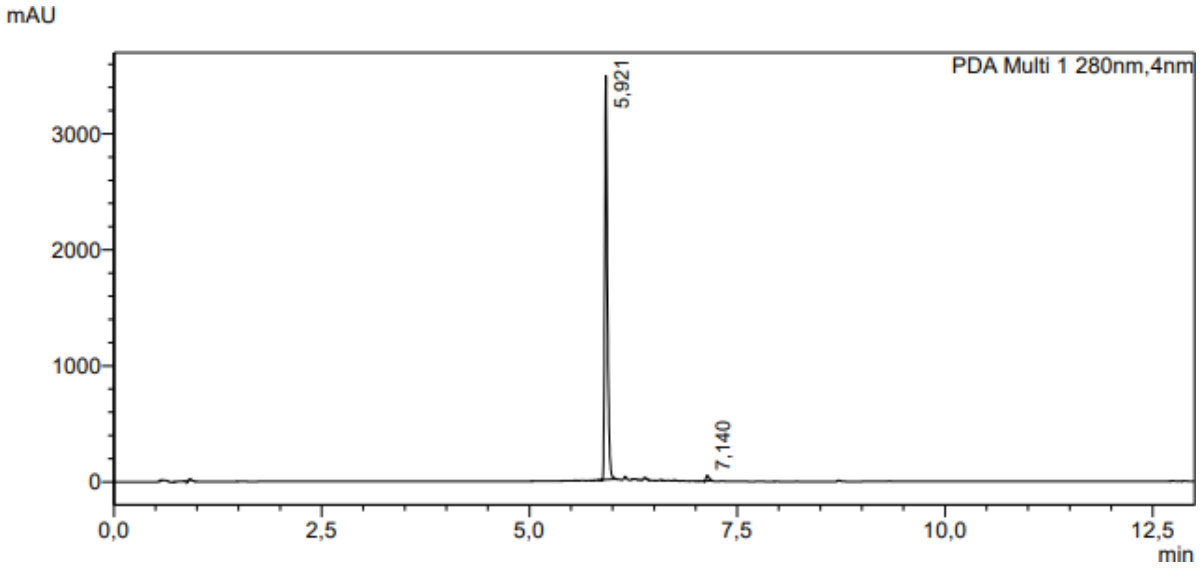

2-(2,4-dimethoxyphenyl)-4-(4-methylpiperazin-1-yl)quinazoline **(3b)**

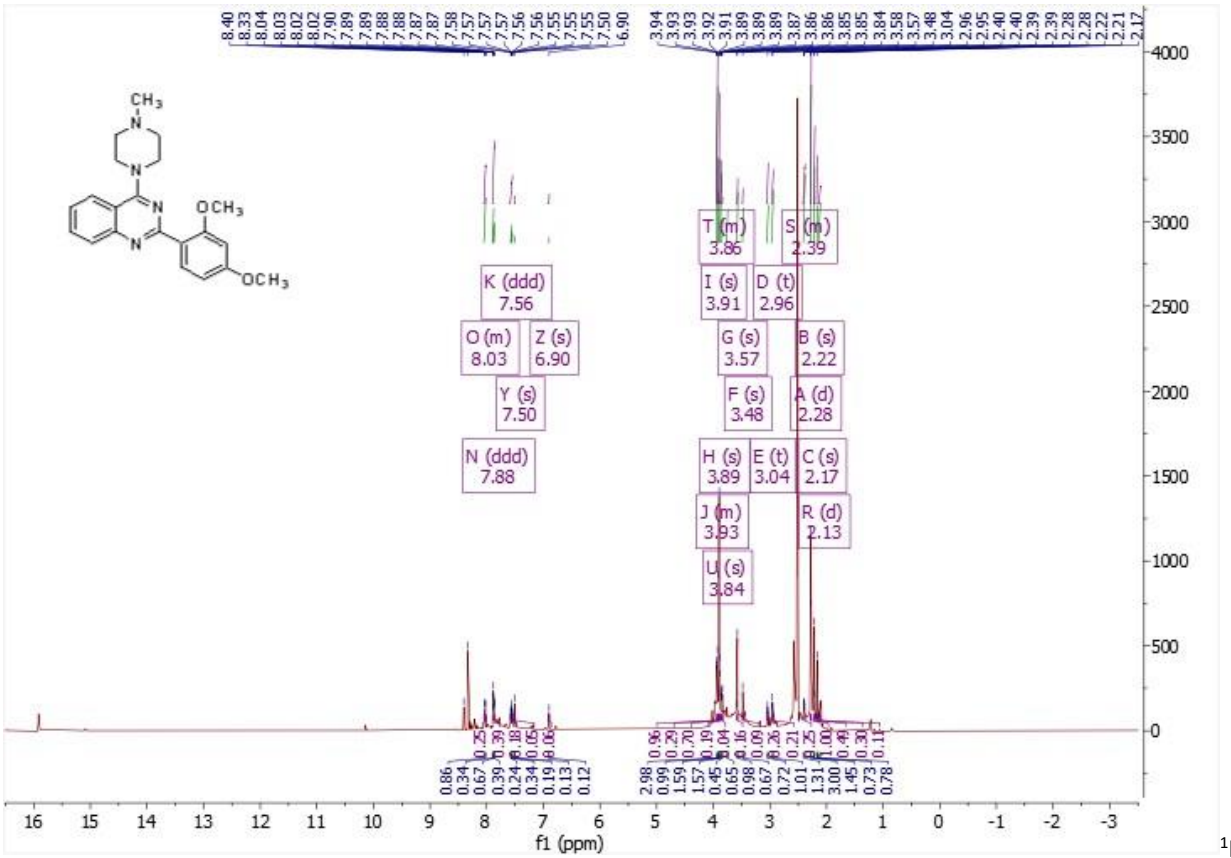

^{1}H NMR

^{13}C NMR

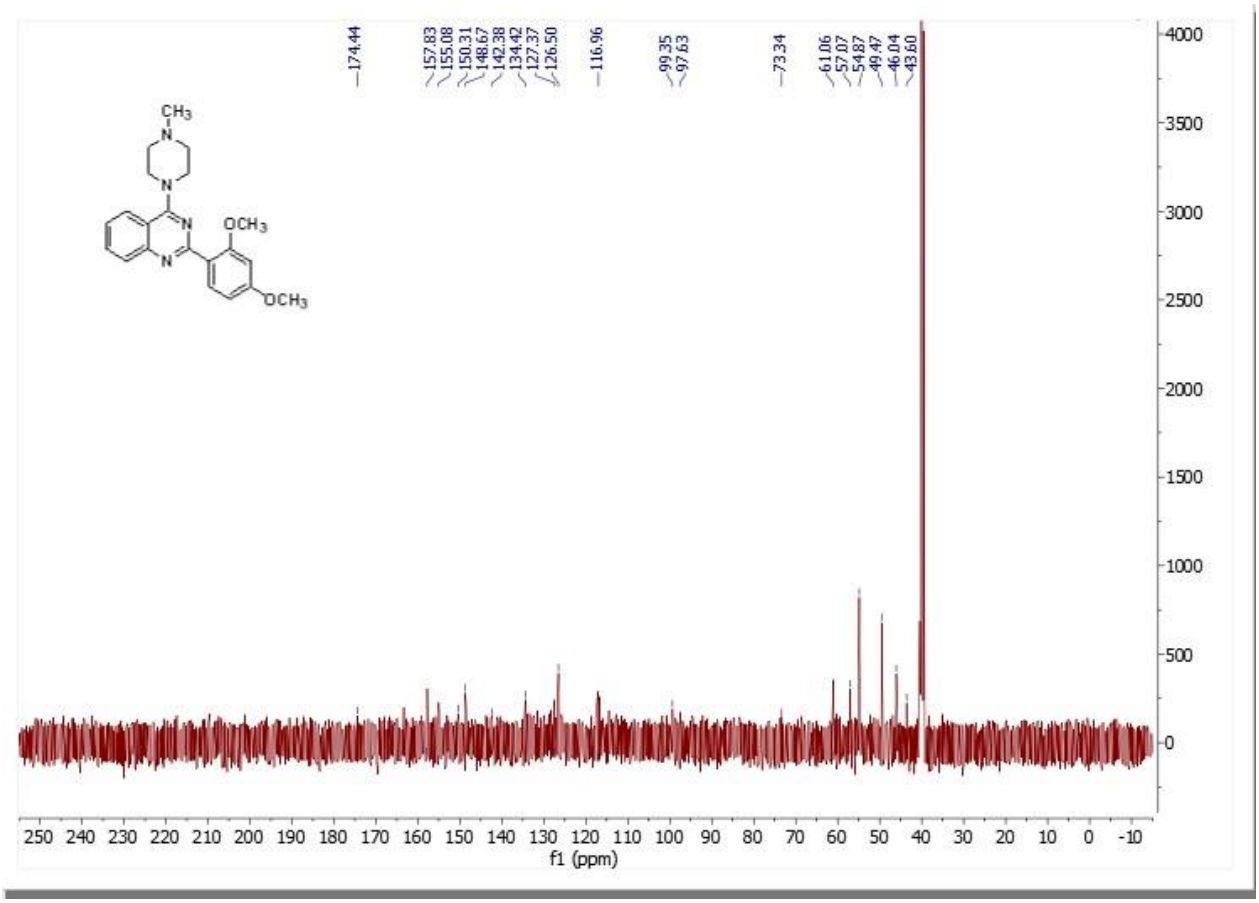
174.44
157.83
155.08
150.31
148.67
142.38
134.42
127.37
126.50
116.96
99.35
97.63
73.34
61.06
57.07
54.87
49.47
46.04
43.60
CH3
OCH3
OCH3
4000
3500
3000
2500
2000
1500
1000
500
0
250 240 230 220 210 200 190 180 170 160 150 140 130 120 110 100 90 80 70 60 50 40 30 20 10 0 -10
f1 (ppm)

FTIR

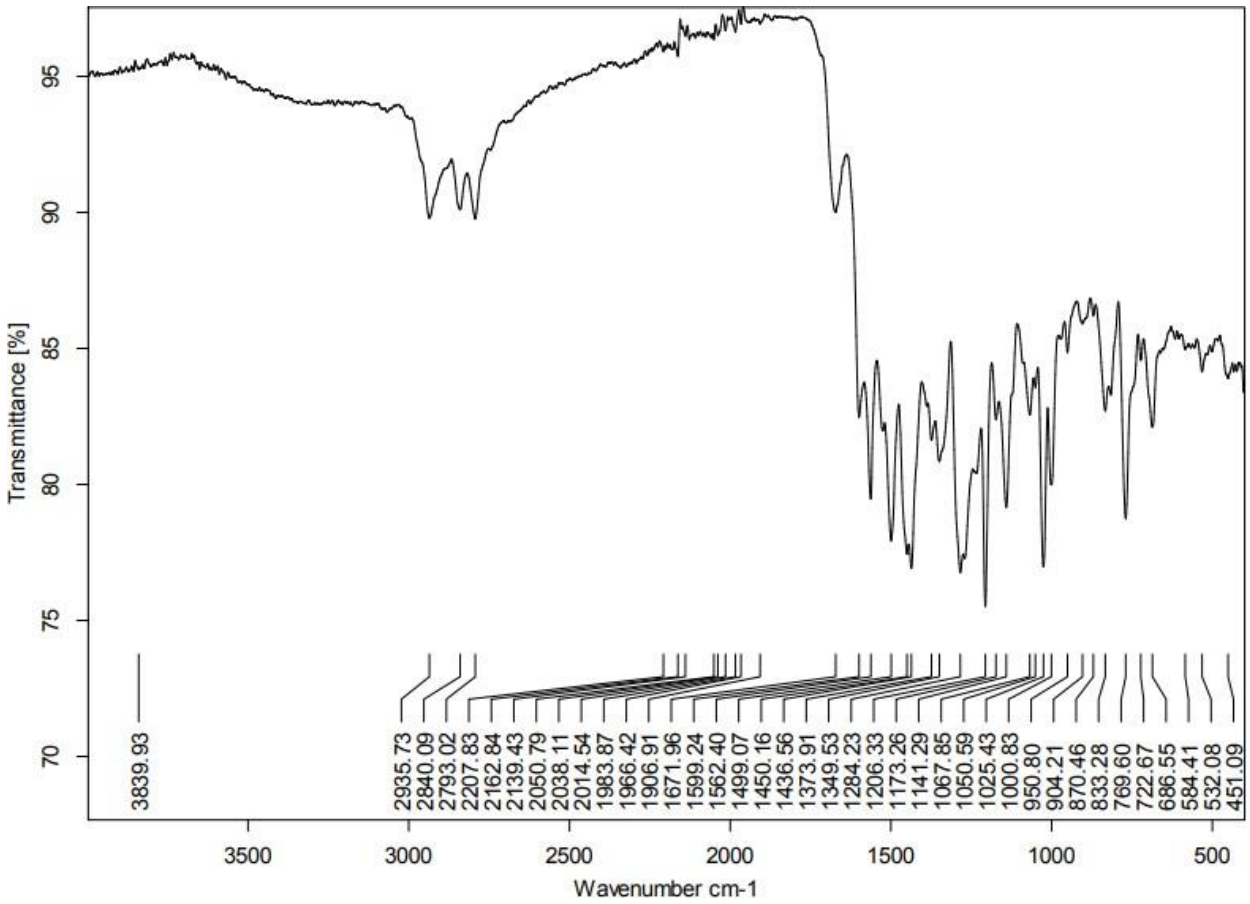
Transmittance [%]
95
90
85
80
75
70
3500
3000
2500
2000
1500
1000
500
Wavenumber cm-1
3839.93
2935.73
2840.09
2793.02
2207.83
2162.84
2139.43
2050.79
2038.11
2014.54
1983.87
1966.42
1906.91
1671.96
1599.24
1562.40
1499.07
1450.16
1436.56
1373.91
1349.53
1284.23
1206.33
1173.26
1141.29
1067.85
1050.59
1025.43
1000.83
950.80
904.21
870.46
833.28
769.60
722.67
686.55
584.41
532.08
451.09

HRMS

Acquisition Parameter

Source Type	APCI	Ion Polarity	Positive	Set Nebulizer	0.8 Bar
Focus	Not active	Set Capillary	4500 V	Set Dry Heater	180 °C
Scan Begin	50 m/z	Set End Plate Offset	-500 V	Set Dry Gas	4.0 l/min
Scan End	2000 m/z	Set Collision Cell RF	100.0 Vpp	Set Divert Valve	Waste

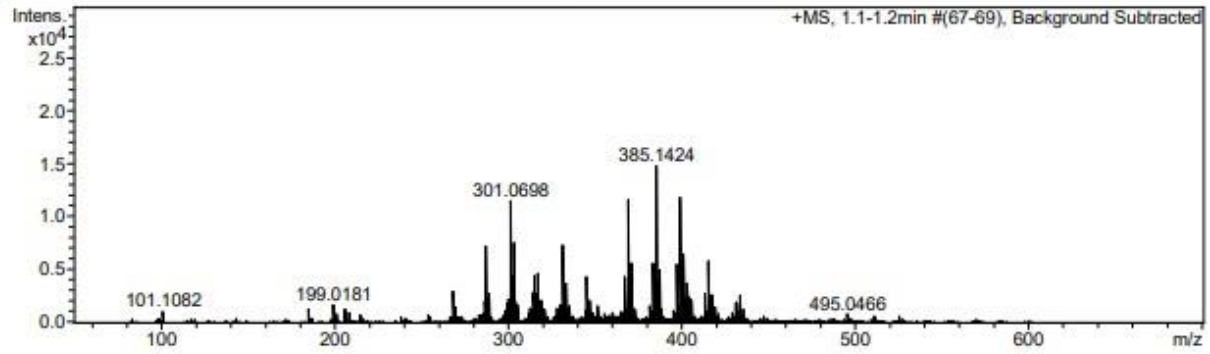

Meas. m/z	#	Formula	Score	m/z	err [mDa]	err [ppm]	mSigma	rdb	e⁻ Conf	N-Rule
287.0589	1	C 21 H 7 N 2	100.00	287.0604	1.5	5.3	207.3	19.5	even	ok
	2	C 18 H 9 N O 3	79.37	287.0577	-1.2	-4.0	212.5	15.0	odd	ok
	3	C 16 H 7 N 4 O 2	20.95	287.0564	-2.5	-8.7	216.4	15.5	even	ok
	4	C 14 H 5 N 7 O	3.37	287.0550	-3.8	-13.4	221.6	16.0	odd	ok
301.0698	1	C 19 H 11 N O 3	47.70	301.0733	3.6	11.8	379.5	15.0	odd	ok
	2	C 17 H 9 N 4 O 2	91.50	301.0720	2.2	7.4	383.5	15.5	even	ok
	3	C 15 H 7 N 7 O	100.00	301.0707	0.9	2.9	388.7	16.0	odd	ok
	4	C 12 H 9 N 6 O 4	23.77	301.0680	-1.8	-6.0	394.1	11.5	even	ok
331.0860	1	C 23 H 11 N 2 O	100.00	331.0866	0.6	1.8	278.5	19.5	even	ok
	2	C 21 H 9 N 5	73.44	331.0852	-0.7	-2.2	280.5	20.0	odd	ok
	3	C 20 H 13 N O 4	29.51	331.0839	-2.1	-6.3	280.9	15.0	odd	ok
369.1449	1	C 25 H 21 O 3	22.81	369.1485	3.6	9.8	255.3	15.5	even	ok
	2	C 23 H 19 N 3 O 2	61.74	369.1472	2.3	6.1	258.0	16.0	odd	ok
	3	C 21 H 17 N 6 O	100.00	369.1458	0.9	2.5	262.0	16.5	even	ok
	4	C 18 H 19 N 5 O 4	50.93	369.1432	-1.8	-4.8	263.3	12.0	odd	ok
385.1424	1	C 28 H 19 N O	29.28	385.1461	3.7	9.6	155.3	20.0	odd	ok
	2	C 25 H 21 O 4	85.75	385.1434	1.0	2.6	171.9	15.5	even	ok
	3	C 26 H 17 N 4	29.44	385.1448	2.4	6.1	173.7	20.5	even	ok
	4	C 23 H 19 N 3 O 3	100.00	385.1421	-0.3	-0.8	174.6	16.0	odd	ok
	5	C 21 H 17 N 6 O 2	37.30	385.1408	-1.7	-4.3	177.5	16.5	even	ok
399.1518	1	C 28 H 19 N 2 O	100.00	399.1492	-2.6	-6.5	265.1	20.5	even	ok
	2	C 26 H 17 N 5	0.71	399.1478	-3.9	-9.9	296.1	21.0	odd	ok
415.1342	1	C 32 H 17 N	100.00	415.1356	1.4	3.4	212.4	25.0	odd	ok
	2	C 29 H 19 O 3	97.71	415.1329	-1.3	-3.1	213.4	20.5	even	ok
	3	C 27 H 17 N 3 O 2	28.33	415.1315	-2.6	-6.3	215.9	21.0	odd	ok
	4	C 25 H 15 N 6 O	0.58	415.1302	-4.0	-9.6	242.0	21.5	even	ok

HPLC

FAILED

2-(4-fluorophenyl)-4-(4-methylpiperazin-1-yl)quinazoline **(3c)**

^{1}H NMR

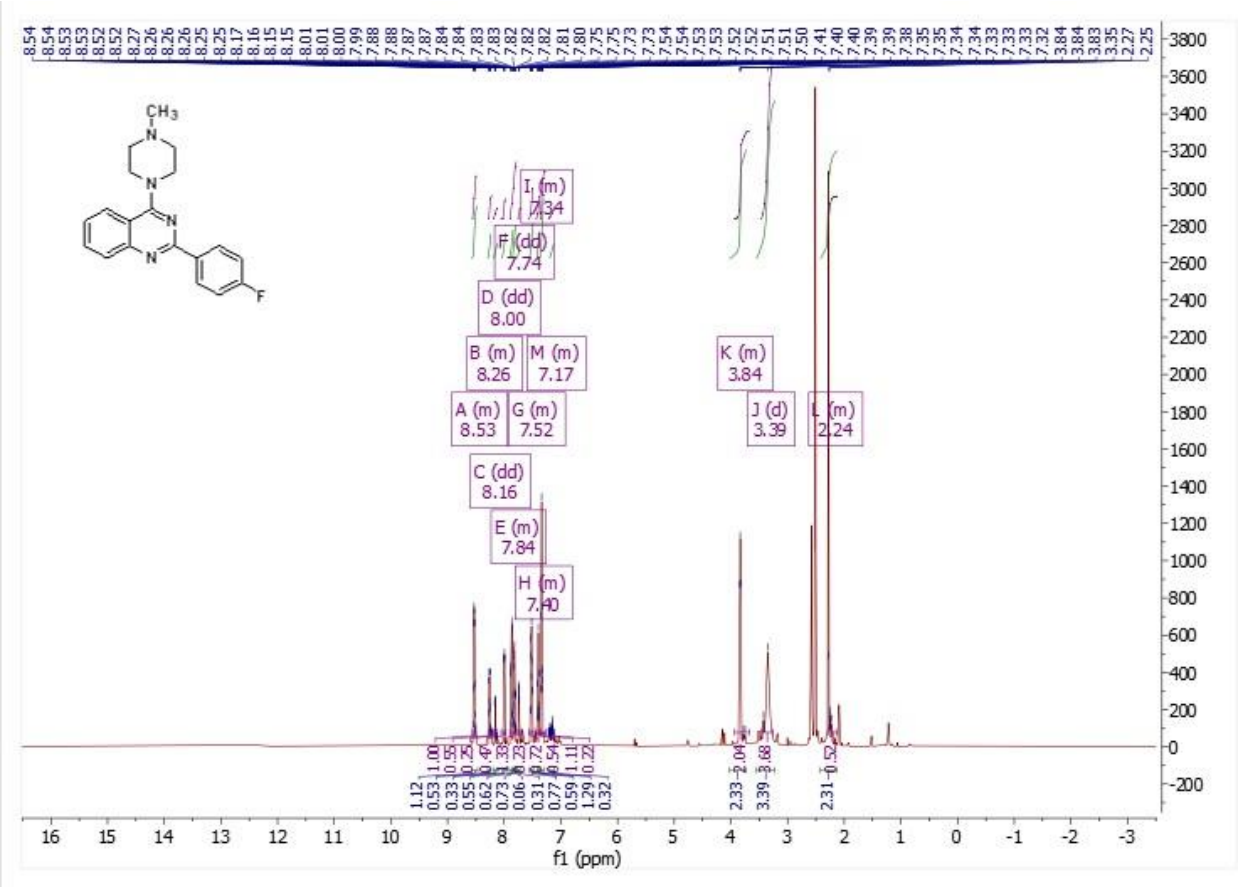

^{13}C NMR

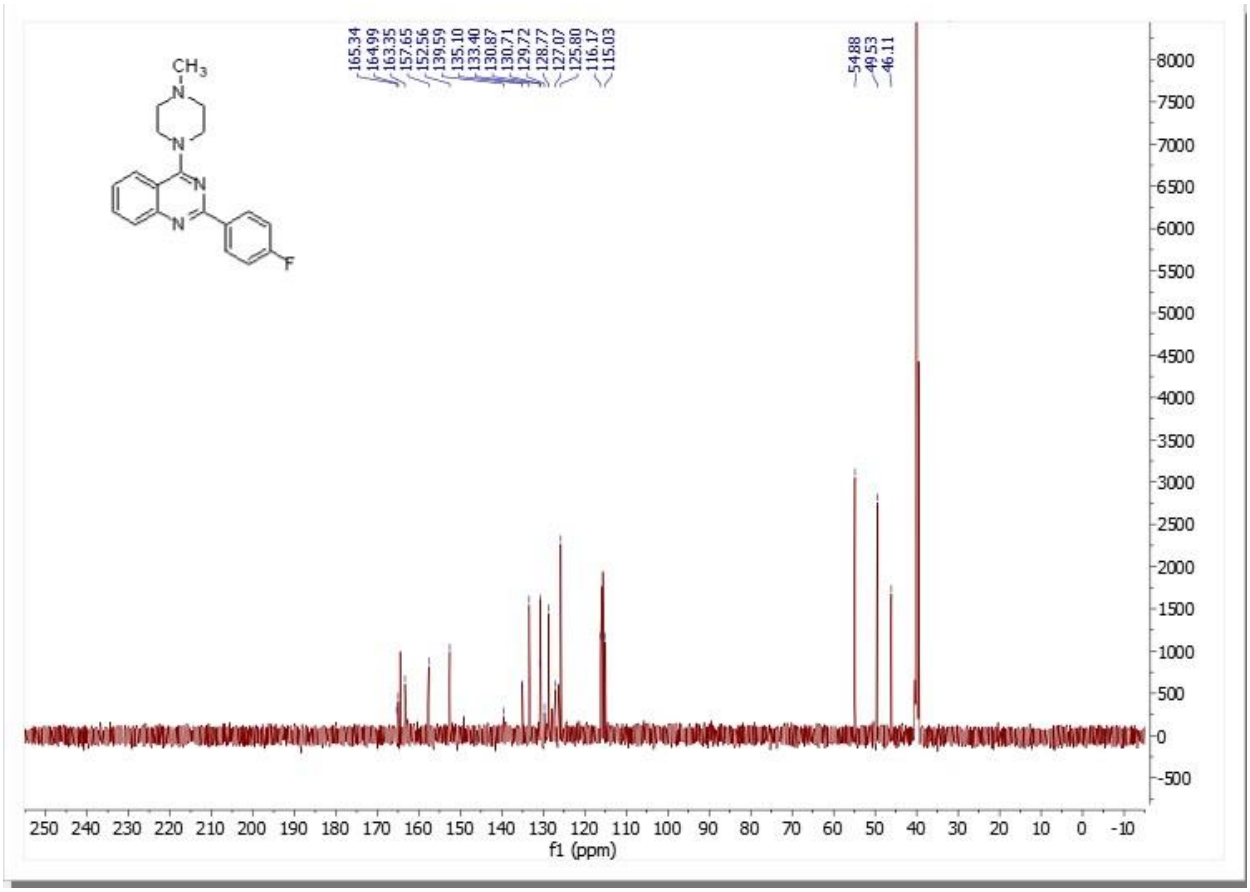
165.34
164.99
163.35
157.65
152.56
139.59
135.10
133.40
130.87
130.71
129.72
128.77
127.07
125.80
116.17
115.03
54.88
49.53
46.11
CH3
N
N
N
N
F
8000
7500
7000
6500
6000
5500
5000
4500
4000
3500
3000
2500
2000
1500
1000
500
0
-500
250 240 230 220 210 200 190 180 170 160 150 140 130 120 110 100 90 80 70 60 50 40 30 20 10 0 -10
f1 (ppm)

FTIR

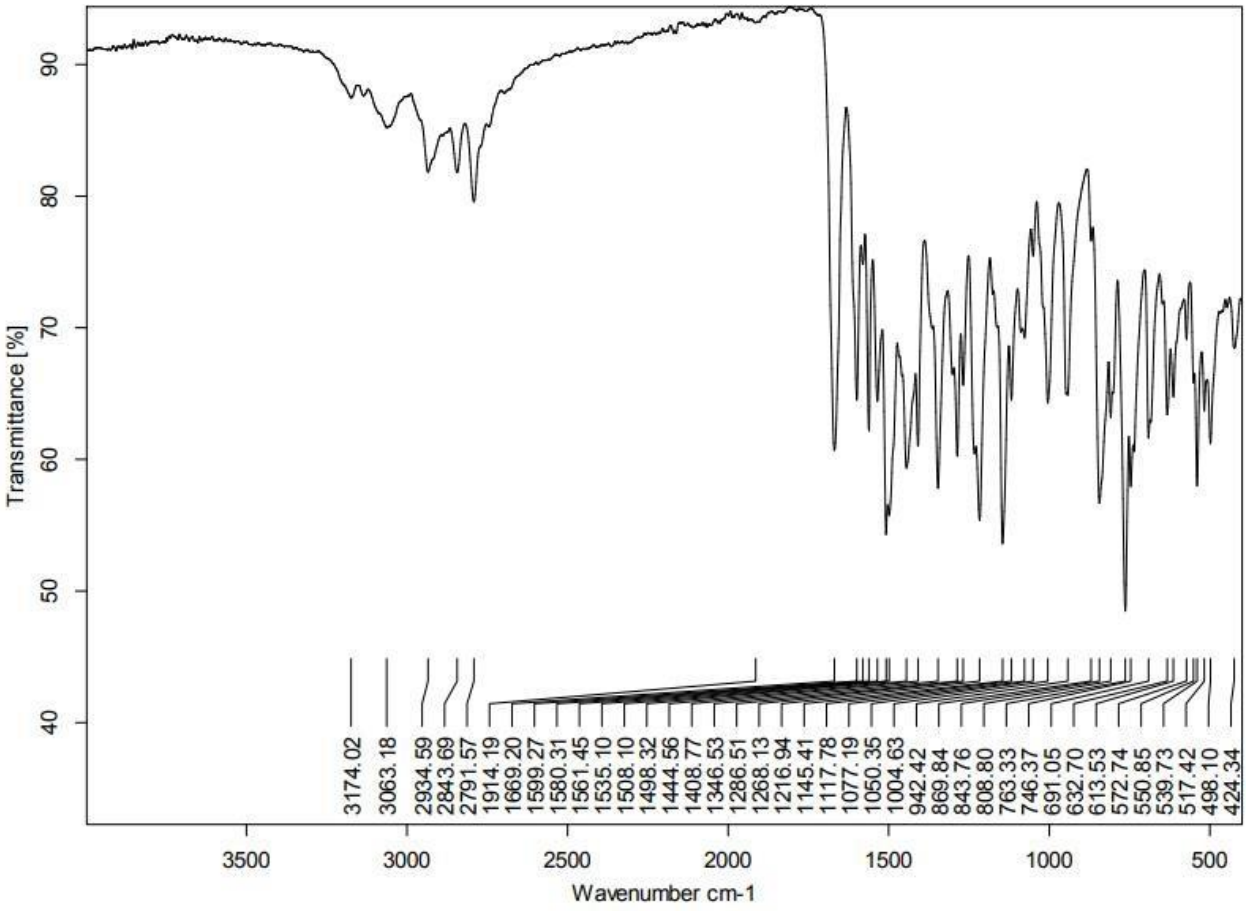

HRMS

Acquisition Parameter

Source Type	APCI	Ion Polarity	Positive	Set Nebulizer	0.8 Bar
Focus	Not active	Set Capillary	4500 V	Set Dry Heater	180 °C
Scan Begin	50 m/z	Set End Plate Offset	-500 V	Set Dry Gas	4.0 l/min
Scan End	2000 m/z	Set Collision Cell RF	100.0 Vpp	Set Divert Valve	Waste

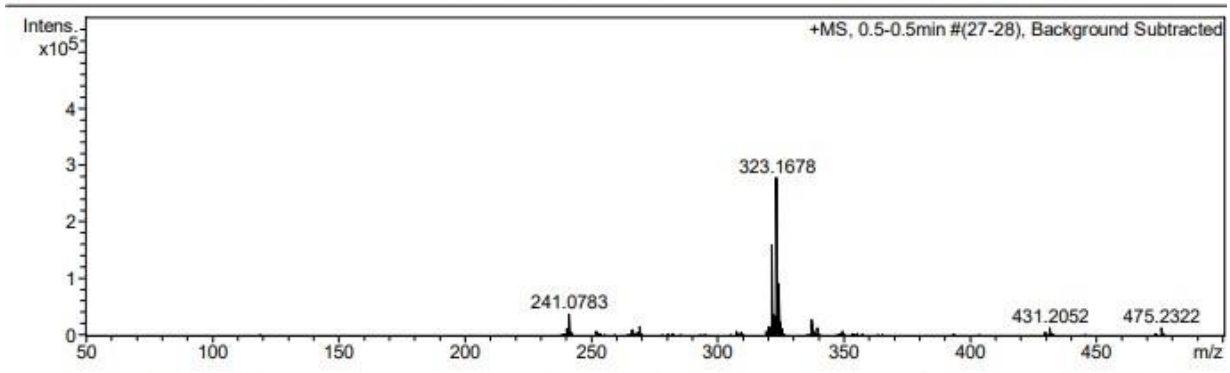

Meas. m/z	#	Formula	Score	m/z	err [mDa]	err [ppm]	mSigma	rdb	e⁻ Conf	N-Rule
323.1678	1	C 19 H 20 F N 4	100.00	323.1667	-1.1	-3.5	66.7	11.5	even	ok

HPLC

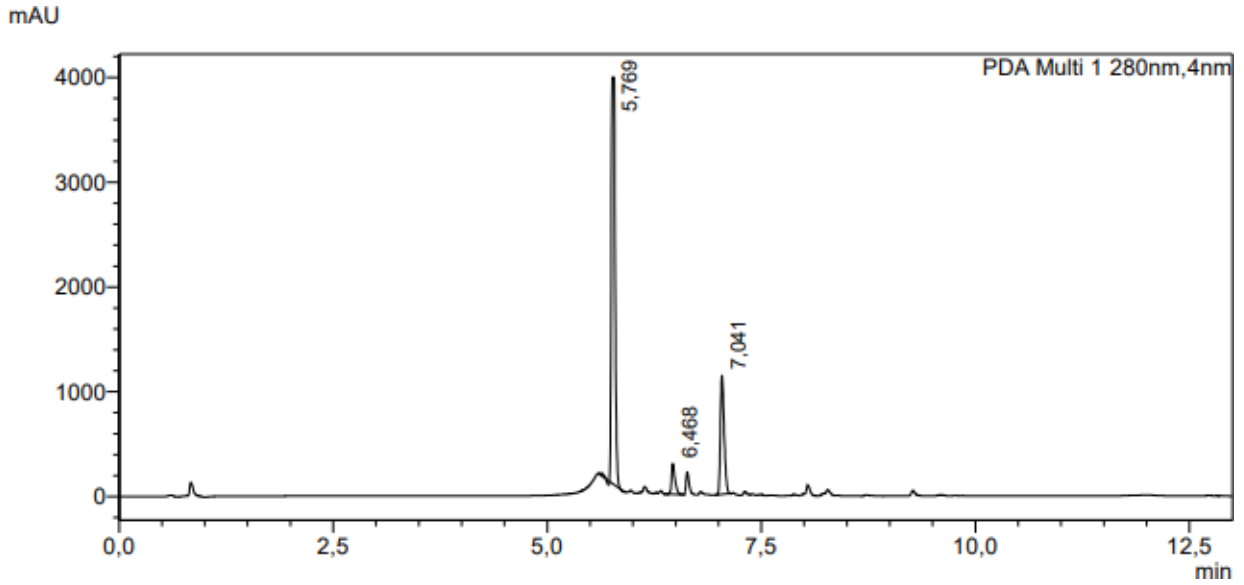

4-(4-methylpiperazin-1-yl)-2-(o-tolyl)quinazoline **(3d)**

^{1}H NMR

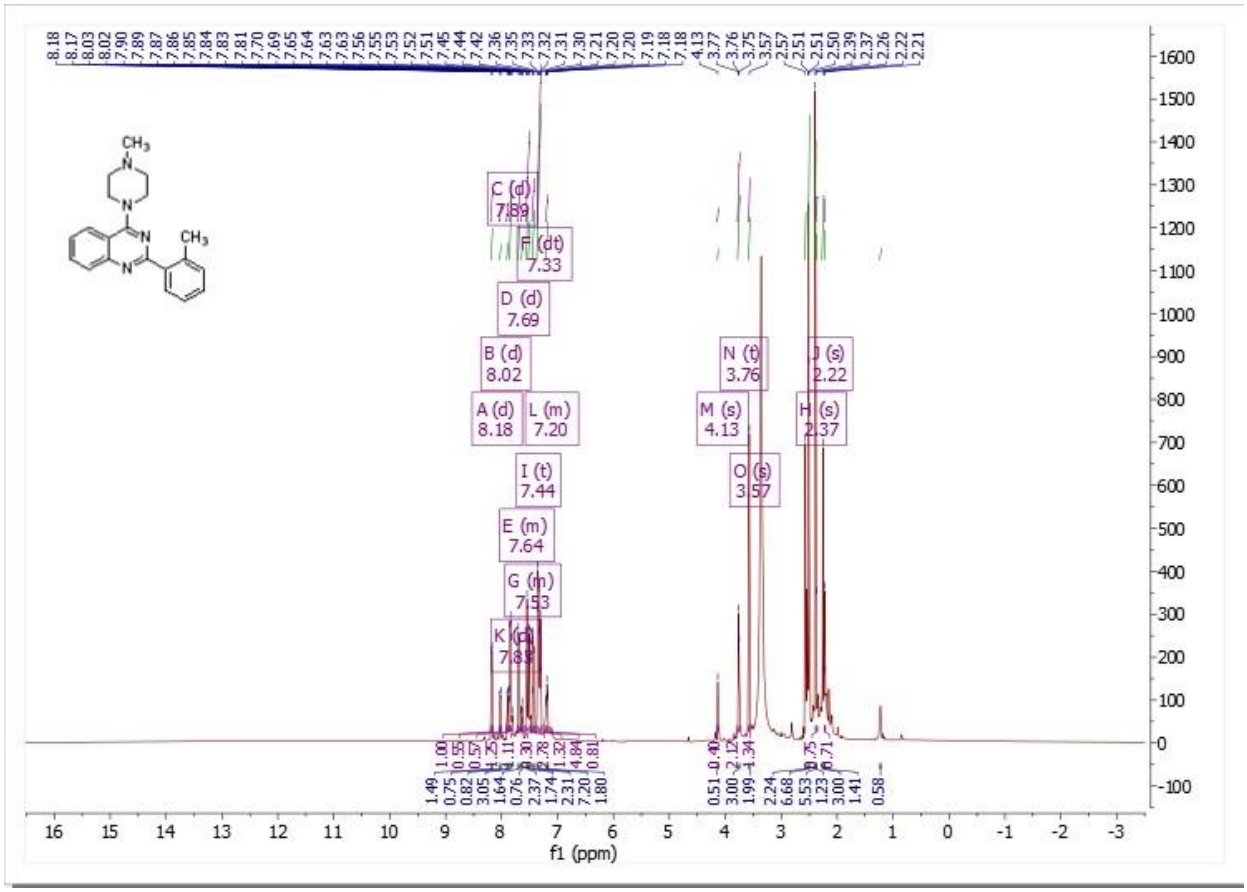

^{13}C NMR

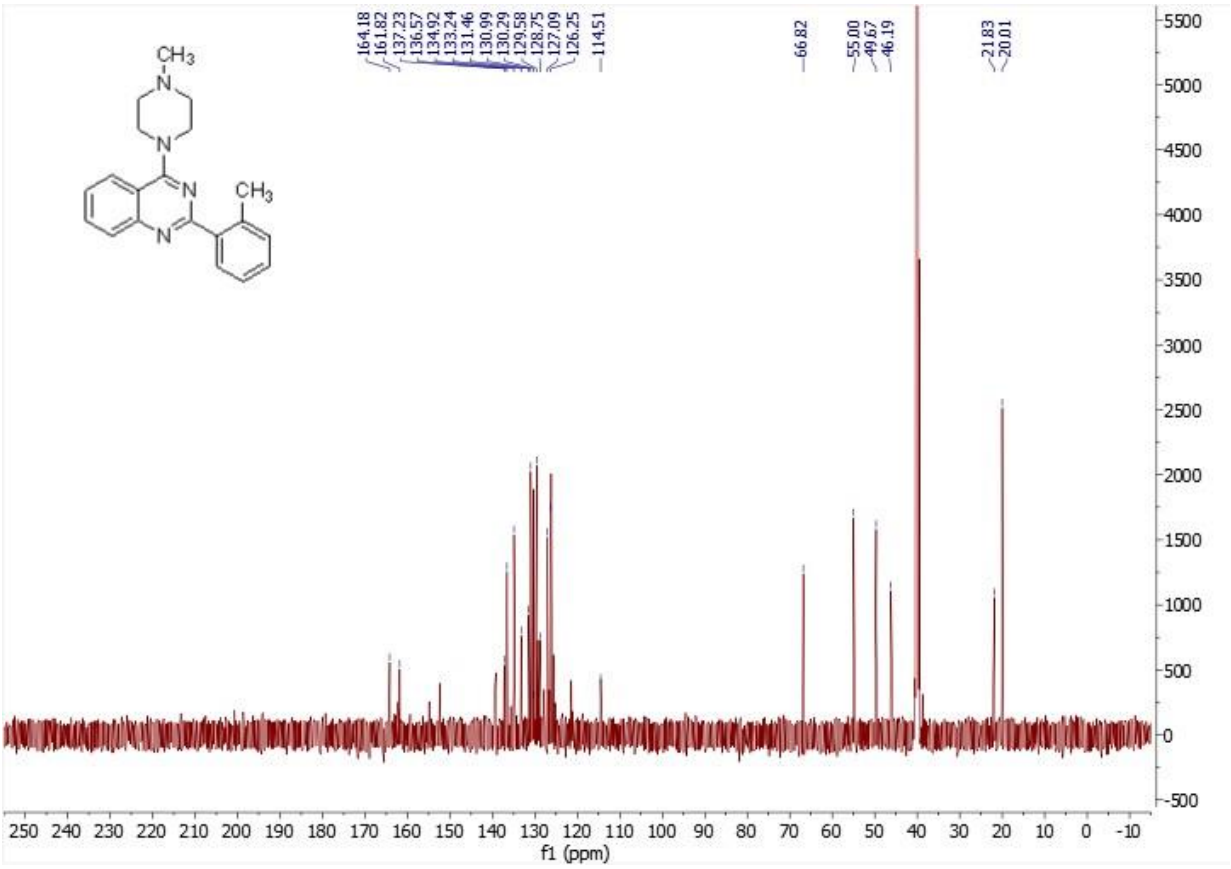
164.18
161.82
137.23
136.57
134.92
133.24
131.46
130.99
130.29
129.58
128.75
127.09
126.25
114.51
66.82
55.00
49.67
46.19
21.83
20.01
CH3
N
N
N
CH3
5500
5000
4500
4000
3500
3000
2500
2000
1500
1000
500
0
-500
250 240 230 220 210 200 190 180 170 160 150 140 130 120 110 100 90 80 70 60 50 40 30 20 10 0 -10
f1 (ppm)

FTIR

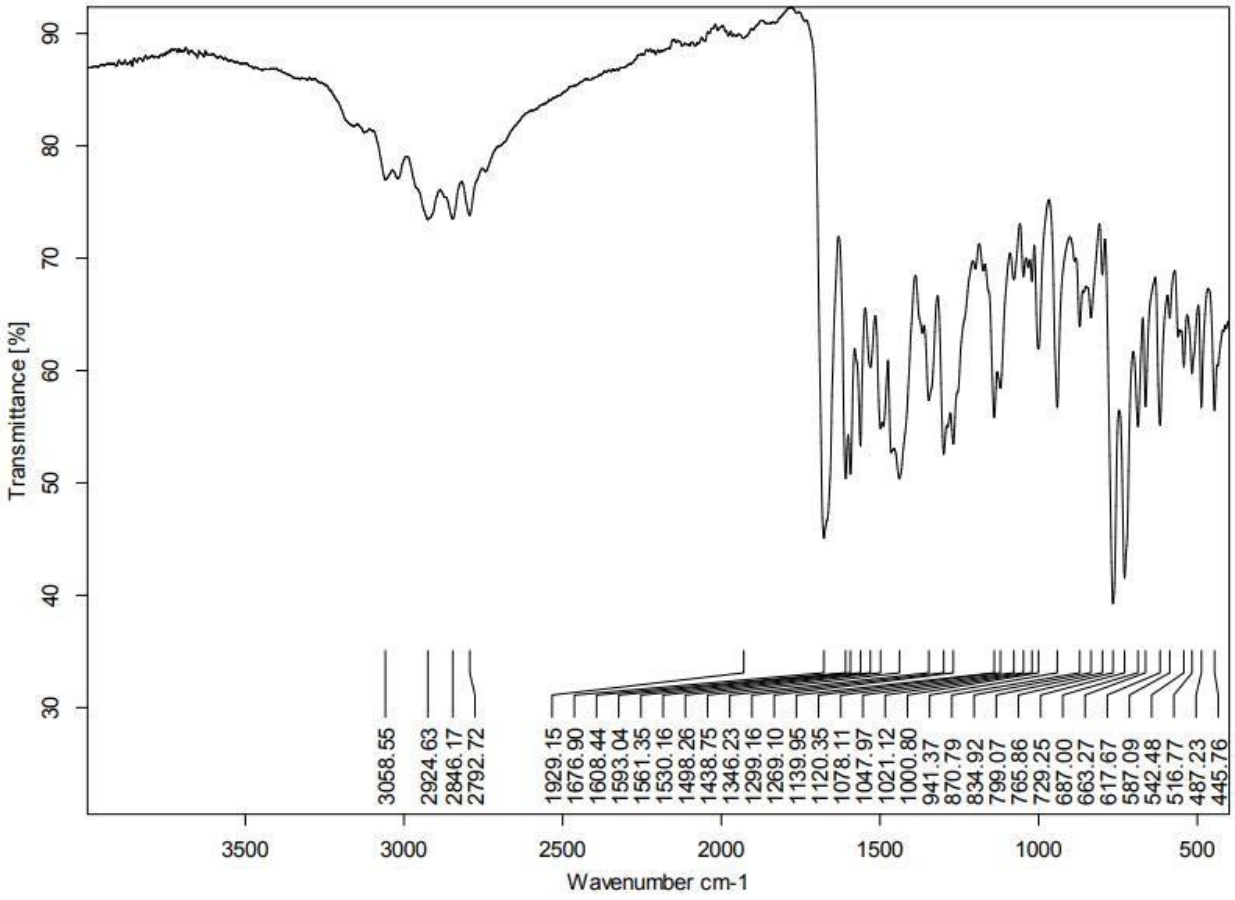

HRMS

Acquisition Parameter

Source Type	APCI	Ion Polarity	Positive	Set Nebulizer	0.8 Bar
Focus	Not active	Set Capillary	4500 V	Set Dry Heater	180 °C
Scan Begin	50 m/z	Set End Plate Offset	-500 V	Set Dry Gas	4.0 l/min
Scan End	2000 m/z	Set Collision Cell RF	100.0 Vpp	Set Divert Valve	Waste

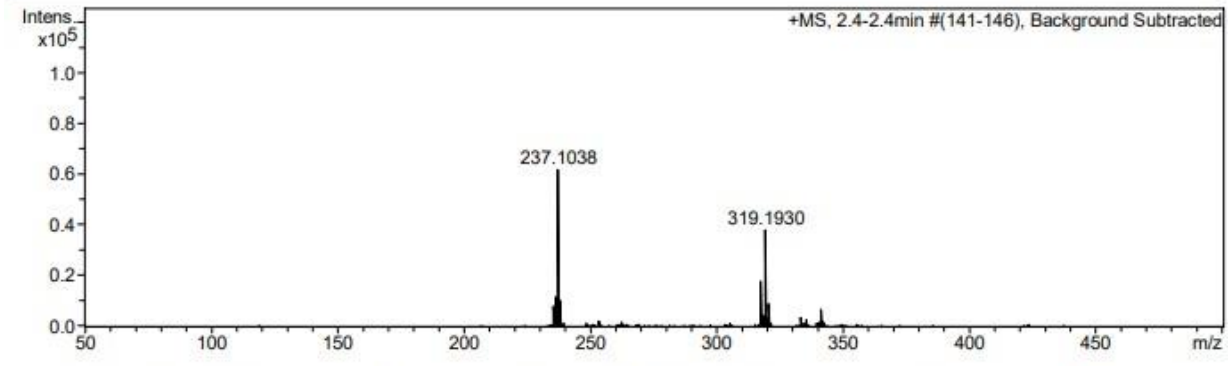

Meas. m/z	#	Formula	Score	m/z	err [mDa]	err [ppm]	mSigma	rdb	e⁻ Conf	N-Rule
237.1038	1	C 14 H 13 N 4	100.00	237.1135	9.7	40.9	4.1	10.5	even	ok
319.1930	1	C 20 H 23 N 4	100.00	319.1917	-1.3	-4.1	9.4	11.5	even	ok

HPLC

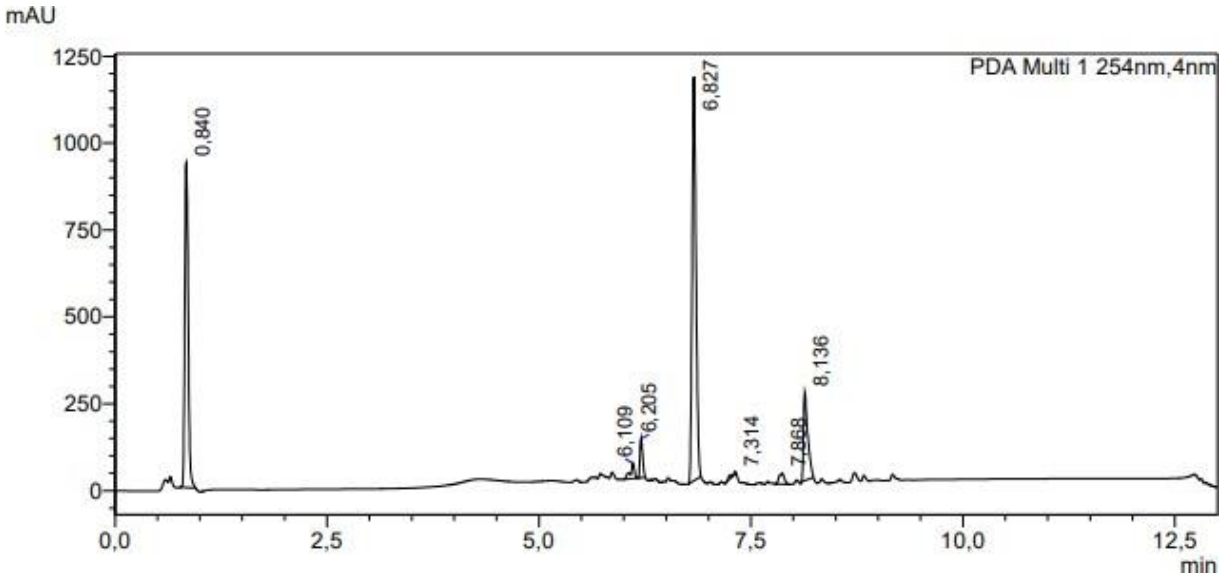

4-(4-methylpiperazin-1-yl)-2-(4-nitrophenyl)quinazoline **(3e)**

^{1}H NMR

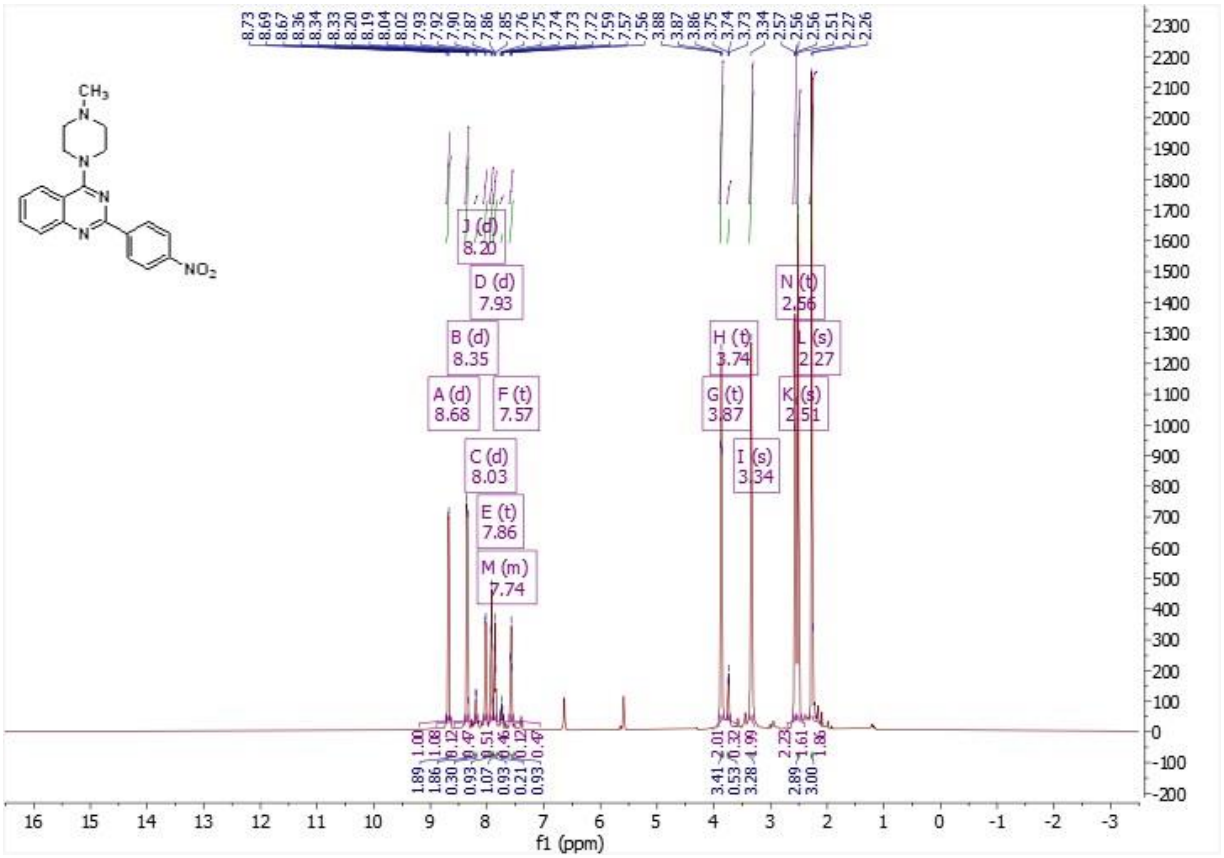

^{13}C NMR

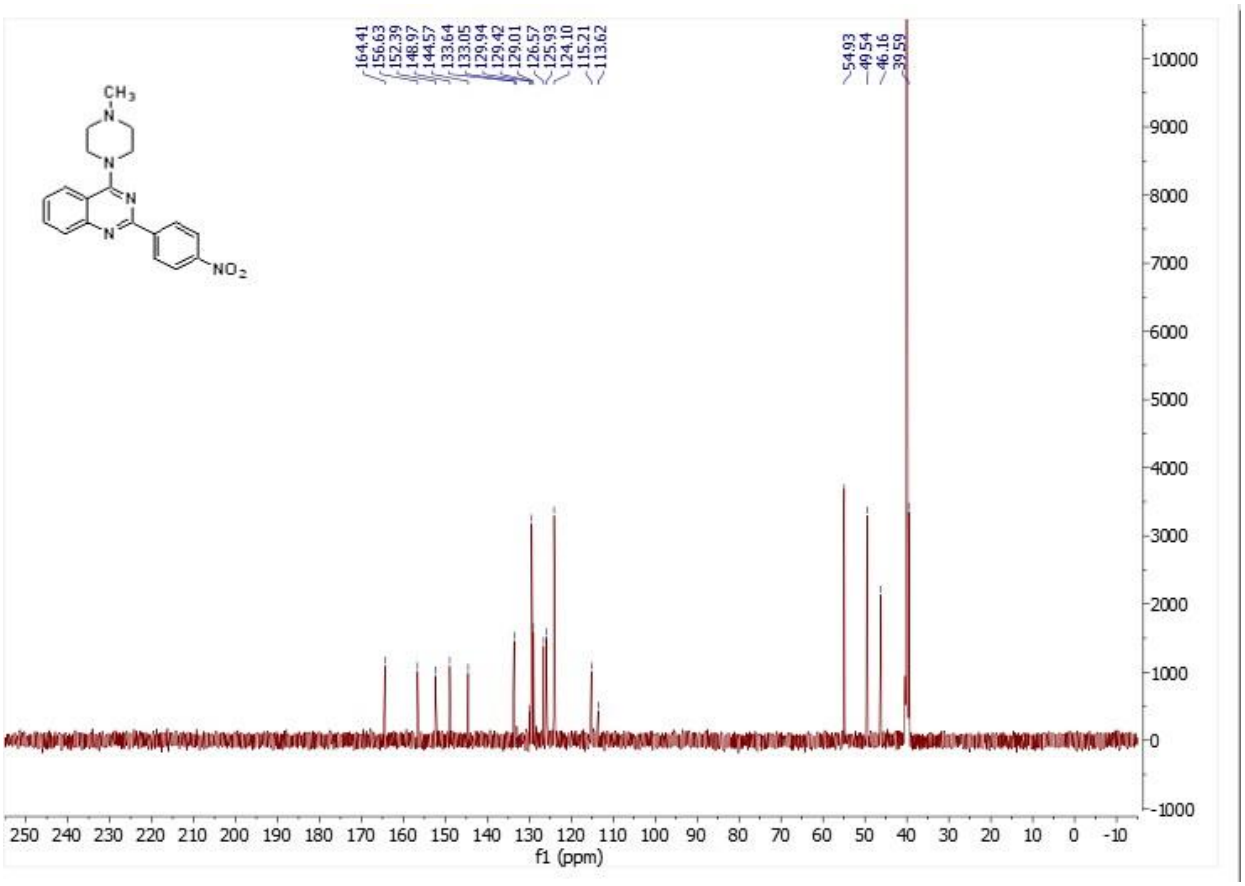
164.41
156.63
152.39
148.97
144.57
133.64
133.05
129.94
129.42
129.01
126.57
125.93
124.10
115.21
113.62
54.93
49.54
46.16
39.59
CH3
N
N
N
N
NO2
10000
9000
8000
7000
6000
5000
4000
3000
2000
1000
0
-1000
250 240 230 220 210 200 190 180 170 160 150 140 130 120 110 100 90 80 70 60 50 40 30 20 10 0 -10
f1 (ppm)

FTIR

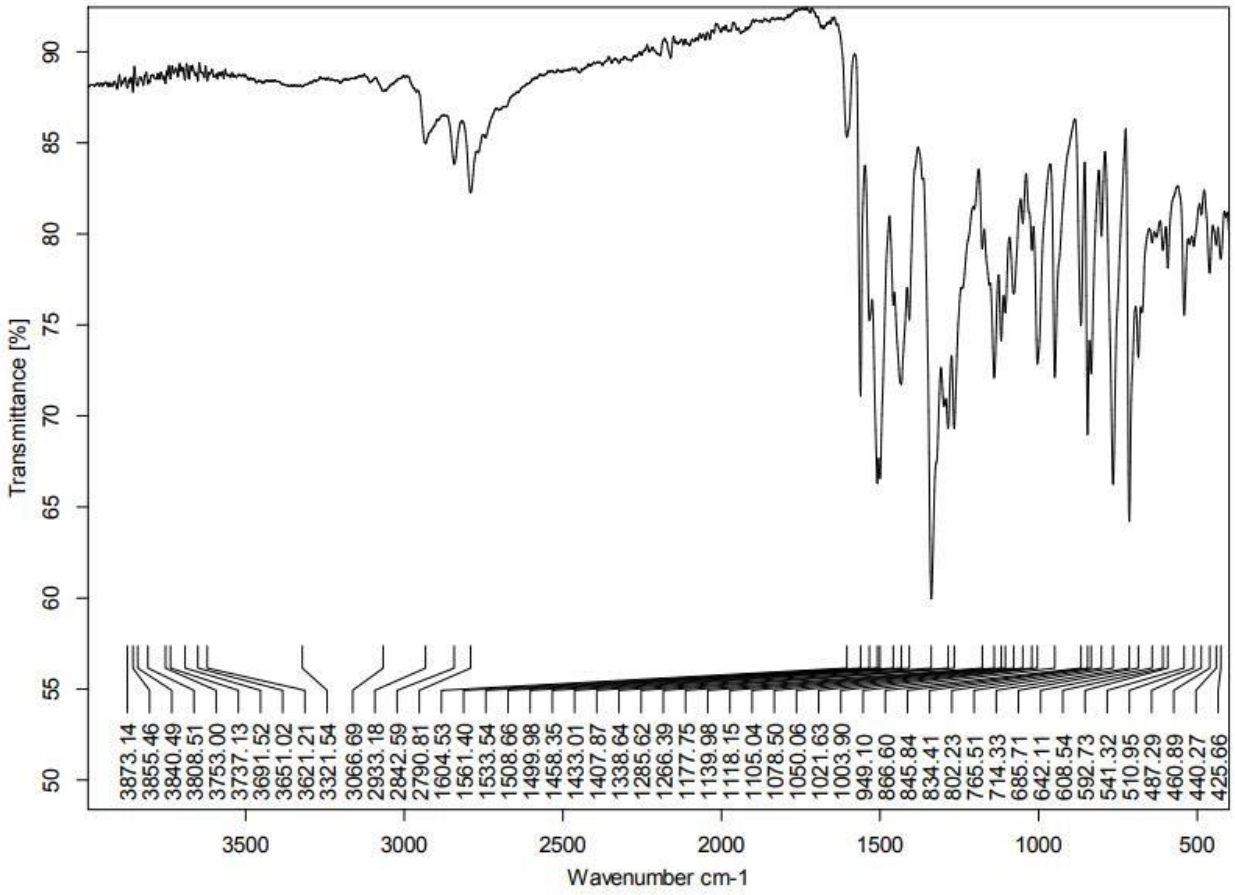

HRMS

Acquisition Parameter

Source Type	APCI	Ion Polarity	Positive	Set Nebulizer	0.8 Bar
Focus	Not active	Set Capillary	4500 V	Set Dry Heater	180 °C
Scan Begin	50 m/z	Set End Plate Offset	-500 V	Set Dry Gas	4.0 l/min
Scan End	2000 m/z	Set Collision Cell RF	100.0 Vpp	Set Divert Valve	Waste

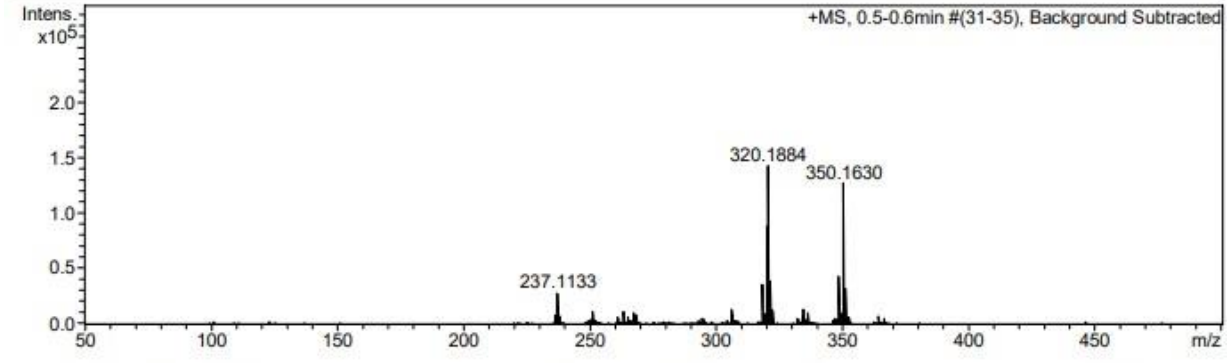

Meas. m/z	#	Formula	Score	m/z	err [mDa]	err [ppm]	mSigma	rdb	e⁻ Conf	N-Rule
320.1884	1	C 21 H 24 N 2 O	100.00	320.1883	-0.1	-0.3	42.1	11.0	odd	ok
	2	C 19 H 22 N 5	42.92	320.1870	-1.4	-4.5	46.8	11.5	even	ok
350.1630	1	C 19 H 20 N 5 O 2	100.00	350.1612	-1.8	-5.2	21.8	12.5	even	ok

HPLC

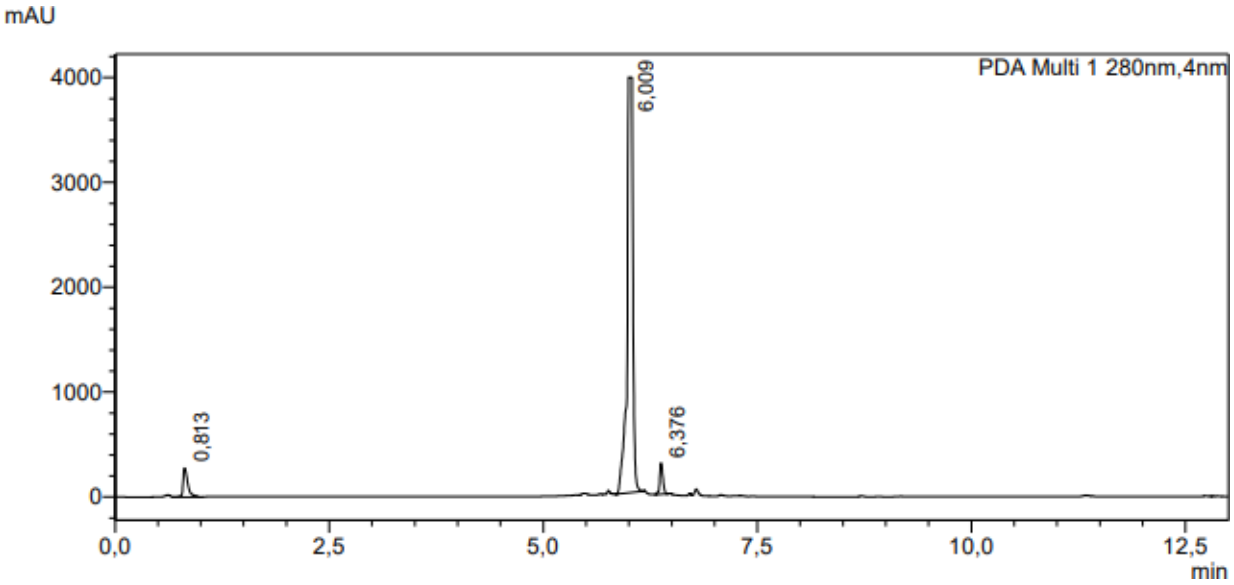
mAU
PDA Multi 1 280nm,4nm
4000
3000
2000
1000
0
6,009
0,813
6,376
0,0
2,5
5,0
7,5
10,0
12,5
min

2-(4-bromophenyl)-4-(4-methylpiperazin-1-yl)quinazoline **(3f)**

^{1}H NMR

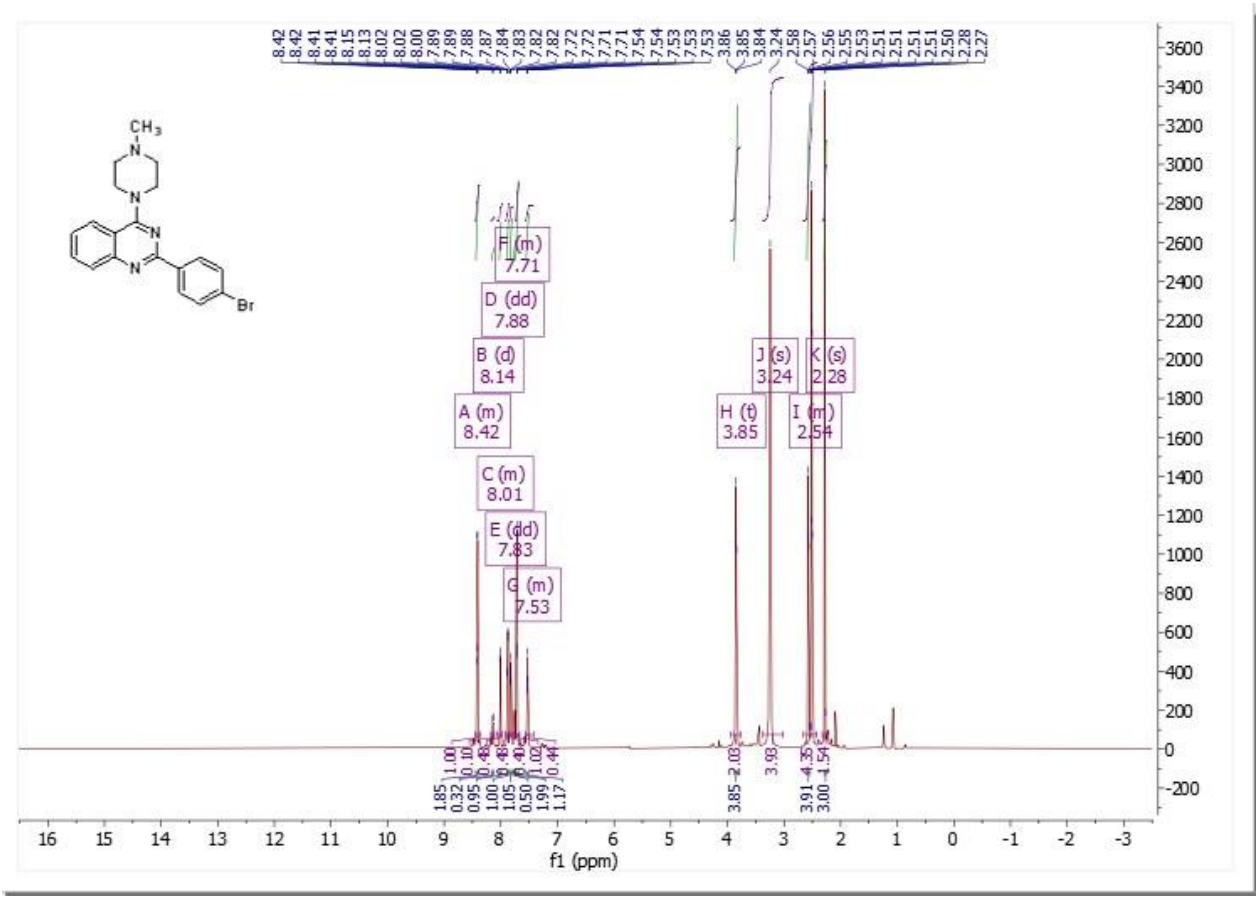

^{13}C NMR

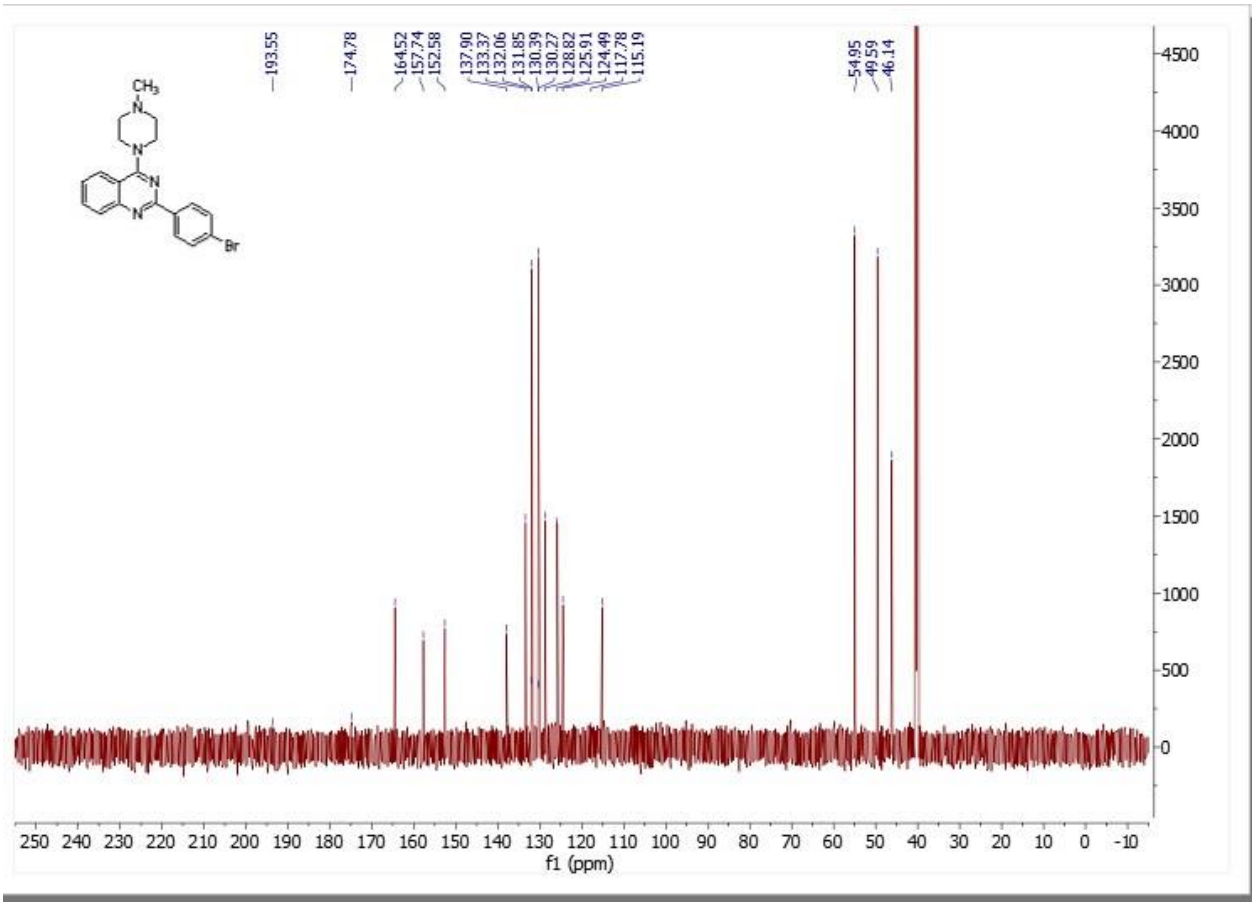
193.55
174.78
164.52
157.74
152.58
137.90
133.37
132.06
131.85
130.39
130.27
128.82
125.91
124.49
117.78
115.19
54.95
49.59
46.14
CH3
N
N
N
N
Br
4500
4000
3500
3000
2500
2000
1500
1000
500
0
250 240 230 220 210 200 190 180 170 160 150 140 130 120 110 100 90 80 70 60 50 40 30 20 10 0 -10
f1 (ppm)

FTIR

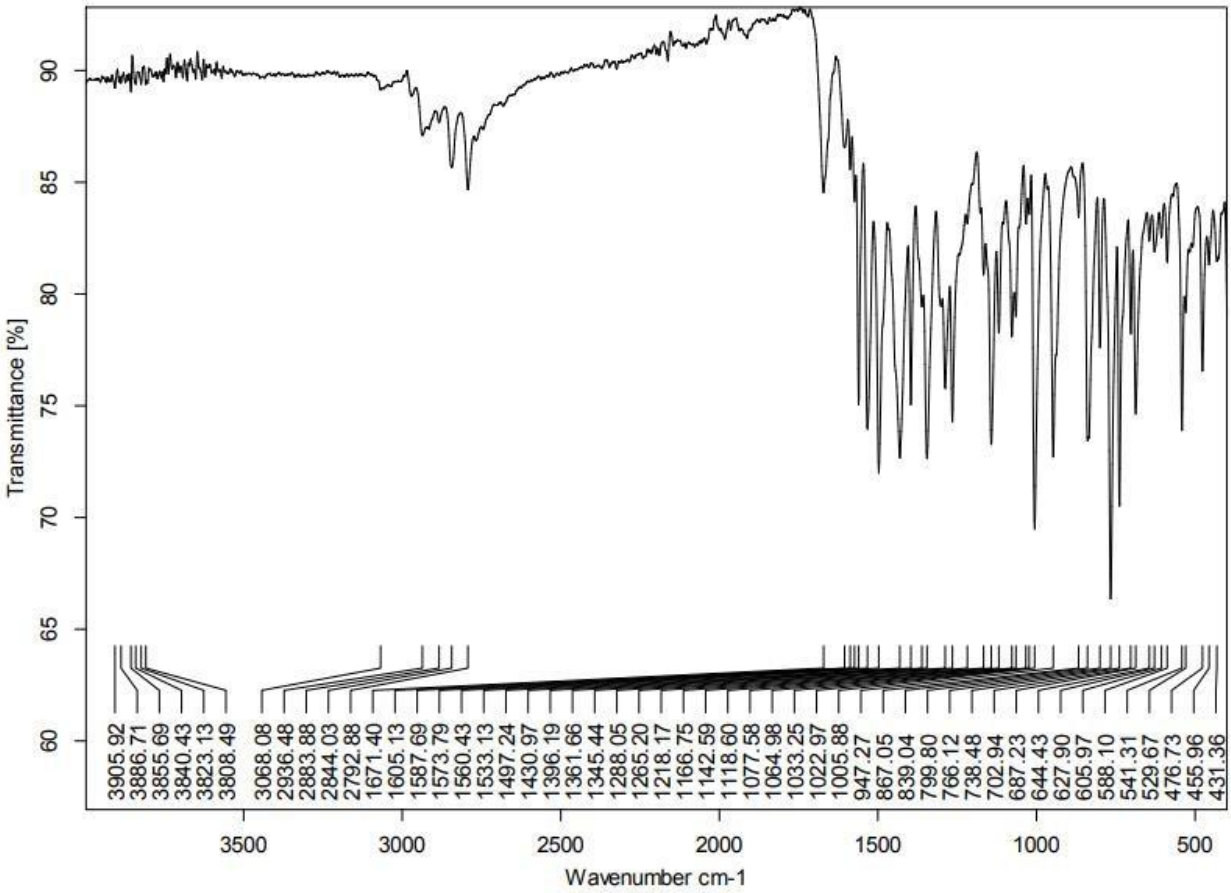

HRMS

Acquisition Parameter

Source Type	APCI	Ion Polarity	Positive	Set Nebulizer	0.8 Bar
Focus	Not active	Set Capillary	4500 V	Set Dry Heater	180 °C
Scan Begin	50 m/z	Set End Plate Offset	-500 V	Set Dry Gas	4.0 l/min
Scan End	2000 m/z	Set Collision Cell RF	100.0 Vpp	Set Divert Valve	Waste

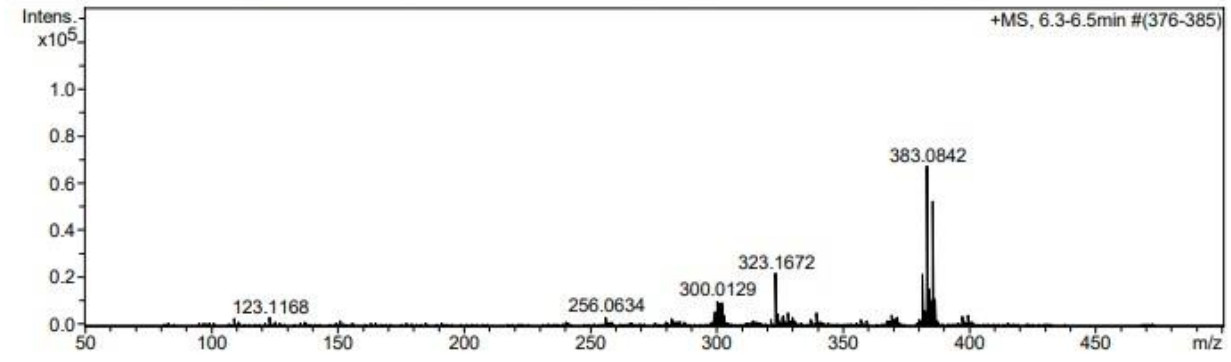

Meas. m/z	#	Formula	Score	m/z	err [mDa]	err [ppm]	mSigma	rdb	e⁻ Conf	N-Rule
381.0722	1	C 19 H 18 Br N 4	100.00	381.0709	-1.3	-3.4	458.6	12.5	even	ok
383.0842	1	C 19 H 20 Br N 4	100.00	383.0866	2.4	6.2	99.5	11.5	even	ok

HPLC

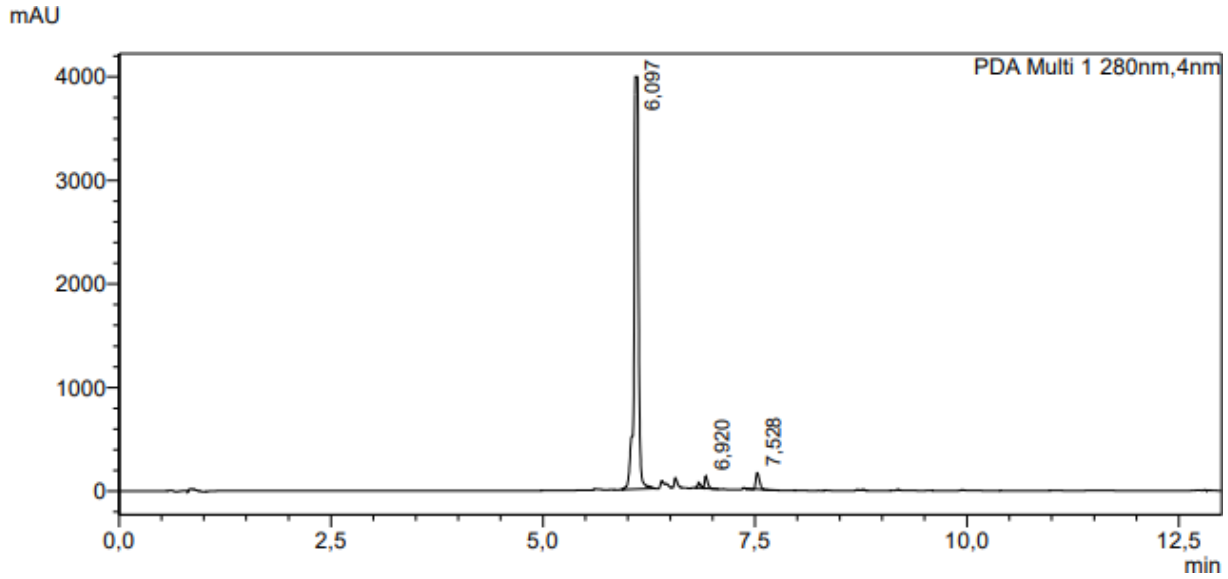

2-(4-bromophenyl)-4-(piperidin-1-yl)quinazoline **(4a)**

^{1}H NMR

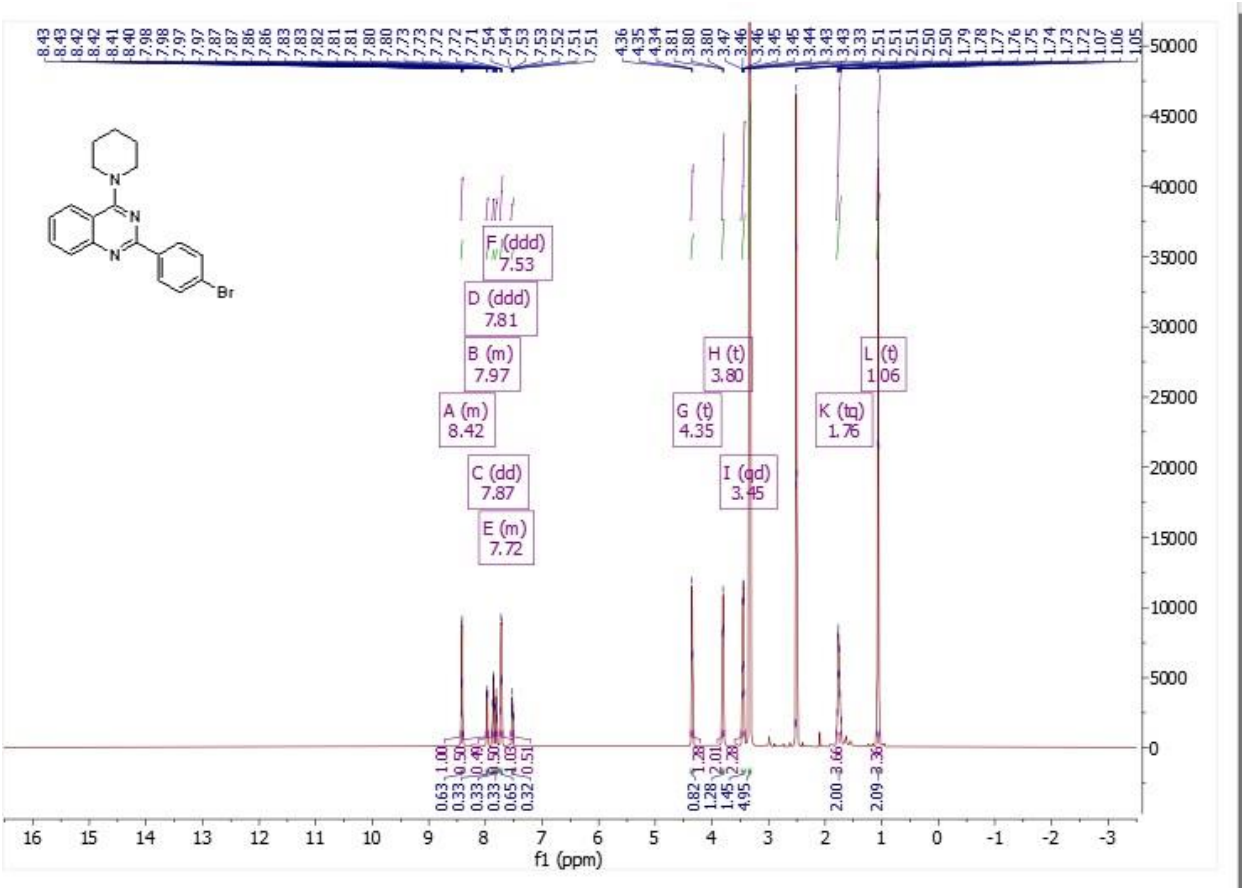

^{13}C NMR

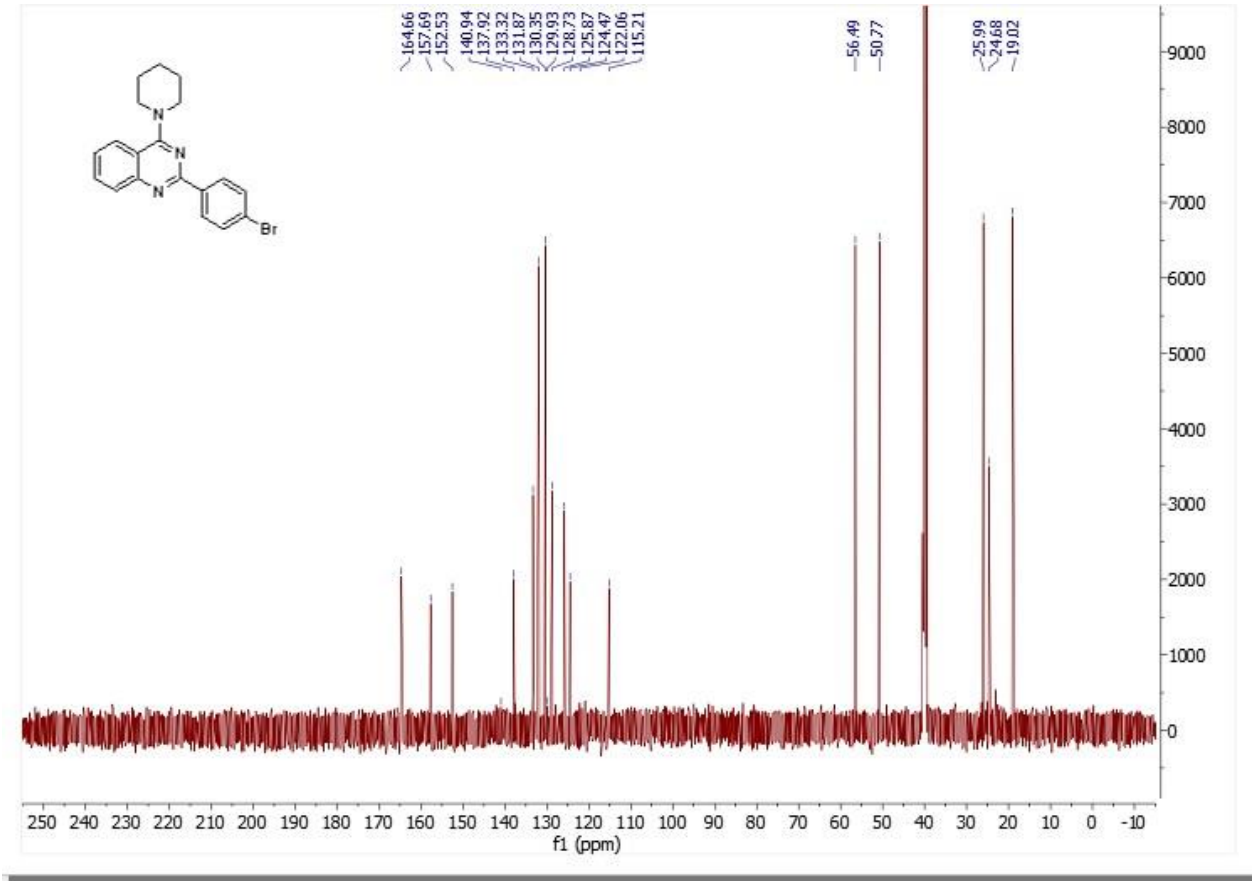
164.66
157.69
152.53
140.94
137.92
133.32
131.87
130.35
129.93
128.73
125.87
124.47
122.06
115.21
56.49
50.77
25.99
24.68
19.02
Br
9000
8000
7000
6000
5000
4000
3000
2000
1000
0
250 240 230 220 210 200 190 180 170 160 150 140 130 120 110 100 90 80 70 60 50 40 30 20 10 0 -10
f1 (ppm)

FTIR

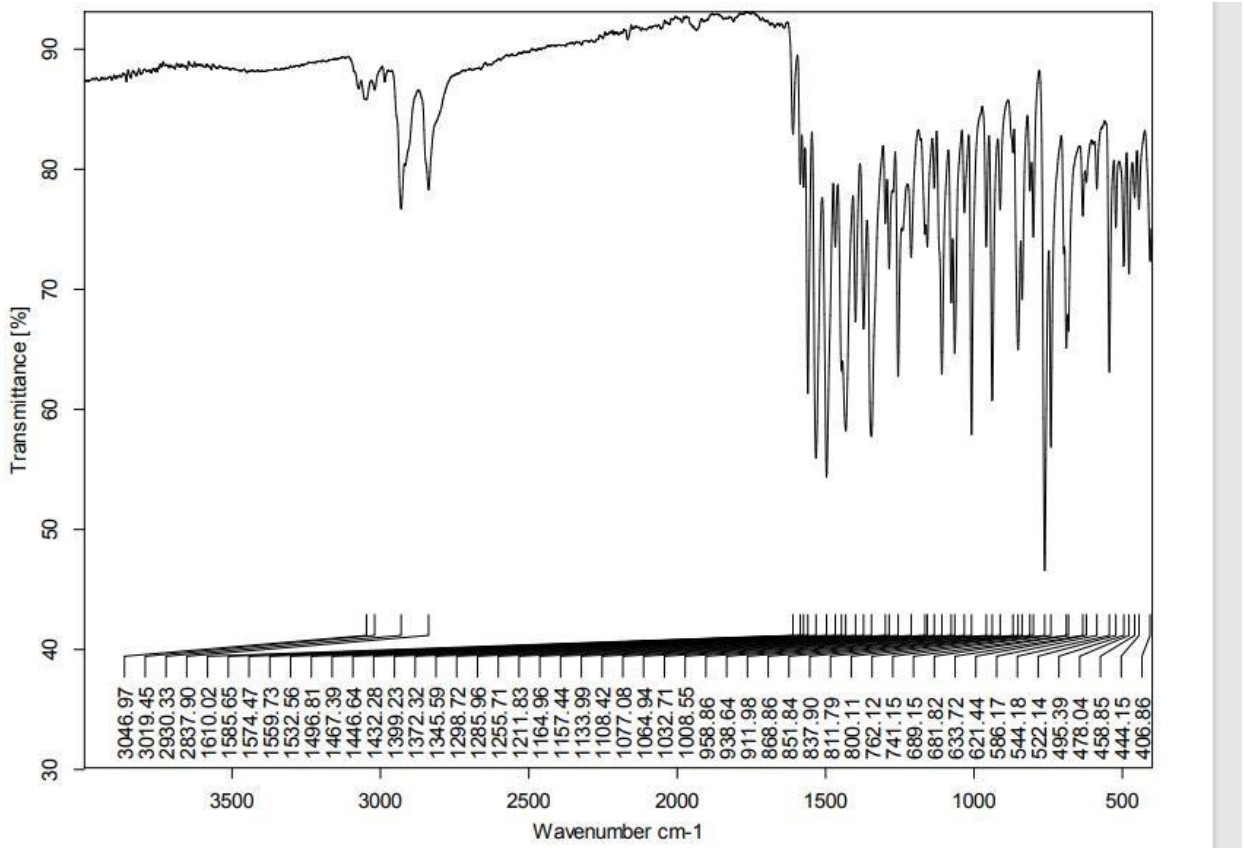

HRMS

Acquisition Parameter

Source Type	APCI	Ion Polarity	Positive	Set Nebulizer	0.8 Bar
Focus	Not active	Set Capillary	4500 V	Set Dry Heater	180 °C
Scan Begin	50 m/z	Set End Plate Offset	-500 V	Set Dry Gas	4.0 l/min
Scan End	2000 m/z	Set Collision Cell RF	100.0 Vpp	Set Divert Valve	Waste

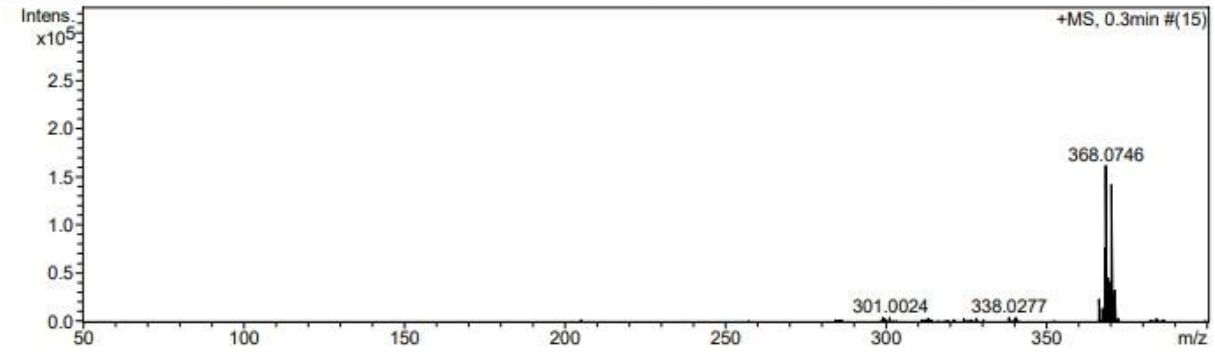

Meas. m/z	#	Formula	Score	m/z	err [mDa]	err [ppm]	mSigma	rdb	e⁻ Conf	N-Rule
368.0746	1	C 19 H 19 Br N 3	100.00	368.0757	1.0	2.9	60.0	11.5	even	ok

HPLC

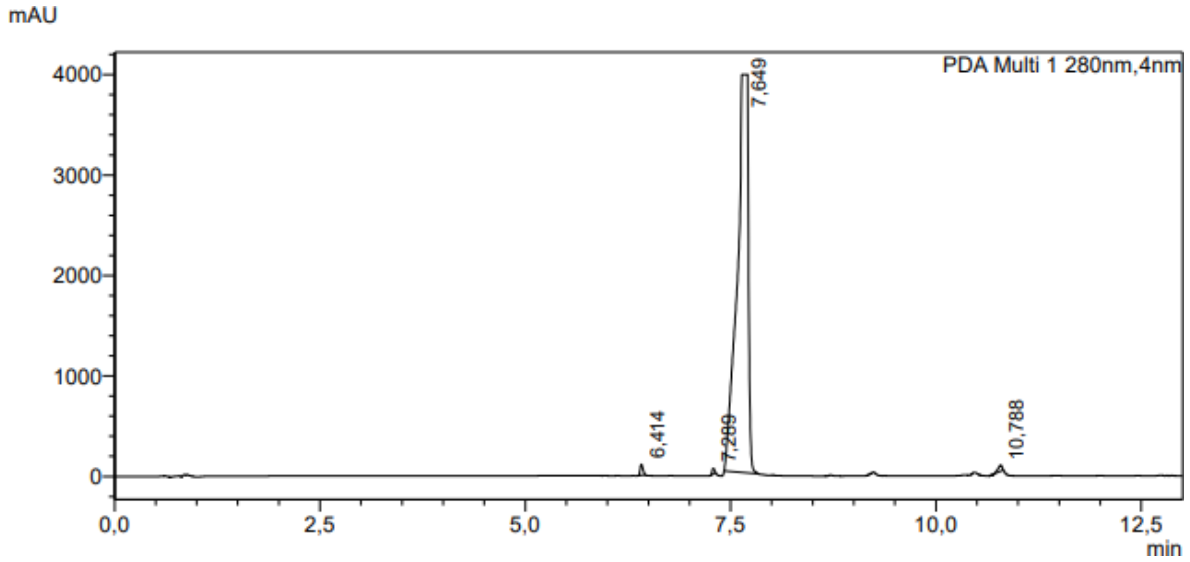

N^1,N^2-bis(2-(4-bromophenyl)quinazolin-4-yl)ethane-1,2-diamine **(5a)**

^{1}H NMR

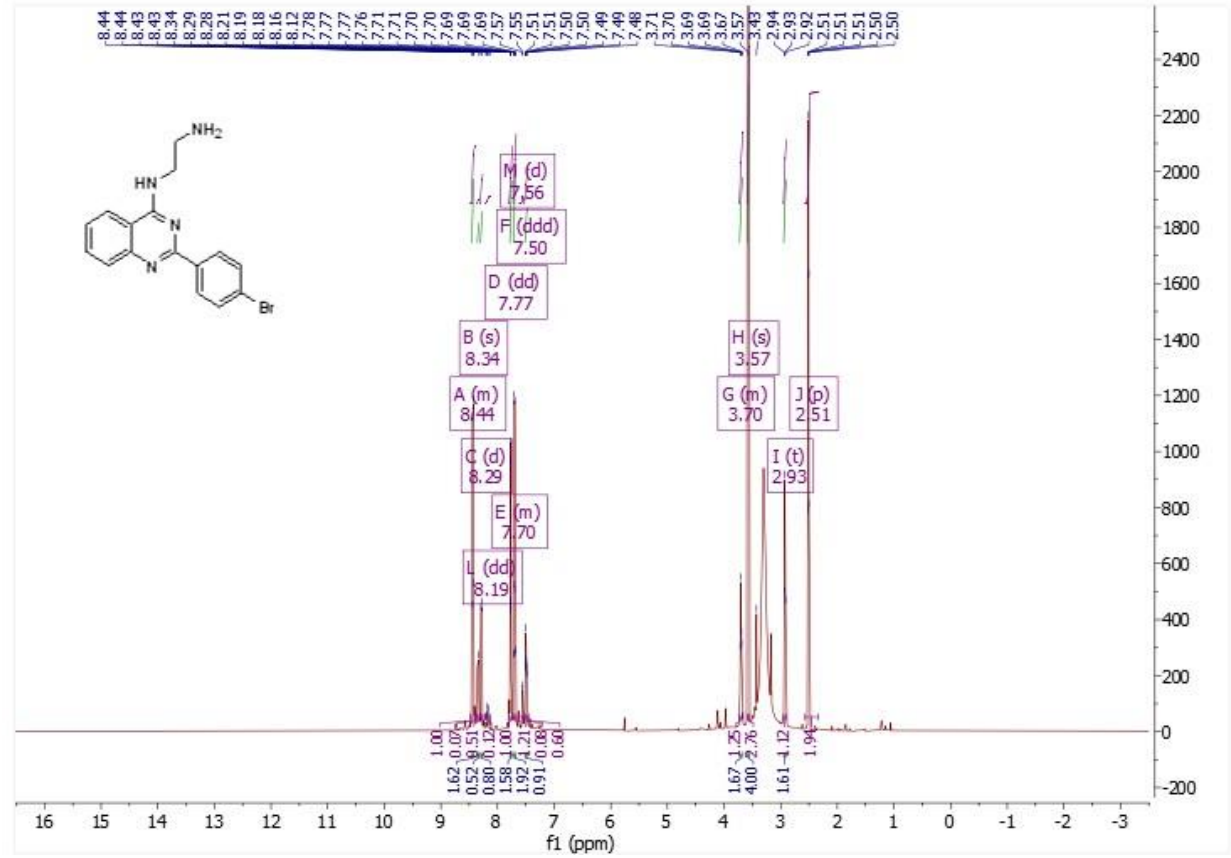

^{13}C NMR

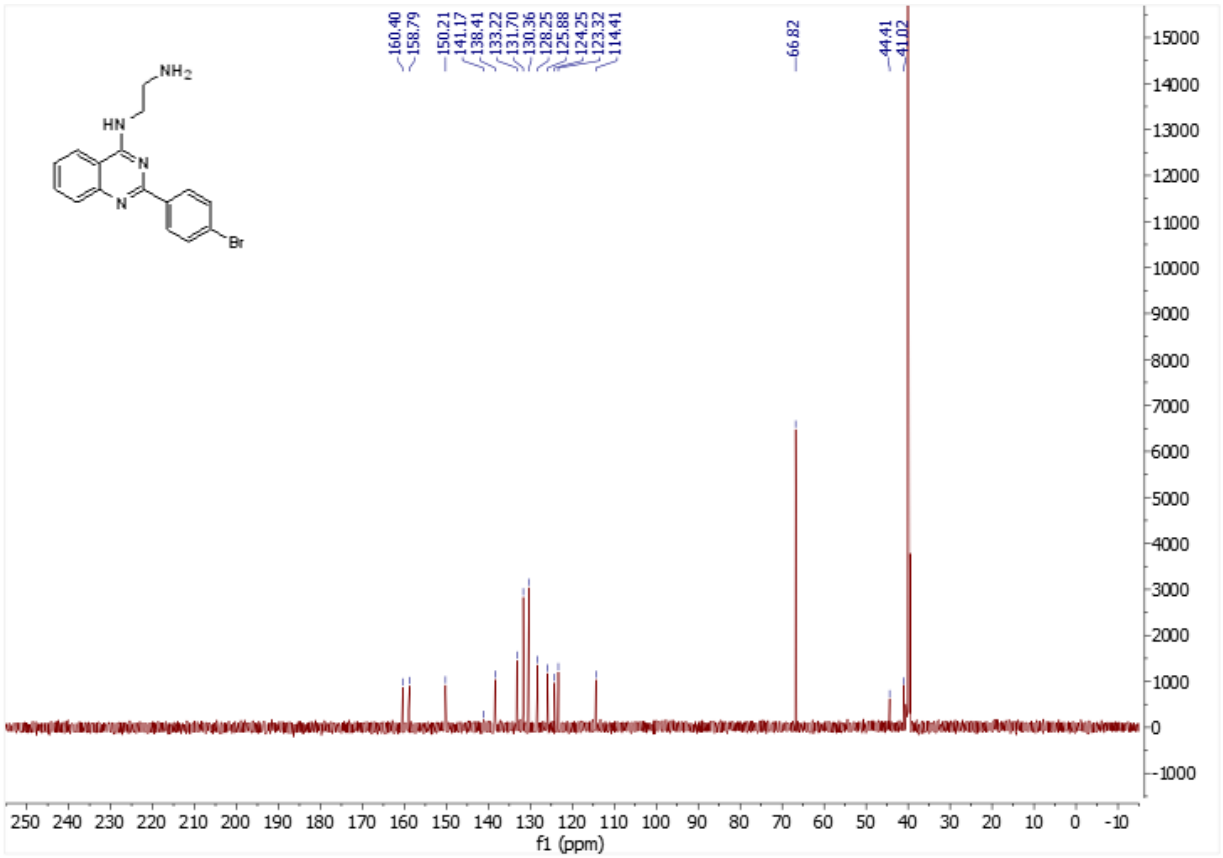
160.40
158.79
150.21
141.17
138.41
133.22
131.70
130.36
128.25
125.88
124.25
123.32
114.41
66.82
44.41
41.02
NH2
HN
N
N
Br
15000
14000
13000
12000
11000
10000
9000
8000
7000
6000
5000
4000
3000
2000
1000
0
-1000
250 240 230 220 210 200 190 180 170 160 150 140 130 120 110 100 90 80 70 60 50 40 30 20 10 0 -10
f1 (ppm)

FTIR

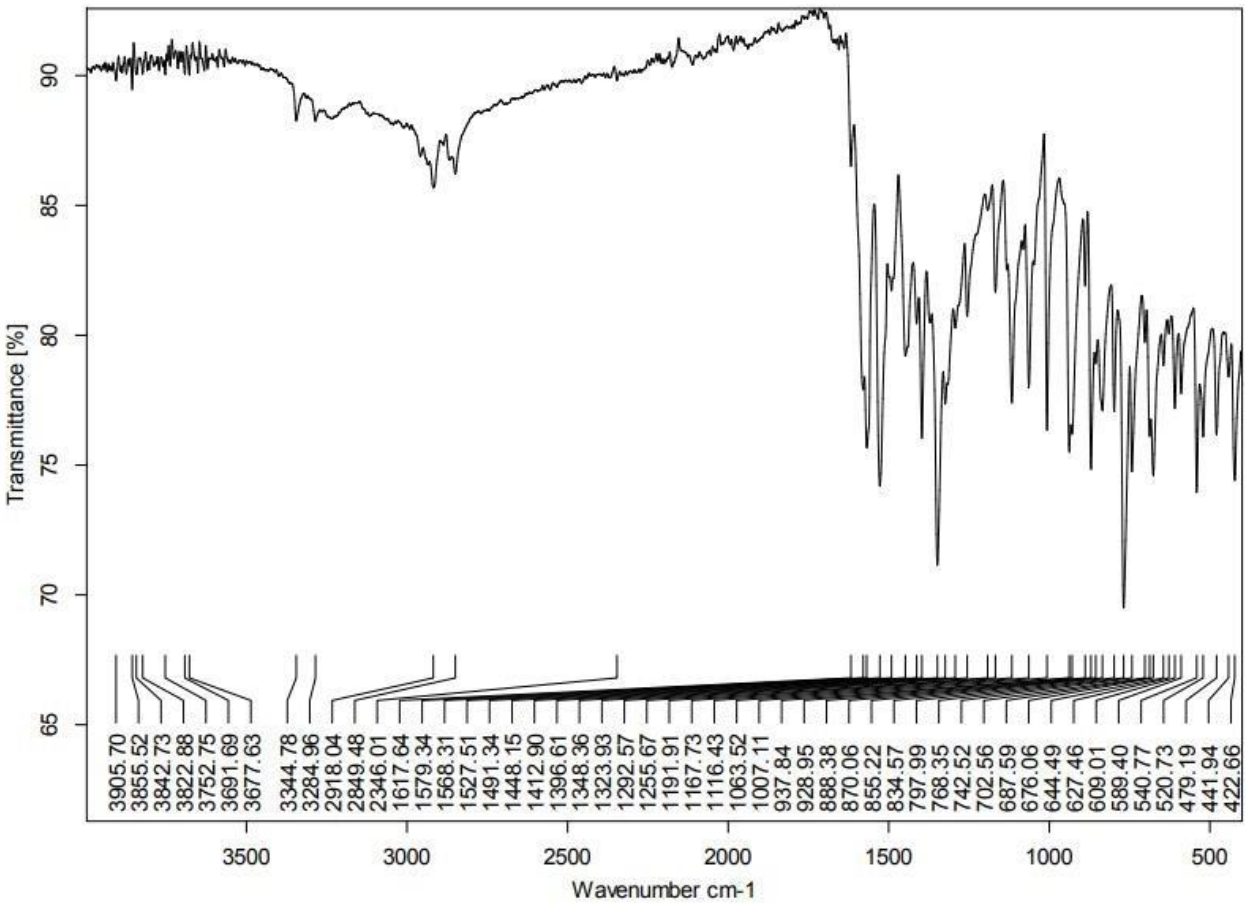

HRMS

Acquisition Parameter

Source Type	APCI	Ion Polarity	Positive	Set Nebulizer	0.8 Bar
Focus	Not active	Set Capillary	4500 V	Set Dry Heater	180 °C
Scan Begin	50 m/z	Set End Plate Offset	-500 V	Set Dry Gas	4.0 l/min
Scan End	2000 m/z	Set Collision Cell RF	100.0 Vpp	Set Divert Valve	Waste

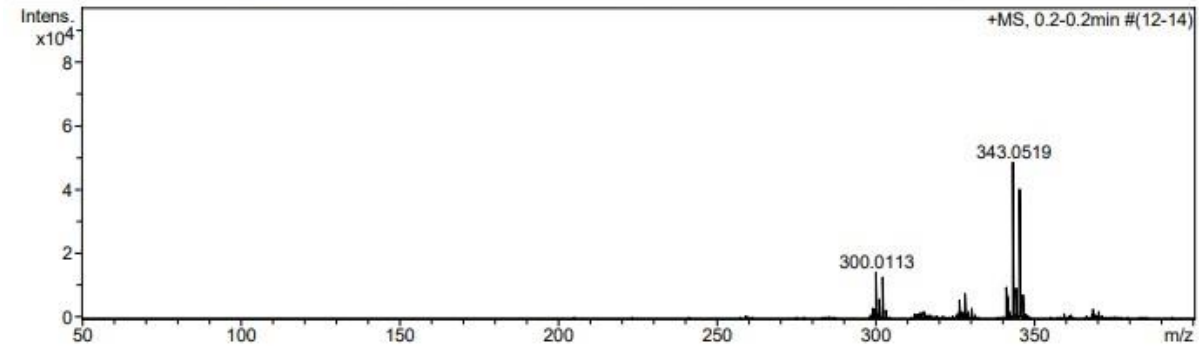

Meas. m/z	#	Formula	Score	m/z	err [mDa]	err [ppm]	mSigma	rdb	e⁻ Conf	N-Rule
343.0519	1	C 15 H 14 Br N 5	0.00	343.0427	-9.2	-26.8	71.0	11.0	odd	ok
	2	C 16 H 16 Br N 4	100.00	343.0553	3.4	9.9	72.0	10.5	even	ok
	3	C 28 H 7	0.00	343.0542	2.3	6.8	404.4	25.5	even	ok

HPLC

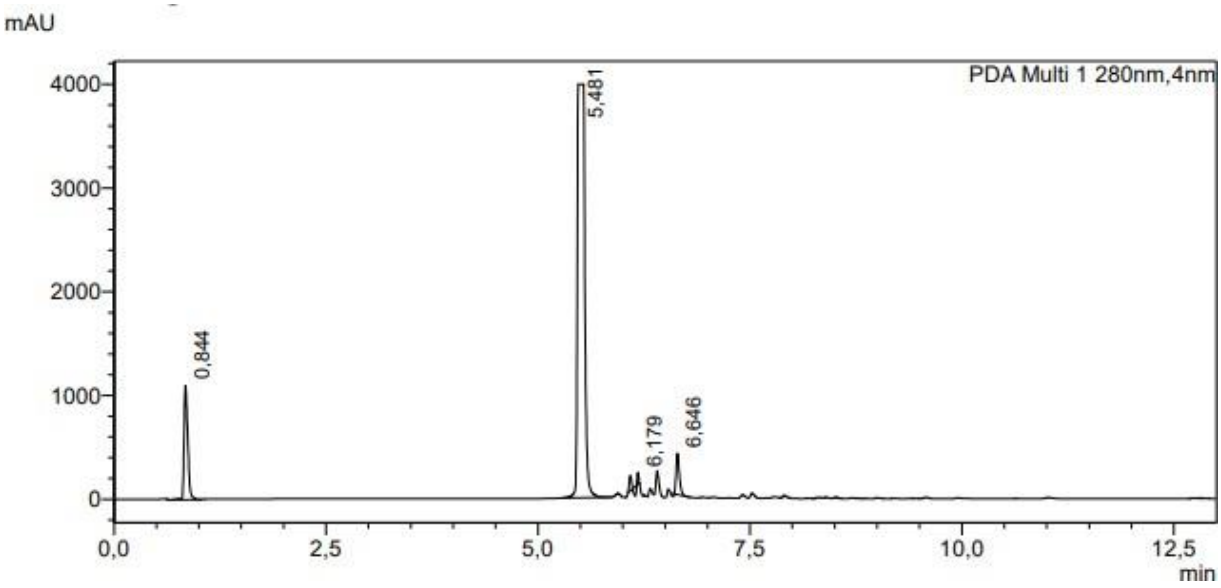

N^1,N^2-bis(2-(4-fluorophenyl)quinazolin-4-yl)ethane-1,2-diamine **(5b)**

^{1}H NMR

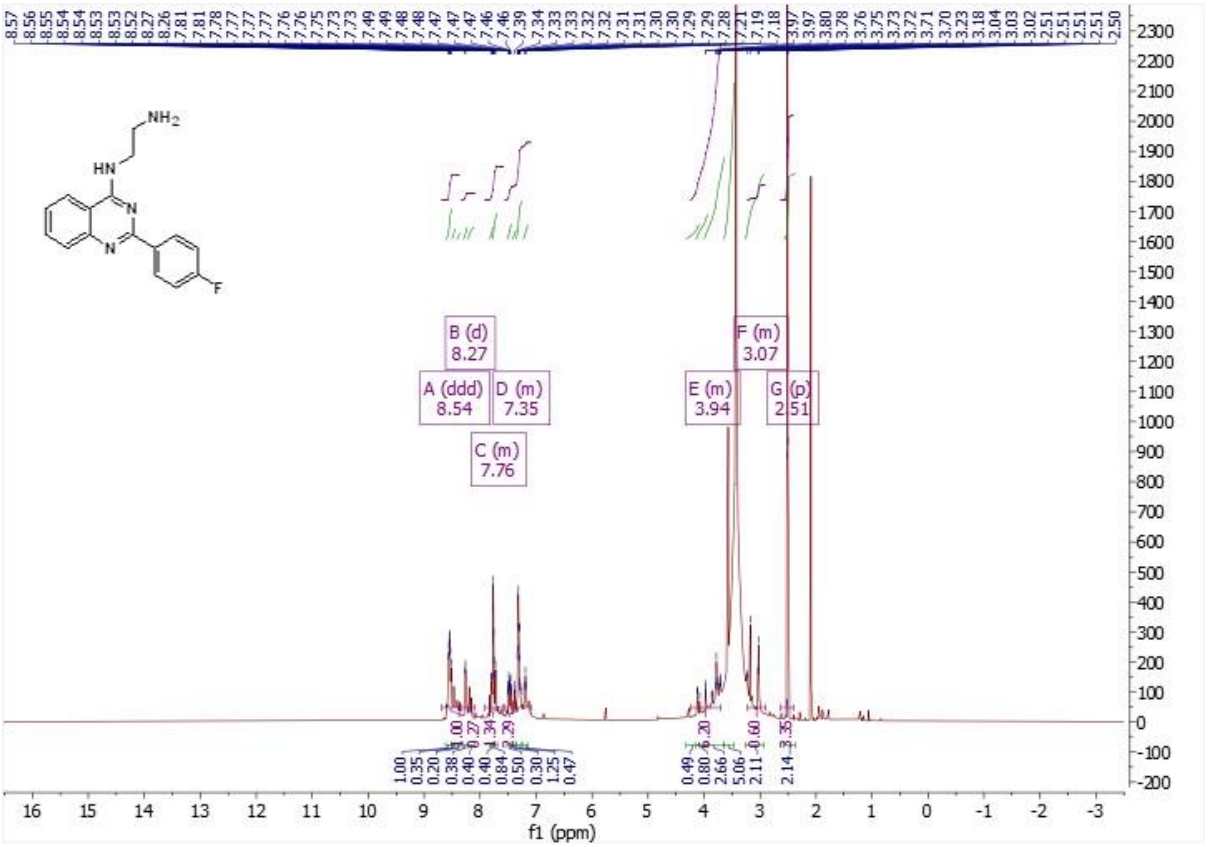

^{13}C NMR

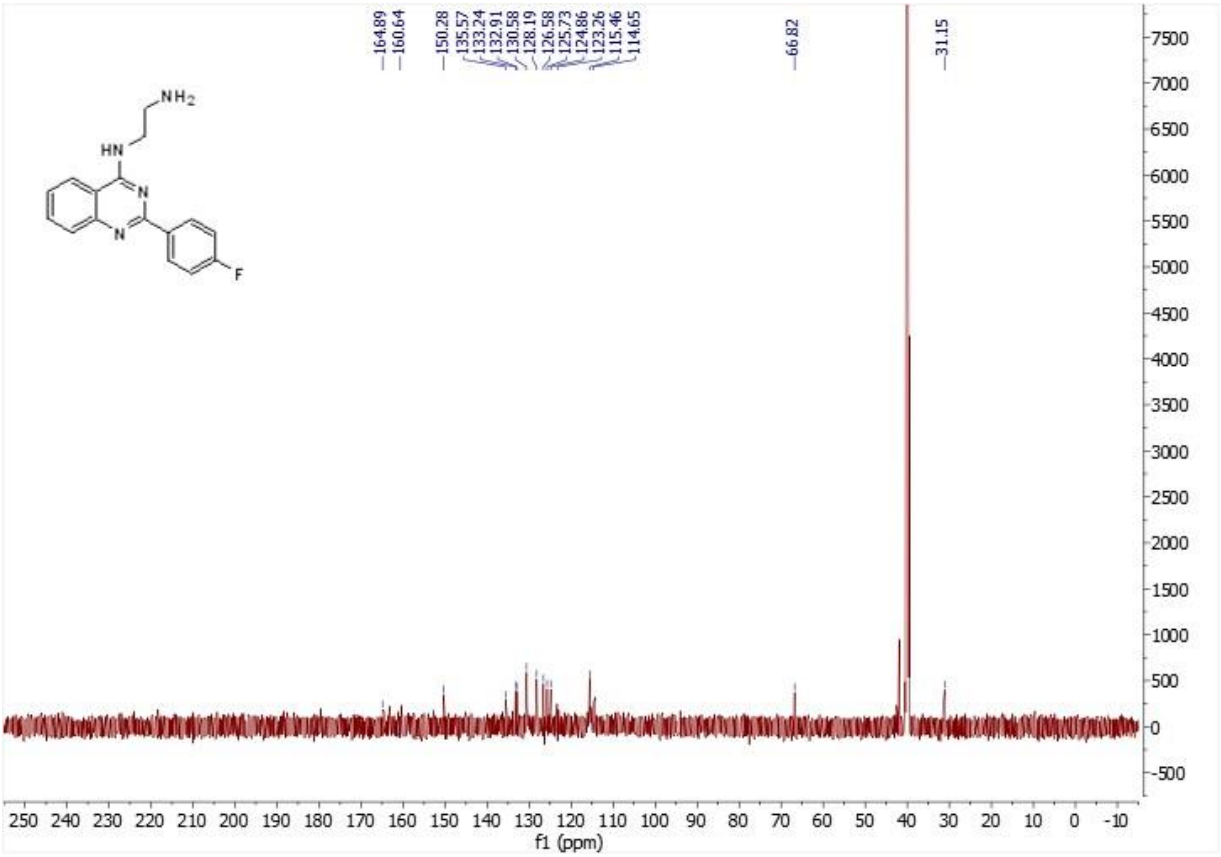
164.89
160.64
150.28
135.57
133.24
132.91
130.58
128.19
126.58
125.73
124.86
123.26
115.46
114.65
66.82
31.15
NH2
HN
N
N
F
7500
7000
6500
6000
5500
5000
4500
4000
3500
3000
2500
2000
1500
1000
500
0
-500
250 240 230 220 210 200 190 180 170 160 150 140 130 120 110 100 90 80 70 60 50 40 30 20 10 0 -10
f1 (ppm)

FTIR

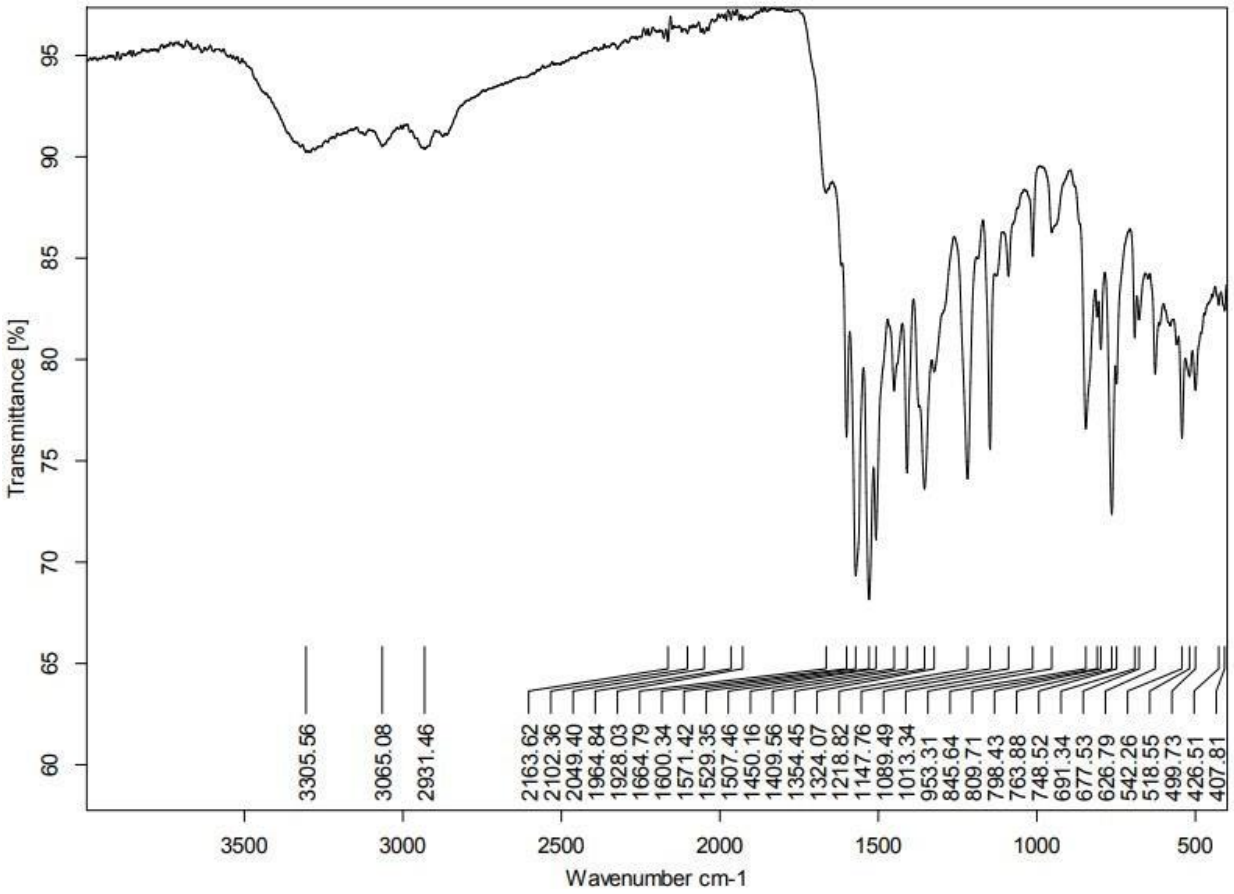
Transmittance [%]
95
90
85
80
75
70
65
60
3305.56
3065.08
2931.46
2163.62
2102.36
2049.40
1964.84
1928.03
1664.79
1600.34
1571.42
1529.35
1507.46
1450.16
1409.56
1354.45
1324.07
1218.82
1147.76
1089.49
1013.34
953.31
845.64
809.71
798.43
763.88
748.52
691.34
677.53
626.79
542.26
518.55
499.73
426.51
407.81
3500
3000
2500
2000
1500
1000
500
Wavenumber cm-1

HRMS

Acquisition Parameter

Source Type	APCI	Ion Polarity	Positive	Set Nebulizer	0.8 Bar
Focus	Not active	Set Capillary	4500 V	Set Dry Heater	180 °C
Scan Begin	50 m/z	Set End Plate Offset	-500 V	Set Dry Gas	4.0 l/min
Scan End	2000 m/z	Set Collision Cell RF	100.0 Vpp	Set Divert Valve	Waste

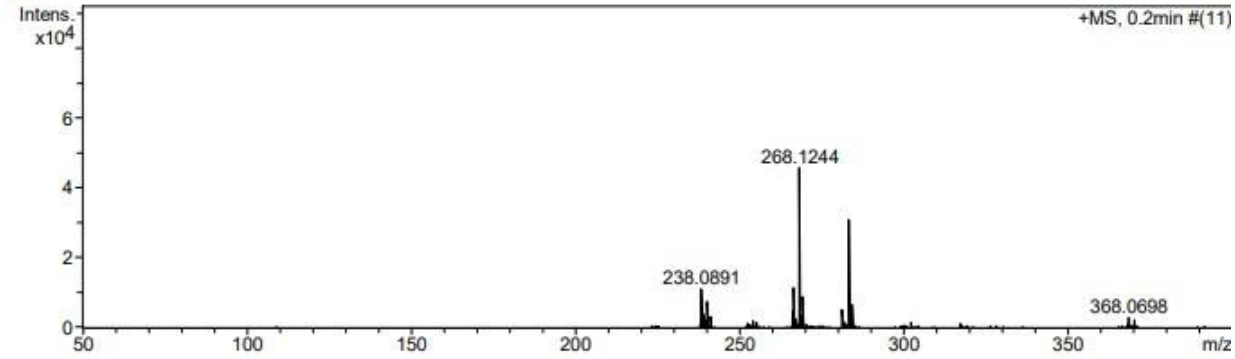

Meas. m/z	#	Formula	Score	m/z	err [mDa]	err [ppm]	mSigma	rdb	e⁻ Conf	N-Rule
238.0891	1	C 15 H 11 F N 2	100.00	238.0901	1.0	4.1	387.8	11.0	odd	ok
	2	C 10 H 10 F 2 N 5	20.53	238.0899	0.8	3.2	398.4	7.5	even	ok
268.1244	1	C 16 H 15 F N 3	100.00	268.1245	0.0	0.1	11.6	10.5	even	ok
	2	C 21 H 16	73.08	268.1247	0.2	0.8	22.8	14.0	odd	ok
284.1339	1	C 15 H 15 F N 5	100.00	284.1306	-3.3	-11.5	104.7	10.5	even	ok
	2	C 19 H 18 F 2	48.35	284.1371	3.2	11.4	119.2	10.0	odd	ok
	3	C 20 H 16 N 2	31.64	284.1308	-3.1	-10.8	129.9	14.0	odd	ok

HPLC

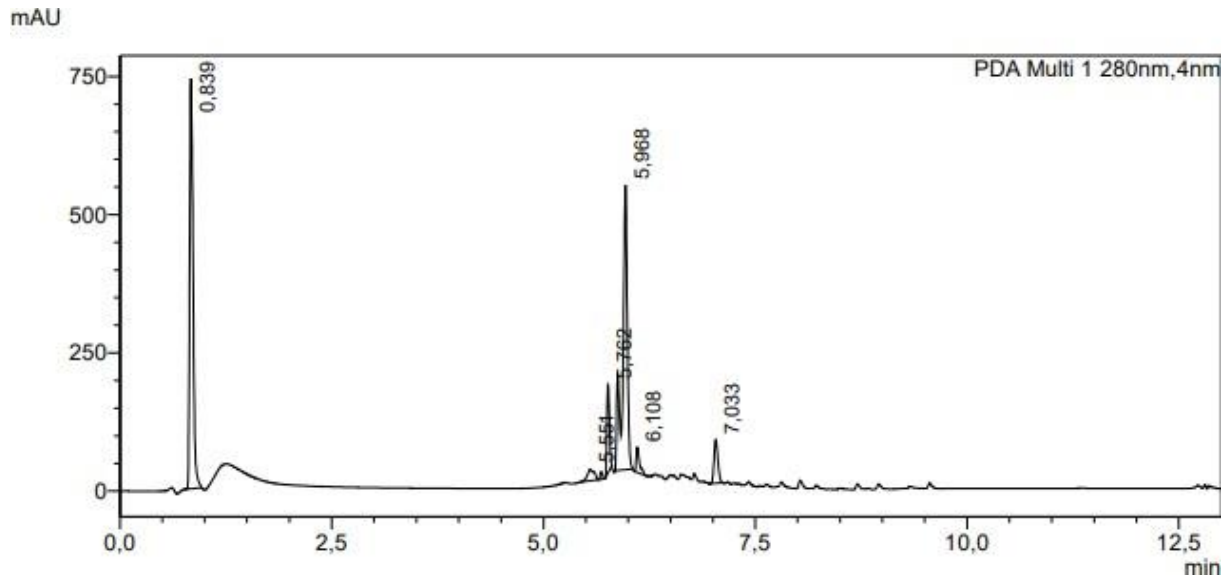

N^1,N^2-bis(2-(3-chlorophenyl)quinazolin-4-yl)ethane-1,2-diamine **(5c)**

^{1}H NMR

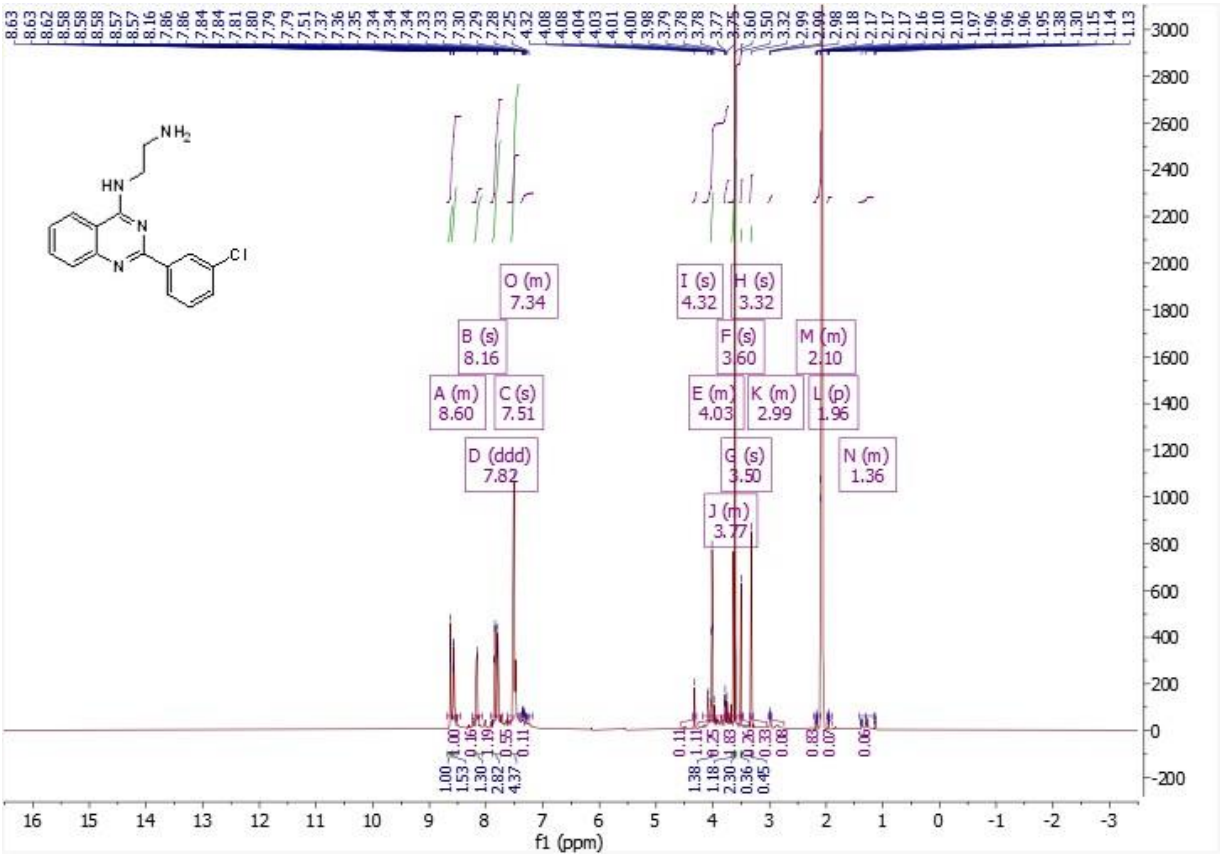

^{13}C NMR

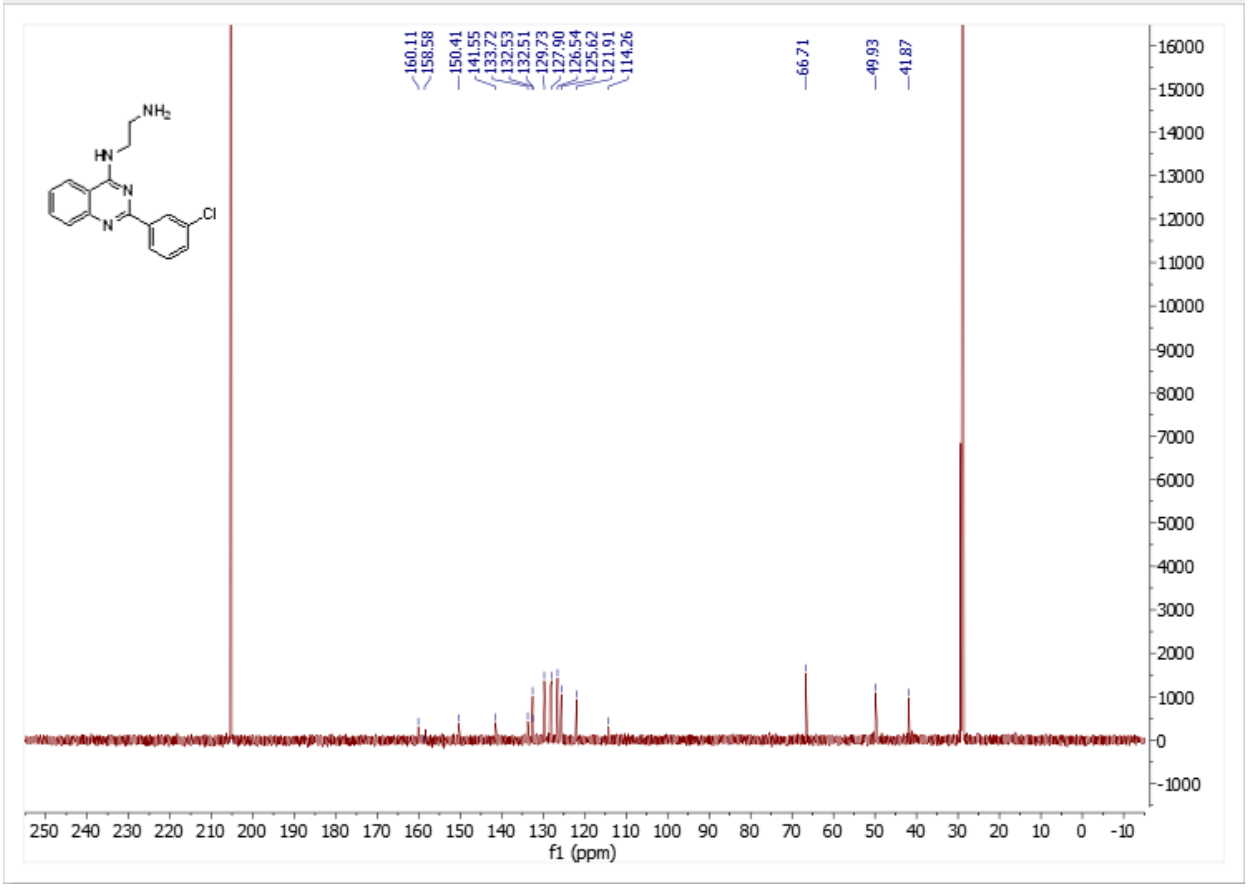
160.11
158.58
150.41
141.55
133.72
132.53
132.51
129.73
127.90
126.54
125.62
121.91
114.26
66.71
49.93
41.87
NH2
HN
N
N
Cl
16000
15000
14000
13000
12000
11000
10000
9000
8000
7000
6000
5000
4000
3000
2000
1000
0
-1000
250 240 230 220 210 200 190 180 170 160 150 140 130 120 110 100 90 80 70 60 50 40 30 20 10 0 -10
f1 (ppm)

FTIR

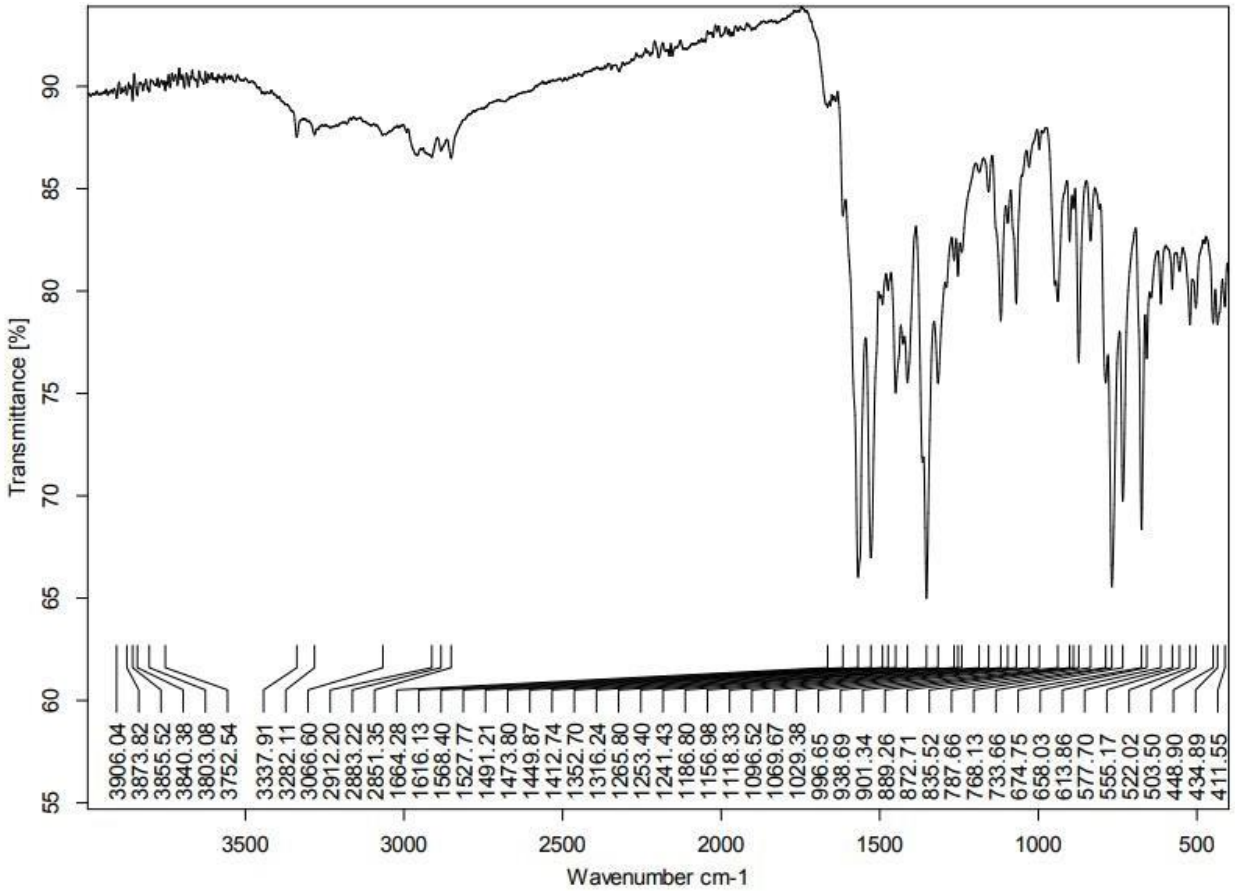
Transmittance [%]
90
85
80
75
70
65
60
55
3906.04
3873.82
3855.52
3840.38
3803.08
3752.54
3337.91
3282.11
3066.60
2912.20
2883.22
2851.35
1664.28
1616.13
1568.40
1527.77
1491.21
1473.80
1449.87
1412.74
1352.70
1316.24
1265.80
1253.40
1241.43
1186.80
1156.98
1118.33
1096.52
1069.67
1029.38
996.65
938.69
901.34
889.26
872.71
835.52
787.66
768.13
733.66
674.75
658.03
613.86
577.70
555.17
522.02
503.50
448.90
434.89
411.55
3500
3000
2500
2000
1500
1000
500
Wavenumber cm-1

HRMS

Acquisition Parameter

Source Type	APCI	Ion Polarity	Positive	Set Nebulizer	0.8 Bar
Focus	Not active	Set Capillary	4500 V	Set Dry Heater	180 °C
Scan Begin	50 m/z	Set End Plate Offset	-500 V	Set Dry Gas	4.0 l/min
Scan End	2000 m/z	Set Collision Cell RF	100.0 Vpp	Set Divert Valve	Waste

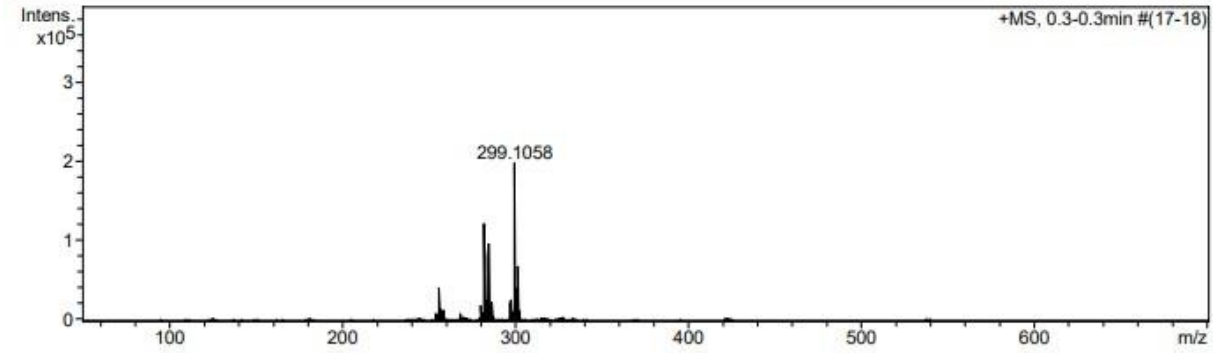

Meas. m/z	#	Formula	Score	m/z	err [mDa]	err [ppm]	mSigma	rdb	e⁻ Conf	N-Rule
256.0626	1	C 14 H 11 Cl N 3	100.00	256.0636	1.0	4.0	43.5	10.5	even	ok
	2	C 13 H 16 Cl 2 N	0.29	256.0654	2.9	11.2	142.4	5.5	even	ok
	3	C 15 H 6 N 5	0.09	256.0618	-0.8	-3.1	180.7	15.5	even	ok
282.0784	1	C 15 H 18 Cl 2 N	100.00	282.0811	2.6	9.4	66.1	6.5	even	ok
	2	C 16 H 13 Cl N 3	0.02	282.0793	0.8	2.9	219.5	11.5	even	ok
	3	C 17 H 8 N 5	0.00	282.0774	-1.0	-3.6	440.5	16.5	even	ok
299.1058	1	C 16 H 16 Cl N 4	100.00	299.1058	-0.0	-0.1	9.7	10.5	even	ok
	2	C 15 H 21 Cl 2 N 2	0.32	299.1076	1.8	6.1	134.0	5.5	even	ok
	3	C 17 H 11 N 6	0.01	299.1040	-1.8	-6.2	188.6	15.5	even	ok
421.0957	1	C 23 H 19 Cl 2 N 4	100.00	421.0981	2.4	5.8	126.8	15.5	even	ok
	2	C 24 H 14 Cl N 6	0.00	421.0963	0.6	1.4	286.5	20.5	even	ok
537.1323	1	C 30 H 23 Cl 2 N 6	100.00	537.1356	3.3	6.1	26.9	21.5	even	ok

HPLC